UNIVERSITÀ
DEGLI STUDI
DI PADOVA

Head Office: Università degli Studi di Padova

Department of Biology

Ph.D. COURSE IN: Biosciences
CURRICULUM: Genetics Genomics and Bioinformatics
SERIES 36°

Integrated metagenomic model insight towards understanding the effects of biochar on microplastics degradation in flooded soil

Coordinator: Prof. Chiara Romualdi
Supervisor: Prof. Stefano Campanaro

Ph.D. student : Mengyuan Ji

Abstract

Soil microbial communities, containing a rich tapestry of bacteria, fungi, and archaea, serve as the cornerstone of terrestrial ecosystems, orchestrating essential biogeochemical processes and maintaining ecological balance. However, the emergence of microplastics pollution has cast a shadow over these vital ecosystems. Microplastics, minute plastic particles measuring less than 5mm, have infiltrated soils globally, ushering in a new era of environmental challenges. Beyond their physical presence, microplastics introduce novel contaminants into these ecosystems, potentially reshaping the composition and functionality of soil microbial communities. Currently, the detection and the removal of microplastics in terrestrial ecosystems have emerged as areas of significant research focus and challenge. Metagenomics is a transformative branch of genomics that allows the direct study of genetic information obtained from environmental samples. It allows for a closer examination of the functionality of complex soil microorganisms and their responses to environmental stressors. To unravel the complex relationship of interactions between microplastic pollution and soil microbial communities, the research reported in this PhD thesis employed an integrated metagenomic strategy, which offers an all-encompassing view of the genetic diversity and metabolic potential of these intricate ecosystems. The studies associated to the present project investigate the capacity of microorganisms and functional materials such as biochar and magnetic biochar to perform soil remediation. The final results showed that members of the genus *Nocardia* and *Pseudomonas* present in the soil are able to degrade microplastics and plasticizers together with magnetic biochar. Additionally, it was observed that polyvinyl chloride microplastics exhibited higher methane emission potential than other thermoplastic microplastics. Furthermore, we extended the application of this integrated genomic approach to a sludge system, also characterized by anaerobic conditions, and elucidated the response of microorganisms within the sludge to nanoparticles. These studies thus shed light on the microbial communities structure and their responses to emerging pollutants. The findings from these investigations hold the promise of informing targeted strategies for the remediation of microplastic-contaminated soils and the sustainable management of waste-activated sludge. In the face of burgeoning environmental challenges, this research endeavors to provide a novel perspective for mitigating the ecological repercussions of emerging pollutants in terrestrial ecosystems, thus safeguarding the delicate balance of our planet's soils and their microbial inhabitants.

Introduction

1.Microbes in the Soil Environment

Soil microorganisms, encompassing bacteria, fungi, and protozoa, exhibit remarkable biodiversity, and a profound ecological significance. Their pivotal functions within terrestrial landscapes encompass organic matter degradation, nutrient cycling orchestration, and diverse pollutant transformations. Soil microorganisms intricately steer material cycles, forming the bedrock of soil fertility and steadfast developmental trajectories (Miransari, 2013). Currently acknowledged as a multitude exceeding billions per gram of soil, with species reaching into the millions, these microorganisms stand as a testament to the Earth's most intricate and diverse biological niche (Williamson et al., 2017). In this grand tapestry, soil stands as an arena of intense material exchange, an intersection where atmospheric, aquatic, geological, and biological realms harmoniously interact. This dynamic orchestration within the soil manifests through various biogeochemical processes, exerting far-reaching influences encompassing global climate modulation, sustenance of food supplies and security, soil reclamation and degradation mitigation (Hille, 2004). These processes thus wield a profound influence on the trajectory of human society's sustainable advancement (Liverman and Cuesta, 2008).

1.1 Soil Microbial Diversity and Function

Soil microbial diversity constitutes an intricate assemblage of microscopic life flourishing within terrestrial ecosystems (Van Elsas et al., 2012). This diversity encompasses a diverse range of taxa, spanning bacteria, fungi, archaea, protozoa, and viruses, collectively shaping the intricate mosaic of subterranean environments (Schmidt and Schaechter, 2011). At its essence, soil microbial diversity embodies a dynamic interplay of genetic, taxonomic, and functional variations intrinsic to these microorganisms (Tripathi et al., 2007). This intricate amalgamation operates synergistically, assuming pivotal roles in fundamental ecological processes such as nutrient cycling, organic matter decomposition, and pollutant biotransformation (Hou et al., 2023). The extensive expanse of soil microbial diversity underscores the intricate interplay among biotic, abiotic, and physicochemical drivers, culminating in a profusion of species, genotypic adaptations, and functional attributes. Ranging from the complex realm of bacteria to the enigmatic domain of fungi, these microorganisms collectively constitute an intangible yet indispensable *substratum* underpinning the vigor, fertility, and adaptability of terrestrial ecosystems (Zhu et al., 2022).

Concurrently, soil microbial function plays a central role in ecosystem dynamics, with organic matter degradation serving as a pivotal process orchestrated by an array of

microorganisms. Collaborative endeavors of bacteria, fungi, and actinomycetes meticulously drive the enzymatic disintegration of a wide range of organic compounds into simpler molecules, releasing essential nutrients and energy, and facilitating the recycling of organic materials crucial for plant growth and overall ecosystem productivity (Blagodatskaya et al., 2021). This intricate sequence starts with enzymatic hydrolysis, followed by microbial assimilation, with fungi notably contributing to the decomposition of recalcitrant compounds such as lignin. Beyond the nutrient cycling, organic matter degradation significantly influences soil structure, moisture retention, and carbon sequestration, ultimately culminating in humuic subtances formation and the enhancement of soil physical properties (Tunlid et al., 2022).

Moreover, soil microbial communities and the biogeochemical processes of soil organic matter are profoundly influenced by biological interactions, encompassing predation, mutualism, and competition (Buchkowski et al., 2017) **(Figure 1)**. The intricate interplay among microorganisms is significantly molded by factors such as mineral heterogeneity, which can impose physical separation, restrict mobility, and dampen hydrological connections (Erktan et al., 2020; Or et al., 2007). Notably, limited competition may be one of the main forces maintaining the incredibly high diversity evident from the presence of tens of thousands of taxa within a gram of soil (Roesch et al., 2007). However, it's worth noting that the density of microbial life in extensive mineral soils is relatively low, as discernible in thin soil sections where clusters of bacterial cells, numbering from tens to hundreds, are widely dispersed, particularly in voluminous soils and at greater soil depths (Raynaud and Nunan, 2014). On the other hand, microbial processes assume significance in bioremediation and in detoxification of pollutants. Factors encompassing pH, moisture, temperature, and substrate availability, alongside human-induced alterations such as land use and pollution, intricately govern bioremediation effects (Warnasuriya et al., 2023). A comprehensive understanding of these intricacies not only advances our knowledge of soil ecosystem function but also holds implications for sustainable agriculture, waste management, and environmental preservation.

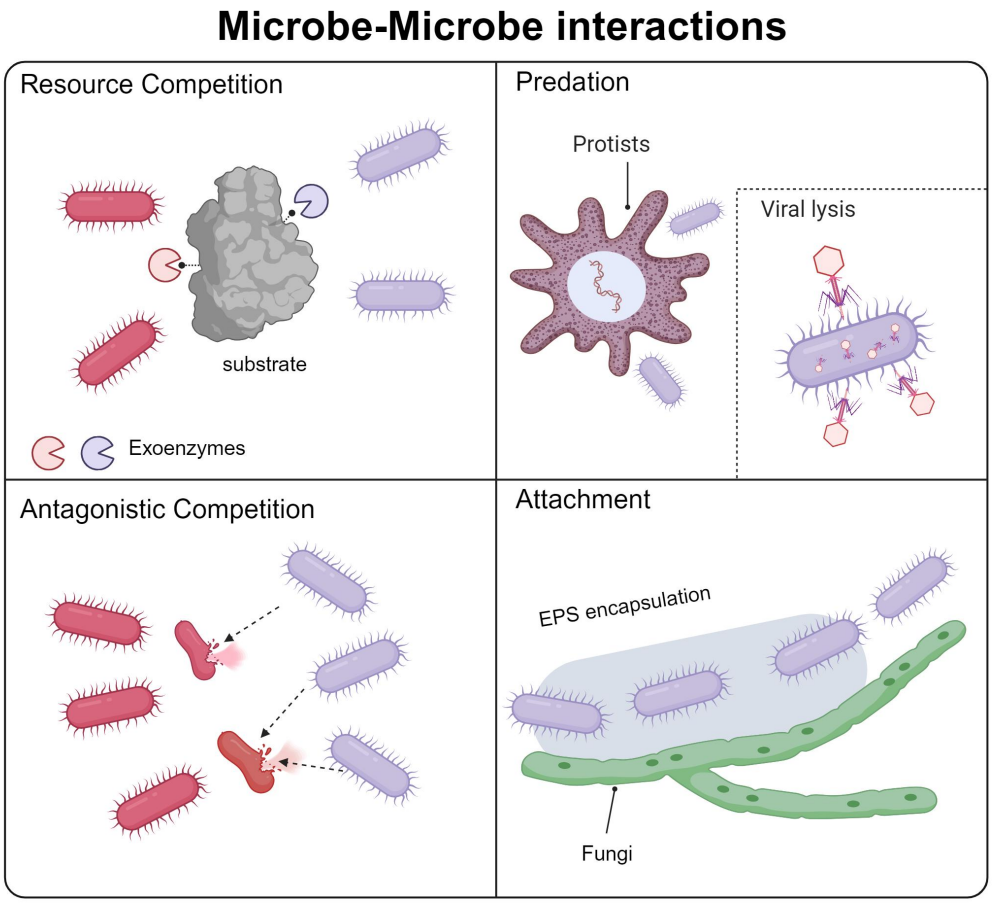

Figure 1. Several different types of interactions among soil microbes

1.2 Research Progress of the Soil Microbiome

Recent years have marked remarkable strides in soil microbial research, driven by the convergence of cutting-edge technologies and interdisciplinary collaboration. High-throughput sequencing techniques, coupled with advanced bioinformatics tools, have revolutionized our ability to unravel the intricate soil microbial diversity and functional dynamics (Jansson and Hofmockel, 2018). Metagenomics, metatranscriptomics, and metaproteomics have emerged as potent methodologies, unveiling insights into the genetic potential, metabolic activity, and complex functional interactions inherent in the soil microbiome (Jansson and Hofmockel, 2018). This holistic approach has unveiled the wide range of roles that specific microbial taxa play in pivotal processes such as nutrient cycling, carbon sequestration, and the modulation of disease dynamics (Hassa et al., 2018; Van Den Bossche et al., 2021).

In parallel, investigations have probed the responses of soil microbial communities to diverse environmental stimuli, ranging from climate fluctuations and land-use transformations to anthropogenic disturbances (Dubey et al., 2019; Philippot et al., 2021). Longitudinal studies and comprehensive surveys have unveiled discernible shifts in microbial composition and activity patterns in response to these influences,

accentuating their implications for ecosystem services and adaptability. This comprehensive approach, harmonizing omics data with soil physicochemical properties, has facilitated the identification of key drivers orchestrating microbial community dynamics across terrestrial biomes. Additionally, intricate trilateral interactions between plants, microbes, and the soil matrix have emerged as focal points. The mutualistic partnerships between mycorrhizal fungi and plants, the intricate dynamics within the rhizosphere microbiota, and the complex plant-microbe signaling pathways have been systematically elucidated (Berrios et al., 2023). These insights not only increased our ecological understanding but also offer strategic avenues for the development of sustainable agricultural practices, enhancing crop productivity while minimizing ecological footprints. Moreover, this trajectory has shifted towards pragmatic applications, with biotechnological interventions harnessing soil microorganisms for enhancing crop yields, disease control, and environmental detoxification gaining traction. The potential of microbial-based biofertilizers, biostimulants, and biopesticides is being explored to usher in a paradigm of ecologically sensitive and economically viable agricultural practices (Fadiji et al., 2022). In short, recent strides in soil microbial research have amplified our understanding of the cryptic subterranean microbiome and beckoned forth opportunities for translating these insights into sustainable land management, ecological restoration, and agro-technological innovation. The continual evolution of technology promises to unveil novel dimensions within the complex soil microbial communities, aligning with the demands of modern agriculture and environmental stewardship.

1.3 Untapped Black Box

The study of the soil microbiome still presents researchers with a complex and pivotal dilemma that stems from its inherent complexity and far-reaching implications. The intricate interplay of diverse microbial species, their intricate interactions, and the multitude of environmental variables influencing their behavior generate a formidable challenge in unraveling the full spectrum of soil microbial diversity and function (Guerra et al., 2021). This dilemma centers around the need to bridge the gap between the massive volume of available sequence data and our capacity to decipher the functional significance of individual microbial taxa and their collective contributions to soil processes (Widder et al., 2016). While advances in high-throughput sequencing technologies have provided unparalleled insights into profiling soil microbial communities, the translation of this wealth of information into actionable insights for sustainable land management and agricultural practices remains a formidable challenge (Lahlali et al., 2021). Striking a balance between elucidating the underlying mechanisms governing soil microbiome dynamics and harnessing this knowledge for

real-world applications necessitates innovative methodologies that integrate multi-omics data, ecological models, and sophisticated computational tools.

Despite these challenges, the future application potential of the soil microbiome is really promising. The burgeoning understanding of microbial diversity, interactions, and functions within the soil microbiome holds the transformative potential to reshape the landscape of sustainable agriculture. Unraveling the microbiome's pivotal role in nutrient cycling, disease suppression, and resilience to environmental stresses lays the groundwork for optimizing crop yields while minimizing dependence on synthetic inputs (Trivedi et al., 2021). Furthermore, the soil microbiome's potential extends to environmental restoration and bioremediation, where harnessing microbial communities can drive soil health restoration, pollution mitigation, and counteracting soil degradation (Coban et al., 2022).

Anticipating the future, the developmental trajectory of soil microbiome research navigates two pivotal dimensions. Firstly, unraveling the intricate functional networks and metabolic pathways within the soil microbiome demands innovative methodologies that synergize high-resolution 'omics' data with sophisticated bioinformatics and modeling approaches. This integration can allows us to dissect the complex interactions that govern soil ecosystem processes, illuminating the molecular basis of microbial functions. Secondly, translating these insights into pragmatic applications requires concerted efforts toward designing targeted microbial interventions, including precision microbiome engineering and formulation of customized microbial consortia. The successful integration of these interventions into agricultural practices necessitates robust field trials and an in-depth comprehension of microbial responses to varying environmental conditions.

In conclusion, the complexity of microbial interactions and the difficulty of translating knowledge into feasible bioaugmentation strategies still face some limitationsfor soil microbiome research. However, the vista of its future application potential is expansive, offering transformative opportunities in sustainable agriculture, ecosystem restoration, and environmental management. To navigate these challenges and seize these opportunities, the developmental trajectory of soil microbiome research entails unraveling functional intricacies, pioneering microbial interventions, and fostering a seamless bridge between foundational science and practical implementation.

2. Emerging Pollutants in Soil

Plastics possess intrinsic durability, rendering their complete degradation really challenging. Following a sequence of natural processes including weathering, solar

irradiation, and radiation, plastic generates small fragments below 5 mm defined as microplastics (MPs). This nomenclature, originally introduced by Thompson et al. (Thompson et al., 2004) in the context of plastic fragments in marine environments, has engendered research predominantly concentrated on aquatic systems. The exploration of MPs in terrestrial ecosystems, particularly soils, started later, with Rillig's seminal proposition in 2012 regarding the potential ecological repercussions of MPs in soil matrices (Rillig, 2012). Existing efforts in this domain have revolved around the identification and spatial dissemination of diverse MP typologies within soil matrices (Guo et al., 2020; Sun et al., 2022). Given the intimate link between soil matrices and agricultural productivity, the scrutiny of MPs in soil has emerged as a compelling research nexus.

2.1 Sources and Distribution of MPs in Soil

The source and distribution of MPs in soil is a complex phenomenon driven by the intricate interplay of anthropogenic activities, environmental processes, and inherent properties of MP particles. Primary sources involve the fragmentation of larger plastic items due to mechanical, chemical, and environmental forces. Secondary sources encompass the deliberate inclusion of MPs in personal care products, industrial abrasives, and other consumer goods (Golwala et al., 2021). These sources collectively release MPs into the environment, where they infiltrate soil matrices via atmospheric deposition, wastewater irrigation, and the application of plastic-based mulches in agriculture (Tian et al., 2022). Additionally, the breakdown of macroplastics within aquatic systems contributes to MP loads in soil via sediment transport and deposition (Rehm and Fiener, 2023).

The distribution of MPs within soil matrices exhibits spatial and vertical heterogeneity, shaped by factors such as land use, hydrological processes, and plastic characteristics. Urban and industrial areas tend to have higher MP concentrations due to higher human activity and plastic input (Rafique et al., 2020). Soil texture, structure, and organic matter content also influence MP distribution, with fine-textured soils having higher retention capacities for MPs compared to coarse-textured soils (Guo et al., 2022). Vertical distribution patterns reveal MPs' propensity to migrate through the soil profile, with studies reporting varying concentrations at different depths, including surface horizons, subsoils, and even groundwater (Huang et al., 2021; Li et al., 2021). This migration is influenced by factors like water movement, root activity, and soil compaction. MPs' association with soil aggregates and organic matter further contributes to their uneven dispersion (Hanun et al., 2021). Furthermore, within the context of farmland soils, the distribution and implications of MPs is particularly. The application of plastic-based mulches, commonly utilized in agricultural practices to

enhance crop yield and conserve moisture, introduces a notable pathway for MP entry into farmland ecosystems. These MPs, sourced from the degradation of plastic mulches or the deliberate incorporation of MPs in some agricultural products, intertwine with the very fabric of agricultural landscapes. Farmland soils serve as both repositories and conduits for these minute particles, which can interact with plant roots, soil biota, and soil organic matter. The intricate interplay between soil physicochemical characteristics, agricultural practices, and MP dynamics in farmland soils underscores the importance of investigating MP prevalence and consequences in these environments (Zhang et al., 2019).

In farmland contexts, the distribution of MPs exhibits complexities influenced by land management practices, irrigation methods, and the incorporation of plastic materials into soil amendments. As MPs pervade farmland soils, the potential for interaction with agricultural crops and their potential entry into the food chain is a critical concern (Pérez-Reverón et al., 2022). Understanding the intricate fate and potential impact of MPs in farmland soils is pivotal for ensuring the integrity of agricultural ecosystems, safeguarding food security, and fostering sustainable land management practices.

2.2 The Impacts of MPs on the Soil Ecological Environment

In response to weathering and exposure to natural agents like sunlight, plastic materials experience internal molecular bond disintegration, leading to the formation of MP particles. These plastics often incorporate chemical additives, such as plasticizers and dyes, which are released into the soil upon degradation, contributing to soil pollution. The MPs obtained after plasticizers addition exhibit hydrophobic attributes and increased surface area, making them potential vectors for the transport of hazardous substances in the environment. Over time, these particles undergo textural changes, developing rougher surfaces with heightened adsorption capabilities (Sutkar et al., 2023).

MPs' presence can induce shifts in soil properties, including pH and electrical conductivity, subsequently affecting their adsorption capacity and overall soil environment. Moreover, MPs influence soil attributes such as bulk density, aggregate size, and quantity, impacting soil porosity, aeration, and water retention capacity (Wang et al., 2022). Besides, MPs exert significant interactions with soil heavy metal elements, influencing their mobility and consequently shaping soil pollution dynamics. They immobilize certain heavy metal elements by decreasing their exchangeable fractions, but also enhance the bioavailability of elements like Cd, Pb, and Zn, aiding their translocation to wheat roots and subsequent desorption (Feng et al., 2022; Medyńska-Juraszek and Jadhav, 2022). Furthermore, MPs demonstrate a propensity to

adsorb soil organic pollutants, with particle size acting as a crucial determinant. For instance, polyethylene MPs in the nanometer range (70 nm) exhibit notably higher adsorption capacities for persistent organic pollutants like polychlorinated biphenyls compared to MPs in the micron range (10-180 μm) (Zhu et al., 2019). However, the adsorption potential varies among MP types, and some may even facilitate the migration of specific organic pollutants (Martín et al., 2022). MPs can also adsorb antibiotics, influencing their degradation rates and transport behaviors. For instance, polyethylene, polyamide, and polystyrene MPs exhibit diverse affinities for tetracycline (Yu et al., 2020). Given the intricacies of soil environments and MP diversity, comprehensive research is needed to understand the complex interactions involved in composite pollution comprising MPs and hazardous substances in soils.

The influence of MPs on soil is also strictly connected to soil attributes such as texture, physicochemical traits, and intrinsic conditions, resulting in variable impacts on soil enzyme activities. Notably affecting nutrient cycling, particularly carbon and nitrogen dynamics, MPs modulate crucial enzyme activities, subsequently impacting nutrient availability and, consequently, crop growth and productivity (Hou et al., 2021). The interaction between MPs and soil microorganisms unfolds in two key dimensions: MPs serve as carriers, fostering microorganism movement and biofilm formation, augmenting enzyme activity and nutrient migration (Ding et al., 2023). Simultaneously, the degradation of plastic releases harmful compounds, contaminating the soil, and leading to disruptions in microbial equilibrium, observable in instances like heightened di-n-butyl phthalate concentrations linked to reduced diversity (Wang et al., 2016). Although some studies have reported soil community changes caused by MPs, the precise relationship between MPs and soil microbial ecology needs further clarification (Zhou et al., 2021). Understanding these complex MP-soil-microbe interactions is crucial for different environments and could help reveal potential environmentally friendly methods for MP degradation.

2.3 The Dilemma of Identification and Removal of MPs in Soil

The challenge of microplastic contamination in soil has prompted a rigorous exploration of two key facets: the accurate identification of these minute plastic particles and the subsequent development of effective removal strategies. Accurately detecting and quantifying microplastics within complex soil compositions presents a formidable obstacle. The intricate amalgamation of organic matter, minerals, and biological entities in soils can obscure microplastics, impeding their successful extraction (Radford et al., 2021). An array of analytical techniques, ranging from spectroscopy and microscopy to chemical analyses, have been employed to distinguish microplastics from their surroundings (Huang et al., 2023). However, the

specific characteristics and limitations of each method must be carefully considered, and the differentiation between anthropogenic microplastics and naturally occurring particles with similar dimensions further compounds the challenge.

The development of effective strategies for removing microplastics from soil also necessitates consideration of the potential impact on soil structure and ecology. The minute size and widespread distribution of microplastics can render conventional soil remediation methods inadequate (Enfrin et al., 2021). Techniques such as sieving, flotation, and magnetic separation, while promising, encounter obstacles related to efficiency, selectivity, and potential soil disturbance (Enfrin et al., 2021; Pathan et al., 2020). Another dimension of this issue pertains to the potential role of microorganisms in removing microplastics from identified soil matrices. Microorganisms possess a remarkable capacity to interact with and modify their environment. Some studies have proposed the potential of microorganisms to facilitate the breakdown of microplastics through processes such as enzymatic degradation or biofilm formation (Anand et al., 2023). These microbial interactions hold promise for enhancing the removal of microplastics from soil, although the effectiveness and scalability of such processes require further investigation. Furthermore, any strategies involving microorganisms must account for their interactions with native soil microbial communities and the potential unintended consequences on soil health and nutrient cycling.

Addressing the intricate dilemma of microplastic identification and removal necessitates a collaborative and interdisciplinary approach. Environmental scientists, materials experts, soil specialists, and microbiologists must collaborate to develop standardized methodologies for detecting, quantifying, and effectively removing microplastics from soil. Furthermore, advocating for sustainable waste management practices and minimizing plastic waste release into the environment remains pivotal in mitigating the overall burden of microplastics in soil ecosystems (Sarkar et al., 2022).

3. Interaction between New Materials and Soil Microorganisms

3.1 Eco-Friendly Remediation Materials

Soil pollution remediation has attracted the attention in the past few years due to its significant ecological and human health implications. Rapid industrialization and urbanization have led to the widespread introduction of contaminants into soil environments, imperiling soil fertility, ecosystem health, and food safety (Carré et al., 2017). To address these challenges, innovative soil remediation strategies have emerged, among which biochar-based approaches seem very promising (Issaka et al., 2022).

Biochar, a carbon-rich material produced through the pyrolysis of organic matter, seems very interesting for soil pollution remediation due to its unique physicochemical properties (Mazarji et al., 2021). The high surface area, porous structure, and substantial ion exchange capacity of biochar render it adept at adsorbing and immobilizing a diverse array of pollutants (Qiu et al., 2022). This encompasses heavy metals like lead, cadmium, and copper, as well as organic compounds including pesticides, hydrocarbons, and pharmaceutical residues (Choudhary et al., 2020; Sohi et al., 2010). The application progress of biochar in recent years has witnessed the development of various biochar types derived from different feedstocks and processed under varying conditions, tailoring their adsorptive capacities to specific contaminants (He et al., 2022). Beyond its adsorptive capabilities, biochar's impact extends to modifying soil properties, enhancing water retention, improving nutrient availability, and fostering microbial activity (Lytand et al., 2023). The biochar-soil interaction is also intricately linked to the soil microbiome, with biochar stimulating microbial growth and altering community composition (Zheng et al., 2022). Furthermore, the intricate interplay between biochar and soil microbiota significantly contributes to the transformation and degradation of pollutants, highlighting its holistic remediation potential (Tan et al., 2022). This microbiome-mediated degradation has a strong potential for addressing recalcitrant pollutants and advancing our understanding of the intricate processes within soil environments. However, the success of biochar as a soil remediation material is based on various factors such as feedstock selection, pyrolysis conditions, and application strategies (Morgan et al., 2020). Despite its promise, challenges remain, including optimizing biochar production methods, tailoring its properties to specific contaminants, and assessing its long-term environmental impact.

3.2 Interactions between Biochar and Soil Microbes

The intricate interplay between biochar and soil microbial communities has garnered significant attention in soil science and environmental research. The diverse and evolving body of scientific literature underscores the complexity of the biochar-soil microbial interaction and its profound implications for soil functioning and ecosystem health (Yu et al., 2018). Studies have demonstrated that biochar amendments can induce shifts in soil microbial community composition, diversity, and functional attributes (Han et al., 2022; Xu et al., 2014). These alterations in microbial populations can further cascade into changes in nutrient cycling dynamics, organic matter decomposition rates, and the breakdown of recalcitrant compounds (Mukherjee et al., 2022). Moreover, the introduction of biochar into soil systems can influence microbial activity by providing a substrate for microbial growth and colonization (Jin, 2010). Simultaneously, biochar's physicochemical properties, such as its high cation

exchange capacity and capacity to sorb organic molecules, contribute to alterations in nutrient availability and the sequestration of contaminants (Ennis et al., 2012; Quilliam et al., 2013).

When combined with microbial agents, such as beneficial bacteria or fungi, the synergistic interaction between biochar and microorganisms can further amplify their individual benefits, resulting in a more robust and efficient strategy for addressing various soil and environmental challenges. Case studies showcasing the biochar-microbial agent interaction underscore its potential across various applications. For instance, in the context of plant growth promotion, the incorporation of biochar combined with plant growth-promoting rhizobacteria has exhibited enhanced nutrient availability, root development, and overall plant vigor (Hafez et al., 2019; Nafees et al., 2022). In agricultural systems, biochar-microbial agent have shown promise in suppressing soil-borne pathogens and enhancing soil health (Kong et al., 2021; Ye et al., 2020). The amalgamation of biochar and microbial agents presents a multifaceted strategy with transformative potential in diverse applications, ranging from soil fertility to the improvement of pollution remediation. While the biochar-microbial interaction has a great potential in bioremediation, comprehensive research efforts are required to elucidate the complex mechanisms governing this synergy, ensuring optimal design and implementation for sustainable soil management and environmental rehabilitation.

As research progresses, investigations are focusing on elucidating the intricate mechanisms underlying the biochar-microbial interaction. This encompasses understanding how biochar's surface properties affect microbial attachment and colonization, the role of biochar in modulating microbial enzymatic activities, and the potential for biochar to foster specific microbial guilds. Additionally, innovative techniques such as stable isotope probing are shedding light on the trophic interactions between soil microbes and biochar-derived carbon, providing insights into carbon flow within the soil microbial food web (Radajewski et al., 2000). As researchers delve deeper into this intricate interplay, a more comprehensive understanding of the mechanisms underlying the biochar-soil microbial interaction will undoubtedly contribute to the optimization of biochar-based strategies for soil management and environmental remediation.

3.3 Prospects and Challenges of Synergistic Remediation

The synergistic remediation of soil organic pollution through the combined use of biochar and microorganisms is based on the complementary attributes of these components. Biochar, characterized by its intricate pore structure and functional groups, offers a favorable microenvironment for microbial colonization and pollutant

degradation. The presence of diverse functional groups, such as phenolic and quinone moieties, on the biochar surface enables electron transfer processes, fostering redox reactions and facilitating the degradation of organic pollutants (Xu et al., 2019; Yuan et al., 2017). Additionally, biochar's surface acts as a platform for electron exchange with microorganisms, supporting redox reactions that contribute to pollutant transformation (Zheng et al., 2022). This intricate interplay between biochar and microorganisms can enhance the overall efficiency of remediation processes by connecting physical and biological mechanisms.

However, the prospects and challenges of this approach warrant careful consideration. Thedesign of biochar to optimize its interaction with microorganisms is a key challenge. Tailoring biochar's properties, including pore structure and surface functional groups, can facilitate microbial colonization and enhance degradation efficiency (Mukherjee et al., 2022). Further, ensuring the compatibility of selected microorganisms with target pollutants is paramount for an effective degradation process. It is crucial to maintain optimal environmental conditions that sustain microbial growth and activity in the presence of biochar. Moreover, understanding the fate of intermediate products generated during biodegradation is essential to mitigate secondary contamination risks.

The remediation potential of the biochar-microorganism synergy is substantial. The adaptable nature of this approach to different soil types and contamination scenarios proposes it as a versatile remediation strategy. The sustained effects of biochar in the soil matrix could lead to prolonged pollutant removal (Ogbonnaya and Semple, 2013). Yet, there are challenges to address, including the need to identify the mechanisms governing biochar's interaction with microorganisms and pollutants at a molecular level. Moreover, elucidating the precise role of biochar in electron transfer processes and redox reactions remains an area of ongoing research (Joseph et al., 2021; Joseph et al., 2015). Additionally, acquiring a deeper understanding of the dynamics of the microbial community within the biochar-microorganism interface could provide valuable insights into the complexities of these interactions (Lin et al., 2023).

4. Application of omics technology in the study of soil ecology

4.1 Development of Sequencing Technology and Genomics

The development of sequencing technology and genomics resultedin a paradigm shift in the understanding of life's fundamental processes and in the exploration of genetic diversity. The origins of this transformative journey can be traced to the pioneering work of Sanger, who introduced the first DNA sequencing method in the late 1970s using chain-terminating nucleotides (Sanger et al., 1977). The landmark sequencing

of the human genome, completed in 2003 through the Human Genome Project, marked a watershed moment, exemplifying the potential of genomics in revolutionizing our understanding of human biology (RUSSO, 2001).

The advent of next-generation sequencing (NGS) technologies in the early 2000s further accelerated genomics research. Platforms such as Illumina and Roche 454 allowed for high-throughput sequencing, enabling the parallel analysis of millions of DNA fragments (Metzker, 2010). This advancement drastically reduced sequencing costs and time, democratizing genomics and enabling large-scale genome sequencing projects across various organisms. Continuing the trajectory of innovation, third-generation sequencing technologies emerged, providing long-read sequencing capabilities that transcend the limitations of short-read NGS. Pacific Biosciences (PacBio) and Oxford Nanopore Technologies introduced single-molecule real-time (SMRT) sequencing and nanopore sequencing, respectively. These technologies offer longer reads, enabling the assembly of complex genomes, the phasing of alleles, and the detection of structural variants with unprecedented accuracy (Goodwin et al., 2015; Rhoads and Au, 2015). The synergy between sequencing technology and genomics has catalyzed breakthroughs across various domains. Comparative genomics has unveiled evolutionary relationships and functional conservation among species. Functional genomics has elucidated the roles of genes and regulatory elements through transcriptomics and epigenomics. Metagenomics has illuminated microbial diversity and interactions within ecosystems. Harnessing genomics has revolutionized environmental science research, enabling in-depth exploration of microbial communities, their functional potential, and their responses to diverse environmental conditions (Dick, 2018).

As genomics continues to evolve, challenges and opportunities arise. The huge amounth of sequencing data demands advanced computational tools and bioinformatics expertise for data analysis and interpretation. Furthermore, the integration of genomics with other omics disciplines, such as proteomics and metabolomics, promises a holistic understanding of biological systems.

4.2 Progress in the Application of Metagenomics to Soil Microorganisms

The application of metagenomics to soil microorganisms has propelled our understanding of the intricate and diverse microbial communities that reside in soil ecosystems (Daniel, 2005). Metagenomics, a potent tool in environmental microbiology, involves the direct sequencing of DNA extracted from environmental samples, obviating the need for microbial cultivation (Tringe and Rubin, 2005). This approach has empowered researchers to delve into the genetic makeup of entire microbial communities, unveiling insights into their functional potential and

ecological roles within soils. By scrutinizing the collective genetic material, or metagenome, researchers can identify functional genes linked to diverse metabolic pathways, enzymatic activities, and interactions that shape soil health and productivity.

Shotgun metagenomic sequencing, a core component of metagenomics, facilitates the reconstruction of genomes from individual microbes within complex soil samples. This capability not only aids in the discovery of novel species but also provides insights into their potential functions (Jansson and Hofmockel, 2018). For instance, the identification of genes implicated in the degradation of complex organic compounds, such as lignocellulose, underscores the pivotal role of soil microbes in carbon cycling and nutrient release (Leis et al., 2013). Moreover, metagenomics unveils insights into microbial interactions and community dynamics. Analyzing co-occurrence patterns and functional correlations among genes and taxa unravels intricate networks underlying the resilience and response of soil microbial communities to environmental variations (Barberán et al., 2012). This knowledge is crucial for predicting how soil ecosystems might respond to disturbances such as changes in land use, climate variations, or pollution events.

However, the application of metagenomics in soil research is not without its challenges. The complexity of soil microbial communities presents computational and analytical hurdles in managing and interpreting extensive sequencing data (Franzosa et al., 2015). Additionally, the scarcity of comprehensive reference databases for soil microbes can hinder accurate taxonomic and functional assignments (Kim et al., 2013). Nevertheless, ongoing advancements in bioinformatics and data sharing are progressively enhancing our capacity to address these challenges.

In summary, metagenomics has determined in a paradigm shift in our understanding of soil microbial communities and their roles in ecosystem functioning. By uncovering the genetic potential of non-cultivable microorganisms and deciphering their interactions, metagenomics provides crucial insights into the enigmatic world beneath our feet. This has profound implications for sustainable agriculture, environmental stewardship, and our broader comprehension of microbial ecology.

4.3 Synergistic Insights from the Integration of Metagenomics and Organic Analysis

The strategic integration of metagenomics and organic matter analysis emerges as a transformative approach to address challenges in soil microbial ecology. Metagenomics serves as a genetic blueprint, detailing the functional potentials within complex microbial communities. For instance, by delineating genes and pathways

associated with complex phenomena such as lignocellulose degradation or nitrogen fixation, researchers are endowed with unparalleled insights into the multifaceted capabilities of soil microorganisms (Kalntremtziou et al., 2023; Pang et al., 2023). An exemplary demonstrationlies in the discovery of microbial enzymes endowed with novel functions, catalyzing the breakdown of recalcitrant compounds, thereby potentially inspiring novel biotechnological applications (Chow et al., 2023).

Concurrently, cobining metagenomics with organic matter analysis provides contextual insights into the intricate functions of microbial activities. Soil organic matter, a very relevant energy source and repository of nutrients, assumes the role of a complex substrate profoundly influencing microbial community composition and functionality. Advanced methodologies such as pyrolysis-gas chromatography/mass spectrometry (Py-GC/MS) enables dissecting the chemical composition of organic matter, unraveling its transformation dynamics (Fuentes et al., 2010). An illustrative instance emerges through Py-GC/MS analysis of soil organic matter, which has unveiled invaluable intelligence concerning the recalcitrant nature of soil carbon in response to shifts in land-use practices (De la Rosa et al., 2018). In addition, the integration of three-dimensional fluorescence spectroscopy further enriches our understanding of organic matter dynamics within soil ecosystems. This advanced technique employs the fluorescence properties of organic molecules to elucidate their composition and interactions in complex matrices. Three-dimensional fluorescence spectroscopy allows researchers to discern the distinct fluorescent signatures associated with different types of organic compounds, shedding light on the diverse biochemical processes occurring within the soil matrix (Li and Hur, 2017). By characterizing the fluorescence spectra emitted by dissolved organic matter, this technique can provide insights into the origins, transformations, and microbial interactions of organic compounds in soil.

The synergistic application of metagenomics and organic matter analysis transcends disciplinary boundaries, addressing fundamental ecological inquiries. Researchers managed to use this integrated toolkit to decipher the intricate mechanisms underpinning the microbial degradation of intricate plant polymers, exemplified by lignocellulose (Zheng et al., 2021). Moreover, this concerted integration facilitates a comprehensive exploration of the intricate interplay between microbial diversity, functional potential, and organic matter transformations, offering an encompassing perspective on ecosystem functioning. In short, by joiningmetagenomics and organic matter analysis furnishes researchers can have a unique vantage point to unravel the intricate tapestry binding soil microorganisms to their dynamic environments. These interdisciplinary insights not only enrich our understanding of soil microbial ecology, but can also boost sustainable agriculture, efficacious ecosystem management, and

innovative environmental conservation strategies.

4.4 Integrating Genomic Technologies Applied to Biochar-Remediated Soils

In order to clarify the intricate interplay between biochar and MPs pollution and their ramifications for soil ecology, a holistic approach merging metagenomics with organic phase analysis is indispensable. This integrative paradigm constitutes a robust instrument for elucidating the dynamics underpinning the synergistic interrelationship amongst microorganisms, pollutants, and remediation materials **(Figure 2)**.

The pivotal role of organic analysis comes to the fore within this integrated framework, particularly concerning the identification of distinctive metabolites concomitant with MPs within the soil matrix. The identification of these metabolites becomes essential to clarify the transformation pathways orchestrated by microbial agents in response to the presence of remediation materials, thereby explicating potential chemical and biochemical processes.

A significant advancement enhancing the integrated model stems from the integration of second-generation and third-generation sequencing hybrid assembly. This hybrid approach harnesses the strengths of both technologies, offering enhanced accuracy, longer read lengths, and improved genome continuity (Jayakumar and Sakakibara, 2019), thus furnishing researchers with a more comprehensive and accurate representation of microbial genomes and their metabolic potential. This refinement in sequencing methodologies strengthens our capacity to decipher the intricate complexities of microbial pollutant degradation and provides a robust foundation for designing effective remediation strategies.

A cornerstone of our integrated model resides in the binning process, which substantiates the identification of pivotal microbial species involved in pollutant degradation and remediation. Through taxonomic categorization of metagenomic sequences, this technique unveils the taxonomically diverse microorganisms wielding pivotal roles in pollutant biotransformation. This enhanced resolution confers the capacity to characterize their prevalence and distribution, thereby providing insights into their ecological significance within contaminated ecosystems (Alneberg et al., 2014).

Metabolic reconstruction allows the predictive identification of potential degradation pathways. By harnessing metagenomic data, a comprehensive identification of the functional gene reservoirs ensconced within designated key microbial species is garnered. This reconstruction augments invaluable insights into the genomic framework governing pollutant degradation, endowing us with the means to delineate

intricate enzymatic cascades and biochemical reactions that underscore pollutant abatement (Frioux et al., 2020).

Significantly, our comprehensive approach further accentuates the pervasiveness of taxa function, as illuminated through the prism of comparative genomics. The exploration of homologous gene content across divergent taxa allows to identify shared functional repertoires that transcend taxonomic delineations. This expanded functional knowledge amplifies our apprehension of the molecular mechanisms orchestrating pollutant degradation, thereby accentuating the convergent evolutionary trajectory of metabolic attributes across microbial lineages (Tettelin et al., 2008).

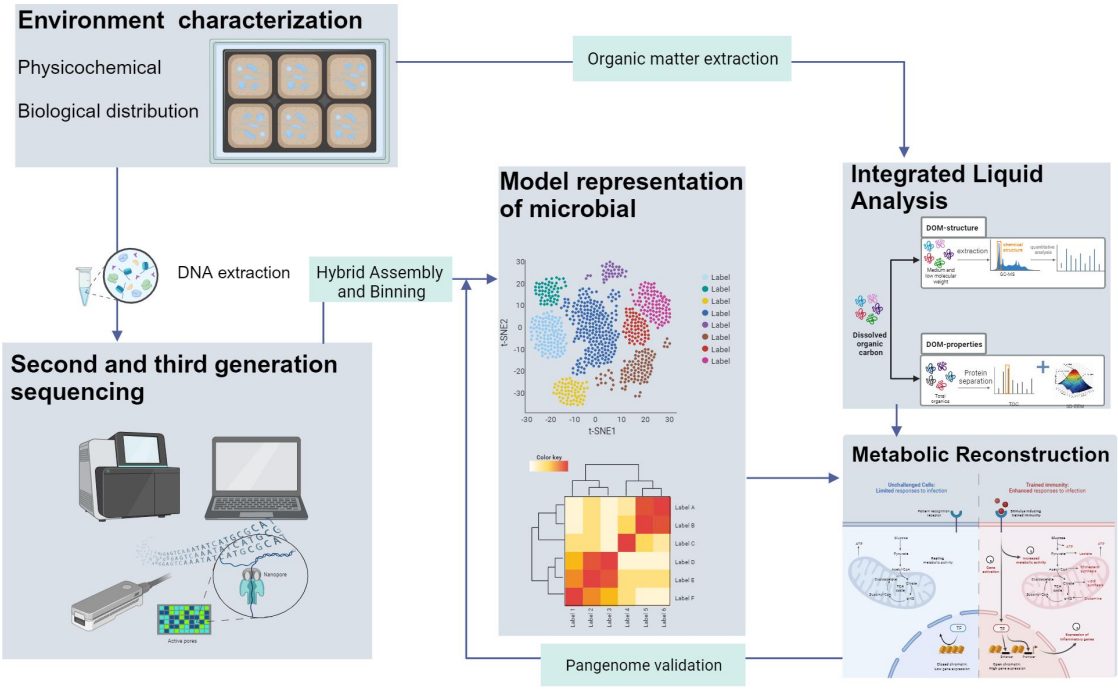

Figure 2. A framework for genome-centric work integrating organic analysis

To resume, the amalgamation of metagenomics and organic phase analysis constitutes a synergistic framework to explore the multi-dimensional interactions betwixt remediation materials, microorganisms, and pollutants within soil ecosystems. This pioneering methodology not only affords elucidation of the identity and functionality of microbial cohorts but also imparts insights into the intricate interplay of chemical and biochemical dynamics steering pollutant attenuation. Thus, it bestows a comprehensive vista upon the adaptive strategies invoked by microorganisms in response to contemporary environmental challenges.

5. Overview on the Selected Manuscripts and Conclusions

For the current PhD thesis, I selected five publications which can shed light on this three years project and evidence the novelty brought from this thesis to the scientific

community. This integrated genomic framework is mainly applied to microplastic-contaminated soils, and we propose potential remediation strategies and simultaneously examine the impact on soil ecology. In addition, this framework was also applied to anaerobic sludge systems to identify microbial mechanisms that can cooperate with nanomaterials in this kind of environment.

PaperI is a review exploring biochar's versatile potential sourced from diverse biomass for remediating diverse soil pollution forms. While prior studies examined singular biochar applications, the evolving understanding of different biochar types necessitates a consolidated overview to customize properties for specific pollution scenarios. This manuscript covers four significant pollution aspects: organic pollution, heavy metal contamination, greenhouse gas reduction, and soil microbial modulation. Biochar's efficacy hinges on source materials; woody biomass biochar, rich in lignin, differs from nutrient-rich waste biochar like animal manure and sludge. These distinctions influence soil remediation outcomes. The review then provides feedstock recommendations, favoring woody and crop residue biochars for organic adsorption, and waste-derived biochars for heavy metal pollution, with stability considerations. It highlights woody biomass biochar's superior greenhouse gas reduction and its appeal to gram-negative bacteria, while soil enzyme activity relates to nutrient content, e.g., phosphorus, potassium, and magnesium.

Based on the previous reports in the literature explored in *PaperI*, *PaperII* and *PaperIII* proposed to prepare magnetic biochar with redox activity to assist in-situ degradation of MPs and their additives. *Paper II* delves into the collaborative dynamics between magnetic biochar and soil microbes in addressing microplastic-contaminated soil. By working together, they significantly enhance the levels of dissolved organic matter within the soil. The research uncovers the pivotal roles of *Nocardioides* and *Rhizobium* species in driving essential steps of long-chain alkane utilization and alkane dehalogenation. These species form partnerships with benzoate-metabolizing organisms, particularly enriched in treatments involving magnetic biochar. *PaperIII* successfully demonstrates the potential of a hybrid approach involving MBC and field microorganisms, specifically *Pseudomonas nitroreducens* sp. upd006, which can uptake Fe(II) and Fe(III), to mineralize the DP plasticizer. Notably, *Pigmentiphaga* sp. upd102 exhibited the capacity to metabolize plasticizers in contaminated soil. A pangenome analysis indicates a shared plasticizer mineralization trait among *Pigmentiphaga* genus members. Importantly, the absence of pathogenic virulence factors in the identified plasticizer-degrading or MBC-cooperating species positions them as promising options for plasticizer removal from both surface water and agricultural soils. Leveraging a hybrid Illumina-Nanopore metagenomic approach, the work effectively dissects the intricate

intricacies of the soil microbiome and its responses to MPs and additives degradation. This work not only unravels the complexity of these processes but also offers insights for the formulation of on-site strategies aimed at remediating soil microplastic pollution.

PaperIV simultaneously investigated the effects of different types and doses of thermoplastic microplastics (MPs) on soil dynamics, focusing on dissolved organic carbon (DOC), microbial communities, and metabolic pathways. Notably, the type of MPs exerts a significant influence on soil bacterial communities, with polyvinyl chloride (PVC) MPs standing out as the major contributor to methane emissions. All three MP types lead to humic substance accumulation, while PVC MPs yield the most diverse DOC composition. Particularly, polyethylene (PE) MPs show a stronger impact on bacterial communities than PVC and polypropylene (PP) MPs on day 30, attributed to distinct plastic structures. The study highlights that MP type holds more sway than dose. Enrichment of competitive species and *Rice Cluster I* in respective PE, PP, and PVC groups accounts for methane emission discrepancies. The analysis also evidenced that elevated quinone reductase levels in PE and PVC groups enhance the oxidative phosphorylation pathway, suggesting the existance of an anaerobic methane oxidation process involving humic acid as an electron acceptor.

PaperV applied this integrated genomic technology to the sludge system. This manuscript offers a comprehensive understanding of the dosage-dependent impact of CuO nanoparticles on anaerobic fermentation of waste-activated sludge for medium-chain carboxylates (MCCs) production. The analysis reveals that MCCs generation is hindered by CuO NPs concentrations surpassing 10 mg/g-TS, with reactive oxygen species stemming from anaerobic conversion systems identified as the main contributor to this inhibition. However, notably, this study unveils that environmentally relevant CuO NPs concentrations below 2.5 mg/g-TS can efficiently promote both short-chain carboxylates and MCCs production. By amalgamating metaproteomic analyses with chemical and molecular approaches, the underlying mechanism is suggested to encompass amplified WAS solubilization, increased electron transfer activities, elevated abundances of crucial microorganisms, and elevated expression levels of pivotal enzymes linked to hydrolysis and acetogenesis processes.

As a concluding observation, it can be said that the five different studies reported in the current study systematically revealed interactions between emerging pollutants and microorganisms in the environment, which highlighted how microbial functions and metabolites respond to these pollutants. The identification of interactions between functional guilds and the reconstruction of metabolic pathways were validated by

shotgun-based metagenomic analysis and metabolome analysis. The results reported in this paper collection serve this goal and highlight the distinct but crucial roles of micro-nanoparticles in two anaerobic systems (flooded soil and sludge).

Cited literature

Alneberg J, Bjarnason BS, De Bruijn I, Schirmer M, Quick J, Ijaz UZ, et al. Binning metagenomic contigs by coverage and composition. Nature methods 2014; 11: 1144-1146.

Anand U, Dey S, Bontempi E, Ducoli S, Vethaak AD, Dey A, et al. Biotechnological methods to remove microplastics: a review. Environmental Chemistry Letters 2023: 1-24.

Barberán A, Bates ST, Casamayor EO, Fierer N. Using network analysis to explore co-occurrence patterns in soil microbial communities. The ISME journal 2012; 6: 343-351.

Berrios L, Yeam J, Holm L, Robinson W, Pellitier PT, Chin ML, et al. Positive interactions between mycorrhizal fungi and bacteria are widespread and benefit plant growth. Current Biology 2023.

Blagodatskaya E, Tarkka M, Knief C, Koller R, Peth S, Schmidt V, et al. Bridging microbial functional traits with localized process rates at soil interfaces. Frontiers in microbiology 2021; 12: 625697.

Buchkowski RW, Bradford MA, Grandy AS, Schmitz OJ, Wieder WR. Applying population and community ecology theory to advance understanding of belowground biogeochemistry. Ecology letters 2017; 20: 231-245.

Carré F, Caudeville J, Bonnard R, Bert V, Boucard P, Ramel M. Soil contamination and human health: a major challenge for global soil security. Global soil security 2017: 275-295.

Choudhary M, Kumar R, Neogi S. Activated biochar derived from Opuntia ficus-indica for the efficient adsorption of malachite green dye, Cu+ 2 and Ni+ 2 from water. Journal of Hazardous Materials 2020; 392: 122441.

Chow J, Perez-Garcia P, Dierkes R, Streit WR. Microbial enzymes will offer limited solutions to the global plastic pollution crisis. Microbial Biotechnology 2023; 16: 195-217.

Coban O, De Deyn GB, van der Ploeg M. Soil microbiota as game-changers in restoration of degraded lands. Science 2022; 375: abe0725.

Daniel R. The metagenomics of soil. Nature reviews microbiology 2005; 3: 470-478.

De la Rosa JM, Merino A, Jiménez Morillo N, Jiménez-González MA, González-Pérez JA, González-Vila FJ, et al. Unveiling the effects of fire on soil organic matter by spectroscopic and thermal degradation methods. Fire Effects in Soil Properties. Current Knowledge and Methods Used 2018: 281-307.

Dick G. Genomic approaches in earth and environmental sciences: John Wiley & Sons, 2018.

Ding R, Ouyang Z, Zhang X, Dong Y, Guo X, Zhu L. Biofilm-Colonized versus Virgin Black Microplastics to Accelerate the Photodegradation of Tetracycline in Aquatic Environments: Analysis of Underneath Mechanisms. Environmental Science & Technology 2023; 57: 5714-5725.

Dubey A, Malla MA, Khan F, Chowdhary K, Yadav S, Kumar A, et al. Soil microbiome: a key player for conservation of soil health under changing climate. Biodiversity and Conservation 2019; 28: 2405-2429.

Enfrin M, Hachemi C, Hodgson PD, Jegatheesan V, Vrouwenvelder J, Callahan DL, et al. Nano/micro plastics–Challenges on quantification and remediation: A review. Journal of Water Process Engineering 2021; 42: 102128.

Ennis CJ, Evans AG, Islam M, Ralebitso-Senior TK, Senior E. Biochar: carbon sequestration, land remediation, and impacts on soil microbiology. Critical Reviews in Environmental Science

and Technology 2012; 42: 2311-2364.

Erktan A, Or D, Scheu S. The physical structure of soil: determinant and consequence of trophic interactions. Soil Biology and Biochemistry 2020; 148: 107876.

Fadiji AE, Babalola OO, Santoyo G, Perazzolli M. The potential role of microbial biostimulants in the amelioration of climate change-associated abiotic stresses on crops. Frontiers in Microbiology 2022; 12: 829099.

Feng X, Wang Q, Sun Y, Zhang S, Wang F. Microplastics change soil properties, heavy metal availability and bacterial community in a Pb-Zn-contaminated soil. Journal of hazardous materials 2022; 424: 127364.

Franzosa EA, Hsu T, Sirota-Madi A, Shafquat A, Abu-Ali G, Morgan XC, et al. Sequencing and beyond: integrating molecular'omics' for microbial community profiling. Nature Reviews Microbiology 2015; 13: 360-372.

Frioux C, Singh D, Korcsmaros T, Hildebrand F. From bag-of-genes to bag-of-genomes: metabolic modelling of communities in the era of metagenome-assembled genomes. Computational and Structural Biotechnology Journal 2020; 18: 1722-1734.

Fuentes M, Baigorri R, González-Vila FJ, González-Gaitano G, García-Mina JM. Pyrolysis–gas chromatography/mass spectrometry identification of distinctive structures providing humic character to organic materials. Journal of environmental quality 2010; 39: 1486-1497.

Golwala H, Zhang X, Iskander SM, Smith AL. Solid waste: An overlooked source of microplastics to the environment. Science of the Total Environment 2021; 769: 144581.

Goodwin S, Gurtowski J, Ethe-Sayers S, Deshpande P, Schatz MC, McCombie WR. Oxford Nanopore sequencing, hybrid error correction, and de novo assembly of a eukaryotic genome. Genome research 2015; 25: 1750-1756.

Guerra CA, Delgado-Baquerizo M, Duarte E, Marigliano O, Görgen C, Maestre FT, et al. Global projections of the soil microbiome in the Anthropocene. Global Ecology and Biogeography 2021; 30: 987-999.

Guo J-J, Huang X-P, Xiang L, Wang Y-Z, Li Y-W, Li H, et al. Source, migration and toxicology of microplastics in soil. Environment international 2020; 137: 105263.

Guo Z, Li P, Yang X, Wang Z, Lu B, Chen W, et al. Soil texture is an important factor determining how microplastics affect soil hydraulic characteristics. Environment International 2022; 165: 107293.

Hafez EM, Alsohim AS, Farig M, Omara AE-D, Rashwan E, Kamara MM. Synergistic effect of biochar and plant growth promoting rhizobacteria on alleviation of water deficit in rice plants under salt-affected soil. Agronomy 2019; 9: 847.

Han Z, Xu P, Li Z, Lin H, Zhu C, Wang J, et al. Microbial diversity and the abundance of keystone species drive the response of soil multifunctionality to organic substitution and biochar amendment in a tea plantation. GCB Bioenergy 2022; 14: 481-495.

Hanun JN, Hassan F, Jiang J-J. Occurrence, fate, and sorption behavior of contaminants of emerging concern to microplastics: Influence of the weathering/aging process. Journal of Environmental Chemical Engineering 2021; 9: 106290.

Hassa J, Maus I, Off S, Pühler A, Scherer P, Klocke M, et al. Metagenome, metatranscriptome, and metaproteome approaches unraveled compositions and functional relationships of microbial communities residing in biogas plants. Applied microbiology and biotechnology 2018; 102: 5045-5063.

He M, Xu Z, Hou D, Gao B, Cao X, Ok YS, et al. Waste-derived biochar for water pollution control and sustainable development. Nature Reviews Earth & Environment 2022; 3: 444-460.

Hille D. Encyclopedia of Soils in the Environment: Academic Press, 2004.

Hou J, Xu X, Yu H, Xi B, Tan W. Comparing the long-term responses of soil microbial structures and diversities to polyethylene microplastics in different aggregate fractions. Environment International 2021; 149: 106398.

Hou Z, Zhou Q, Mo F, Kang W, Ouyang S. Enhanced carbon emission driven by the interaction between functional microbial community and hydrocarbons: An enlightenment for carbon cycle. Science of The Total Environment 2023; 867: 161402.

Huang J, Chen H, Zheng Y, Yang Y, Zhang Y, Gao B. Microplastic pollution in soils and groundwater: Characteristics, analytical methods and impacts. Chemical Engineering Journal 2021; 425: 131870.

Huang Z, Hu B, Wang H. Analytical methods for microplastics in the environment: a review. Environmental Chemistry Letters 2023; 21: 383-401.

Issaka E, Fapohunda FO, Amu-Darko JNO, Yeboah L, Yakubu S, Varjani S, et al. Biochar-based composites for remediation of polluted wastewater and soil environments: Challenges and prospects. Chemosphere 2022; 297: 134163.

Jansson JK, Hofmockel KS. The soil microbiome—from metagenomics to metaphenomics. Current opinion in microbiology 2018; 43: 162-168.

Jayakumar V, Sakakibara Y. Comprehensive evaluation of non-hybrid genome assembly tools for third-generation PacBio long-read sequence data. Briefings in bioinformatics 2019; 20: 866-876.

Jin H. Characterization of microbial life colonizing biochar and biochar-amended soils. 2010.

Joseph S, Cowie AL, Van Zwieten L, Bolan N, Budai A, Buss W, et al. How biochar works, and when it doesn't: A review of mechanisms controlling soil and plant responses to biochar. Gcb Bioenergy 2021; 13: 1731-1764.

Joseph S, Husson O, Graber ER, Van Zwieten L, Taherymoosavi S, Thomas T, et al. The electrochemical properties of biochars and how they affect soil redox properties and processes. Agronomy 2015; 5: 322-340.

Kalntremtziou M, Papaioannou IA, Vangalis V, Polemis E, Pappas KM, Zervakis GI, et al. Evaluation of the lignocellulose degradation potential of Mediterranean forests soil microbial communities through diversity and targeted functional metagenomics. Frontiers in Microbiology 2023; 14: 1121993.

Kim M, Lee K-H, Yoon S-W, Kim B-S, Chun J, Yi H. Analytical tools and databases for metagenomics in the next-generation sequencing era. Genomics & informatics 2013; 11: 102.

Kong J, He Z, Chen L, Yang R, Du J. Efficiency of biochar, nitrogen addition, and microbial agent amendments in remediation of soil properties and microbial community in Qilian Mountains mine soils. Ecology and Evolution 2021; 11: 9318-9331.

Lahlali R, Ibrahim DS, Belabess Z, Roni MZK, Radouane N, Vicente CS, et al. High-throughput molecular technologies for unraveling the mystery of soil microbial community: Challenges and future prospects. Heliyon 2021; 7.

Leis B, Angelov A, Liebl W. Screening and expression of genes from metagenomes. Advances in applied microbiology 2013; 83: 1-68.

Li H, Lu X, Wang S, Zheng B, Xu Y. Vertical migration of microplastics along soil profile under

different crop root systems. Environmental Pollution 2021; 278: 116833.
Li P, Hur J. Utilization of UV-Vis spectroscopy and related data analyses for dissolved organic matter (DOM) studies: A review. Critical Reviews in Environmental Science and Technology 2017; 47: 131-154.
Lin M, Li F, Li X, Rong X, Oh K. Biochar-clay, biochar-microorganism and biochar-enzyme composites for environmental remediation: a review. Environmental Chemistry Letters 2023; 21: 1837-1862.
Liverman DM, Cuesta RMR. Human interactions with the Earth system: people and pixels revisited. Earth Surface Processes and Landforms: The Journal of the British Geomorphological Research Group 2008; 33: 1458-1471.
Lytand W, Singh BV, Katiyar D. Biochar's Influence on Soil Microorganisms: Understanding the Impacts and Mechanisms. Int. J. Plant Soil Sci 2023; 35: 455-464.
Martín J, Santos JL, Aparicio I, Alonso E. Microplastics and associated emerging contaminants in the environment: Analysis, sorption mechanisms and effects of co-exposure. Trends in Environmental Analytical Chemistry 2022; 35: e00170.
Mazarji M, Bayero MT, Minkina T, Sushkova S, Mandzhieva S, Tereshchenko A, et al. Realizing united nations sustainable development goals for greener remediation of heavy metals-contaminated soils by biochar: Emerging trends and future directions. Sustainability 2021; 13: 13825.
Medyńska-Juraszek A, Jadhav B. Influence of Different Microplastic Forms on pH and Mobility of Cu2+ and Pb2+ in Soil. Molecules 2022; 27: 1744.
Metzker ML. Sequencing technologies—the next generation. Nature reviews genetics 2010; 11: 31-46.
Miransari M. Soil microbes and the availability of soil nutrients. Acta physiologiae plantarum 2013; 35: 3075-3084.
Morgan H, Sohi S, Shackley S. Biochar: An Emerging Carbon Abatement and Soil Management Strategy. Oxford Research Encyclopedia of Environmental Science, 2020.
Mukherjee S, Sarkar B, Aralappanavar VK, Mukhopadhyay R, Basak BB, Srivastava P, et al. Biochar-microorganism interactions for organic pollutant remediation: Challenges and perspectives. Environmental Pollution 2022; 308: 119609.
Nafees M, Ullah S, Ahmed I. Modulation of drought adversities in Vicia faba by the application of plant growth promoting rhizobacteria and biochar. Microscopy Research and Technique 2022; 85: 1856-1869.
Ogbonnaya U, Semple KT. Impact of biochar on organic contaminants in soil: a tool for mitigating risk? Agronomy 2013; 3: 349-375.
Or D, Smets BF, Wraith J, Dechesne A, Friedman S. Physical constraints affecting bacterial habitats and activity in unsaturated porous media–a review. Advances in Water Resources 2007; 30: 1505-1527.
Pérez-Reverón R, Álvarez-Méndez SJ, Kropp RM, Perdomo-González A, Hernández-Borges J, Díaz-Peña FJ. Microplastics in agricultural systems: analytical methodologies and effects on soil quality and crop yield. Agriculture 2022; 12: 1162.
Pang Z, Mao X, Zhou S, Yu S, Liu G, Lu C, et al. Microbiota-mediated nitrogen fixation and microhabitat homeostasis in aerial root-mucilage. Microbiome 2023; 11: 85.
Pathan SI, Arfaioli P, Bardelli T, Ceccherini MT, Nannipieri P, Pietramellara G. Soil pollution from micro-and nanoplastic debris: A hidden and unknown biohazard. Sustainability 2020; 12:

7255.

Philippot L, Griffiths BS, Langenheder S. Microbial community resilience across ecosystems and multiple disturbances. Microbiology and Molecular Biology Reviews 2021; 85: 10.1128/mmbr. 00026-20.

Qiu M, Liu L, Ling Q, Cai Y, Yu S, Wang S, et al. Biochar for the removal of contaminants from soil and water: a review. Biochar 2022; 4: 19.

Quilliam RS, Glanville HC, Wade SC, Jones DL. Life in the 'charosphere'–Does biochar in agricultural soil provide a significant habitat for microorganisms? Soil Biology and Biochemistry 2013; 65: 287-293.

Radajewski S, Ineson P, Parekh NR, Murrell JC. Stable-isotope probing as a tool in microbial ecology. Nature 2000; 403: 646-649.

Radford F, Zapata-Restrepo LM, Horton AA, Hudson MD, Shaw PJ, Williams ID. Developing a systematic method for extraction of microplastics in soils. Analytical Methods 2021; 13: 1695-1705.

Rafique A, Irfan M, Mumtaz M, Qadir A. Spatial distribution of microplastics in soil with context to human activities: a case study from the urban center. Environmental Monitoring and Assessment 2020; 192: 1-13.

Raynaud X, Nunan N. Spatial ecology of bacteria at the microscale in soil. PloS one 2014; 9: e87217.

Rehm R, Fiener P. Model-based analysis of erosion-induced microplastic delivery from arable land to the stream network of a mesoscale catchment. EGUsphere 2023; 2023: 1-43.

Rhoads A, Au KF. PacBio sequencing and its applications. Genomics, proteomics & bioinformatics 2015; 13: 278-289.

Rillig MC. Microplastic in terrestrial ecosystems and the soil? ACS Publications, 2012.

Roesch LF, Fulthorpe RR, Riva A, Casella G, Hadwin AK, Kent AD, et al. Pyrosequencing enumerates and contrasts soil microbial diversity. The ISME journal 2007; 1: 283-290.

RUSSO E. Behind the sequence. The Scientist 2001; 15: 1-1.

Sanger F, Nicklen S, Coulson AR. DNA sequencing with chain-terminating inhibitors. Proceedings of the national academy of sciences 1977; 74: 5463-5467.

Sarkar B, Dissanayake PD, Bolan NS, Dar JY, Kumar M, Haque MN, et al. Challenges and opportunities in sustainable management of microplastics and nanoplastics in the environment. Environmental Research 2022; 207: 112179.

Schmidt TM, Schaechter M. Topics in ecological and environmental microbiology: Academic Press, 2011.

Sohi SP, Krull E, Lopez-Capel E, Bol R. A review of biochar and its use and function in soil. Advances in agronomy 2010; 105: 47-82.

Sun Q, Li J, Wang C, Chen A, You Y, Yang S, et al. Research progress on distribution, sources, identification, toxicity, and biodegradation of microplastics in the ocean, freshwater, and soil environment. Frontiers of Environmental Science & Engineering 2022; 16: 1.

Sutkar PR, Gadewar RD, Dhulap VP. Recent trends in degradation of Microplastics in the environment: A state-of-the-art review. Journal of Hazardous Materials Advances 2023: 100343.

Tan S, Narayanan M, Huong DTT, Ito N, Unpaprom Y, Pugazhendhi A, et al. A perspective on the interaction between biochar and soil microbes: A way to regain soil eminence. Environmental Research 2022: 113832.

Tettelin H, Riley D, Cattuto C, Medini D. Comparative genomics: the bacterial pan-genome. Current

opinion in microbiology 2008; 11: 472-477.
Thompson RC, Olsen Y, Mitchell RP, Davis A, Rowland SJ, John AW, et al. Lost at sea: where is all the plastic? Science 2004; 304: 838-838.
Tian L, Jinjin C, Ji R, Ma Y, Yu X. Microplastics in agricultural soils: sources, effects, and their fate. Current Opinion in Environmental Science & Health 2022; 25: 100311.
Tringe SG, Rubin EM. Metagenomics: DNA sequencing of environmental samples. Nature reviews genetics 2005; 6: 805-814.
Tripathi C, Tripathi D, Praveen V, Bihari V. Microbial diversity–Biotechnological and industrial perspectives. 2007.
Trivedi P, Mattupalli C, Eversole K, Leach JE. Enabling sustainable agriculture through understanding and enhancement of microbiomes. New Phytologist 2021; 230: 2129-2147.
Tunlid A, Floudas D, Op De Beeck M, Wang T, Persson P. Decomposition of soil organic matter by ectomycorrhizal fungi: Mechanisms and consequences for organic nitrogen uptake and soil carbon stabilization. Frontiers in Forests and Global Change 2022; 5: 934409.
Van Den Bossche T, Arntzen MØ, Becher D, Benndorf D, Eijsink VG, Henry C, et al. The Metaproteomics Initiative: a coordinated approach for propelling the functional characterization of microbiomes. Microbiome 2021; 9: 1-4.
Van Elsas JD, Chiurazzi M, Mallon CA, Elhottovā D, Krištůfek V, Salles JF. Microbial diversity determines the invasion of soil by a bacterial pathogen. Proceedings of the National Academy of Sciences 2012; 109: 1159-1164.
Wang F, Wang Q, Adams CA, Sun Y, Zhang S. Effects of microplastics on soil properties: current knowledge and future perspectives. Journal of Hazardous Materials 2022; 424: 127531.
Wang J, Lv S, Zhang M, Chen G, Zhu T, Zhang S, et al. Effects of plastic film residues on occurrence of phthalates and microbial activity in soils. Chemosphere 2016; 151: 171-177.
Warnasuriya SD, Udayanga D, Manamgoda DS, Biles C. Fungi as environmental bioindicators. Science of The Total Environment 2023: 164583.
Widder S, Allen RJ, Pfeiffer T, Curtis TP, Wiuf C, Sloan WT, et al. Challenges in microbial ecology: building predictive understanding of community function and dynamics. The ISME journal 2016; 10: 2557-2568.
Williamson KE, Fuhrmann JJ, Wommack KE, Radosevich M. Viruses in soil ecosystems: an unknown quantity within an unexplored territory. Annual review of virology 2017; 4: 201-219.
Xu H-J, Wang X-H, Li H, Yao H-Y, Su J-Q, Zhu Y-G. Biochar impacts soil microbial community composition and nitrogen cycling in an acidic soil planted with rape. Environmental science & technology 2014; 48: 9391-9399.
Xu Y, Yan Y, Obadamudalige NL, Ok YS, Bolan N, Li Q. Redox-mediated biochar-contaminant interactions in soil. Biochar from biomass and waste. Elsevier, 2019, pp. 409-419.
Ye J, Liao W, Zhang P, Li J, Nabi M, Wang S, et al. Fe1-xS/biochar combined with thiobacillus enhancing lead phytoavailability in contaminated soil: preparation of biochar, enrichment of thiobacillus and their function on soil lead. Environmental Pollution 2020; 267: 115447.
Yu F, Yang C, Huang G, Zhou T, Zhao Y, Ma J. Interfacial interaction between diverse microplastics and tetracycline by adsorption in an aqueous solution. Science of the Total Environment 2020; 721: 137729.
Yu J, Deem LM, Crow SE, Deenik JL, Penton CR. Biochar application influences microbial assemblage complexity and composition due to soil and bioenergy crop type interactions. Soil

Biology and Biochemistry 2018; 117: 97-107.

Yuan Y, Bolan N, Prévoteau A, Vithanage M, Biswas JK, Ok YS, et al. Applications of biochar in redox-mediated reactions. Bioresource Technology 2017; 246: 271-281.

Zhang M, Zhao Y, Qin X, Jia W, Chai L, Huang M, et al. Microplastics from mulching film is a distinct habitat for bacteria in farmland soil. Science of the Total Environment 2019; 688: 470-478.

Zheng R, Cai R, Liu R, Liu G, Sun C. Maribellus comscasis sp. nov., a novel deep-sea Bacteroidetes bacterium, possessing a prominent capability of degrading cellulose. Environmental Microbiology 2021; 23: 4561-4575.

Zheng X, Xu W, Dong J, Yang T, Shangguan Z, Qu J, et al. The effects of biochar and its applications in the microbial remediation of contaminated soil: A review. Journal of Hazardous Materials 2022; 438: 129557.

Zhou J, Gui H, Banfield CC, Wen Y, Zang H, Dippold MA, et al. The microplastisphere: biodegradable microplastics addition alters soil microbial community structure and function. Soil Biology and Biochemistry 2021; 156: 108211.

Zhu P, Yang S, Wu Y, Ru Y, Yu X, Wang L, et al. Shifts in soil microbial community composition, function, and co-occurrence network of phragmites australis in the yellow river delta. Frontiers in Microbiology 2022; 13: 858125.

Zhu Z-l, Wang S-c, Zhao F-f, Wang S-g, Liu F-f, Liu G-z. Joint toxicity of microplastics with triclosan to marine microalgae Skeletonema costatum. Environmental pollution 2019; 246: 509-517.

Selected Publications

I **Ji, Mengyuan**, Xiaoxia Wang, Muhammad Usman, Feihong Liu, Yitong Dan, Lei Zhou, Stefano Campanaro, Gang Luo, and Wenjing Sang. "Effects of different feedstocks-based biochar on soil remediation: A review." Environmental Pollution 294 (2022): 118655.

II **Ji, Mengyuan**, Ginevra Giangeri, Fengbo Yu, Filippo Sessa, Chao Liu, Wenjing Sang, Paolo Canu, Fangbai Li, Laura Treu, and Stefano Campanaro. "An integrated metagenomic model to uncover the cooperation between microbes and magnetic biochar during microplastics degradation in paddy soil." Journal of Hazardous Materials 458 (2023): 131950.

III **Ji, Mengyuan**, Ginevra Giangeri, Muhammad Usman, Chao Liu, Matteo Bosaro, Filippo Sessa, Paolo Canu, Laura Treu, and Stefano Campanaro. "An integrated Metagenomic-Pangenomic strategy revealed native microbes and magnetic biochar cooperation in plasticizer degradation." Chemical Engineering Journal 468 (2023): 143589.

IV **Ji, Mengyuan**, Lurui Xiao, Muhammad Usman, Chao Liu, Wenjing Sang, Laura Treu, Stefano Campanaro, Gang Luo, and Yalei Zhang. "Different microplastics in anaerobic paddy soils: Altering methane emissions by influencing organic matter composition and microbial metabolic pathways." Chemical Engineering Journal (2023): 144003.

V Liu, Chao, Haiqing Wang, Muhammad Usman, **Mengyuan Ji**, Jun Sha, Zhenda Liang, Lishan Zhu, Li Zhou, and Bing Yan. "Nonmonotonic effect of CuO nanoparticles on medium-chain carboxylates production from waste activated sludge." Water Research 230 (2023): 119545.

Chapter I

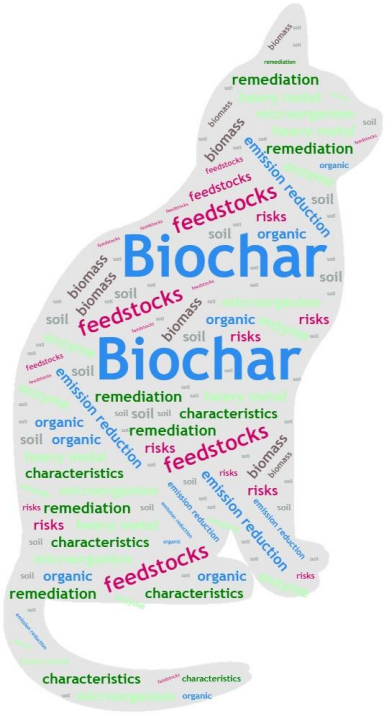

Effects of different feedstocks-based biochar on soil remediation: A review

Mengyuan Ji[a,b] , Xiaoxia Wang [a] , Muhammad Usman [c,d] , Feihong Liu [a] , Yitong Dan [a] , Lei Zhou [a] , Stefano Campanaro [b] , Gang Luo [d] , Wenjing Sang [a,*]

Environmental Pollution, Volume 458, 15 September 2023, 131950
https://doi.org/10.1016/j.envpol.2021.118655

[a] Textile Pollution Controlling Engineering Center of Ministry of Environmental Protection, College of Environmental Science and Engineering, Donghua University, Shanghai, 201620, China
[b] Department of Biology, University of Padua, 35131, Padova, Italy
[c] Bioproducts Science & Engineering Laboratory (BSEL), Department of Biological Systems Engineering, Washington State University (WSU), Richland, WA, USA
[d] Shanghai Key Laboratory of Atmospheric Particle Pollution and Prevention (LAP3), Department of Environmental Science and Engineering, Fudan University, Shanghai, 200433, China

*Corresponding author

Environmental Pollution 294 (2022) 118655

Contents lists available at ScienceDirect

Environmental Pollution

journal homepage: www.elsevier.com/locate/envpol

Effects of different feedstocks-based biochar on soil remediation: A review☆

Mengyuan Ji [a,b], Xiaoxia Wang [a], Muhammad Usman [c,d], Feihong Liu [a], Yitong Dan [a], Lei Zhou [a], Stefano Campanaro [b], Gang Luo [d], Wenjing Sang [a,*]

[a] Textile Pollution Controlling Engineering Center of Ministry of Environmental Protection, College of Environmental Science and Engineering, Donghua University, Shanghai, 201620, China
[b] Department of Biology, University of Padua, 35131, Padova, Italy
[c] Bioproducts Science & Engineering Laboratory (BSEL), Department of Biological Systems Engineering, Washington State University (WSU), Richland, WA, USA
[d] Shanghai Key Laboratory of Atmospheric Particle Pollution and Prevention (LAP3), Department of Environmental Science and Engineering, Fudan University, Shanghai, 200433, China

ARTICLE INFO

Keywords:
Feedstocks
Biochar
Soil remediation
Characteristic

ABSTRACT

As a promising amendment, biochar has excellent characteristics and can be used as a remediation agent for diverse types of soil pollution. Biochar is mostly made from agricultural wastes, forestry wastes, and biosolids (eg, sewage sludge), but not all the biochar has the same performance in the improvement of soil quality. There is a lack of guidelines devoted to the selection of biochar to be used for different types of soil pollution, and this can undermine the remediation efficiency. To shed light on this sensitive issue, this review focus on the following aspects, (i) how feedstocks affect biochar properties, (ii) the effects of biochar on heavy metals and organic pollutants in soil, and (iii) the impact on greenhouse gas emissions from soil. Generally, the biochars produced from crop residue and woody biomass which are composed of lignin, cellulose, and hemicellulose are more suitable for organic pollution remediation and greenhouse gas emission reduction, while biochar with high ash content are more suitable for cationic organic pollutant and heavy metal pollution (manure and sludge, etc.). Additionally, the effect of biochar on soil microorganisms shows that gram-negative bacteria in soil tend to use WB biochar with high lignin content, while biochar from OW (rich in P, K, Mg, and other nutrients) is more able to promote enzyme activity. Finally, our recommendations on feedstocks selection are presented in the form of a flow diagram, which is precisely intended to be used as a support for decisions on the crucial proportioning conditions to be selected for the preparation of biochar having specific properties and to maximize its efficiency in pollution control.

1. Introduction

Increasing economy and industry have stirred a great deal of interest for soil security globally and regionally. The multi-layer porous structure, high carbon content, and abundant functional groups of biochar make it a promising soil amendment. It has been proven to be effective in improving soil quality, such as adjusting soil water retention, nutrient content, and soil aggregates (Aslam et al., 2014). Returning biochar to soil is a potentially valuable soil remediation method, which can reduce heavy metal (Wang et al., 2020) and organic pollution (Dai et al., 2019), control greenhouse gas emissions (Li et al., 2018b) (CO_2, CH_4 and N_2O), and stimulate the activities of soil microorganisms (Plaza et al., 2016). Reasonable application of biochar could be a cost-beneficial technology to reduce soil pollution, mitigate climate change, and preserve soil quality.

Soil contamination by organic pollutants (pesticides, fertilizers, antibiotics, polycyclic aromatic hydrocarbons (PAHs), polychlorinated biphenyls (PCBs), etc.) and heavy metals (Cd, Pb, Cr, Cu, Zn, As, Co, Ni, etc.) (Sun et al., 2018; Yang et al., 2014). These pollutants that enter the soil environment mainly through sewage irrigation, atmospheric deposition, fertilizers and pesticides, industrial wastes, mineral resources, etc., not only affect crop yields and soil quality, but also cause carcinogenesis, teratogenesis, mutagenesis, and genetic toxicity, and ultimately threat human health through the food chain (Qin et al., 2020; Sun et al., 2018). In order to control hazardous effects and effectively restore the ecosystem of contaminated soil, a series of in-situ and ex-situ

☆ This paper has been recommended for acceptance by Dr. Yong Sik Ok.

* Corresponding author.
E-mail address: wjsang@dhu.edu.cn (W. Sang).

https://doi.org/10.1016/j.envpol.2021.118655
Received 18 April 2021; Received in revised form 19 October 2021; Accepted 5 December 2021
Available online 8 December 2021

remediation technologies (including surface coverage, encapsulation, landfill, soil washing, soil washing, etc.) have been developed. Biochar has become a promising restoration strategy due to its superior physical and chemical properties.

Biochar is generated by the combustion of biomass under an oxygen-limited environment with a relatively low temperature (<700 °C) (Gupta et al., 2019). The average carbon content of biochar is usually 70%–80% (except for biosolid biochar) (Tan et al., 2017) and presents an aromatic carbon structure including a crystalline phase (fused poly-aromatic hydrocarbon sheet) and an amorphous phase (random aromatic ring). The biochar properties largely depend upon the type of feedstocks and also on pyrolysis conditions like temperature, heating rate and duration (Li et al., 2019a). Due to its porous structure and surface functional groups, biochar has become a promising solution to various environmental problems (Suliman et al., 2017). Generally, biochar consists high C, N, P, Ca, and K (Steiner et al., 2010) and returning it to soils can increase soil water retention, improve the soil fertility and improve the plant yield (Rajkovich et al., 2012). The effect of biochar on soil pollution varies remarkably among the different feedstocks and their interaction with the soil (such as ion exchange, functional groups complexation, physical adsorption, and surface precipitation). This is further determined by the feedstock composition, pyrolysis condition (Kuzyakov et al., 2009), soil condition, and type of the pollution (Beesley et al., 2010). Although the preparation temperature of biochar is considered to be of great significance to the biochar properties (Novak et al., 2009), the importance of its feedstocks cannot be ignored. To date, mostly previous studies have focused on the effects of biochar on plant growth and soil functions, and there is a lack of systematic consideration of the effects of biochar on the remediation of different types of soil pollution.

The amount of research related to biochar is increasing year by year (Fig. 1), and most of them are related to the functionality of biochar, mainly focusing on improving soil physicochemical properties (Zhang et al., 2021), enhancing crop yield (Ye et al., 2020a), adsorbing various pollutants (Liu et al., 2017) and improving the bioavailability of soil nutrient elements (e.g., C, N, and K) (Liu et al., 2018). Some studies have discussed the remediation effect of biochar on a certain type of soil pollution based on feedstock type and production condition (Dutta et al., 2017; Wang et al., 2019). Furthermore, He et al. have discussed the effects of biochar on soil health and biota health by selecting changes in soil biological and non-biological indicators (He et al., 2021). In addition, the role of the redox reactivity of biochar in environmental remediation has received extensive attention in recent years. Currently,

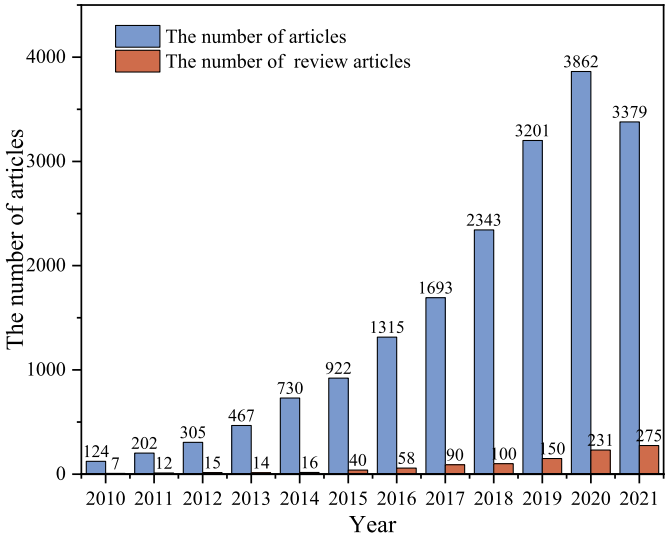

Fig. 1. The number of articles related to biochar published in 01.2010–09.2021 (database: web of science).

researches on the multifunctional synergy between the electroactive components of different types of biochar are still deficient. Wan et al. (2020) critically reviewed the latest progress in electron-mediated biochar applied to sustainable remediation, from the perspective of reactive-active moieties (RAMs) (such as amino-NHx, phenolic –OH and ketonic group), environmental persistent free radicals (EPFRs), defect sites, and metal/heteroatom doping. Their review is of great significance for the future engineering application of biochar as a green and sustainable metal-free catalyst. However, the relationship between the characteristics of different feedstocks and their effect on different soil remediation is still unclear. Therefore, the objective of this review is to establish corresponding evaluation methods that can be used to remediate multiple soil pollution with biochar based on different feedstocks, which are achieved from the perspectives of (1) the impact of the type of feedstocks on the key properties of biochar that can affect the quality of soil and the C and N cycles (e.g. nutrition, the proportion of aromatic and aliphatic C fractions (El-Naggar et al., 2019)); (2) The relationship between the physicochemical indicators of biochar (porosity, alkalinity, CEC, element content, and nutrient content, etc.) and soil heavy metal remediation, organic pollution remediation, and greenhouse gas emission reduction. In addition, because the functional and diversity of the soil microbiome is closely related to soil health, (3) the effects of biochar based on different feedstocks on soil community and enzyme activities were further evaluated. It finally highlights (4) the popularization prospects of various biochar in soil remediation and the challenges faced by the mixed feedstock's biochar used in different pollution aspects.

2. Differences in the properties of biochar from different raw material sources

2.1. Classification of biomass feedstocks

Studies have shown that different feedstocks have significantly affected the properties of biochar (e.g., yield, ash, element content, functional groups, aromaticity, porosity and specific surface area, etc.) (Gul et al., 2015; Suliman et al., 2016). Therefore, the comparison of the properties of biochar from different feedstocks is the basis for preferential application of biochar to remediate different types of soil pollution. In order to provide guidance for the subsequent remediation of different pollutants, we mainly discussed the characteristics of three feedstocks: crop straw, woody biomass and organic waste. Many studies have used crop residues and woody biomass (Hoslett et al., 2020) (mainly corn stalks, wheat stalks, straw and rice husks, potatoes, soybeans, sugar cane and bagasse, cotton, grapes, oranges, peanuts, rapeseed/straw, etc.) as feedstocks to produce biochar (Al Afif et al., 2020; Hoslett et al., 2020). In general, the cellulose and lignin in crop residue can decay into smaller molecules during the pyrolysis process, resulting in lower O/C and H/C of crop residue biochar. For woody biomass, the proportions of hemicellulose, cellulose and lignin are often different according to the type of wood species, which further affects the properties of the products (e.g., C, H, O content, etc.) after pyrolysis (Gholizadeh et al., 2019). This kind of biomass has the characteristics of low ash content, low moisture, high calorific value and few voids (Jafri et al., 2018). organic wastes (sewage sludge, manure, and compost) usually has the characteristics of higher moisture and ash content, lower calorific value and bulk density, and higher porosity, so that requires higher heat energy and longer time for pyrolysis (Jafri et al., 2018). Among them, sewage sludge contains heavy metals, parasites, and other microbial pathogens, which may cause damages to the environment. On the other hand, if sludge contains more available phosphorus, the prepared biochar has a higher P element content (Han et al., 2013; Jing et al., 2011).

2.2. Impacts on SSA, PH, CEC, and ASH content of biochar

Specific surface area (SSA) and porosity are important

physicochemical properties of biochar, which play a decisive role in the available active sites of biochar. It can further affect the properties of biochar (for example cation exchange capacity, water holding capacity and adsorption capacity, etc.). When feedstocks undergoes pyrolysis, the loss of water during dehydration and the release of volatile components in the carbon matrix contribute to the formation and development of the pore structure of biochar (Williams and Reed, 2006). Sources of biomass feedstocks are one of the main factors affecting the pore structure. Alkali metals in biomass can be used as self-activators for pore development during pyrolysis. In general, high ash content leads to low micropore surface area, while high organic carbon content promotes the generation of micropores (Leng et al., 2020). This phenomenon is closely related to the release of volatiles, and ash can easily block the pores. Organic wastes (OW) such as manure, compost, and sludge often contain more inorganic minerals (more ash), which can cause a lot of pore-clogging, especially micropore clogging, resulting in a lower surface area (Zhang et al., 2019c). For woody biomass (WB) biochar, the thermal stability of lignin keeps the pore structure and therefore has a higher specific surface area and porosity (Özçimen and Ersoy-Meriçboyu, 2010). Biochar can also impact soil pH (Ahmad et al., 2014). Generally, the pH of WB biochar is lower than that of crop residue (CR) and OW (El-Gamal et al., 2017). The content of non-pyrolyzable inorganic elements in organic matter and the degradation degree of organic components are closely related to the pH value of biochar (García-Jaramillo et al., 2015). Fig. 2 further compares the pH, ash content, and specific surface area of selected biochar derived from different feedstocks (Here we select the relevant literature between 2010 and 2021 from the Web of Science and Google Scholar database for meta-analysis and compare the physicochemical properties of biochar in the three temperature ranges of high (700 ± 50 °C), middle (500 ± 50 °C), and low (300 ± 50 °C). All the relevant references are listed in Table S1.). It can be seen clearly that the pH of OW biochar is lower than that of CR- and WB-biochar when the temperature is low. As the temperature increases, the pH of WB becomes the lowest of the three. The ash content of OW is significantly higher than that of CR and WB. As the increase of temperature, the SSA of the three has obviously increased and generally decreased in the order of WB, CR, and OW. Cation exchange capacity (CEC) is a significant indicator of the ability of biochar to reversely adsorb cations. Since the CEC data clearly recorded in the 2010–2021 data set is not sufficient for meta-analysis, we refer to the typical cases in the previous literature. Compared with WB biochar, CR- and OW-based biochar generally have higher CEC (Cely et al., 2015; Tag et al., 2016). CEC indicates the ability of biochar to sorb cationic. It is reported that the CEC of biochar mainly depends on the amounts and distribution of O-containing functional groups on the surface of the biochar (Banik et al., 2018). For example, the negatively charged carboxyl and phenolic groups on the surface of the biochar can act as sorption sites for cations. In addition, previous studies have shown that biomass with higher ash content shows a higher CEC value. The main components of ash are soluble alkali metal salts (Ca^{2+}, K^{+}, Mg^{2+}, etc.) and mineral components (PO_4^{3-}, CO_3^{2-}, etc.). These negatively charged mineral components have a strong electrostatic attraction to cationic components (Zhou et al., 2014). Moreover, the soluble metal salt can play a role in ion exchange during the adsorption process (Zhu et al., 2018). As the ash content in woody biomass, crop residue, and organic waste biochar increases in sequence, the CEC of OW biochar tends to be the largest, which could be attributed to the fact that alkali metals in biomass promote the formation of oxygen-containing functional groups on the surface of the biochar during the pyrolysis process (Kharel et al., 2019).

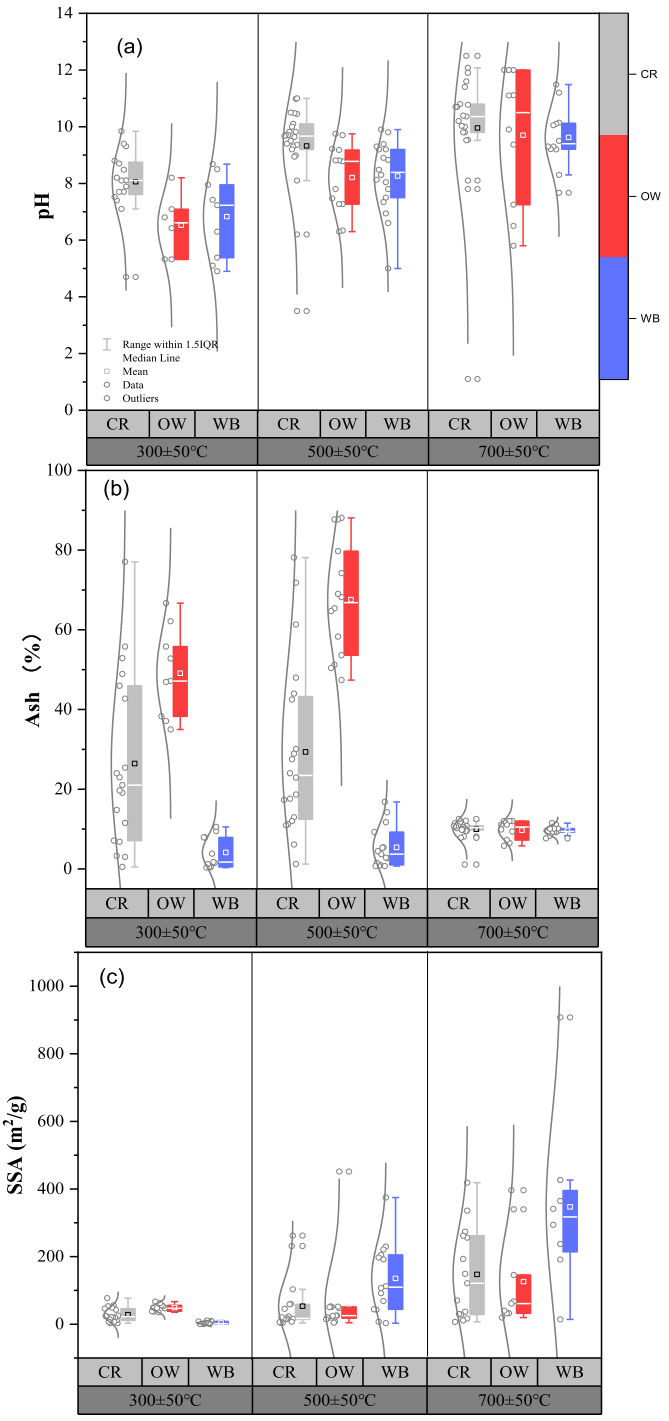

Fig. 2. Differences in properties of biochar from different feedstocks. (The gray circles in the figure are the original data points, and the brown curves are the scattered point distribution curve. Data comes from Table S1 (a): pH difference; (b): ash content difference; (c): specific surface area difference.). (For interpretation of the references to colour in this figure legend, the reader is referred to the Web version of this article.)

2.3. Impacts on biochar element content

In terms of elemental composition, the carbon content of woody biomass biochar is usually higher than that of crop residue- and organic wastes-biochar (the content of elements such as N, P, K, and Ca in woody feedstocksis relatively lower) (Domingues et al., 2017). The C content in sewage sludge shows a decrease during the pyrolysis process, and the loss of C can be attributed to the increase in the volatility of C as the pyrolysis temperature increases (Agrafioti et al., 2013). In a few cases, the increase of C content during sludge pyrolysis is due to the loss of –OH surface functional groups during the biomass dehydroxyl process (Zielińska et al., 2015). Previous study showed that the C content of biochar formed at different temperatures varies with raw materials, and the

general order was pine wood > rice straw > pig manure ≈ sewage sludge (Wei et al., 2019). If the purpose of soil remediation is carbon sequestration and emission reduction, it is more suitable to use biochar with high aromatic carbon content (low O/C and H/C), which we explained further in section 5.1. Generally, the K and Ca content of WB are relatively high, while the contents of N, S, P Na and Mg in OW are higher than that of other feedstocks (Domingues et al., 2017). Therefore, if the goal is to supplement nitrogen, phosphorus and potassium fertilizers, biochar derived from manure can be used. Moreover, feedstock is a key factor in determining the total nitrogen content of biochar. If the content of macromolecular amino acids and protein in the feedstocks is high, correspondingly, the nitrogen content in biochar is also high (Chen et al., 2020). Previous studies have shown that the order of nitrogen content in raw materials is "WB < CR < OW" (Pariyar et al., 2020). As the pyrolysis temperature increases, a large amount of N is released in gaseous form (NO, N_2O, NO_2, NH_3, N_2), which reduces the N content in biochar (Mukherjee et al., 2011). In addition, Ippolito et al. (2020) have used meta-data analysis to predict the availability of nutrient elements in different biochar, and the results showed that: (i) The percentage of available N in manure biochar is relatively high (e.g., pig manure, and cattle manure, etc.) (ii) The percentage of available P in typical CR (e.g., wheat, rice, corn stalk, etc.). is relatively high. (iii) The percentage of available K in WB is relatively high.

2.4. Impacts on the functional groups of biochar surface

The functional groups on the surface of biochar determine the characteristics of trace elements or their binding characteristic to pollutants. The functional groups can be modified or introduced to enhance the required adsorption characteristics. Some techniques such as FT-IR andX-ray photoelectron spectroscopy (XPS) have been applied to study these functional groups (Amin et al., 2016).

FT-IR spectroscopy can be used to reveal the changes in the characteristics of biochar surface functional groups with feedstocks. In addition, it also describes the stretching of C–H bands associated with aliphatic functional groups. The structure of biochar mainly presents an aromatic ring skeleton and is rich in electron-withdrawing functional groups (Keiluweit et al., 2010). According to the research of Mukome (Mukome et al., 2013), the aromatic functional groups of WBbiochar show a considerably similarity, showing the tensile vibrations belonging to C–H, C═C and C═O (peaks between 700 and 900 cm^{-1}/1587 cm^{-1}). Moreover, there is a significant difference in the 870 cm^{-1} aromatic C–H stretch peak intensity among WB biochar and OW biochar, which is related to the abundant cellulose and sugars in plant raw materials. Janu et al. (2021) also confirmed that the difference in surface functional groups of biochar produced from different feedstocks at the same pyrolysis temperature is related to the lignin content of the unpyrolyzed biomass. In addition, with the increase of the pyrolysis temperature, the acidic functional groups connected with carbon evaporate faster, and the ash content is closely related to the basic functional groups. The functional groups on the biochar surface determine its binding characteristics to heavy metals or organic pollutants. Compared with OW biochar, WB biochar with more functional groups (hydroxyl and carboxyl groups) is easier to combine with heavy metal (such as Pb^{2+} and Zn^{2+}) (Fan et al., 2018; Zhao et al., 2020). The characterization of CR biochar showed that the aged biochar was functionalized with peroxide functional groups (C–O–O-) (Kumar et al., 2018), and these polar groups can interact with positively charged metal cations, leading to a series of reactions between surface carboxyl/phenolic functional groups and cations, thus further reducing metal ion mobility (Zhang et al., 2013).

XPS is also called electron spectroscopy for chemical analysis (ESCA). It is a surface-specific quantitative technique that can determine the relative abundance of different types of elements (Singh et al., 2014). Previous studies have extensively used XPS to characterize the functional groups on the surface of biochar. The previous results show that there are mainly four deconvoluted peaks of C 1s at 284.89 (C–C/C–H), 286.49 (C–O), 287.89 (C═O), and 288.79 eV (O═C–O) on the surface of biochar, and according to the pyrolysis temperature and the source of feedstocks, the proportion of aliphatic -C-C, –C═O, and –COOH groups changed significantly (Singh et al., 2014; Suliman et al., 2016). Moreover, the oxygen content on the surface of biochar also decreased with the increase of pyrolysis temperature. Qiu et al. (2014) compared the surface elemental composition of woody biomass and animal manure biochar and found that the (O + N)/C value of the manure biochar surface was significantly higher than that of plant-derived biochar. Additionally, the ash content of these biochar was positively correlated with the (O + N)/C of the surface of biochar. Thus, they speculate that the minerals of biochars could contribute to the high content of surface O of these biochar.

3. Remediation of soil organic pollutants by the application of biochar

3.1. Comparison of the sorption effect of different types of biochar

Biochar is increasingly used in the field of multiple soil organic pollution remediation (Chen et al., 2019b; Trinh et al., 2017). The efficiency of biochar in removing organic pollutants depends on the properties of biochar and pollutants. In order to visualize the relationship between the properties of biochar and the removal efficiency, the differences in the removal of organic pollutants among CR, WB, and OW-biochar were compared in Table 1. We mainly searched the relevant papers from 2010 to 2021 and divided them into CR, WB, and OW according to the source of feedstocks. The pyrolysis temperature of biochar in the table is ranked from high to low to facilitate the comparison of sorption capacity and mechanism from different feedstocks in three different pyrolysis intervals (300 ± 50 °C), (500 ± 50 °C), and (700 ± 50 °C). In addition, in order to highlight the impact of feedstocks, a series of biochar-based synthetic and modified materials are not included in the table. The types of organics selected for analysis mainly include antibiotics, fuels, oils, pesticides, and persistent organics.

As shown in Table 1, the sorption mechanism of cationic organic pollutants is significantly different from other organics. Wang et al. (Wang and Liu, 2017) compared the ability of different biochar to sorb methylene blue. The results showed that the WB biochar produced at low temperature has a better removal effect on methylene blue than other biochars. In this process, the main contributors are ash and dissolved carbon, and the main mechanism is an electrostatic interaction. Lonappan et al. (2016) proved that pig manure biochar has excellent sorption effect on methylene blue, this can be attributed to the cationic properties of methylene blue and the general anionic properties of manure. In addition, the remediation effect of biochar on typical soil organic pollutants-pesticide residues has also been extensively studied (Khorram et al., 2017). The sorption effect of biochar on pesticides in the soil is largely depends on the characteristics of biochar (e.g., porosity, H/C, etc.), the hydrophobicity of pesticides, soil properties (pH, moisture content) and environmental factors (Qiu et al., 2009). Due to the hydrophobicity of pesticides, most of them have a strong affinity for biochar (Zheng et al., 2010). Jin et al. (2016) evaluated the sorption capacity of various biochar-amended soil to imidacloprid, isoproturon and atrazine, and the results have showed that for a certain amount of biochar, the sorption rate of biochar to the mixture is usually proportional to the organic carbon (OC) content of the biochar and negatively correlated with the ash content. As one kind of persistent organic pollutants, polycyclic aromatic hydrocarbons (PAHs) are one of the most difficult pollutants in soil to remove (Cerniglia, 1992). Recently, the combination of surfactants (dodecyl tetramethylene glycol ether) and ligno-based biochar is considered to be an efficacious method to remove PAHs from the soil (Cao et al., 2016; Masrat et al., 2013). Nevertheless, PAHs in biochar has the risk of being released, previous studies have shown that PAHs in sludge based biochar can be leached in water (Chen

Table 1
The removal effect of biochar from different feedstocks on organic pollutants.

Feedstocks	Pyrolysis Temperature (°C)	Types of Biomass	Types of organic pollutants	Adsorption capacity (Q_m mg/g)	Main mechanism	References
Crop residue	700 ± 50	Rice straw	Tetracycline	552.00	H-bonding, π-π electron donor acceptor (EDA) interaction	Chen et al. (2018)
		Straw	Sunset yellow	29.50	π-π EDA interaction	Ji et al. (2016)
		Corn straw	perfluorooctane sulfonate	169.30	Hydrophobic and electrostatic interaction	Guo et al. (2017)
	500 ± 50	Peanut shells	Doxycycline hydrochloride	52.37	Strong complexation, electrostatic interactions	Li et al. (2017a)
		Rice husk	Crude	3230.00	Hydrophobic interaction and oleophilicity	Kandanelli et al. (2018)
	300 ± 50	Soybean stover; Peanut shells	Trichloroethylene	21.94; 24.30	chemisorption and pore diffusion	Ahmad et al. (2013)
		Corncob	Bisphenol A	2.39	H-bonding, π-π EDA	Li et al. (2017b)
Woody biomass	700 ± 50	Woody tree (*Gliricidia sepium*)	Crystal violet	125.53	Pore diffusion, π-π EDA	Wathukarage et al. (2019)
		Bamboo	Fuel oil	38.40	π-π EDA and acid-base interaction	Yang et al. (2018)
		Pine sawdust	Sulfamethoxazole	13.83	Hydrophobic interaction	Foo and Hameed (2012)
	500 ± 50	Eucalyptus sawdust	Dimetridazole	200.00	Physisorption and chemisorption	Wan et al. (2016)
		Maple wood	Crude oil	4800.00	Pore-filling	Nguyen and Pignatello (2013)
	300 ± 50	Herb	Metolachlor	2.32	pore-filling and polar functional groups	Wei et al. (2020b)
		Woody tree (*Gliricidia sepium*)	crystal violet dye	4.4	Pore diffusion, π-π EDA, H-bonding	Wathukarage et al. (2019)
Organic wastes	700 ± 50	Paper and pulp sludge	Methyl orange	20.53	Complexation	Chaukura et al. (2017)
		Pig manure	Tetracycline	365.40	H-bonding and π-π EDA	Chen et al. (2018)
	500 ± 50	Sewage sludge	2,4-Dichlorophenol	17.51	π-π EDA	Kalderis et al. (2017)
		Sewage sludge	Fluoroquinolone	19.80	Positive correlation with volatile solid content	Yao et al. (2013)
	300 ± 50	Paper mill sludge	pentachlorophenol	6.11	partition on uncarbonized organic matter	Devi and Saroha (2015)

et al., 2019c; José et al., 2016). Therefore, special care should be taken when applying sludge biochar.

The mechanism of biochar sorption of organic pollutants roughly includes pore filling, electrostatic interaction, electron donor and acceptor interaction, and hydrophobic interaction (Abbas et al., 2018; Keiluweit et al., 2010). Pore filling occurs due to the existence of mesopores and micropores in biochar (Nguyen et al., 2007) (Nguyen and Pignatello, 2013), and WB biochar usually has a significant advantage in this reaction due to its relatively high porosity. Ming et al. also verified that peanut shell biochar has good phosphate adsorption capacity due to its larger BET surface area (up to 328.96 m^2/g) and narrower pore size distribution (Wathukarage et al., 2019). Electrostatic interaction occupies an important position in the adsorption of ionic organics. Generally, the surface of biochar is negatively charged when kept at a higher pH condition (Mukherjee et al., 2011), which will cause electrostatic attraction between biochar and positively charged organics, and the magnitude of this electrostatic attraction depends on the magnitude of the charge of each atom and the distance between the two atoms. Hydrophobicity plays a major role in the sorption of neutral and hydrophobic organic matter. Biochar with low surface oxidation is generally hydrophobic and can react with hydrophobic organic compounds to achieve the purpose of eliminating organic pollutants (Inyang and Dickenson, 2015). The interaction between electron donor and acceptor occupies a dominant position in the sorption of aromatic organics (Spokas, 2010). The amount of adsorbed organic pollutants is proportional to the number of oxygen functional groups on the surface of biochar, partly due to the interaction of the π-π electron donor acceptor, and the functional groups (hydroxyl and amine groups, etc.) can be used as -π electron donor sites (Ahmed et al., 2018; Yang et al., 2018).

3.2. Degradation mechanism

In addition to being used as an adsorbent, biochar and its composite materials can be used as catalysts to degrade organic pollutants. First, the environmentally persistent free radicals (EPFRs) of biochar can react with O_2 to produce hydroxyl radicals without adding oxidants (Ruan et al., 2019). Moreover, when there is an external oxidant, the redox-active part (phenolic hydroxyl, etc.) on biochar can act as electron shuttles to interact with oxidants and enhance the formation of strong oxidizing free radicals such as hydroxyl radicals (·OH) and sulfate radicals ($SO_4^{\cdot-}$) (Fang et al., 2015). In recent years, an increasing number of studies have showed that magnetic biochar doped with transition metal ions can activate active oxygen (ROS) generated by persulfate/hydrogen peroxide to effectively degrade organic pollutants in aqueous solutions (Fu et al., 2019; Rong et al., 2019). However, whether it can degrade organics in soil environment needs further investigation. Secondly, biochar can serve as electron acceptors and support materials for photocatalysts to improve the photodegradability of the catalysts (Lu et al., 2019; Mian and Liu, 2018). The pore structure and carbon sources of biochar can also affect the activity and diversity of microorganisms (Zhu et al., 2017), thereby indirectly promoting the biodegradation of organic pollutants. To further understand the long-term effects of biochar on the interaction of persistent organic pollutants-root exudates-rhizosphere microorganisms, one recent research focused on the effect of biochar on the in situ remediations of rhizosphere soil. They found that high-temperature biochar with large sorption capacity can ensure the rapid adsorption and fixation of organic pollutants in the soil, and low-temperature biochar with high nutrients content can stimulate soil microbes to promote the biodegradation of persistent organic pollutants in the rhizosphere and reduce its environmental risk (Ni et al., 2020). At present, there are few studies on the analysis of differences in the degradation mechanism of various types biochar. Combining the amount of oxygen-containing functional groups on the surface of

biochar and its redox potential, we conclude that WB, which is rich in carboxyl and hydroxyl groups, is more suitable for use as feedstocks for helping degradation. Further research is needed to explore the feasibility of optimizing the production system to produce biochar that can be effectively used for specific soil organic remediation.

It is a very slow process to use environmental microorganisms to biodegrade organic pollutants under natural conditions. One of the potential solutions to improve the biodegradation efficiency in the soil is to implement enhancement of biodegradation through biostimulation. Biochar can improve the chemical properties of the soil, such as increasing soil pH, organic carbon, nutrients, and cation exchange capacity, also, the introduction of biochar would affect the activity of soil enzymes. Hence, it can further change the soil microbial community and promote the in-situ degradation of organic pollution. Many studies have showed that WB biochar is a good biodegradation promoter of soil PAHs (Anyika et al., 2015). Moreover, Zhang et al. (2018) investigated the effects of several biochars on the biodegradation rate of PAH from the perspective of microbial community and soil enzyme activity, and the results showed that there is no significant difference in the biodegradation rate of total PAH in soils treated with different biochars. However, the feedstocks selected in their study are all crop residue, and their properties are not so different. He et al., compared the effects of pig manure biochar (PB) and bamboo biochar (BB), and the result shows that adding PB to the soil with low organic matter content promotes the degradation of phthalates higher than BB (He et al., 2018). The sixth section of this review further analyzes the impact of biochar on soil microbes. In order to investigate the biodegradation effect of different feedstocks on the organic pollutants, the impact of these compounds on the soil microecology has to be taken into account.

WB biochar generally exhibits superior sorption performance due to the existence of a pore-filling mechanism, while OW biochar such as manure shows a higher sorption efficiency for cationic organic pollutants due to its high ash content (as we mentioned in section 2.2, high ash content often has a high CEC value). Moreover, biochar with a larger surface area and higher OC content is more suitable for the removal of pesticides and persistent organic pollutants (generally derived from biomass with higher lignin content).

3.3. Feedstocks selection recommendations and research limitations

In short, the properties of biochar such as negative charge, SSA, ash, porosity, and OC content are closely related to its adsorption effect. The lignin content has a significant impact on these properties. It is recommended to use woody biomass with high lignin content to undergo high-temperature pyrolysis to produce biochar as an adsorbent for organic pollutants. It is worth noting that due to the nature of cationic organic pollutants, it is more appropriate to choose OW as the precursor or use low-temperature pyrolysis WB. On the other hand, since the catalytic degradation effect is closely related to the EPFRs of biochar, it is recommended to use WB with high lignin content as the precursor and pyrolyze at about 500 ± 50 °C (when the pyrolysis temperature is higher than 700 °C, the free radical content would be significantly reduced (Qin et al., 2018).

So far, most of the studies about the sorption mechanism of organic pollution on biochar are still at the level of experience or observation, and there is a lack of long-term research on the removal of organic pollutants on field. Compared with the soil alone, the agglomerate of biochar and soil exhibits a multiplying adsorption capacity (Teixidó et al., 2013). Hence, biochar is a very promising strategy for the remediation of soil organic pollutants. However, for contaminated soil, the separation of biochar with pollutants adsorbed from the soil is also a problem, and the long-term toxicity of biochar remaining in the environment deserve further study.

4. Remediation of heavy metal pollution by the application of biochar

Soil contaminated by different heavy metals (i.e. Cd, Pb, Cu, Hg etc.) has become a serious worldwide issue, which not only affect the crop yield, soil fertility and quality reduction, but also conclusively affects the human health by food cycle (Hayyat et al., 2016; Wang et al., 2017a). These heavy metals can persist in soil and bring environmental risks.

4.1. Remediation of heavy metals contamination in soil by biochar

Biochar can be used in soil heavy metal remediation, for example, biochar could efficiently adsorb the heavy metals in the soil, and reduce the toxin stress and bioavailability to plants and microbes (Dhaliwal et al., 2020; Hayyat et al., 2016). Previous studies showed that various biochar have diversified capacity to decrease the bioaccessibility of heavy metals (O'Connor et al., 2018b). Biochars based on various feedstocks exhibit different characteristics (surface area, porosity, functional groups, etc.), which are important in repairing heavy metal pollution.

We adopt the same method as section 3.1 to select relevant papers and compare the removal effects of different biochars on diverse heavy metals. The results are shown in Table 2. It can be seen from Table 2 that the higher the CEC value of biochar, the higher its adsorption capacity for heavy metals. Biochar derived from manure generally has a higher Cu^{2+} removal rate than straw biochar (Meier et al., 2017; Park et al., 2011). Lei et al. confirmed that ion exchange is the main mechanism for OW biochar to fix Cd^{2+} and Cu^{2+}(Lei et al., 2019). In addition, sludge and manure hold higher ash content and pH value compared with other types of biochar. The ash in the biomass may adhere to the surface of the material during the pyrolysis process to prevent the escape of volatile gases and hinder the contact between air and the surface of the material (Wang et al., 2021b), Which probably hinders the pyrolysis process. In addition, the accumulation of ash containing soluble alkali metal salts and minerals can lead to biochar sequestering heavy metals mainly through ion exchange and co-precipitation, as we mentioned before. WB biochar (straw, husks, forest waste etc.) mainly adsorbed heavy metals by forming surface complexes (Cui et al., 2011; Cui et al., 2012). The functional groups on biochar (such as –OH, –COOH, –C double bond O- and C double bond N) provided binding sites for heavy metal ions, thereby increasing the specific adsorption of metals. In general, the mineral-rich biochar obtained from OW are more suitable for heavy metal fixation. However, it is worth noting that the soil properties and maturing process will seriously disturb the stability of biochar. Generally, the pyrolysis temperature range of lignin is much wider than that of cellulose and hemicellulose, and the average activation energy required for its degradation is also higher (Pasangulapati et al., 2012). Therefore, WB biochar with higher lignin content shows higher stability, whereas the sludge or manure biochar showed a more unstable carbon (low resistance to mineralization) structure, which promotes the microbial decomposition of biochar in the soil (Li et al., 2019b). Therefore, the stability layout of biochar derived from various feedstocks could be "OW < CR < WB". Thus, from the long-term of view, modified woody biochar pyrolysis at high temperature should be the better choice. Moreover, the consequence of biochar during the treatment of heavy metal contaminated soil also transformed the metal speciation and varied the physicochemical properties of the soil (i.e. pH, redox potential, nutrient balance etc.) (Lahori et al., 2017). These variations can subsequently influence the interaction between metals and soil, thereby affecting the metal mobility and bioavailability after biochar modification. For example, with the addition of biochar, more negatively charged surface sites lead to a decrease in zeta potential and an increase in the CEC of soil surface. Therefore, the electrostatic attraction between the positively charged heavy metals and the soil can be enhanced (Jiang et al., 2012). In terms of metal speciation, the use of biochar might

Table 2
Effect of different types of biochar on the remediation of heavy metals in different types of contaminated soil.

Feedstocks	Pyrolysis temperature (°C)	Types of Biomass	Concentration & time	Types of Soil	Metal concentration	Removal (%)	Reference
Crop residue	700 ± 50	Soybean stover	10% for 90 days	Agricultural soil	1945 mg As/kg; 1945 mg Pb/kg	95% Pb	Ahmad et al. (2016)
		Red pepper stalk	2.5% for 45 days	Agricultural soil	1445 mg Pb/kg	65%	Igalavithana et al. (2019)
	500 ± 50	Maize straw	30 t/ha for 3 months	Paddy soil	2.04 mg Cd/kg	50.4%	Zhang et al. (2019b)
		Corn stalk	2% for 30 days	Arable land soil	2 mg Cd/kg	91%	Gao et al. (2019)
		Rice husk	1–5% for 10 days	Field soil	1000 mg Hg/kg	>94%	O'Connor et al. (2018a)
		Rice straw	40 t/ha for 4 months	Paddy field soil	432.8 mg Cr/kg	22.3%	Zhou et al. (2019)
		Sugarcane bagasse	1.5% for 4 months	Agricultural soil	50 mg Cd/kg; 50 mg Cr/kg	40.4% Cd; 48.1–49.6% Cr	Bashir et al. (2018)
		Hickory nut shell	30 t/ha for 6 months	Paddy soil	2.04 mg Cd/kg	53.6%	Zhang et al. (2019b)
		Vegetable waste	5% for 45 days	Agricultural soil	1445 mg Pb/kg	87%	Igalavithana et al. (2019)
		Orange bagasse	60 t/ha for 24 months	Fallow field soil	100 mg Cu/kg	28%	Gonzaga et al. (2020)
		Orange bagasse	60 t/ha for 6 months	Fallow field soil	100 mg Cu/kg	41%	Gonzaga et al. (2018)
		Rice straw	3% for 30 days	Paddy soil	120 mg As/kg	234.5%	Wang et al. (2017b)
		Wheat straw	0-40 t/ha for 3 years	Farmland soil	1.78 and 3.81 mg Cd/kg; 118 and 230 mg Pb/kg	16–20% Cd; 24–67% Pb	Sui et al. (2018)
		Wheat straw	0-40 t/ha for 2 years	Farmland soil	0.9 mg Cd/kg; 171 mg Zn/kg	57–86% Cd	Chen et al. (2016)
		Corn stalks, peanut husks and rice husks	0–4% for 3 years	Farmland soil	3.98 mg Cd/kg	28.5–59.4%	He et al. (2017)
		Rice straw	0-20 t/ha for 2 years	Farmland soil	0.85 mg Cd/kg	8.6–50.2%	Sui et al. (2020)
		Wheat straw	0-40 t/ha for 5 years	Farmland soil	22.65 mg Cd/kg; 621.23 mg Pb/kg	7.5–23.3% Cd; 3.7–19.8% Pb	Cui et al. (2016)
		Rice straw	1–3% for 96 days	Paddy field soil	212 mg As/kg; 10.8 mg Cd/kg	49–68% Cd; 26–49% As	Yin et al. (2017)
	300 ± 50	Soybean straw	3% for 6 days	Agricultural soil	1.36 mg Cd/kg	65.7%	Li et al. (2018a)
		Wheat straw	72 t/ha for 118 days	Farmland soil	129 mg Hg/kg	26%	Xing et al. (2019)
		Oat hull	5% for 24 months	Sedimentary alfisol	338 mg Cu/kg	68%	Moore et al. (2018)
Woody biomass	700 ± 50	Poplar branch	5% for 1 day	Vegetable garden soil	434 μg Pb/g: 353 μg Zn/g,	24.46% Zn; 46.56% Pb	Wang et al. (2017a)
		Holm oak	0–4% for 3 years	Farmland soil	11 mg Cd/kg; 247 mg Pb/kg; 298 mg Zn/kg	40–66% Cd; 48–77% Zn	Egene et al. (2018)
	500 ± 50	Poplar	0–3% for 2 years	Farmland soil	6.65–11.0 mg Cd/kg; 1124–1148 mg Pb/kg; 1151–1852 mg Zn/kg	75% Cd; 86% Pb; 92% Zn	Karer et al. (2018)
	300 ± 50	Kenaf	24 g biochar mixed with 600 g soil for 2 years	Farmland soil	2050 mg Pb/kg; 495 mg Zn/kg; 654 mg Cu/kg; 0.705 mg Cd/kg; 1177 mg As/kg	34.8–63.8% Pb; 22.6–37.2% Cu; 15–20.1% Cd; 116–210% Zn;	(He et al., 2019a; He et al., 2019b)
		Poplar branch	5% for 1 day	Vegetable garden soil	434 μg Pb/g; 353 μg Zn/g,	< 5% Zn; < 3% Pb	Wang et al. (2017a)
Organic wastes	700 ± 50	Sewage sludge	5% for 17 weeks	Paddy field soil	2.1 mg Hg/kg & 65.3 mg Hg/kg	67% & 29%	Zhang et al. (2019a)
	500 ± 50	Chicken manure	5% for 14 days	Mine soil, Hills soil	1805 & 160 mg Cu/kg	79% & −45%	Park et al. (2011)
		Sewage sludge	5% for 77 days	clay texture, basic pH and high organic matter content	1000 mg Ni kg −1	88%	Mendez et al. (2014)
		Sewage sludge	30 t/ha for 6 months	Fallow field soil	100 mg Cu/kg	−18%	Gonzaga et al. (2018)
		Chicken manure	5% for 14 days	Sedimentary alfisol	800 mg Cu/kg	73%	Meier et al. (2017)
	300 ± 50	Sewage sludge	3% for 6 days	Agricultural soil	98.7 mg As/kg	11.7–28.5%	Li et al. (2018a)

decrease the exchangeable contents of heavy metals in the soil. Xu et al. (2020) reported that the application of biochar switches the state of heavy metals composition (Cd, Pb) from reducible and acid-soluble state to oxidizable and residual state, therefore, lowering the bioavailability of Cd and Pb. In addition, this study also showed that the utilization of biochar resulted in a reduced amount of superoxide dismutase and peroxidase in the soil.

4.2. Sorption mechanism

Previous studies proposed various mechanisms for the interaction of biochar with heavy metals. The mineral substance, alkaline metal ions, π-electrons, pore structures of micro pores, abundant surface functional groups and organic matters actually provide the binding sites for biochar remediation of heavy metals. Biochar has the ability to sorb heavy metals in contaminated soil through precipitation, complexation, electrostatic attraction, cation exchange of the heavy metals from inorganic to organic states that varied the heavy metals motility and bioavailability (Wang et al., 2018; Xu et al., 2018), and results in the improvement of agronomic benefits of the soil. Therefore, the interaction mechanism of biochar and heavy metals are critical for the soil remediation. Many studies evidenced a link between the availability of pollutants in the soil after applying the biochar and the microbial composition (Nie et al., 2018; Tang et al., 2020). However, the effect of microbes on the morphological transformation of heavy metals adsorbed via biochar is still unclear, which needs more investigation.

4.3. Feedstocks selection recommendations and research limitations

In short, the remediation effect of heavy metals in the soil by biochar is inseparable from its CEC, zeta potential, ash content, functional groups, and mineral content. Besides, Ion exchange and co-precipitation occupy an important position in the sorption mechanism for heavy metals. From the perspective of resource reuse, we recommend that OW should be given priority consideration to be used as feedstocks for remediation of heavy metal pollution in the soil, but how to improve the long-term stability of this type of biochar in the soil is still a problem worthy of attention. In addition, sewage sludge may contain heavy metals. It is better to pay attention to its composition and concentration before use, and then determine whether it is necessary to adopt reasonable pretreatment methods to reduce its heavy metal content. Futhermore, it is still unclear how the type of feedstocks affects the speciation of heavy metals adsorbed on biochar through the roles of microorganisms.

Biochar still has some limitations in the remediation of soil contaminated by heavy metals. Firstly, the common situation in actual soil pollution is compound heavy metal pollution. The use of biochar to fix certain metals has the risk of promoting the migration and toxicity of other metals at the same time (Xiang et al., 2021). Second, in-situ passivation is more sensitive to environmental pH changes, microbial activity, and other factors. The passivated heavy metals may be re-released under certain conditions, and more long-term field tests and environmental monitoring are required to verify the remediation effect of biochar (Wang et al., 2021a). Therefore, it is particularly important to develop multi-material composite biochar materials with superior performance to compensate for the shortcomings of single biochar. In addition, fixed heavy metals are difficult to separate and eradicate from the soil. In the future, the combined use of multiple remediation technologies (such as combined with phytoremediation) can be considered to gradually remove heavy metals in the soil and completely eliminate its potential risks.

5. The impact of biochar application on greenhouse gas emission reduction in soil

5.1. Factors affecting greenhouse emissions

Farmland ecosystem is one of the important emission sources of greenhouse gases (GHG) (mainly CO_2, CH_4, N_2O), accounting for 10%–20% of total global greenhouse gas emissions. Therefore, developing a green and effective soil greenhouse gas emission reduction technology has become a hot issue in the related field (Ameloot et al., 2016). Biochar has been proven to regulate greenhouse gas emissions in several ways: (1) It can regulate nitrification and denitrification reactions by adjusting soil properties and microbial activity, thereby inhibiting N_2O production. Firstly, biochar increases the permeability of the soil and inhibits denitrification (Subedi et al., 2016). Secondly, it increases the soil pH value and enhances the N_2O reductase enzyme activity, thus reducing the N_2O content (Ming et al., 2016). (2) Biochar are able to affect the composition and function of soil microbial community and inhibit the activity of certain microorganisms, thereby inhibiting the degradation of organics, and reduce the emission of C and N (Ji et al., 2020). In addition, Luo et al. (2016) found that biochar can reduce urease activity (Due to high C/N ratio (Tarin et al., 2020)), inhibit N mineralization and help to increase soil N content. (3) Biochar adsorbs C, N and organic matter to produce more stable substances (Abagandura et al., 2019). Previous studies have shown that the high SSA and mineral content (such as $Fe(OH)_3$, $CaCO_3$, etc.) of biochar have a strong physical and chemical fixation effect on CO_2 emission (Plaza et al., 2016). This immobilization promotes the formation of organic-inorganic complexes between biochar, soil and organic matter, resulting in tighter aggregates (Nguyen et al., 2020; Xu et al., 2016b). Biochar mainly exists in soil aggregates as additional availability organic carbon, it can promote the transformation of organic carbon in the soil from large aggregates to small aggregates (Sun et al., 2020). (4) Biochar can inhibit soil respiration by reducing enzyme activity. Wei et al. (2020c) found that biochar application reduced the total soil microbial biomass, β-glucosidase and urease, and significantly inhibited soil respiration. They believed that biochar application has little effect on the overall soil organic carbon level, which is conducive to long-term carbon storage. However, some research studies believed that the application of biochar would not cause a significant impact on soil respiration, and its carbon sequestration effect is mainly because biochar promotes crop growth and improves soil carbon utilization (Gianfreda and Rao, 2008).

5.2. Comparison of the emission reduction effects of biochar from different feedstocks

Table 3 shows the greenhouse gas emission reduction effects of different biochar. Dissolved organic matter (DOM) is the most mobile and bioavailable part of the soil. It occupies an important position in the soil carbon cycle. The higher the soluble organic matter content, the easier the mineralization of soil carbon (Lévesque et al., 2020). Studies have shown that the application of biochar increases the content of DOM in soil pore water and soil leachate (Venegas et al., 2016). In addition, Wang et al. (2016) reported that CR biochar promoted the conversion of native organic matter into soluble organic carbon, which might be relate to the following three aspects: a) the release of DOM from native soil organic is increased. b) The electronegative functional groups on the surface of the humic acid are improved. c) The increase in the number of base ions, especially the K^+ content, competes for cation exchange sites on the surface of clay and SOM, thereby dispersing the clay and SOM and increasing the release of soluble organic C. The ratio of unstable C and stable C of biochar is closely related to the feedstock and temperature (Ashry et al., 2016). The content of aromatic carbon in biochar is usually positively correlated with pyrolysis temperature, so high-temperature biochar is more suitable for carbon sequestration and emission reduction (Purakayastha et al., 2016). Studies showed that the H/C of biochar prepared from CR and WB at 500–700 °C is usually less than 0.7 (Ahmad et al., 2016), and the stable C content is above 98% (Tag et al., 2016). In addition, high-temperature biochar has a low mineralized carbon and nitrogen content (Taherymoosavi et al., 2016), without significant impact on the mineralization and release of carbon and nitrogen (Ahmad et al., 2016).

From Table 3, the emission reduction rate of WB biochar is usually higher than that of CR biochar (Suddick and Six, 2013), which may be closely related to its higher number of micropores (Shi et al., 2016), lower C/P (Vandecasteele et al., 2016) and lower ash content (Gao et al., 2016). The biochar emission reduction of several CR and OW are ranked as follows: corn straw > rice husk and wheat straw > manure and sludge

Table 3
Effect of different types of biochar on soil green house gas emission.

Feedstocks	Pyrolysis Temperature (°C)	Types of Biomass	Types of soil	Greenhouse gas	Emission reduction effect	Reference
Crop waste	700 ± 50	Peanut shell	acidic soil	CO_2, and CH_4	CO_2 reduced from 45 to 35%; CH_4 reduced from 47% to 36%.	Ibrahim et al. (2017)
		Willow, Pine maize And Wood mixture	Silt loam soil	Nox	Reduced both NO (52–84%) and NO_2 (47–67%) emissions	Nelissen et al. (2014)
	500 ± 50	Corn stalk	Paddy	CH_4	Reduced by 61–63%	Feng et al. (2012)
	300 ± 50	Rice straw	Paddy	CH_4	mitigated methane emissions from cow manure-added soil.	Nguyen et al. (2020)
Woody biomass	700 ± 50	Plantation tree	Acidic soil and alkaline soil	N_2O	Acidic soil: reduced by 34% Alkaline soil: reduced by 37%	Lai et al. (2013)
	500 ± 50	Coppiced woodlands (beech, hazel, oak and birch)	Silty-loam	Nox	reduced by 26–76%	Castaldi et al. (2011)
	300 ± 50	Korean pine	Clay-loam	CO_2 and N_2O	no significant effect	Pokharel et al. (2018)
Organic waste	700 ± 50	Sewage sludge	Acidic soil	CO_2, and CH_4	CO_2: reduced from 34 to 27%; CH_4: reduced from 36% to 31%.	Ibrahim et al. (2017)
	500 ± 50	Sewage sludge	Acidic paddy	N_2O & CH_4	Total cumulative N2O emissions have been reduced by 95.6% and 98.4%	Khan et al. (2013)
		Chicken manure	Paddy and Forest	CH_4	Lower moderate soil (30 & 60%) methane emissions are reduced.	Yu et al. (2013)

biochar. Biochar with high DOM content is not suitable for greenhouse gas emission reduction.

5.3. Feedstocks selection recommendations and research limitations

In short, the impact of biochar on soil greenhouse gas emissions is related to its C/N, SSA, mineral content, DOM content, and aromatic. High-temperature WB or CR biochar with a low mineralizable carbon and nitrogen content is the preferred choice for greenhouse gas emission reduction materials.

Current research have mainly studied the effects of biochar on soil greenhouse gas production from the perspective of soil properties (pH, DOC, bulk density, etc.). However, there is a lack of more detailed researches on the effects of biochar properties (porosity, specific surface area, oxygen functional groups, electron transferability, etc.) on greenhouse gas emission reduction, which hinders the construction of the correlation between different biochar and emission reduction rate. Exploring the characteristics of biochar for reducing greenhouse gas emissions will also help to develop new biochar materials, formulate reasonable returning strategies and explore long-term mechanisms for reducing soil greenhouse gas emissions.

6. The effect of biochar application on soil microorganisms

When evaluating the impact of biochar on soil biological characteristics, microbial functional activities and community structure can be regarded as useful indicators. The application of biochar can affect the growth of microorganisms by improving soil properties, such as increasing soil pH, soil porosity, water retention capacity, and nutrients (C, N, P, K, Mg and Ca, etc) (Cayuela et al., 2014). Evaluation of the biome structure in the soil after biochar addition, revealed that feedstocks of biochar and soil are key factors. However, the relationship among the types of biochar, microbial community and soil enzyme activity is still unclear. The next-generation sequencing and meta-omics are promising methods for understanding how changes in the soil microbial composition and functions are affected by different biochars.

6.1. Comparison of community structure changes

In this section, we summarize the effects of biochar on soil microorganism. Table 4 shows the effect of different biochar on soil microecology. The results based on the weighted UniFrac distance matrix confirmed that the feedstocks are the main source of soil fungal community variation, and explains 18.8% of the overall variability ($P < 0.01$) (Yu et al., 2018). In addition, Yu et al. (2018) also proved that cellulose-rich biochar caused the largest priming effect (PE), while peanut-biochar caused the smallest priming effect, including the only negative PE. According to the results, the ratio of cellulose and lignin content might be one of the key factor to explain this difference. In early studies, Phospholipid fatty acid (PLFA) was often used to analyze the composition of soil communities. The increase or decrease in PLFA content is related to the type of biochar and the redox potential of the soil (Bamminger et al., 2014; Xu et al., 2016a). Chen et al. (2013) characterized the microbial distribution structure of biochar added soil using marker gene based analysis and sequencing 16S rRNA and 18S rRNA genes, the result showed that biochar increased bacterial abundance but decreased fungal gene abundance. Gram-positive and gram-negative bacteria use different types of carbon sources, the ratio and abundance of them are important indicators of changes in soil microbial communities. Farrell et al. (2013) found that Gram-negative bacteria prefer to use WB biochar compared to CR biochar, and the ratio of fungi and bacteria in the soil largely depends on the C/N ratio of soil. Biochar can change the microbial community structure by changing the C/N of the metabolic substrate in the soil. Consequently, microorganisms which have the ability to degrade refractory organics (fungi and actinomycetes, etc.) are more likely to be predominant in biochar-amended soils (Khodadad et al., 2011). WB, CR, and OW have identified significantly different lignin and cellulose contents, and biochar derived from them has significantly different induction of soil microorganisms. So far, studies generally believe that the pore structure, ash content, C/N, and DOM content of biochar are the main determinants for the community modifications. Furthermore, the oxygen-containing functional groups on the surface of biochar can act as electron acceptors, affecting the electron transfer process between related microorganisms (denitrifying bacteria, iron-reducing bacteria, etc.) in the soil (Kappler et al., 2014; Yuan et al., 2021). WB biochar has been found to hinder cell-to-cell communication of gram-negative bacteria with agar-based acetic acid regulated by serine acetic acid, and this barrier effect of high-temperature biochar (700 °C) is 10 times higher than for low-temperature biochar (300 °C) (Masiello et al., 2013).

6.2. Comparison of soil enzyme activity changes

Soil enzymes are mainly derived from the secretions of animals, plants, and microorganisms. Their activity roughly reflects the activity of biochemical reactions, microbial activity and nutrient substances in

Table 4
Effect of different types of biochar on soil microbial.

Feedstocks	Pyrolysis Temperature (°C)	Types of Biomass	Types of soil	Soil microbial changes	Mechanism	Reference
Crop residue	700 ± 50	Miscanthus giganteus	Low pH clay loam	ATP increased by 22% and 38% at day 90 and 180, respectively	pH increased from 3.64 to 5.14, and this decreased the toxic concentrations of extractable Al and Mn	Luo et al. (2013)
	500 ± 50	Rice husk	River sediment	Application of biochar reduced bacterial abundance and diversity	The addition of BC changes the characteristics of river sediments, which has a negative impact on microorganisms	Bamminger et al. (2014)
		Rice husk	River sediment	Application of biochar reduced bacterial abundance and diversity	The addition of BC changes the characteristics of river sediments, which has a negative impact on microorganisms	Bamminger et al. (2014)
		maize straw	calcareous soil	The relative abundance of bacteria increased, and the relative abundance of fungi and arbuscular mycorrhizal fungi decreased.	DOC and microbial biomass carbon are the main factors affecting soil microbial biomass	Song et al. (2019)
		Maize straw	Fluvo-aquic soil, light loamy soil	Increased activity of soil extracellular enzymes which involved in C, N, and S cycling	Significantly increased SOC, total N, and exchangeable K	Wang et al. (2015)
		Maize straw	Silt soil	Significantly increased the PLFAs of arbuscular mycorrhizal fungi	SOC ($P < 0.01$), KMnO4–C ($P < 0.01$) and CMI ($P < 0.01$) induced an important impact on the composition of soil microbial communities	Luo et al. (2017)
	300 ± 50	Wheat straw	acid soil	Fungal gene abundance decreases and dehydrogenase and alkaline phosphatase activities increase significantly	The addition of BC increased soil SOC and pH, and also changed the activity of soil enzymes	Chen et al. (2013)
		Corn residue	Calcareous soil	Addition of corn residue biochar significantly increased microbial biomass, and respiration as well as the catalase and dehydrogenase activity,	Appreciably increase soil P and K availability and SOC content	Karimi et al. (2020)
Woody biomass	700 ± 50	Oak pellet	Sandy and clay loam	The abundance of gram-negative bacteria has gradually increased	biochar can potentially improve soil fertility, and BC can act as a substrate for microbial activity	Gomez et al. (2014)
	500 ± 50	Eucalyptus	Field dry soil	MBC decreased significantly, but MBN remained unchanged, and the community structure of ammonia-oxidizing bacteria only changed when biochar and N source were added together.	BC reduces soil MBC, which in turn causes the decomposition of soil organic matter and the reduction of nitrogen mineralization	Dempster et al. (2012)
		Oak and hickory hardwood sawdust	Portneuf silt loam	Biochar has no significant effect on microbial community structure and soil enzyme activity	This biochar has a low nitrogen content, which has little effect on the soil microbial nutrient cycling process	Elzobair et al. (2016)
Organic wastes	700 ± 50	Sewage sludge	High organic matter content and sandy loam texture	β-glucosidase activity diminished in the biochar-amended soils	this enzyme is particularly sensitive to th e additions of sludges and its activity declines exponentially with increasing concentrations of heavy metals	Paz-Ferreiro et al. (2012)
	500 ± 50	husk and paper fiber sludge	calcareous sandy soil; acidic sandy soil	Biochar increased microbial activity, and the respiration activity of acidic sandy soil was higher than that of calcareous soil	Biochar significantly increased the nutrient concentration and provided a more livable habitat for microorganisms in acidic sandy soil	Farkas et al. (2020)
	300 ± 50	swine manure	Clay-loam soil	Increased the abundance of bacteria and fungi, the growth rate of bacteria is faster than that of fungi	The addition of MB reduced the nitrogen utilization rate in the soil	Liang et al. (2018)

soil, which are important indicators of soil quality (Burns et al., 2013). Soil enzyme activity is affected by soil nutrient content, pH, CEC, water holding capacity and pore structure. Previous studies have shown that biochar can increase soil enzyme activity. Oleszczuk et al. (2014) found that when the application rate of wheat straw biochar is 30 t hm^{-2}, it can significantly increase the activities of soil dehydrogenase, urease, protease and alkaline phosphatase, whereas has no significant effect on the activity of acid phosphatase, and when the application rate rises to 45 t hm^{-2}, the activities of soil dehydrogenase, protease and alkaline phosphatase start declining. Ameloot et al. (2014) found that high temperature (700 °C) and low temperature (350 °C) biochar have different effects on soil dehydrogenase enzyme activity, indicating that the effect of biochar on soil enzyme activity varies with biochar type and soil enzyme types. Biochar contains P, K, Mg and other nutrients which can promote soil microbial activity, thereby improving global enzymatic activity in the soil (Lehmann et al., 2011). Because of the strong sorption performance of biochar, it also increases the complexity of soil enzymes. the sorption of biochar to the reaction substrate helps the enzymatic reaction and promotes soil enzyme activity. On the other hand, the sorption of enzymes on biochar can reduce the availability of the binding sites, which are crucial for catalyzing enzymatic reactions, thereby inhibiting the progress of enzymatic reactions (Bailey et al., 2011; Lehmann and Joseph, 2015). However, due to the wide variety of soil enzymes and biochar types, it is difficult to draw conclusions about the causal relationship between these two. Biochar can also protect soil microorganisms from grazing. Previous studies (Baran et al., 2004; Gianfreda and Rao, 2008) revealed that biochar can fix and inactivate enzymes produced by *Fusarium oxysporum f. sp. radicislycopersici*,

thereby degrading cell walls and protecting crops from soil pathogens (Jaiswal et al., 2020). However, excessive application of biochar may introduce toxic substances (heavy metals and polycyclic aromatic hydrocarbons etc.) into the soil, thereby inhibiting the activity of soil enzymes, which has to be considered in the future application of biochar. Another research focus point after biochar application is the relationship between plant rhizosphere soil microorganisms and enzyme activities. Lehmann et al. (2017) believe that adding biochar to the soil can promote the formation of symbiosis between bacteria and other mycorrhizas and improve the bacterial diversity in the soil ecosystem.

6.3. Feedstocks selection recommendations and research limitations

The impact of biochar on soil microorganisms is closely related to its pore structure, ash content, C/N, and DOM content, nutrients. In general, gram-negative bacteria in the soil are more inclined to use WB biochar with high lignin content, but high-temperature WB biochar may form a barrier to the communication between cells and may prevent the process of enzymatic reactions due to high adsorption. From the perspective of promoting enzyme activity, organic waste rich in P, K, Mg, and other nutrients is a better choice. Combining the optimized functional microorganisms to prepare biochar inoculum materials is a field worth further exploring.

So far, the research on biochar and microbial activity and interaction in soil has mainly focused on small-scale laboratory incubation and greenhouse pot experiment. In addition, depending on the type of biochar, soil type, and microbial composition, the interaction of microorganisms with soil and plants may vary greatly. Research on the interaction of microorganisms with various biochars, different biochar application rates, and different plant species is still lacking. The development of technologies such as metagenomics and metatranscriptomics makes the research on the effect of biochar on soil microbiome, functions, and enzyme activities more available (Jansson and Hofmockel, 2018). However, it is still hard to distinguish the effects of biochar on specific soil biological characteristics or specific soil microorganisms in the complex microbial community. Fluorescence in situ hybridization (FISH) and nanoscale secondary ion mass spectrometry (NanoSIMs) can provide technical support for the advancement of this research investigation (Dubey et al., 2020; Zumstein et al., 2018). Soil components and properties have different effects on the living habitats and functions of different bacterial populations. Changes in bacterial communities may cause changes in soil enzyme activity. Therefore, soil nutrient content, enzyme activity and the relative abundance of bacterial communities are closely related. At present, there is no accurate correlation between different feedstocks of biochar and soil microbial activities. More comparable research should be done in this area.

7. Stability and potential toxicity of biochar in soil environment

7.1. Comparison of the long-term stability of different biochar

The stability of biochar in the environment determines the stability of the environmental remediation effect. Generally, biochar contains two parts of carbon: stable-C (high resistance to mineralization) and unstable-C (low resistance to mineralization) (Wei et al., 2019). Therefore, discussing the stability of biochar in soil is inseparable from discussing its impact on organic carbon (OC). The large-scale application of biochar in the soil would inevitably affect the amount and composition of soil organic carbon. Generally, the stability of biochar in the soil will be affected by physical decomposition, chemical decomposition, and biological decomposition. Most of researches have focused on the chemical and biological decomposition of biochar in the soil (Chen et al., 2019a; Kuzyakov et al., 2014), but there is still a lack of clear understanding of the differences in the long-term environmental stability of biochar induced by different feedstocks.

Biochar shows different stability with different chemical structures. The percentage of mineralized OC of biochar from OW and CR (average: 4.35%) is often higher than that of WB-based biochar (average: 1.52%) (Han et al., 2020), which is related to the content of lignin in the feedstocks. In addition, the mineralization rate of biochar in the soil will decrease with the increase of pyrolysis temperature, this is related to the increases of biochar aromatic condensation (Singh et al., 2012). In addition, the active minerals in the soil (such as phyllosilicate and iron oxide) can interact with biochar to form a complex and affect its stability (Han et al., 2016). The organic carbon derived from biochar can be combined with the soil background organic matter, and the stable OC in biochar will directly change the composition of soil organic matter through physical mixing. In addition, biochar can interact with soil organic carbon to protect them from being used by microorganisms. Table 5 further compares the organic matter released by different biochar and its impact on the soil environment.

From Table 5, humic acid, fulvic acid, microbial by-products, aromatic proteins and tryptophan-like components were identified in the DOM derived from biochar (Gui et al., 2020; Li et al., 2017c). As the pyrolysis temperature of manure biochar increases, the protein-like substances of biochar first decrease and then increase, while the humic acid substances show the opposite trend. The characterization of DOM extracted from lignocellulose-rich biochar shows that increasing the pyrolysis temperature from 300 °C to 700 °C can lead to an increase in the aromaticity of DOM and a decrease in the content of phenol and carboxyl groups (Wei et al., 2020a). In addition, research further shows that the aliphatic and fulvic acid-like compounds in biochar-derived DOM decrease with the increase of pyrolysis temperature, while fused polycyclic aromatic hydrocarbons, humic acids, and soluble microbial by-products increase at the same time (Zhang et al., 2020a). In addition to changes in DOM content and mineralization, the application of biochar in the soil can also affect the composition of soil natural DOM. It is foreseeable that the participation of biochar in the soil system would affect the overall biodegradability of SOM, the dissimilation reduction reaction, and the sorption of pollutants in the soil.

7.2. Comparison of potential toxicity of different biochar

Previous studies have confirmed that biochar contains a variety of pollutants, such as polycyclic aromatic hydrocarbons (PAHs), potentially toxic elements (PTEs), dioxins, volatile organic compounds (VOCs) (Considering its volatility, its toxicity in the soil environment would not be discussed emphatically in this section.), persistent free radicals (PFR), and metal cyanide (MCN) (Freddo et al., 2012; Godlewska et al., 2021).

PAHs are the most common pollutants from biochar, which are classified as one of the persistent organic pollutants (POPs). The decomposition and subsequent recombination reactions of biomass during the pyrolysis process generate PAHs. Hale et al. (2012) compared the content of available PAHs in biochar derived from 23 different feedstocks in the temperature range of 250–900 °C. Among them, food waste biochar has the highest concentration (10.0 ng/L) of available PAHs and pine wood biochar shows the lowest concentration (0.17 ng/L). The characterization of sewage sludge biochar (500–700 °C) found that its PAHs concentration ranged from 81 ng/L to 126 ng/L, and tricyclic PAHs occupy a dominant position in the bioavailable PAHs (Zielińska and Oleszczuk, 2016).

PTEs, such as As, Cd, Cr, Co, Cu, Pb, Hg, Ni, Zn, and Mo, is another major pollutant in biochar, and their enrichment in biochar may constitute a threat to soil microorganisms and plants (Shaheen et al., 2019). The content of PTEs in biochar depends on the initial concentration of PTE in the feedstocks. After the pyrolysis process, most of the PTE is concentrated in biochar (Shen et al., 2020). In general, biochar derived from CR and WB shows relatively low PTE levels (Except for phytoremediation residues (Huang et al., 2018)), while OW have higher initial PTE levels (Huang et al., 2020; Meng et al., 2018), so the PTE content of biochar produced is also relatively high. Currently, the co-pyrolysis of mixed high-PTE and low-PTE biomass is an effective

Table 5
DOM characteristics of different biochar and its influence on soil.

Feedstocks	Pyrolysis Temperature (°C)	Types of Biomass	Types of soil	DOM composition of biochar	Impact on the soil	Reference
Crop residue	700 ± 50	Wheat straw	Loamy sand soil	Humic-like (%): 18.30 ± 0.30 More conjugated bonds: 3.66 ± 0.01 humic acid with highly aromatic (%): 78.10 ± 0.30	Reduced the amount of soil DOM (2.6–12.7 mg L^{-1})	Feng et al. (2021)
	500 ± 50	Cacao shell Rice husk	Acidic and neutral agricultural soils	NA	Increased soil DOC concentration (4.5–69 mg L^{-1}); increased the molecular size and aromaticity of soil DOM	Smebye et al. (2016)
		Wheat straw	Vegetable farm soil	TOC:97.5 (mg L^{-1}) Hydrophobic: 0.315 Biopolymer: 0.007 Humics: 0.256 Building blocks: 0.145 LMW-neutrals: 0.200 LMW-acids: 0.077	Crop yield increased by 22.56%	Bian et al. (2019)
	300 ± 50	Rice straw	Framland soil	Both fulvic and protein-like substance were dominant in biochar-derived DOM whereas humic-like was presented at the lowest level.	Specific fluorescent components in DOM can promote its complexation with heavy metals	Huang et al. (2019)
		Wheat straw	Loamy sand soil	Humic-like (%): 55.80 ± 0.60 More conjugated bonds: 19.50 ± 0.90 humic acid with highly aromatic (%): 24.70 ± 0.30	Increased soil DOM (3.1–12.2 mg L^{-1}).	Feng et al. (2021)
Woody biomass	800–1000	Wood chips	HMs contaminated Soil	NA	Soil DOC increased by 27%; Increased tryptophan-like abundance	Yang et al. (2019)
	500 ± 50	Fir tree Lignin	As contaminated soil	Sawdust TOC: 175–504 mg L^{-1} Lignin TOC: 41–304 mg L^{-1} The amount of oxalic acid decreased with increased lignin content of biomass	Biochar increased the concentration of soil DOM, which not only enhanced the reduction of iron, but also increased As Liquidity (1.4–7.4 times)	Kim et al. (2020)
		Mixed woodchips	sandy loam	NA	Enhance the mobility of Mo and As	Kloss et al. (2015)
Organic wastes	700 ± 50	Cow manure	Loamy sand soil	Humic-like (%): 65.10 ± 0.10 More conjugated bonds: 2.64 ± 0.13 humic acid with highly aromatic (%): 32.2 ± 0.2	Reduced the amount of soil DOM (2.8–9.0 mg L^{-1}).	Feng et al. (2021)
	500 ± 50	Compost	Paddy soil and sandy soil	DOM is constituted by highly humified molecules	Decreased liquidity of pesticides	García-Jaramillo et al. (2014)
	300 ± 50	Sewage sludge	Agricultural field soil	•Tryptophan-like •UVA humic-like substance and UVC humic-like substance	Increased the proportion of protein-like components in soil DOM (SSB3 > SSB5); Decreased the Cu(II) complexation capacities of soil DOM (SSB3 > SSB5)	Xing et al. (2020)
		Cow manure	Loamy sand soil	Tryptophan-like (%):11.50 ± 0.20 Humic-like (%): 59.10 ± 0.50 More conjugated bonds: 29.50 ± 0.30	Increased soil DOM (3.6–13.7 mg L^{-1}).	Feng et al. (2021)

strategy to reduce the PTE content of biochar. For example, after co-pyrolysis of woody biomass and sewage sludge with high PTEs, the PTEs content of the resulting mixed biochar is reduced (Jin et al., 2017). In addition, high-temperature pyrolysis would evaporate part of PTE with low-boiling point, reducing the ecological risk of biochar (Buss et al., 2016).

PFR is abundant and ubiquitous in various of biochar (Liao et al., 2014). As an emerging pollutant, PFR can induce the formation of reactive oxygen species, which in turn poses a huge risk to the agricultural environment and ecosystem health. Generally, the content of PFRs in biochar increases with the increase of pyrolysis temperature (300–600 °C), and then drops sharply at 700 °C (Tao et al., 2020). Lignin, cellulose, and hemicellulose are the main precursors to control the formation of PFR in biochar (Nzihou et al., 2013). The abundant phenol or quinone moiety in biochar can induce the formation of PFR on the surface of biochar by transferring electrons to transition metals (Fang et al., 2014). It can be seen that the high proportion of lignin in biomass (e.g. crop waste) is the main contributor to the PFR of biochar, and some organic wastes containing transition metals or phenolic compounds are also prone to form PFR. Due to the electron transfer between the carbon surface and microbial cells during the pollutant remediation process, the reaction induced by PFRs may change the microbial community structure, which may cause potential toxicity to certain soil microorganisms. It is necessary to pay special attention to the toxicity and negative effects of PFR when using it to degrade pollutants.

Organic nitrogen and metal can combine to form metal cyanide (MCN) (Luo et al., 2019), a highly toxic substance. Metal elements and organic nitrogen are commonly found in biomass from food waste, sludge, fungal residues, and algae. The corresponding biochar produced from them carries MCN (Luo et al., 2020). Moreover, special attention should be paid to the biochar prepared from biomass rich in unstable alkali metal salts such as Na_2CO_3, K_2CO_3, and K_2SO_4, because they can combine with the organic nitrogen in the biomass to produce MOCN, Then MCN is generated by carbothermal reduction (Han et al., 2021). Luo et al. (2020) proposed that the use of metal chloride salts is an efficient and low-cost technology to inhibit the production of CN-biochar. At present, there are few studies on the long-term toxicity and ecological risks of MAN contained in biochar. If engineering applications are considered, more relevant verifications are needed.

It is worth noting that what we mentioned above are mainly the toxic substances contained in biochar. The actual environmental toxicity should be based on its availability degree. Although the formation of PAHs is inevitable due to the production of biochar, the level of

bioavailable PAHs in biochar is not so high. For PTEs in biochar, some available part of PTE is gradually transformed into a stable part after pyrolysis (Zhang et al., 2020b), reducing the risk of leaching. The level of toxicity in biochar depends on the feedstocks and pyrolysis temperature. For PTE-rich biomass, such as food waste, sewage sludge, pig manure, and phytoremediation residues, Co-pyrolysis with low PTE feedstocks (such as woody biomass, crop residues) reduces the levels of PTE (PFR controlling can also follow this strategy). For PFR, high pyrolysis temperature can effectively reduce its content. In addition, since natural organic matter or clay particles can inactivate PFR in biochar, clay-biochar composites probably be good candidates for soil amendments in the future. For MCN, avoiding the use of biomass containing unstable oxygen-containing alkali salts can effectively limit the level of MCN in biochar. Since biochar has a variety of complex toxic substances, it is still very challenging to get the correlation between different kinds of substances and specific soil pollution. In general, if the strategy of feedstocks selection and biochar production is followed, the environmental toxicity of biochar can be considered ignorable, and this risk should not hinder the application of biochar in the engineering field in the future.

8. Conclusion

This review emphasizes the remediation effect of biochar from different feedstocks on various types of soil pollution: organic pollution, heavy metal pollution, reduction of greenhouse gas emission and soil microbial community structure, which are usually considered as important aspects of biochar application. Although the application of

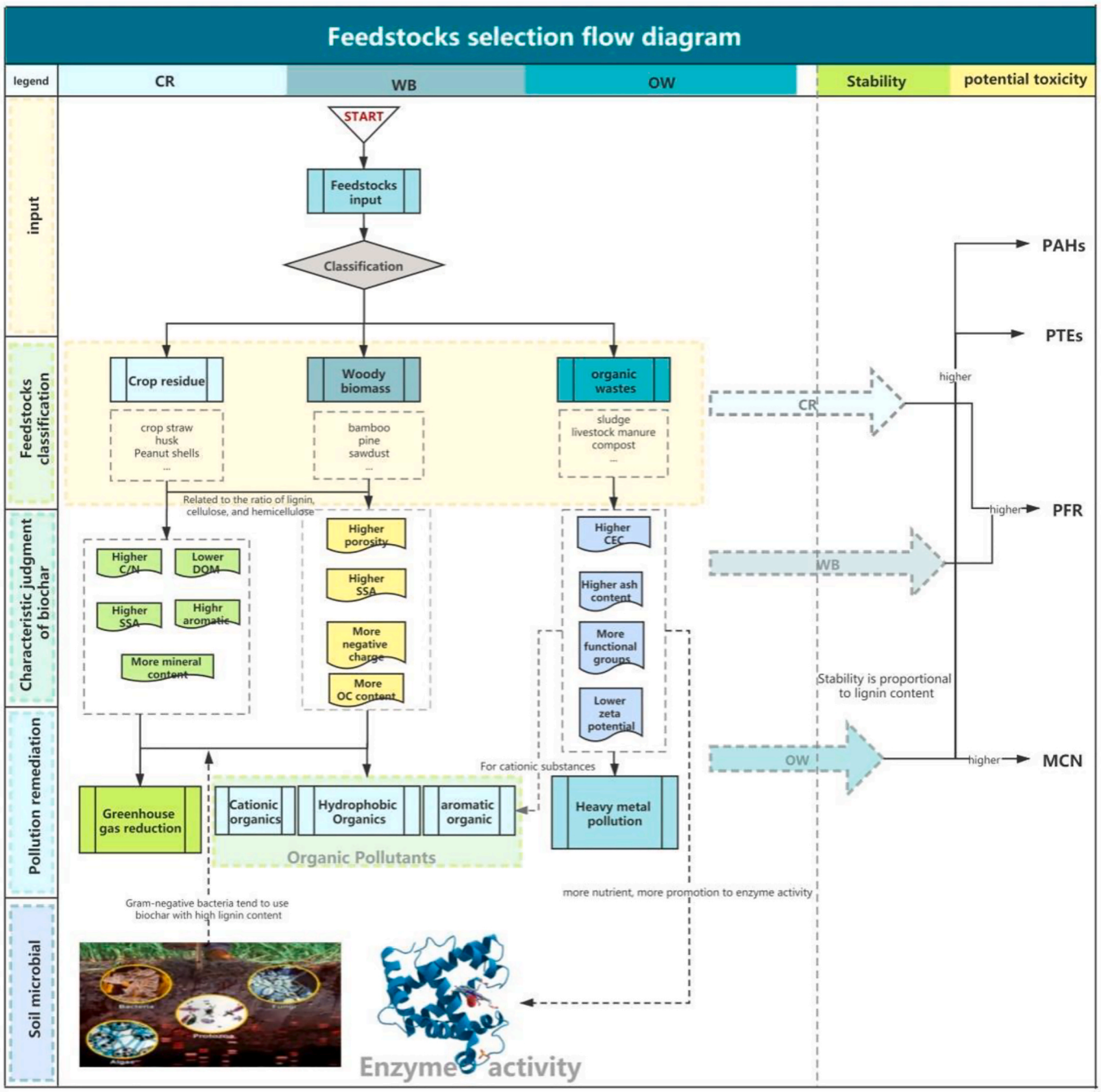

Fig. 3. Flow diagram of feedstocks selection.

biochar in various fields has been reviewed individually, the rapid renovation of scientific knowledge on different biochar encourage us to summarize the issues to optimizing the biochar properties for specific pollution. woody biomass contain high lignin content, while organic wastes such as animal manure and sludge have a higher content of mineral elements, ash, and nutrients. It is because of these differences in properties that different biochar have varying effects on soil remediation.

Our recommendations regarding feedstocks selection are shown in Fig. 3, when biochar are used in the organics adsorption, WB and CR biochar generally exhibits superior sorption performance due to the existence of the pore-filling mechanism, while OW biochar such as manure exhibits a better adsorption efficiency of cationic dyes due to its high ash content. As for the remediation of soil heavy metal pollution, statistical results show that OW (manure and sludge biochar) biochar is more suitable than woody biochar, but the stability of biochar should be specially considered in practical applications. The effect of biochar on greenhouse gas emission reduction is closely related to its porosity, H/C, and C/N ratio. In general, WB biochar shows better emission reduction effects than CR and OW-based biochar. In terms of soil microorganisms, gram-negative bacteria in the soil prefer to use WB biochar than CR biochar. Additionally, soil enzyme activity is closely related to the content of P, K, Mg, and other nutrients in biochar.

8.1. *Future perspectives*

The main objects discussed in this review are individual feedstocks. On this basis, strengthening the research on mixed materials or loaded materials and promoting the development of modified biochar can expand the application of biochar in the field of environmental remediation. More research combines catalytic technology or biodegradation technology with biochar preparation, providing a new perspective for environmental pollution remediation. For example, biochar combined with *Pseudomonas* sp shows good performance in fixing Cd and Cu in soil (Tu et al., 2020). Magnetic biochar can promote the removal of attached metals in aging microplastics in some cases (Ye et al., 2020b). Therefore, further modification of selected feedstocks to enhance the removal of emerging pollutants is a research direction worth investigating in the future.

In future research, there are still some issues that need attention:

First, the potential toxicity in the biochar still needs to be paid attention to (PAHs, PTEs, ((PAHs, PTEs, PFR), and MCN, etc.). These pollutants are basically derived from biomass, so the biomass raw materials need to be screened and pretreated. Although this review gives some suggestions for the selection of feedstocks, the relationship between some process parameters (pyrolysis temperature, residence time, pyrolysis atmosphere, pressure conditions, etc.) and secondary pollutants is still not so clear. In addition, does the treated biochar have an antagonistic effect with other target compounds in the environment, and whether the modified biochar may cause secondary pollution to the environment? Is it possible for the adsorbed pollutants to be desorbed again? How to separate the treated biochar from the water or soil environment? These are all issues worth considering.

Second, the soil environment is more complex. Biochar may react with soil components, such as soil minerals and organic matter, plant roots, earth organisms, and soil microorganisms (Joseph et al., 2010). The research between biochar with different characteristics and soil microbiome is still scarce, especially the intervention of biochar on soil microbial function and enzyme activity. More advanced technologies can be applied in the future to study the relationship between biochar and soil microorganisms.

Third, most of the current research is conducted on a laboratory scale. Therefore, more research is needed to focus on field soil remediation under natural conditions to fully understand the behavior of biochar under actual conditions. Various biochars with different physical and chemical properties have been tested for their ability to remove pollutants from soil and water. There is no conclusive evidence that there is optimal biochar for the target pollutants. A lot of work is required to ensure the specific use and accuracy of biochar in terms of biochar type, preparation conditions, application rate, application time, and recovery procedures.

Credit author statement

Mengyuan Ji: Conceptualization, Methodology, Writing. **Xiaoxia Wang, Muhammad Usman:** Data curation, Writing – original draft. **Feihong Liu:** Data curation, Investigation. **Yitong Dan, Lei Zhou:** Data curation. **Stefano Campanaro, Gang Luo:** Supervision. **Wenjing Sang:** Conceptualization, Writing- Reviewing and Editing.

Declaration of competing interest

The authors declare that they have no known competing financial interests or personal relationships that could have appeared to influence the work reported in this paper.

Acknowledgements

The authors would like to acknowledge the support provided by the Fundamental Research Funds for the Central Universities of China (No. 2232018D3-15), China Scholarship Council (No. 202008310162) and State Key Laboratory of Pollution Control and Resource Reuse Foundation (No. PCRRF19001).

Appendix A. Supplementary data

Supplementary data to this article can be found online at https://doi.org/10.1016/j.envpol.2021.118655.

References

Abagandura, G.O., Chintala, R., Sandhu, S.S., Kumar, S., Schumacher, T.E., 2019. Effects of biochar and manure applications on soil carbon dioxide, methane, and nitrous oxide fluxes from two different soils. J. Environ. Qual. 48, 1664–1674.

Abbas, Z., Ali, S., Rizwan, M., Zaheer, I.E., Malik, A., Riaz, M.A., et al., 2018. A critical review of mechanisms involved in the adsorption of organic and inorganic contaminants through biochar. Arab. J. Geosci. 11, 448.

Agrafioti, E., Bouras, G., Kalderis, D., Diamadopoulos, E., 2013. Biochar production by sewage sludge pyrolysis. J. Anal. Appl. Pyrol. 101, 72–78.

Ahmad, M., Lee, S.S., Oh, S.-E., Mohan, D., Moon, D.H., Lee, Y.H., et al., 2013. Modeling adsorption kinetics of trichloroethylene onto biochars derived from soybean stover and peanut shell wastes. Environ. Sci. Pollut. Control Ser. 20, 8364–8373.

Ahmad, M., Ok, Y.S., Kim, B.-Y., Ahn, J.-H., Lee, Y.H., Zhang, M., et al., 2016. Impact of soybean stover-and pine needle-derived biochars on Pb and as mobility, microbial community, and carbon stability in a contaminated agricultural soil. J. Environ. Manag. 166, 131–139.

Ahmad, M., Rajapaksha, A.U., Lim, J.E., Zhang, M., Bolan, N., Mohan, D., et al., 2014. Biochar as a sorbent for contaminant management in soil and water: a review. Chemosphere 99, 19–33.

Ahmed, M.B., Zhou, J.L., Ngo, H.H., Johir, M.A.H., Sun, L., Asadullah, M., et al., 2018. Sorption of hydrophobic organic contaminants on functionalized biochar: protagonist role of π-π electron-donor-acceptor interactions and hydrogen bonds. J. Hazard Mater. 360, 270–278.

Al Afif, R., Anayah, S.S., Pfeifer, C., 2020. Batch pyrolysis of cotton stalks for evaluation of biochar energy potential. Renew. Energy 147, 2250–2258.

Ameloot, N., Maenhout, P., De Neve, S., Sleutel, S., 2016. Biochar-induced N2O emission reductions after field incorporation in a loam soil. Geoderma 267, 10–16.

Ameloot, N., Sleutel, S., Case, S.D., Alberti, G., McNamara, N.P., Zavalloni, C., et al., 2014. C mineralization and microbial activity in four biochar field experiments several years after incorporation. Soil Biol. Biochem. 78, 195–203.

Amin, F.R., Huang, Y., He, Y., Zhang, R., Liu, G., Chen, C., 2016. Biochar applications and modern techniques for characterization. Clean Technol. Environ. Policy 18, 1457–1473.

Anyika, C., Majid, Z.A., Ibrahim, Z., Zakaria, M.P., Yahya, A., 2015. The impact of biochars on sorption and biodegradation of polycyclic aromatic hydrocarbons in soils—a review. Environ. Sci. Pollut. Control Ser. 22, 3314–3341.

Ashry, A., Bailey, E.H., Chenery, S., Young, S.D., 2016. Kinetic study of time-dependent fixation of UVI on biochar. J. Hazard Mater. 320, 55–66.

Aslam, Z., Khalid, M., Aon, M., 2014. Impact of biochar on soil physical properties. Sch. J. Agric. Sci. 4, 280–284.

Bailey, V.L., Fansler, S.J., Smith, J.L., Bolton Jr., H., 2011. Reconciling apparent variability in effects of biochar amendment on soil enzyme activities by assay optimization. Soil Biol. Biochem. 43, 296–301.
Bamminger, C., Zaiser, N., Zinsser, P., Lamers, M., Kammann, C., Marhan, S., 2014. Effects of biochar, earthworms, and litter addition on soil microbial activity and abundance in a temperate agricultural soil. Biol. Fertil. Soils 50, 1189–1200.
Banik, C., Lawrinenko, M., Bakshi, S., Laird, D.A., 2018. Impact of pyrolysis temperature and feedstock on surface charge and functional group chemistry of biochars. J. Environ. Qual. 47, 452–461.
Baran, S., Bielińska, J.E., Oleszczuk, P., 2004. Enzymatic activity in an airfield soil polluted with polycyclic aromatic hydrocarbons. Geoderma 118, 221–232.
Bashir, S., Hussain, Q., Akmal, M., Riaz, M., Hu, H., Ijaz, S.S., et al., 2018. Sugarcane bagasse-derived biochar reduces the cadmium and chromium bioavailability to mash bean and enhances the microbial activity in contaminated soil. J. Soils Sediments 18, 874–886.
Beesley, L., Moreno-Jiménez, E., Gomez-Eyles, J.L., 2010. Effects of biochar and greenwaste compost amendments on mobility, bioavailability and toxicity of inorganic and organic contaminants in a multi-element polluted soil. Environ. Pollut. 158, 2282–2287.
Bian, R., Joseph, S., Shi, W., Li, L., Taherymoosavi, S., Pan, G., 2019. Biochar DOM for plant promotion but not residual biochar for metal immobilization depended on pyrolysis temperature. Sci. Total Environ. 662, 571–580.
Burns, R.G., DeForest, J.L., Marxsen, J., Sinsabaugh, R.L., Stromberger, M.E., Wallenstein, M.D., et al., 2013. Soil enzymes in a changing environment: current knowledge and future directions. Soil Biol. Biochem. 58, 216–234.
Buss, W., Graham, M.C., Shepherd, J.G., Mašek, O., 2016. Suitability of marginal biomass-derived biochars for soil amendment. Sci. Total Environ. 547, 314–322.
Cao, Y., Yang, B., Song, Z., Wang, H., He, F., Han, X., 2016. Wheat straw biochar amendments on the removal of polycyclic aromatic hydrocarbons (PAHs) in contaminated soil. Ecotoxicol. Environ. Saf. 130, 248–255.
Castaldi, S., Riondino, M., Baronti, S., Esposito, F., Marzaioli, R., Rutigliano, F.A., et al., 2011. Impact of biochar application to a Mediterranean wheat crop on soil microbial activity and greenhouse gas fluxes. Chemosphere 85, 1464–1471.
Cayuela, M., Van Zwieten, L., Singh, B., Jeffery, S., Roig, A., Sánchez-Monedero, M., 2014. Biochar's role in mitigating soil nitrous oxide emissions: a review and meta-analysis. Agric. Ecosyst. Environ. 191, 5–16.
Cely, P., Gascó, G., Paz-Ferreiro, J., Méndez, A., 2015. Agronomic properties of biochars from different manure wastes. J. Anal. Appl. Pyrol. 111, 173–182.
Cerniglia, C.E., 1992. Biodegradation of polycyclic aromatic hydrocarbons. Biodegradation 3, 351–368.
Chaukura, N., Murimba, E.C., Gwenzi, W., 2017. Synthesis, characterisation and methyl orange adsorption capacity of ferric oxide–biochar nano-composites derived from pulp and paper sludge. Appl. Water Sci. 7, 2175–2186.
Chen, C., Liu, G., An, Q., Lin, L., Shang, Y., Wan, C., 2020. From wasted sludge to valuable biochar by low temperature hydrothermal carbonization treatment: insight into the surface characteristics. J. Clean. Prod. 121600.
Chen, D., Guo, H., Li, R., Li, L., Pan, G., Chang, A., et al., 2016. Low uptake affinity cultivars with biochar to tackle Cd-tainted rice—a field study over four rice seasons in Hunan, China. Sci. Total Environ. 541, 1489–1498.
Chen, G., Wang, X., Zhang, R., 2019a. Decomposition temperature sensitivity of biochars with different stabilities affected by organic carbon fractions and soil microbes. Soil Tillage Res. 186, 322–332.
Chen, J., Liu, X., Zheng, J., Zhang, B., Lu, H., Chi, Z., et al., 2013. Biochar soil amendment increased bacterial but decreased fungal gene abundance with shifts in community structure in a slightly acid rice paddy from Southwest China. Appl. Soil Ecol. 71, 33–44.
Chen, Q., Rao, P., Cheng, Z., Yan, L., Qian, S., Song, R., et al., 2019b. Novel soil remediation technology for simultaneous organic pollutant catalytic degradation and nitrogen supplementation. Chem. Eng. J. 370, 27–36.
Chen, T., Luo, L., Deng, S., Shi, G., Zhang, S., Zhang, Y., et al., 2018. Sorption of tetracycline on H3PO4 modified biochar derived from rice straw and swine manure. Bioresour. Technol. 267, 431–437.
Chen, X., Yang, L., Myneni, S.C., Deng, Y., 2019c. Leaching of polycyclic aromatic hydrocarbons (PAHs) from sewage sludge-derived biochar. Chem. Eng. J. 373, 840–845.
Cui, L., Li, L., Zhang, A., Pan, G., Bao, D., Chang, A., 2011. Biochar amendment greatly reduces rice Cd uptake in a contaminated paddy soil: a two-year field experiment. BioResources 6, 2605–2618.
Cui, L., Pan, G., Li, L., Bian, R., Liu, X., Yan, J., et al., 2016. Continuous immobilization of cadmium and lead in biochar amended contaminated paddy soil: a five-year field experiment. Ecol. Eng. 93, 1–8.
Cui, L., Pan, G., Li, L., Yan, J., Zhang, A., Bian, R., et al., 2012. The reduction of wheat Cd uptake in contaminated soil via biochar amendment: a two-year field experiment. Bioresources 7, 5666–5676.
Dai, Y., Zhang, N., Xing, C., Cui, Q., Sun, Q., 2019. The adsorption, regeneration and engineering applications of biochar for removal organic pollutants: a review. Chemosphere 223, 12–27.
Dempster, D., Gleeson, D., Zi, Solaiman, Jones, D., Murphy, D., 2012. Decreased soil microbial biomass and nitrogen mineralisation with Eucalyptus biochar addition to a coarse textured soil. Plant Soil 354, 311–324.
Devi, P., Saroha, A.K., 2015. Effect of pyrolysis temperature on polycyclic aromatic hydrocarbons toxicity and sorption behaviour of biochars prepared by pyrolysis of paper mill effluent treatment plant sludge. Bioresour. Technol. 192, 312–320.
Dhaliwal, S.S., Singh, J., Taneja, P.K., Mandal, A., 2020. Remediation techniques for removal of heavy metals from the soil contaminated through different sources: a review. Environ. Sci. Pollut. Control Ser. 27, 1319–1333.
Domingues, R.R., Trugilho, P.F., Silva, C.A., Melo, ICNd, Melo, L.C., Magriotis, Z.M., et al., 2017. Properties of biochar derived from wood and high-nutrient biomasses with the aim of agronomic and environmental benefits. PLoS One 12, e0176884.
Dubey, R.K., Tripathi, V., Prabha, R., Chaurasia, R., Singh, D.P., Rao, C.S., et al., 2020. Methods for Exploring Soil Microbial Diversity. Unravelling the Soil Microbiome. Springer, pp. 23–32.
Dutta, T., Kwon, E., Bhattacharya, S.S., Jeon, B.H., Deep, A., Uchimiya, M., et al., 2017. Polycyclic aromatic hydrocarbons and volatile organic compounds in biochar and biochar-amended soil: a review. Gcb Bioenergy 9, 990–1004.
Egene, C.E., Van Poucke, R., Ok, Y.S., Meers, E., Tack, F., 2018. Impact of organic amendments (biochar, compost and peat) on Cd and Zn mobility and solubility in contaminated soil of the Campine region after three years. Sci. Total Environ. 626, 195–202.
El-Gamal, E.H., Saleh, M., Elsokkary, I., Rashad, M., Abd El-Latif, M.M., 2017. Comparison between properties of biochar produced by traditional and controlled pyrolysis. Alexandria Sci. Exch. J 38, 412–425.
El-Naggar, A., El-Naggar, A.H., Shaheen, S.M., Sarkar, B., Chang, S.X., Tsang, D.C., et al., 2019. Biochar composition-dependent impacts on soil nutrient release, carbon mineralization, and potential environmental risk: a review. J. Environ. Manag. 241, 458–467.
Elzobair, K.A., Stromberger, M.E., Ippolito, J.A., Lentz, R.D., 2016. Contrasting effects of biochar versus manure on soil microbial communities and enzyme activities in an Aridisol. Chemosphere 142, 145–152.
Fan, Q., Sun, J., Chu, L., Cui, L., Quan, G., Yan, J., et al., 2018. Effects of chemical oxidation on surface oxygen-containing functional groups and adsorption behavior of biochar. Chemosphere 207, 33–40.
Fang, G., Gao, J., Liu, C., Dionysiou, D.D., Wang, Y., Zhou, D., 2014. Key role of persistent free radicals in hydrogen peroxide activation by biochar: implications to organic contaminant degradation. Environ. Sci. Technol. 48, 1902–1910.
Fang, G., Liu, C., Gao, J., Dionysiou, D.D., Zhou, D., 2015. Manipulation of persistent free radicals in biochar to activate persulfate for contaminant degradation. Environ. Sci. Technol. 49, 5645–5653.
Farkas, É., Feigl, V., Gruiz, K., Vaszita, E., Fekete-Kertész, I., Tolner, M., et al., 2020. Long-term effects of grain husk and paper fibre sludge biochar on acidic and calcareous sandy soils–A scale-up field experiment applying a complex monitoring toolkit. Sci. Total Environ. 731, 138988.
Farrell, M., Kuhn, T.K., Macdonald, L.M., Maddern, T.M., Murphy, D.V., Hall, P.A., et al., 2013. Microbial utilisation of biochar-derived carbon. Sci. Total Environ. 465, 288–297.
Feng, Y., Xu, Y., Yu, Y., Xie, Z., Lin, X., 2012. Mechanisms of biochar decreasing methane emission from Chinese paddy soils. Soil Biol. Biochem. 46, 80–88.
Feng, Z., Fan, Z., Song, H., Li, K., Lu, H., Liu, Y., et al., 2021. Biochar induced changes of soil dissolved organic matter: the release and adsorption of dissolved organic matter by biochar and soil. Sci. Total Environ. 783, 147091.
Foo, K., Hameed, B., 2012. Microwave-assisted regeneration of activated carbon. Bioresour. Technol. 119, 234–240.
Freddo, A., Cai, C., Reid, B.J., 2012. Environmental contextualisation of potential toxic elements and polycyclic aromatic hydrocarbons in biochar. Environ. Pollut. 171, 18–24.
Fu, H., Ma, S., Zhao, P., Xu, S., Zhan, S., 2019. Activation of peroxymonosulfate by graphitized hierarchical porous biochar and MnFe2O4 magnetic nanoarchitecture for organic pollutants degradation: structure dependence and mechanism. Chem. Eng. J. 360, 157–170.
Gao, S., Hoffman-Krull, K., Bidwell, A., DeLuca, T., 2016. Locally produced wood biochar increases nutrient retention and availability in agricultural soils of the San Juan Islands, USA. Agric. Ecosyst. Environ. 233, 43–54.
Gao, X., Peng, Y., Zhou, Y., Adeel, M., Chen, Q., 2019. Effects of magnesium ferrite biochar on the cadmium passivation in acidic soil and bioavailability for packoi (Brassica chinensis L.). J. Environ. Manag. 251, 109610.
García-Jaramillo, M., Cox, L., Cornejo, J., Hermosín, M., 2014. Effect of soil organic amendments on the behavior of bentazone and tricyclazole. Sci. Total Environ. 466, 906–913.
García-Jaramillo, M., Cox, L., Knicker, H.E., Cornejo, J., Spokas, K.A., Hermosín, M.C., 2015. Characterization and selection of biochar for an efficient retention of tricyclazole in a flooded alluvial paddy soil. J. Hazard Mater. 286, 581–588.
Gholizadeh, M., Hu, X., Liu, Q., 2019. A mini review of the specialties of the bio-oils produced from pyrolysis of 20 different biomasses. Renew. Sustain. Energy Rev. 114, 109313.
Gianfreda, L., Rao, M.A., 2008. Interactions between xenobiotics and microbial and enzymatic soil activity. Crit. Rev. Environ. Sci. Technol. 38, 269–310.
Godlewska, P., Ok, Y.S., Oleszczuk, P., 2021. The dark side of black gold: ecotoxicological aspects of biochar and biochar-amended soils. J. Hazard Mater. 403, 123833.
Gomez, J., Denef, K., Stewart, C., Zheng, J., Cotrufo, M., 2014. Biochar addition rate influences soil microbial abundance and activity in temperate soils. Eur. J. Soil Sci. 65, 28–39.
Gonzaga, M.I.S., Mackowiak, C., de Almeida, A.Q., Wisniewski Jr., A., de Souza, D.F., da Silva Lima, I., et al., 2018. Assessing biochar applications and repeated Brassica juncea L. production cycles to remediate Cu contaminated soil. Chemosphere 201, 278–285.
Gonzaga, M.I.S., Matias, MIdAS., Andrade, K.R., de Jesus, A.N., da Costa Cunha, G., de Andrade, R.S., et al., 2020. Aged biochar changed copper availability and distribution among soil fractions and influenced corn seed germination in a copper-contaminated soil. Chemosphere 240, 124828.
Gui, X., Liu, C., Li, F., Wang, J., 2020. Effect of pyrolysis temperature on the composition of DOM in manure-derived biochar. Ecotoxicol. Environ. Saf. 197, 110597.

Gul, S., Whalen, J.K., Thomas, B.W., Sachdeva, V., Deng, H., 2015. Physico-chemical properties and microbial responses in biochar-amended soils: mechanisms and future directions. Agric. Ecosyst. Environ. 206, 46–59.
Guo, W., Huo, S., Feng, J., Lu, X., 2017. Adsorption of perfluorooctane sulfonate (PFOS) on corn straw-derived biochar prepared at different pyrolytic temperatures. J. Taiwan Institute Chem. Eng. 78, 265–271.
Gupta, G.K., Gupta, P.K., Mondal, M.K., 2019. Experimental process parameters optimization and in-depth product characterizations for teak sawdust pyrolysis. Waste Manag. 87, 499–511.
Hale, S.E., Lehmann, J., Rutherford, D., Zimmerman, A.R., Bachmann, R.T., Shitumbanuma, V., et al., 2012. Quantifying the total and bioavailable polycyclic aromatic hydrocarbons and dioxins in biochars. Environ. Sci. Technol. 46, 2830–2838.
Han, D.G., Li, C., Zhao, X.H., 2013. Prospect of Sludge Treatment Technology in Tianjin. Advanced Materials Research, vol. 765. Trans Tech Publ, pp. 2916–2921.
Han, H., Buss, W., Zheng, Y., Song, P., Rafiq, M.K., Liu, P., et al., 2021. Contaminants in biochar and suggested mitigation measures-a review. Chem. Eng. J. 132287.
Han, L., Sun, K., Jin, J., Xing, B., 2016. Some concepts of soil organic carbon characteristics and mineral interaction from a review of literature. Soil Biol. Biochem. 94, 107–121.
Han, L., Sun, K., Yang, Y., Xia, X., Li, F., Yang, Z., et al., 2020. Biochar's stability and effect on the content, composition and turnover of soil organic carbon. Geoderma 364, 114184.
Hayyat, A., Javed, M., Rasheed, I., Ali, S., Shahid, M.J., Rizwan, M., et al., 2016. Role of Biochar in Remediating Heavy Metals in Soil. Phytoremediation. Springer, pp. 421–437.
He, E., Yang, Y., Xu, Z., Qiu, H., Yang, F., Peijnenburg, W.J., et al., 2019a. Two years of aging influences the distribution and lability of metal (loid) s in a contaminated soil amended with different biochars. Sci. Total Environ. 673, 245–253.
He, L., Fan, S., Müller, K., Wang, H., Che, L., Xu, S., et al., 2018. Comparative analysis biochar and compost-induced degradation of di-(2-ethylhexyl) phthalate in soils. Sci. Total Environ. 625, 987–993.
He, L., Zhong, H., Liu, G., Dai, Z., Brookes, P.C., Xu, J., 2019b. Remediation of heavy metal contaminated soils by biochar: mechanisms, potential risks and applications in China. Environ. Pollut. 252, 846–855.
He, M., Xiong, X., Wang, L., Hou, D., Bolan, N.S., Ok, Y.S., et al., 2021. A critical review on performance indicators for evaluating soil biota and soil health of biochar-amended soils. J. Hazard Mater. 125378.
He, T., Meng, J., Chen, W., Liu, Z., Cao, T., Cheng, X., et al., 2017. Effects of biochar on cadmium accumulation in rice and cadmium fractions of soil: a three-year pot experiment. BioResources 12, 622–642.
Hoslett, J., Ghazal, H., Katsou, E., Jouhara, H., 2020. The removal of tetracycline from water using biochar produced from agricultural discarded material. Sci. Total Environ. 751, 141755.
Huang, H., Yao, W., Li, R., Ali, A., Du, J., Guo, D., et al., 2018. Effect of pyrolysis temperature on chemical form, behavior and environmental risk of Zn, Pb and Cd in biochar produced from phytoremediation residue. Bioresour. Technol. 249, 487–493.
Huang, M., Li, Z., Luo, N., Yang, R., Wen, J., Huang, B., et al., 2019. Application potential of biochar in environment: insight from degradation of biochar-derived DOM and complexation of DOM with heavy metals. Sci. Total Environ. 646, 220–228.
Huang, Y.-F., Huang, Y.-Y., Chiueh, P.-T., Lo, S.-L., 2020. Heterogeneous Fenton oxidation of trichloroethylene catalyzed by sewage sludge biochar: experimental study and life cycle assessment. Chemosphere 249, 126139.
Ibrahim, M., Li, G., Khan, S., Chi, Q., Xu, Y., 2017. Biochars mitigate greenhouse gas emissions and bioaccumulation of potentially toxic elements and arsenic speciation in Phaseolus vulgaris L. Environ. Sci. Pollut. Control Ser. 24, 19524–19534.
Igalavithana, A.D., Kwon, E.E., Vithanage, M., Rinklebe, J., Moon, D.H., Meers, E., et al., 2019. Soil lead immobilization by biochars in short-term laboratory incubation studies. Environ. Int. 127, 190–198.
Inyang, M., Dickenson, E., 2015. The potential role of biochar in the removal of organic and microbial contaminants from potable and reuse water: a review. Chemosphere 134, 232–240.
Ippolito, J.A., Cui, L., Kammann, C., Wrage-Mönnig, N., Estavillo, J.M., Fuertes-Mendizabal, T., et al., 2020. Feedstock choice, pyrolysis temperature and type influence biochar characteristics: a comprehensive meta-data analysis review. Biochar 1–18.
Jafri, N., Wong, W., Doshi, V., Yoon, L., Cheah, K.H., 2018. A review on production and characterization of biochars for application in direct carbon fuel cells. Process Saf. Environ. Protect. 118, 152–166.
Jaiswal, A.K., Alkan, N., Elad, Y., Sela, N., Philosoph, A.M., Graber, E.R., et al., 2020. Molecular insights into biochar-mediated plant growth promotion and systemic resistance in tomato against Fusarium crown and root rot disease. Sci. Rep. 10, 1–15.
Jansson, J.K., Hofmockel, K.S., 2018. The soil microbiome—from metagenomics to metaphenomics. Curr. Opin. Microbiol. 43, 162–168.
Janu, R., Mrlik, V., Ribitsch, D., Hofman, J., Sedláček, P., Bielská, L., et al., 2021. Biochar surface functional groups as affected by biomass feedstock, biochar composition and pyrolysis temperature. Carbon Res. Conversion 4, 36–46.
Ji, M., Zhou, L., Zhang, S., Luo, G., Sang, W., 2020. Effects of biochar on methane emission from paddy soil: focusing on DOM and microbial communities. Sci. Total Environ. 743, 140725.
Ji, X., Lü, L., Chen, F., Yang, C., 2016. Sorption properties and mechanisms of organic dyes by straw biochar. Acta Sci. Circumstantiae 36, 1648–1654.
Jiang, T.-Y., Jiang, J., Xu, R.-K., Li, Z., 2012. Adsorption of Pb (II) on variable charge soils amended with rice-straw derived biochar. Chemosphere 89, 249–256.
Jin, J., Kang, M., Sun, K., Pan, Z., Wu, F., Xing, B., 2016. Properties of biochar-amended soils and their sorption of imidacloprid, isoproturon, and atrazine. Sci. Total Environ. 550, 504–513.
Jin, J., Wang, M., Cao, Y., Wu, S., Liang, P., Li, Y., et al., 2017. Cumulative effects of bamboo sawdust addition on pyrolysis of sewage sludge: biochar properties and environmental risk from metals. Bioresour. Technol. 228, 218–226.
Jing, G., Luan, M., Chen, T., 2011. Prospects for development of oily sludge treatment. Chem. Technol. Fuels Oils 47, 312.
José, M., Paneque, M., Hilber, I., Blum, F., Knicker, H.E., Bucheli, T.D., 2016. Assessment of polycyclic aromatic hydrocarbons in biochar and biochar-amended agricultural soil from Southern Spain. J. Soils Sediments 16, 557–565.
Joseph, S.D., Camps-Arbestain, M., Lin, Y., Munroe, P., Chia, C., Hook, J., et al., 2010. An investigation into the reactions of biochar in soil. Soil Res. 48, 501–515.
Kalderis, D., Kayan, B., Akay, S., Kulaksız, E., Gözmen, B., 2017. Adsorption of 2, 4-dichlorophenol on paper sludge/wheat husk biochar: process optimization and comparison with biochars prepared from wood chips, sewage sludge and hog fuel/demolition waste. J. Environ. Chem. Eng. 5, 2222–2231.
Kandanelli, R., Meesala, L., Kumar, J., Raju, C.S.K., Peddy, V.R., Gandham, S., et al., 2018. Cost effective and practically viable oil spillage mitigation: comprehensive study with biochar. Mar. Pollut. Bull. 128, 32–40.
Kappler, A., Wuestner, M.L., Ruecker, A., Harter, J., Halama, M., Behrens, S., 2014. Biochar as an electron shuttle between bacteria and Fe (III) minerals. Environ. Sci. Technol. Lett. 1, 339–344.
Karer, J., Zehetner, F., Dunst, G., Fessl, J., Wagner, M., Puschenreiter, M., et al., 2018. Immobilisation of metals in a contaminated soil with biochar-compost mixtures and inorganic additives: 2-year greenhouse and field experiments. Environ. Sci. Pollut. Control Ser. 25, 2506–2516.
Karimi, A., Moezzi, A., Chorom, M., Enayatizamir, N., 2020. Application of biochar changed the status of nutrients and biological activity in a calcareous soil. J. Soil Sci. Plant Nutr. 20, 450–459.
Keiluweit, M., Nico, P.S., Johnson, M.G., Kleber, M., 2010. Dynamic molecular structure of plant biomass-derived black carbon (biochar). Environ. Sci. Technol. 44, 1247–1253.
Khan, S., Chao, C., Waqas, M., Arp, H.P.H., Zhu, Y.-G., 2013. Sewage sludge biochar influence upon rice (Oryza sativa L) yield, metal bioaccumulation and greenhouse gas emissions from acidic paddy soil. Environ. Sci. Technol. 47, 8624–8632.
Kharel, G., Sacko, O., Feng, X., Morris, J.R., Phillips, C.L., Trippe, K., et al., 2019. Biochar surface oxygenation by ozonization for super high cation exchange capacity. ACS Sustain. Chem. Eng. 7, 16410–16418.
Khodadad, C.L., Zimmerman, A.R., Green, S.J., Uthandi, S., Foster, J.S., 2011. Taxa-specific changes in soil microbial community composition induced by pyrogenic carbon amendments. Soil Biol. Biochem. 43, 385–392.
Khorram, M.S., Lin, D., Zhang, Q., Zheng, Y., Fang, H., Yu, Y., 2017. Effects of aging process on adsorption–desorption and bioavailability of fomesafen in an agricultural soil amended with rice hull biochar. J. Environ. Sci. 56, 180–191.
Kim, H.-B., Kim, J.-G., Kim, T., Alessi, D.S., Baek, K., 2020. Mobility of arsenic in soil amended with biochar derived from biomass with different lignin contents: relationships between lignin content and dissolved organic matter leaching. Chem. Eng. J. 393, 124687.
Kloss, S., Zehetner, F., Buecker, J., Oburger, E., Wenzel, W.W., Enders, A., et al., 2015. Trace element biogeochemistry in the soil-water-plant system of a temperate agricultural soil amended with different biochars. Environ. Sci. Pollut. Control Ser. 22, 4513–4526.
Kumar, A., Joseph, S., Tsechansky, L., Privat, K., Schreiter, I.J., Schüth, C., et al., 2018. Biochar aging in contaminated soil promotes Zn immobilization due to changes in biochar surface structural and chemical properties. Sci. Total Environ. 626, 953–961.
Kuzyakov, Y., Bogomolova, I., Glaser, B., 2014. Biochar stability in soil: decomposition during eight years and transformation as assessed by compound-specific 14C analysis. Soil Biol. Biochem. 70, 229–236.
Kuzyakov, Y., Subbotina, I., Chen, H., Bogomolova, I., Xu, X., 2009. Black carbon decomposition and incorporation into soil microbial biomass estimated by 14C labeling. Soil Biol. Biochem. 41, 210–219.
Lévesque, V., Rochette, P., Hogue, R., Jeanne, T., Ziadi, N., Chantigny, M.H., et al., 2020. Greenhouse Gas Emissions and Soil Bacterial Community as Affected by Biochar Amendments after Periodic Mineral Fertilizer Applications. BIOLOGY AND FERTILITY OF SOILS.
Lahori, A.H., Zhanyu, G., Zhang, Z., Ronghua, L., Mahar, A., Awasthi, M.K., et al., 2017. Use of biochar as an amendment for remediation of heavy metal-contaminated soils: prospects and challenges. Pedosphere 27, 991–1014.
Lai, W.-Y., Lai, C.-M., Ke, G.-R., Chung, R.-S., Chen, C.-T., Cheng, C.-H., et al., 2013. The effects of woodchip biochar application on crop yield, carbon sequestration and greenhouse gas emissions from soils planted with rice or leaf beet. J. Taiwan Institute Chem. Eng. 44, 1039–1044.
Lehmann, A., Leifheit, E., Rillig, M., 2017. Mycorrhizas and Soil Aggregation. Mycorrhizal Mediation of Soil. Elsevier, pp. 241–262.
Lehmann, J., Joseph, S., 2015. Biochar for Environmental Management: Science, Technology and Implementation. Routledge.
Lehmann, J., Rillig, M.C., Thies, J., Masiello, C.A., Hockaday, W.C., Crowley, D., 2011. Biochar effects on soil biota–a review. Soil Biol. Biochem. 43, 1812–1836.
Lei, S., Shi, Y., Qiu, Y., Che, L., Xue, C., 2019. Performance and mechanisms of emerging animal-derived biochars for immobilization of heavy metals. Sci. Total Environ. 646, 1281–1289.
Leng, L., Xiong, Q., Yang, L., Li, H., Zhou, Y., Zhang, W., et al., 2020. An overview on engineering the surface area and porosity of biochar. Sci. Total Environ. 144204.
Li, C., Zhang, L., Xia, H., Peng, J., Cheng, S., Shu, J., et al., 2017a. Analysis of devitalization mechanism and chemical constituents for fast and efficient

regeneration of spent carbon by means of ultrasound and microwaves. J. Anal. Appl. Pyrol. 124, 42–50.
Li, G., Khan, S., Ibrahim, M., Sun, T.-R., Tang, J.-F., Cotner, J.B., et al., 2018a. Biochars induced modification of dissolved organic matter (DOM) in soil and its impact on mobility and bioaccumulation of arsenic and cadmium. J. Hazard Mater. 348, 100–108.
Li, J., Liang, N., Jin, X., Zhou, D., Li, H., Wu, M., et al., 2017b. The role of ash content on bisphenol A sorption to biochars derived from different agricultural wastes. Chemosphere 171, 66–73.
Li, M., Zhang, A., Wu, H., Liu, H., Lv, J., 2017c. Predicting potential release of dissolved organic matter from biochars derived from agricultural residues using fluorescence and ultraviolet absorbance. J. Hazard Mater. 334, 86–92.
Li, S., Harris, S., Anandhi, A., Chen, G., 2019a. Predicting biochar properties and functions based on feedstock and pyrolysis temperature: a review and data syntheses. J. Clean. Prod. 215, 890–902.
Li, X., Li, Y., Zhang, X., Zhao, X., Sun, Y., Weng, L., et al., 2019b. Long-term effect of biochar amendment on the biodegradation of petroleum hydrocarbons in soil microbial fuel cells. Sci. Total Environ. 651, 796–806.
Li, Y., Hu, S., Chen, J., Müller, K., Li, Y., Fu, W., et al., 2018b. Effects of biochar application in forest ecosystems on soil properties and greenhouse gas emissions: a review. J. Soils Sediments 18, 546–563.
Liang, X., Chen, L., Liu, Z., Jin, Y., He, M., Zhao, Z., et al., 2018. Composition of microbial community in pig manure biochar-amended soils and the linkage to the heavy metals accumulation in rice at harvest. Land Degrad. Dev. 29, 2189–2198.
Liao, S., Pan, B., Li, H., Zhang, D., Xing, B., 2014. Detecting free radicals in biochars and determining their ability to inhibit the germination and growth of corn, wheat and rice seedlings. Environ. Sci. Technol. 48, 8581–8587.
Liu, L., Tan, Z., Gong, H., Huang, Q., 2018. Migration and transformation mechanisms of nutrient elements (N, P, K) within biochar in straw–biochar–soil–plant systems: a review. ACS Sustain. Chem. Eng. 7, 22–32.
Liu, X., Sun, J., Duan, S., Wang, Y., Hayat, T., Alsaedi, A., et al., 2017. A valuable biochar from poplar catkins with high adsorption capacity for both organic pollutants and inorganic heavy metal ions. Sci. Rep. 7, 1–12.
Lonappan, L., Rouissi, T., Das, R.K., Brar, S.K., Ramirez, A.A., Verma, M., et al., 2016. Adsorption of methylene blue on biochar microparticles derived from different waste materials. Waste Manag. 49, 537–544.
Lu, L., Shan, R., Shi, Y., Wang, S., Yuan, H., 2019. A novel TiO2/biochar composite catalysts for photocatalytic degradation of methyl orange. Chemosphere 222, 391–398.
Luo, J., Jia, C., Shen, M., Zhang, S., Zhu, X., 2019. Enhancement of adsorption and energy storage capacity of biomass-based N-doped porous carbon via cyclic carbothermal reduction triggered by nitrogen dopants. Carbon 155, 403–409.
Luo, J., Lin, L., Liu, C., Jia, C., Chen, T., Yang, Y., et al., 2020. Reveal a hidden highly toxic substance in biochar to support its effective elimination strategy. J. Hazard Mater. 399, 123055.
Luo, S., Wang, S., Tian, L., Li, S., Li, X., Shen, Y., et al., 2017. Long-term biochar application influences soil microbial community and its potential roles in semiarid farmland. Appl. Soil Ecol. 117, 10–15.
Luo, X., Chen, L., Zheng, H., Chang, J., Wang, H., Wang, Z., et al., 2016. Biochar addition reduced net N mineralization of a coastal wetland soil in the Yellow River Delta, China. Geoderma 282, 120–128.
Luo, Y., Durenkamp, M., De Nobili, M., Lin, Q., Devonshire, B., Brookes, P., 2013. Microbial biomass growth, following incorporation of biochars produced at 350 C or 700 C, in a silty-clay loam soil of high and low pH. Soil Biol. Biochem. 57, 513–523.
Masiello, C.A., Chen, Y., Gao, X., Liu, S., Cheng, H.-Y., Bennett, M.R., et al., 2013. Biochar and microbial signaling: production conditions determine effects on microbial communication. Environ. Sci. Technol. 47, 11496–11503.
Masrat, R., Maswal, M., Dar, A.A., 2013. Competitive solubilization of naphthalene and pyrene in various micellar systems. J. Hazard Mater. 244, 662–670.
Meier, S., Curaqueo, G., Khan, N., Bolan, N., Cea, M., Eugenia, G.M., et al., 2017. Chicken-manure-derived biochar reduced bioavailability of copper in a contaminated soil. J. Soils Sediments 17, 741–750.
Mendez, A., Paz-Ferreiro, J., Araujo, F., Gasco, G., 2014. Biochar from pyrolysis of deinking paper sludge and its use in the treatment of a nickel polluted soil. J. Anal. Appl. Pyrol. 107, 46–52.
Meng, J., Liang, S., Tao, M., Liu, X., Brookes, P.C., Xu, J., 2018. Chemical speciation and risk assessment of Cu and Zn in biochars derived from co-pyrolysis of pig manure with rice straw. Chemosphere 200, 344–350.
Mian, M.M., Liu, G., 2018. Recent progress in biochar-supported photocatalysts: synthesis, role of biochar, and applications. RSC Adv. 8, 14237–14248.
Ming, L., Ming, L., Li, Z-p, Jiang, C-y, Meng, W., 2016. Soil N transformation and microbial community structure as affected by adding biochar to a paddy soil of subtropical China. J. Intergrative Agri. 15, 209–219.
Moore, F., González, M.-E., Khan, N., Curaqueo, G., Sanchez-Monedero, M., Rilling, J., et al., 2018. Copper immobilization by biochar and microbial community abundance in metal-contaminated soils. Sci. Total Environ. 616, 960–969.
Mukherjee, A., Zimmerman, A., Harris, W., 2011. Surface chemistry variations among a series of laboratory-produced biochars. Geoderma 163, 247–255.
Mukome, F.N., Zhang, X., Silva, L.C., Six, J., Parikh, S.J., 2013. Use of chemical and physical characteristics to investigate trends in biochar feedstocks. J. Agric. Food Chem. 61, 2196–2204.
Nelissen, V., Saha, B.K., Ruysschaert, G., Boeckx, P., 2014. Effect of different biochar and fertilizer types on N2O and NO emissions. Soil Biol. Biochem. 70, 244–255.
Nguyen, B.T., Trinh, N.N., Bach, Q.-V., 2020. Methane emissions and associated microbial activities from paddy salt-affected soil as influenced by biochar and cow manure addition. Appl. Soil Ecol. 152, 103531.
Nguyen, H.N., Pignatello, J.J., 2013. Laboratory tests of biochars as absorbents for use in recovery or containment of marine crude oil spills. Environ. Eng. Sci. 30, 374–380.
Nguyen, T.H., Cho, H.-H., Poster, D.L., Ball, W.P., 2007. Evidence for a pore-filling mechanism in the adsorption of aromatic hydrocarbons to a natural wood char. Environ. Sci. Technol. 41, 1212–1217.
Ni, N., Kong, D., Wu, W., He, J., Shan, Z., Li, J., et al., 2020. The role of biochar in reducing the bioavailability and migration of persistent organic pollutants in soil–plant systems: a review. Bull. Environ. Contam. Toxicol. 104, 157–165.
Nie, C., Yang, X., Niazi, N.K., Xu, X., Wen, Y., Rinklebe, J., et al., 2018. Impact of sugarcane bagasse-derived biochar on heavy metal availability and microbial activity: a field study. Chemosphere 200, 274–282.
Novak, J.M., Lima, I., Xing, B., Gaskin, J.W., Steiner, C., Das, K., et al., 2009. Characterization of designer biochar produced at different temperatures and their effects on a loamy sand. Annals Enviro. Sci. 3.1 (195–206.).
Nzihou, A., Stanmore, B., Sharrock, P., 2013. A review of catalysts for the gasification of biomass char, with some reference to coal. Energy 58, 305–317.
O'Connor, D., Peng, T., Li, G., Wang, S., Duan, L., Mulder, J., et al., 2018a. Sulfur-modified rice husk biochar: a green method for the remediation of mercury contaminated soil. Sci. Total Environ. 621, 819–826.
O'Connor, D., Peng, T., Zhang, J., Tsang, D.C., Alessi, D.S., Shen, Z., et al., 2018b. Biochar application for the remediation of heavy metal polluted land: a review of in situ field trials. Sci. Total Environ. 619, 815–826.
Oleszczuk, P., Jośko, I., Futa, B., Pasieczna-Patkowska, S., Pałys, E., Kraska, P., 2014. Effect of pesticides on microorganisms, enzymatic activity and plant in biochar-amended soil. Geoderma 214, 10–18.
Özçimen, D., Ersoy-Meriçboyu, A., 2010. Characterization of biochar and bio-oil samples obtained from carbonization of various biomass materials. Renew. Energy 35, 1319–1324.
Pariyar, P., Kumari, K., Jain, M.K., Jadhao, P.S., 2020. Evaluation of change in biochar properties derived from different feedstock and pyrolysis temperature for environmental and agricultural application. Sci. Total Environ. 713, 136433.
Park, J.H., Choppala, G.K., Bolan, N.S., Chung, J.W., Chuasavathi, T., 2011. Biochar reduces the bioavailability and phytotoxicity of heavy metals. Plant Soil 348, 439.
Pasangulapati, V., Ramachandriya, K.D., Kumar, A., Wilkins, M.R., Jones, C.L., Huhnke, R.L., 2012. Effects of cellulose, hemicellulose and lignin on thermochemical conversion characteristics of the selected biomass. Bioresour. Technol. 114, 663–669.
Paz-Ferreiro, J., Gascó, G., Gutiérrez, B., Méndez, A., 2012. Soil biochemical activities and the geometric mean of enzyme activities after application of sewage sludge and sewage sludge biochar to soil. Biol. Fertil. Soils 48, 511–517.
Plaza, C., Giannetta, B., Fernández, J.M., López-de-Sá, E.G., Polo, A., Gascó, G., et al., 2016. Response of different soil organic matter pools to biochar and organic fertilizers. Agric. Ecosyst. Environ. 225, 150–159.
Pokharel, P., Kwak, J.-H., Ok, Y.S., Chang, S.X., 2018. Pine sawdust biochar reduces GHG emission by decreasing microbial and enzyme activities in forest and grassland soils in a laboratory experiment. Sci. Total Environ. 625, 1247–1256.
Purakayastha, T., Das, K., Gaskin, J., Harris, K., Smith, J., Kumari, S., 2016. Effect of pyrolysis temperatures on stability and priming effects of C3 and C4 biochars applied to two different soils. Soil Tillage Res. 155, 107–115.
Qin, G., Niu, Z., Yu, J., Li, Z., Ma, J.-Y., Xiang, P., 2020. Soil heavy metal pollution and food safety in China: effects, sources and removing technology. Chemosphere 129205.
Qin, Y., Li, G., Gao, Y., Zhang, L., Ok, Y.S., An, T., 2018. Persistent free radicals in carbon-based materials on transformation of refractory organic contaminants (ROCs) in water: a critical review. Water Res. 137, 130–143.
Qiu, M., Sun, K., Jin, J., Gao, B., Yan, Y., Han, L., et al., 2014. Properties of the plant-and manure-derived biochars and their sorption of dibutyl phthalate and phenanthrene. Sci. Rep. 4, 1–10.
Qiu, Y., Xiao, X., Cheng, H., Zhou, Z., Sheng, G.D., 2009. Influence of environmental factors on pesticide adsorption by black carbon: pH and model dissolved organic matter. Environ. Sci. Technol. 43, 4973–4978.
Rajkovich, S., Enders, A., Hanley, K., Hyland, C., Zimmerman, A.R., Lehmann, J., 2012. Corn growth and nitrogen nutrition after additions of biochars with varying properties to a temperate soil. Biol. Fertil. Soils 48, 271–284.
Rong, X., Xie, M., Kong, L., Natarajan, V., Ma, L., Zhan, J., 2019. The magnetic biochar derived from banana peels as a persulfate activator for organic contaminants degradation. Chem. Eng. J. 372, 294–303.
Ruan, X., Sun, Y., Du, W., Tang, Y., Liu, Q., Zhang, Z., et al., 2019. Formation, characteristics, and applications of environmentally persistent free radicals in biochars: a review. Bioresour. Technol. 281, 457–468.
Shaheen, S.M., Niazi, N.K., Hassan, N.E., Bibi, I., Wang, H., Tsang, D.C., et al., 2019. Wood-based biochar for the removal of potentially toxic elements in water and wastewater: a critical review. Int. Mater. Rev. 64, 216–247.
Shen, X., Zeng, J., Zhang, D., Wang, F., Li, Y., Yi, W., 2020. Effect of pyrolysis temperature on characteristics, chemical speciation and environmental risk of Cr, Mn, Cu, and Zn in biochars derived from pig manure. Sci. Total Environ. 704, 135283.
Shi, K., Qiu, Y., Li, B., Stenstrom, M.K., 2016. Effectiveness and potential of straw-and wood-based biochars for adsorption of imidazolium-type ionic liquids. Ecotoxicol. Environ. Saf. 130, 155–162.
Singh, B., Fang, Y., Cowie, B.C., Thomsen, L., 2014. NEXAFS and XPS characterisation of carbon functional groups of fresh and aged biochars. Org. Geochem. 77, 1–10.
Singh, B.P., Cowie, A.L., Smernik, R.J., 2012. Biochar carbon stability in a clayey soil as a function of feedstock and pyrolysis temperature. Environ. Sci. Technol. 46, 11770–11778.

Smebye, A., Alling, V., Vogt, R.D., Gadmar, T.C., Mulder, J., Cornelissen, G., et al., 2016. Biochar amendment to soil changes dissolved organic matter content and composition. Chemosphere 142, 100–105.
Song, D., Xi, X., Zheng, Q., Liang, G., Zhou, W., Wang, X., 2019. Soil nutrient and microbial activity responses to two years after maize straw biochar application in a calcareous soil. Ecotoxicol. Environ. Saf. 180, 348–356.
Spokas, K.A., 2010. Review of the stability of biochar in soils: predictability of O: C molar ratios. Carbon Manag. 1, 289–303.
Steiner, C., Das, K., Melear, N., Lakly, D., 2010. Reducing nitrogen loss during poultry litter composting using biochar. J. Environ. Qual. 39, 1236–1242.
Subedi, R., Taupe, N., Pelissetti, S., Petruzzelli, L., Bertora, C., Leahy, J.J., et al., 2016. Greenhouse gas emissions and soil properties following amendment with manure-derived biochars: influence of pyrolysis temperature and feedstock type. J. Environ. Manag. 166, 73–83.
Suddick, E.C., Six, J., 2013. An estimation of annual nitrous oxide emissions and soil quality following the amendment of high temperature walnut shell biochar and compost to a small scale vegetable crop rotation. Sci. Total Environ. 465, 298–307.
Sui, F., Wang, J., Zuo, J., Joseph, S., Munroe, P., Drosos, M., et al., 2020. Effect of amendment of biochar supplemented with Si on Cd mobility and rice uptake over three rice growing seasons in an acidic Cd-tainted paddy from central South China. Sci. Total Environ. 709, 136101.
Sui, F., Zuo, J., Chen, D., Li, L., Pan, G., Crowley, D.E., 2018. Biochar effects on uptake of cadmium and lead by wheat in relation to annual precipitation: a 3-year field study. Environ. Sci. Pollut. Control Ser. 25, 3368–3377.
Suliman, W., Harsh, J.B., Abu-Lail, N.I., Fortuna, A.-M., Dallmeyer, I., Garcia-Pérez, M., 2017. The role of biochar porosity and surface functionality in augmenting hydrologic properties of a sandy soil. Sci. Total Environ. 574, 139–147.
Suliman, W., Harsh, J.B., Abu-Lail, N.I., Fortuna, A.-M., Dallmeyer, I., Garcia-Perez, M., 2016. Influence of feedstock source and pyrolysis temperature on biochar bulk and surface properties. Biomass Bioenergy 84, 37–48.
Sun, J., Pan, L., Tsang, D.C., Zhan, Y., Zhu, L., Li, X., 2018. Organic contamination and remediation in the agricultural soils of China: a critical review. Sci. Total Environ. 615, 724–740.
Sun, Z., Zhang, Z., Zhu, K., Wang, Z., Zhao, X., Lin, Q., et al., 2020. Biochar altered native soil organic carbon by changing soil aggregate size distribution and native SOC in aggregates based on an 8-year field experiment. Sci. Total Environ. 708, 134829.
Tag, A.T., Duman, G., Ucar, S., Yanik, J., 2016. Effects of feedstock type and pyrolysis temperature on potential applications of biochar. J. Anal. Appl. Pyrol. 120, 200–206.
Taherymoosavi, S., Joseph, S., Munroe, P., 2016. Characterization of organic compounds in a mixed feedstock biochar generated from Australian agricultural residues. J. Anal. Appl. Pyrol. 120, 441–449.
Tan, Z., Lin, C.S., Ji, X., Rainey, T.J., 2017. Returning biochar to fields: a review. Appl. Soil Ecol. 116, 1–11.
Tang, J., Zhang, L., Zhang, J., Ren, L., Zhou, Y., Zheng, Y., et al., 2020. Physicochemical features, metal availability and enzyme activity in heavy metal-polluted soil remediated by biochar and compost. Sci. Total Environ. 701, 134751.
Tao, W., Duan, W., Liu, C., Zhu, D., Si, X., Zhu, R., et al., 2020. Formation of persistent free radicals in biochar derived from rice straw based on a detailed analysis of pyrolysis kinetics. Sci. Total Environ. 715, 136575.
Tarin, M.W.K., Khaliq, M.A., Fan, L., Xie, D., Tayyab, M., Chen, L., et al., 2020. Divergent consequences of different biochar amendments on carbon dioxide (CO2) and nitrous oxide (N2O) emissions from the red soil. Sci. Total Environ. 754, 141935.
Teixidó, M., Hurtado, C., Pignatello, J.J., Beltrán, J.L., Granados, M., Peccia, J., 2013. Predicting contaminant adsorption in black carbon (biochar)-amended soil for the veterinary antimicrobial sulfamethazine. Environ. Sci. Technol. 47, 6197–6205.
Trinh, B.S., Werner, D., Reid, B.J., 2017. Application of a full-scale wood gasification biochar as a soil improver to reduce organic pollutant leaching risks. J. Chem. Technol. Biotechnol. 92, 1928–1937.
Tu, C., Wei, J., Guan, F., Liu, Y., Sun, Y., Luo, Y., 2020. Biochar and bacteria inoculated biochar enhanced Cd and Cu immobilization and enzymatic activity in a polluted soil. Environ. Int. 137, 105576.
Vandecasteele, B., Sinicco, T., D'Hose, T., Nest, T.V., Mondini, C., 2016. Biochar amendment before or after composting affects compost quality and N losses, but not P plant uptake. J. Environ. Manag. 168, 200–209.
Venegas, A., Rigol, A., Vidal, M., 2016. Changes in heavy metal extractability from contaminated soils remediated with organic waste or biochar. Geoderma 279, 132–140.
Wan, S., Hua, Z., Sun, L., Bai, X., Liang, L., 2016. Biosorption of nitroimidazole antibiotics onto chemically modified porous biochar prepared by experimental design: kinetics, thermodynamics, and equilibrium analysis. Process Saf. Environ. Protect. 104, 422–435.
Wan, Z., Sun, Y., Tsang, D.C., Hou, D., Cao, X., Zhang, S., et al., 2020. Sustainable remediation with an electroactive biochar system: mechanisms and perspectives. Green Chem. 22, 2688–2711.
Wang, D., Griffin, D.E., Parikh, S.J., Scow, K.M., 2016. Impact of biochar amendment on soil water soluble carbon in the context of extreme hydrological events. Chemosphere 160, 287–292.
Wang, H., Xia, W., Lu, P., 2017a. Study on adsorption characteristics of biochar on heavy metals in soil. Kor. J. Chem. Eng. 34, 1867–1873.
Wang, J., Shi, L., Zhai, L., Zhang, H., Wang, S., Zou, J., et al., 2021a. Analysis of the long-term effectiveness of biochar immobilization remediation on heavy metal contaminated soil and the potential environmental factors weakening the remediation effect: a review. Ecotoxicol. Environ. Saf. 207, 111261.
Wang, M., Zhu, Y., Cheng, L., Andserson, B., Zhao, X., Wang, D., et al., 2018. Review on utilization of biochar for metal-contaminated soil and sediment remediation. J. Environ. Sci. 63, 156–173.
Wang, N., Xue, X.-M., Juhasz, A.L., Chang, Z.-Z., Li, H.-B., 2017b. Biochar increases arsenic release from an anaerobic paddy soil due to enhanced microbial reduction of iron and arsenic. Environ. Pollut. 220, 514–522.
Wang, X., Song, D., Liang, G., Zhang, Q., Ai, C., Zhou, W., 2015. Maize biochar addition rate influences soil enzyme activity and microbial community composition in a fluvo-aquic soil. Appl. Soil Ecol. 96, 265–272.
Wang, X., Zhai, M., Guo, H., Panahi, A., Dong, P., Levendis, Y.A., 2021b. High-temperature pyrolysis of biomass pellets: the effect of ash melting on the structure of the char residue. Fuel 285, 119084.
Wang, Y., Liu, R., 2017. Comparison of characteristics of twenty-one types of biochar and their ability to remove multi-heavy metals and methylene blue in solution. Fuel Process. Technol. 160, 55–63.
Wang, Y., Liu, Y., Zhan, W., Zheng, K., Wang, J., Zhang, C., et al., 2020. Stabilization of heavy metal-contaminated soils by biochar: challenges and recommendations. Sci. Total Environ. 729, 139060.
Wang, Y., Wang, H.-S., Tang, C.-S., Gu, K., Shi, B., 2019. Remediation of heavy-metal-contaminated soils by biochar: a review. Environ. Geotech. 40, 1–14.
Wathukarage, A., Herath, I., Iqbal, M., Vithanage, M., 2019. Mechanistic understanding of crystal violet dye sorption by woody biochar: implications for wastewater treatment. Environ. Geochem. Health 41, 1647–1661.
Wei, J., Tu, C., Yuan, G., Zhou, Y., Wang, H., Lu, J., 2020a. Limited Cu (II) binding to biochar DOM: evidence from C K-edge NEXAFS and EEM-PARAFAC combined with two-dimensional correlation analysis. Sci. Total Environ. 701, 134919.
Wei, L., Huang, Y., Huang, L., Li, Y., Huang, Q., Xu, G., et al., 2020b. The ratio of H/C is a useful parameter to predict adsorption of the herbicide metolachlor to biochars. Environ. Res. 184, 109324.
Wei, S., Zhu, M., Fan, X., Song, J., Li, K., Jia, W., et al., 2019. Influence of pyrolysis temperature and feedstock on carbon fractions of biochar produced from pyrolysis of rice straw, pine wood, pig manure and sewage sludge. Chemosphere 218, 624–631.
Wei, Z., Wang, J.J., Fultz, L.M., White, P., Jeong, C., 2020c. Application of biochar in estrogen hormone-contaminated and manure-affected soils: impact on soil respiration, microbial community and enzyme activity. Chemosphere 128625.
Williams, P.T., Reed, A.R., 2006. Development of activated carbon pore structure via physical and chemical activation of biomass fibre waste. Biomass Bioenergy 30, 144–152.
Xiang, L., Liu, S., Ye, S., Yang, H., Song, B., Qin, F., et al., 2021. Potential hazards of biochar: the negative environmental impacts of biochar applications. J. Hazard Mater. 126611.
Xing, J., Xu, G., Li, G., 2020. Analysis of the complexation behaviors of Cu (II) with DOM from sludge-based biochars and agricultural soil: effect of pyrolysis temperature. Chemosphere 250, 126184.
Xing, Y., Wang, J., Xia, J., Liu, Z., Zhang, Y., Du, Y., et al., 2019. A pilot study on using biochars as sustainable amendments to inhibit rice uptake of Hg from a historically polluted soil in a Karst region of China. Ecotoxicol. Environ. Saf. 170, 18–24.
Xu, C., Zhao, J., Yang, W., He, L., Wei, W., Tan, X., et al., 2020. Evaluation of biochar pyrolyzed from kitchen waste, corn straw, and peanut hulls on immobilization of Pb and Cd in contaminated soil. Environ. Pollut. 261, 114133.
Xu, M., Wu, J., Luo, L., Yang, G., Zhang, X., Peng, H., et al., 2018. The factors affecting biochar application in restoring heavy metal-polluted soil and its potential applications. Chem. Ecol. 34, 177–197.
Xu, N., Tan, G., Wang, H., Gai, X., 2016a. Effect of biochar additions to soil on nitrogen leaching, microbial biomass and bacterial community structure. Eur. J. Soil Biol. 74, 1–8.
Xu, X., Kan, Y., Zhao, L., Cao, X., 2016b. Chemical transformation of CO2 during its capture by waste biomass derived biochars. Environ. Pollut. 213, 533–540.
Yang, E., Yao, C., Liu, Y., Zhang, C., Jia, L., Li, D., et al., 2018. Bamboo-derived porous biochar for efficient adsorption removal of dibenzothiophene from model fuel. Fuel 211, 121–129.
Yang, H., Huang, X., Thompson, J.R., Flower, R.J., 2014. Soil pollution: urban brownfields. Science 344, 691–692.
Yang, X., Tsibart, A., Nam, H., Hur, J., El-Naggar, A., Tack, F.M., et al., 2019. Effect of gasification biochar application on soil quality: trace metal behavior, microbial community, and soil dissolved organic matter. J. Hazard Mater. 365, 684–694.
Yao, H., Lu, J., Wu, J., Lu, Z., Wilson, P.C., Shen, Y., 2013. Adsorption of fluoroquinolone antibiotics by wastewater sludge biochar: role of the sludge source. Water, Air, Soil Pollut. 224, 1–9.
Ye, L., Camps-Arbestain, M., Shen, Q., Lehmann, J., Singh, B., Sabir, M., 2020a. Biochar effects on crop yields with and without fertilizer: a meta-analysis of field studies using separate controls. Soil Use Manag. 36, 2–18.
Ye, S., Cheng, M., Zeng, G., Tan, X., Wu, H., Liang, J., et al., 2020b. Insights into catalytic removal and separation of attached metals from natural-aged microplastics by magnetic biochar activating oxidation process. Water Res. 179, 115876.
Yin, D., Wang, X., Peng, B., Tan, C., Ma, L.Q., 2017. Effect of biochar and Fe-biochar on Cd and as mobility and transfer in soil-rice system. Chemosphere 186, 928–937.
Yu, L., Tang, J., Zhang, R., Wu, Q., Gong, M., 2013. Effects of biochar application on soil methane emission at different soil moisture levels. Biol. Fertil. Soils 49, 119–128.
Yu, Z., Chen, L., Pan, S., Li, Y., Kuzyakov, Y., Xu, J., et al., 2018. Feedstock determines biochar-induced soil priming effects by stimulating the activity of specific microorganisms. Eur. J. Soil Sci. 69, 521–534.
Yuan, D., Yuan, H., He, X., Hu, H., Qin, S., Clough, T., et al., 2021. Identification and verification of key functional groups of biochar influencing soil N 2 O emission. Biol. Fertil. Soils 1–10.
Zhang, G., Guo, X., Zhu, Y., Liu, X., Han, Z., Sun, K., et al., 2018. The effects of different biochars on microbial quantity, microbial community shift, enzyme activity, and biodegradation of polycyclic aromatic hydrocarbons in soil. Geoderma 328, 100–108.

Zhang, J., Wu, S., Xu, Z., Wang, M., Man, Y.B., Christie, P., et al., 2019a. The role of sewage sludge biochar in methylmercury formation and accumulation in rice. Chemosphere 218, 527–533.
Zhang, M., Shan, S., Chen, Y., Wang, F., Yang, D., Ren, J., et al., 2019b. Biochar reduces cadmium accumulation in rice grains in a tungsten mining area-field experiment: effects of biochar type and dosage, rice variety, and pollution level. Environ. Geochem. Health 41, 43–52.
Zhang, P., Huang, P., Xu, X., Sun, H., Jiang, B., Liao, Y., 2020a. Spectroscopic and molecular characterization of biochar-derived dissolved organic matter and the associations with soil microbial responses. Sci. Total Environ. 708, 134619.
Zhang, P., Li, Y., Cao, Y., Han, L., 2019c. Characteristics of tetracycline adsorption by cow manure biochar prepared at different pyrolysis temperatures. Bioresour. Technol. 285, 121348.
Zhang, P., Zhang, X., Li, Y., Han, L., 2020b. Influence of pyrolysis temperature on chemical speciation, leaching ability, and environmental risk of heavy metals in biochar derived from cow manure. Bioresour. Technol. 302, 122850.
Zhang, W., Mao, S., Chen, H., Huang, L., Qiu, R., 2013. Pb (II) and Cr (VI) sorption by biochars pyrolyzed from the municipal wastewater sludge under different heating conditions. Bioresour. Technol. 147, 545–552.
Zhang, Y., Wang, J., Feng, Y., 2021. The effects of biochar addition on soil physicochemical properties: a review. Catena 202, 105284.
Zhao, M., Dai, Y., Zhang, M., Feng, C., Qin, B., Zhang, W., et al., 2020. Mechanisms of Pb and/or Zn adsorption by different biochars: biochar characteristics, stability, and binding energies. Sci. Total Environ. 717, 136894.
Zheng, W., Guo, M., Chow, T., Bennett, D.N., Rajagopalan, N., 2010. Sorption properties of greenwaste biochar for two triazine pesticides. J. Hazard Mater. 181, 121–126.
Zhou, J., Chen, H., Tao, Y., Thring, R.W., Mao, J., 2019. Biochar amendment of chromium-polluted paddy soil suppresses greenhouse gas emissions and decreases chromium uptake by rice grain. J. Soils Sediments 19, 1756–1766.
Zhou, L., Huang, J., He, B., Zhang, F., Li, H., 2014. Peach gum for efficient removal of methylene blue and methyl violet dyes from aqueous solution. Carbohydr. Polym. 101, 574–581.
Zhu, X., Chen, B., Zhu, L., Xing, B., 2017. Effects and mechanisms of biochar-microbe interactions in soil improvement and pollution remediation: a review. Environ. Pollut. 227, 98–115.
Zhu, Y., Yi, B., Yuan, Q., Wu, Y., Wang, M., Yan, S., 2018. Removal of methylene blue from aqueous solution by cattle manure-derived low temperature biochar. RSC Adv. 8, 19917–19929.
Zielińska, A., Oleszczuk, P., 2016. Effect of pyrolysis temperatures on freely dissolved polycyclic aromatic hydrocarbon (PAH) concentrations in sewage sludge-derived biochars. Chemosphere 153, 68–74.
Zielińska, A., Oleszczuk, P., Charmas, B., Skubiszewska-Zięba, J., Pasieczna-Patkowska, S., 2015. Effect of sewage sludge properties on the biochar characteristic. J. Anal. Appl. Pyrol. 112, 201–213.
Zumstein, M.T., Schintlmeister, A., Nelson, T.F., Baumgartner, R., Woebken, D., Wagner, M., et al., 2018. Biodegradation of synthetic polymers in soils: tracking carbon into CO2 and microbial biomass. Sci. Adv. 4, eaas9024.

Chapter II

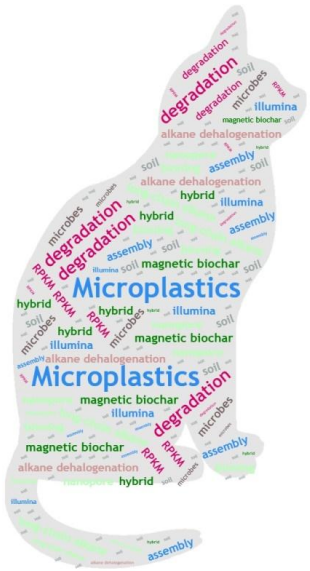

An integrated metagenomic model to uncover the cooperation between microbes and magnetic biochar during microplastics degradation in paddy soil

Mengyuan Ji [a] , Ginevra Giangeri [a] , Fengbo Yu [c] , Filippo Sessa [b] , Chao Liu [d] , Wenjing Sang [e] , Paolo Canu [b] , Fangbai Li [d] , Laura Treu [a] , Stefano Campanaro [a,*]

Journal of Hazardous Materials, Volume 294, 1 February 2022, 118655

https://doi.org/10.1016/j.jhazmat.2023.131950

[a] Department of Biology, University of Padova, Via U. Bassi 58/b, 35121 Padova, Italy

[b] Department of Industrial Engineering, University of Padova, Via Marzolo 9, 35131 Padova, Italy

[c] Shanghai Key Laboratory of Atmospheric Particle Pollution and Prevention, Department of Environmental Science and Engineering, Fudan University, Shanghai 200433,
China

[d] Guangdong Key Laboratory of Integrated Agro-Environmental Pollution Control and Management, Institute of Eco-environmental and Soil Sciences, Guangdong Academy of Sciences, Guangzhou 510650, China

[e] Textile Pollution Controlling Engineering Center of Ministry of Environmental Protection, College of Environmental Science and Engineering, Donghua University, Shanghai 201620, China

*Corresponding author

Journal of Hazardous Materials 458 (2023) 131950

Contents lists available at ScienceDirect

Journal of Hazardous Materials

journal homepage: www.elsevier.com/locate/jhazmat

An integrated metagenomic model to uncover the cooperation between microbes and magnetic biochar during microplastics degradation in paddy soil

Mengyuan Ji [a], Ginevra Giangeri [a], Fengbo Yu [c], Filippo Sessa [b], Chao Liu [d], Wenjing Sang [e], Paolo Canu [b], Fangbai Li [d], Laura Treu [a], Stefano Campanaro [a,*]

[a] Department of Biology, University of Padova, Via U. Bassi 58/b, 35121 Padova, Italy
[b] Department of Industrial Engineering, University of Padova, Via Marzolo 9, 35131 Padova, Italy
[c] Shanghai Key Laboratory of Atmospheric Particle Pollution and Prevention, Department of Environmental Science and Engineering, Fudan University, Shanghai 200433, China
[d] Guangdong Key Laboratory of Integrated Agro-Environmental Pollution Control and Management, Institute of Eco-environmental and Soil Sciences, Guangdong Academy of Sciences, Guangzhou 510650, China
[e] Textile Pollution Controlling Engineering Center of Ministry of Environmental Protection, College of Environmental Science and Engineering, Donghua University, Shanghai 201620, China

HIGHLIGHTS

- MEBC treatments resulted in marked increases in dissolved organic carbon.
- Hybrid assembly strategy obtained high-quality paddy soil microbiome information.
- The RPKM values of some genes encoding pathways related to MPs degradation increased in different treatments.
- *Nocardioides* sp. was identified as a potential species that cooperated with MEBC to utilize MPs.
- Complex soil microbes made biological dechlorination possible of MPs.

GRAPHICAL ABSTRACT

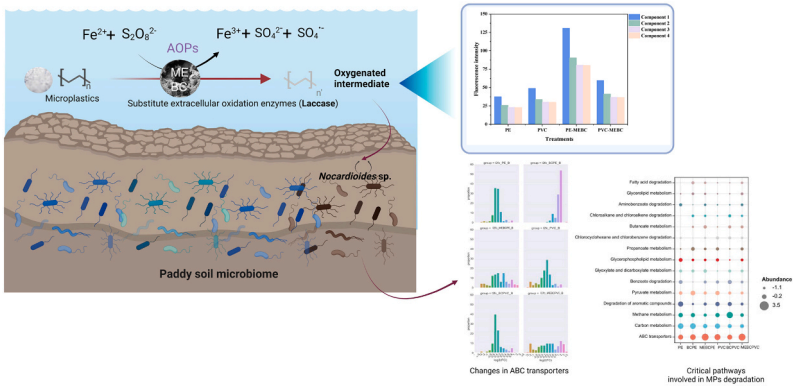

ARTICLE INFO

Edited By: Baiyu Zhang

Keywords:
Microplastics
Magnetic biochar
Degradation pathways
Hybrid assembly
Soil microbiome

ABSTRACT

The free radicals released from the advanced oxidation processes can enhance microplastics degradation, however, the existence of microbes acting synergistically in this process is still uncertain. In this study, magnetic biochar was used to initiate the advanced oxidation process in flooded soil. paddy soil was contaminated with polyethylene and polyvinyl chloride microplastics in a long-term incubation experiment, and subsequently subjected to bioremediation with biochar or magnetic biochar. After incubation, the total organic matter present in the samples containing polyvinyl chloride or polyethylene, and treated with magnetic biochar, significantly increased compared to the control. In the same samples there was an accumulation of "UVA humic" and

* Correspondence to: Via Ugo Bassi 58/b, 35131 Padova, Italy.
E-mail address: stefano.campanaro@unipd.it (S. Campanaro).

https://doi.org/10.1016/j.jhazmat.2023.131950
Received 17 January 2023; Received in revised form 20 June 2023; Accepted 25 June 2023
Available online 27 June 2023

"protein/phenol-like" substances. The integrated metagenomic investigation revealed that the relative abundance of some key genes involved in fatty acids degradation and in dehalogenation changed in different treatments. Results from genome-centric investigation suggest that a *Nocardioides* species can cooperate with magnetic biochar in the degradation of microplastics. In addition, a species assigned to the *Rhizobium* taxon was identified as a candidate in the dehalogenation and in the benzoate metabolism. Overall, our results suggest that cooperation between magnetic biochar and some microbial species involved in microplastic degradation is relevant in determining the fate of microplastics in soil.

1. Introduction

In the last few years microplastics (MPs) pollution has become a global environmental problem. Conventional microplastics in soil are difficult to degrade and negatively affect soil functions [1,2]. Due to sewage irrigation, mulching, and other agricultural practices, the annual input of MPs in farmland soil exceeds the one estimated for the global marine environment; according to that, farmland soil has become a major sink for MPs [3,4]. Previous studies have focused on the response of soil microorganisms to MPs, or on the effect of MPs on biogeochemical cycles including nitrogen [5]. While most of the strategies adopted in these studies merely focused on overall changes occurring in the microbial community, genes playing key roles in functional processes have not been deeply investigated. Currently, studies considering the degradation pathways of MPs in soil environments are scarce, and external factors that may drive MPs degradation must therefore be in-depth investigated.

Studies have shown that complete degradation of MPs in soil is slow in normal environmental conditions [6]. For instance, it has been reported that polyethylene (PE) can exist stably in soil for 200–400 years, and the mass loss of PE can reach 1.5% when *Cupriavidus Necator H16* is participating in the degradation process [7]. Additionally, polyolefins (such as PE and polyvinyl chloride (PVC)) degrade far more slowly than polyesters [8]. Under natural soil conditions, fungi involved in degradation (e.g. *Aspergillus*, *Fusarium*, *Penicillium*) cannot reduce PE weight by more than 10–30% [9]. The unique flooded environment of paddy soil provides favorable conditions for various chemical reactions such as redox to occur. Therefore, it is needed to further study the degradation potential of different MPs in paddy soil with chemical treatment, to explore the degradation mechanism, so as to efficiently control the pollution level and promote the safer use of plastic film. In addition, approximately 99% of the soil microbiome cannot be cultured by standard cultivation methods [10], while metagenomics can access rich genetic resources of unculturable microbes, revealing strain-level details of the genes and metabolic processes [11,12]. Therefore, the potential degraders and degradation pathways of MPs in paddy soil can be identified through a genome-centric metagenomic approach.

Biochar (BC) is an eco-friendly material and it has been used extensively to control soil pollution [13]. It has been reported that the MPs transport in the soil can be significantly inhibited in porous biochar [14]. However, when unmodified, biochar generally exhibits low efficiency in terms of stimulating degradation or adsorption of organic matter [15]. Magnetic biochar (MEBC) is formed by the pyrolysis activation, or chemical co-precipitation of (oxides) transition metals (Fe, Co, Ni, etc.) together with the biochar substrate [16]. MEBC not only retains the original characteristics of BC, but it also has more oxygen-containing functional treatments (OFGs), persistent free radicals (PFRs), and magnetic material [17]. Therefore, peroxodisulfate (PS), peroxymonosulfate and H_2O_2 can be activated by MEBC to generate reactive oxygen species (ROS) [18], thereby effectively degrading refractory organic pollutants such as polycyclic aromatic hydrocarbons (PAHs) and phthalates [19,20]. The chemically-mediated catalytic degradation of MPs is significantly more efficient compared to natural biodegradation. For instance, Kang and colleagues combined hydrothermal and advanced oxidation methods to achieve a 50% mass loss of PE MPs within eight hours [21]. According to a recent report, mixed plastics can be efficiently degraded and recycled by combining oxidation and bioconversion processes [22]. However, few studies have focused on the degradation potential obtained when soil microbes act in cooperation with external chemical oxidation toward MPs. Most of the studies only focused on changes in soil microbial communities in the presence of MPs or remediation materials, without paying particular attention to the functional responses of microbial species. Therefore, which microorganisms are responsible for the degradation of MPs in paddy soil, and whether BC/MEBC can promote MPs mineralization by soil microorganisms remain unclear.

Here, we hypothesized that redox-active MEBC has the potential to replace oxidases, thereby increasing the overall MPs degradation potential. To verify this hypothesis, a 50-day incubation experiment was conducted to investigate the effects of the PE and PVC MPs on the composition and functions of microbial communities in paddy soil. BC and MEBC were also included to study their capability for improving the degradation of MPs. The excitation emission matrix (EEM) spectra revealed responses of soil dissolved organic matter (DOM) structure in each set of conditions. Take advantage of the high precision of Illumina short-reads and the large span of nanopore long-reads to provide high-resolution information on complex soil microbial communities. Compared with short reads-based methods, the total length of the hybrid assembly was increased by order of magnitude. Genome-centric metagenomic analysis was used to evaluate the functional traits of the paddy soil microbiome and investigation of the functional pathways, thus, allowing for the evaluation of changes in the relative abundance of genes in response to various treatments as well as assessments of the general metabolic activities.

2. Materials and Methods

2.1. Soil, MPs, and chemicals

Soil samples were collected in November 2020 at 2–20 cm depth in a paddy rice field located in Grumolo delle Abbadesse (VI, Italy) (45°30'36.8"N 11°39'29.3"E). The soil samples were sieved using a 2 mm mesh screen following air drying and mixing. The basic physicochemical properties of the soil are listed in Table S1. The PE and PVC used in this study were provided by Euronewpack. Before the experiment, a crusher was used to fragment plastics which were then passed through a sieve (<5 mm) to obtain the MPs. Sodium persulfate (SP, $Na_2S_2O_8$, $\geq$ 99.5%), urea (NH_2CONH_2, 99%), and ascorbic acid were purchased from Sigma-Aldrich.

2.2. BC and MEBC preparation

Rice straw, one the most common biomasses, was used for biochar preparation. Soil used in the experiment and rice straw were collected at the same sampling site. Raw materials were prepared for usage by being dried, crushed, sieved, ground using a 60 mesh sieve, and sieved. Some of the pretreated rice straw was then submerged in a solution containing urea, ascorbic acid, and $FeSO_4 \bullet 7\ H_2O$. (The molar ratio of ascorbic acid to iron salt was 2:1), and the mixture was put into a Teflon-lined autoclave, sealed, and heated for 10 h at 160 °C. After that, the material was dried for 24 h at 80 °C. The material was pyrolyzed at 700 °C under N_2 gas for 2 h, with a temperature ramp rate of roughly 10 °C/min [23,24]. The pyrolyzed biochar that had either metal loading or not was referred

to as BC or MEBC, respectively. The structure characteristics of BC and MEBC is shown in Fig. S1. The physical and chemical properties of biochar and magnetic carbon are shown in Table 1.

2.3. Paddy soil microcosm incubation

In order to simulate the field flooding conditions of paddy fields, a hypoxia soil incubation was performed. The experimental design included MPs contaminated treatments (PE and PVC), BC and MPs treatments, MEBC and MPs treatments, and blank control, with three replicates each (n = 21). Each 120 mL serum bottle added 50 g dry soil, then PE and PVC MPs were added to obtain a concentration of 1.5% by weight of soil. In the amendment treatments, BC or MEBC was added at 1.5% of soil dry weight. Then, SP was added to the MEBC treatment to activate the advanced oxidation process (AOPs). All bottles were saturated with 80 mL of sterile ultrapure water. Microcosms were kept at 25 °C in the dark and covered with aluminum foil to avoid evaporation during incubation.

Liquid sampling was performed at days 7, 21, 35, and 49. The mixture was collected using a 2 mL syringe, and centrifuged at 4000 rpm (Eppendorf 5804 R centrifuge) for 10 min. The upper liquid layer was stored at −20 °C for subsequent DOM analysis. Destructive soil sample was done 49 days after the start of incubation. The soil mixture was put in a tube and centrifuged in a high-speed centrifuge for 10 min at 4000 rpm (Eppendorf 5804 R centrifuge). Before DNA extraction, the obtained solid was stored at 80 °C. Concomitantly with the sampling of the solid phase, 15 mL of upper liquid phase were collected after the centrifugation step, and immediately frozen for subsequent organic structure analysis.

2.4. Characterization of soil leachate dissolved organic matter

The dissolved organic carbon of samples was determined using a TOC analyzer (TOC-L CPH, Shimadzu, Japan). The liquid samples were filtered through 0.45 μm filters, and diluted 1:25 before measurement.

DOM structural characterization was conducted using the 3D-fluorescence spectrophotometer (Aqualog; Horiba-Jobin Yvon, USA) with an excitation (Ex) range from 240 to 600 nm, and an emission (Em) range from 280 to 550 nm. With 3 nm excitation and emission slit band widths, the spectra were captured. Rayleigh scattering was subtracted from the original EEM data. To counteract the impact of Raman scattering, the same circumstances were used to run the fluorescence spectra of Milli-Q water. As previously mentioned, parallel factor analysis (PARAFAC) was used to investigate DOM fluorescence features [25]. MATLAB version 8.5.0197613 was used to carry out the PARAFAC modeling [26].

2.5. Illumina and Nanopore sequencing

Genomic DNA of the microbiota present in the soil samples collected on day 49 were extracted using DNeasy PowerSoil® (QIAGEN GmbH, Hilden, Germany) with minor modifications (https://doi.org/10.1016/j.watres.2018.02.001). NanoDrop (ThermoFisher Scientific, Waltham, MA) and Qubit fluorometer (Life Technologies, Carlsbad, CA) were used to check the samples' quantity and quality. Metagenomic sequencing was performed using Illumina NovaSeq platform at the Department of Biology sequencing facility. Total DNA pooled from all samples was adopted for the construction of a long-read library with the Rapid Barcoding kit (SQK-RBK004) and sequenced using a FLO-MIN106 R9 flow cell on a MinION device (Oxford Nanopore Technologies, Oxford, UK).

410 millions Illumina paired-end reads (150 +150 bp) and 2.66 millions Nanopore long reads with average length 4.043 Kb (10.75 Gbp) were used for downstream analysis.

2.6. Hybrid assembly and gene prediction

The quality check, filtering, and adaptor removal from Illumina reads were done with Trimmomatic (v0.39) and BBDuck. MEGAHIT (v1.2.9) was used for Illumina reads assembly with parameters "–presets meta-large" and "–min-contig-len 1000″ [27]. Basecalling of Nanopore raw fasta files, barcode assignment, and read filtering were performed using Guppy (v5.0.11 +2b6dbff). Nanopore long reads were assembled de novo using the meta-mode of Flye (v.2.9-b1768) [28]. Then, Pilon (v1.23) was used for error correction of Nanopore assembly based on Illumina reads [29]. Quickmerge v0.3 [30] was used to generate the final hybrid assembly results. Assembly metrics were calculated using QUAST (v5.0.2) [31] (The quality comparison of contigs obtained from different assembly methods is shown in Table S2). The binning process was performed with CONCOCT [32], MetaBAT2 [33], MetaBAT1 [34], VAMB (v3.0.2) [35] and MaxBin2 (v2.2.6) [36] to reconstruct the genome bins (GBs). The GBs generated from the above five binning softwares were dereplicated and aggregated via DAS_Tool [37] to obtain the final GBs. The completeness and contamination of each GB were estimated using checkM (v1.0.18) [38]. GBs having quality lower than 50% of completeness or contamination higher than 10% were discarded and the taxonomy was assigned to the remaining metagenome assembled genomes (MAGs) using GTDB-Tk (v1.3.0) based on the release 95 of the database GTD [39] and converted to the NCBI annotation using gtdb_to_ncbi_majority_vote.py. The 16 S rRNA genes were identified for each MAG with the in-house developed perl script extract_16S_using_hmm.pl (https://sourceforge.net/projects/extract-16s-rrna-from-genomes/) using Hidden Markov Models obtained from RNAmmer [40] and taxonomy was assigned using SILVA database release 138 [41]. The taxonomy obtained from 16 S rRNA genes was used when possible to improve the assignment obtained from GTDB-Tk.

2.7. Functional annotation and classification

Protein-coding genes were predicted using Prodigal (v2.6.2) with default parameters [42] and associated with KEGG IDs using EggNOG (v2.0.1–1) and DIAMOND (v0.9.22) [43]. To calculate the number of aligned reads per gene, HQ Illumina shotgun reads were mapped back to the assembly using Bowtie 2. Only the alignments with the highest scores were maintained. Read counts from each station were normalized by dividing them by the gene length in million kb to get reads per kilobase million (RPKM), which took into consideration the length of the gene and the total amount of reads for each sample In order to obtain a better insight on the functional capabilities of input genomes, EggNOG (v2.0.1–1) was used [44]. Metagenomic sequences were submitted to the NCBI Sequence Read Archive database under the Bioproject accession number PRJNA892267.

Table 1
Physicochemical Properties of Biochar and Magnetic Biochar.

	C content (wt %)	H content (wt %)	N content (wt %)	O content (wt %)	Fe content (wt %)	S content (wt %)	H/C	O/C	C/N	specific surface area (m^2/g)
BC	52.01	1.05	0.57	17.87	-	-	0.24	0.26	106.41	80.92
MEBC	18.47	-	2.11	5.96	30.37	33.56	-	0.24	10.21	120.84

2.8. Statistical analysis

Differences in TOC content between treatments were statistically compared using a one-way or two-way ANOVA ($\alpha < 0.05$) in SPSS 19.0. The two sided Welch's t-test was used to determine significantly different MAGs and genes between each treatment and blank samples. A permutational multivariate analysis of variance was conducted using the adonis function to evaluate significant effects of various treatments. Using the EnrichM's "annotate" and "enrichment" function (v0.6.30), enzymes enriched in particular treatments of MAGs were found based on statistical findings from the Fisher exact test (https://github.com/geronimp/enrichM). To identify enriched species in every single treatment, the fold change was calculated and a 2-fold threshold was selected.

3. Results

3.1. Evidence of Changes in Soil Dissolved Organic Matter

The fraction of soil organic matter that can be extracted using aqueous or diluted salt solutions is known as DOM (Bolan et al., 2011). Changes in TOC of soil DOM among different treatments during the incubation period are reported in Fig. 1 A. Overall, changes in the TOC are significantly different among amendments ($p < 0.05$). When compared to blank, PE and PVC MPs increased TOC respectively by 69.02% and 93.49% on day seven. However, after 35 and 40 days, the TOC values for the two MPs treatments were significantly lower than that of the blank, indicating a long-term inhibitory effect of MPs on soil organic content. These results are consistent with previous reports that PE MPs altered soil aggregate structure and decrease solubility, ultimately leading to a reduction in organic carbon [45]. On day 49 the TOC of treatments treated with PE and PVC MPs decreased by 31.61% and 42.80%, respectively compared to the blank. The application of BC further reduced the content of TOC in MPs-contaminated soil throughout the incubation period, especially on samples with PE MPs. In contrast, the MEBC resulted in a significant increase in TOC during the same period. On day 49, the TOC value in the MEBC-PE treatment was as high as 405.98 mg/kg soil, and that in the MEBC-PVC treatment reached 287.4 mg/kg soil.

Given that the organic molecules released directly from MPs are likely to be high molecular weight polymers, we further investigated the DOM structure through 3D-EEM. The fluorescence spectra of the oscillatory release of MPs are shown in Fig. S2. Compared with initial PE and PVC MPs, the fluorescence intensity and total amount of the MPs aqueous solution treated with MEBC were increased noticeably, supporting the role of MEBC in promoting the release of organic matter from MPs. After 50 days, two main components were identified in all the soil leachate samples (Fig. 1B). Fig. 1 C provides a comparative view of the fluorescence intensity measured for each component in the different treatments. Table 1 shows the peak positions and corresponding descriptions for different DOM components. Component 1 featured two peaks of excitation/emission (Ex/Em), one at 250/325 nm and another at 250/425 nm, which are classified as typical UVA humic in paddy soil [46]. The fluorescence intensity of C1 in MPs PE was higher than that identified in PVC, and the application of BC resulted in a similar intensity of C1 between these two treatments. Unlike the fluorescence quenching determined by other pollutants, polypropylene MPs have been demonstrated to enhance the accumulation of high molecular weight humic-like material [47], which seems to be consistent with the increase in C1 intensity brought about by PE treatment in this work. Component 2 (C2) presented an Ex/Em maximum at 275/340 nm which was related to the protein/phenol-like substances [48]. In general, Protein/Phenol-like compounds are biodegradable, and it is worth noting that the content of C2 in the PE and PVC MPs treatments increased significantly with MEBC treatment.(Table 2).

3.2. Influence of multiple treatments on the microbial community composition

Microbial colonization was observed around MPs isolated from soil (Fig. S1D), which provided evidence to some extent that MPs were utilized by soil microorganisms as a carbon source. In order to investigate the effect of the MP, BC and MEBC on the microbial community, soil samples from the blank control and six different treatments were collected after 49 days of incubations. The role of the microbiome in microcosm bottles was determined by both analyzing the entire set of genes predicted on the assembly (defined as "global assembly analysis" in the rest of the paper), and using a genome-centric metagenomic approach (defined as "genome-centric investigation"). Shotgun sequences were obtained with a mixed strategy based on Illumina and Nanopore reads, and their assembly resulted in 1.3 millions contigs larger than 1 kbp, for a total size of 2.91 Gbp.

Binning of the scaffolds allowed to recover 193 MAGs, 52 of them having high-quality (completeness $\geq$ 90% and contamination $\leq$ 5%), while the remaining 141 MAGs had medium quality (50% $\leq$ completeness $\geq$ 90% and 5% $\leq$ contamination $\leq$ 10%). The relative abundance of 105 MAGs exceeds 1%, and they were taxonomically assigned to 14 bacterial phyla, as shown in Fig. 2. Among them, *Proteobacteria* (48 MAGs) dominated the microbial community. *Proteobacteria* species are highly different in terms of metabolic properties, and for this reason they can play many important roles in global nutrient cycling and carbohydrate degradation. The significant reduction of *Proteobacteria* relative abundance in the BCPE and PVC treatments is consistent with the low organics found in these samples, indicating a less efficient carbohydrate metabolism. The phylum *Actinobacteria* (18 MAGs) and *Acidobacteria* (6 MAGs) possess a series of genes involved in multiple metabolic pathways, which are involved in the regulation of biogeochemical cycles, the breakdown of biopolymers, and the secretion of exopolysaccharides [49,50]. It is worth noting that the abundance of these two taxa did not show an increase in MEBC treatments. However, they were found to be enriched in BCPE and PVC treatments. This difference in microbial community composition could be attributed to the fact that in MEBC treatments, the initial deterioration of the polymer was likely due to free radical attack. *Candidatus Saccharibacteria* (2 MAGs) was significantly enriched only in the MEBC treatment; it was previously associated with soil humus fermentation, which can result into acetic and lactic acid accumulation [51]. *Bacteroidetes* (6 MAGs) are more prevalent in soils with higher levels of organic carbon; a rise in their relative abundance after exposure to MEBC-PVCs suggests a high rate of soil carbon mineralization [52,53]. In addition to the taxonomic groups mentioned above, other phyla commonly identified in soils include *Firmicutes* (9 MAGs), *Gemmatimonadetes* (4 MAGs), *Planctomycetes* (2 MAGs), and *Chloroflexi* (9 MAGs).

3.3. Key genes involved in MPs degradation on the global level

Analysis of the RPKM values of the genes among all the samples was used to clarify the effect of different treatments on the functional activity of the microbial community. By checking all the genes in the assembly, it was found that 1.83% of them were showing a significant change in relative abundance between PE and blank. When BC and MEBC were added, the percentage of significantly different genes accounted for 1.35% and 6.48%, respectively. While comparing PVC and blank samples, the fraction of significantly different genes was 0.97%, and BC and MEBC addition increased this fraction to 1.48% and 14.33%, respectively (Fig. S7). These findings suggest that MEBC is impacting more functions than the other treatments.

In the following section, RPKM values of genes associated with the pathways were used as "proxy" to define the impact of the treatments on the different functions. Analysis was refined by checking specific functional pathways, tailoring the process on transport systems and metabolic pathways involved in the utilization of potentially available

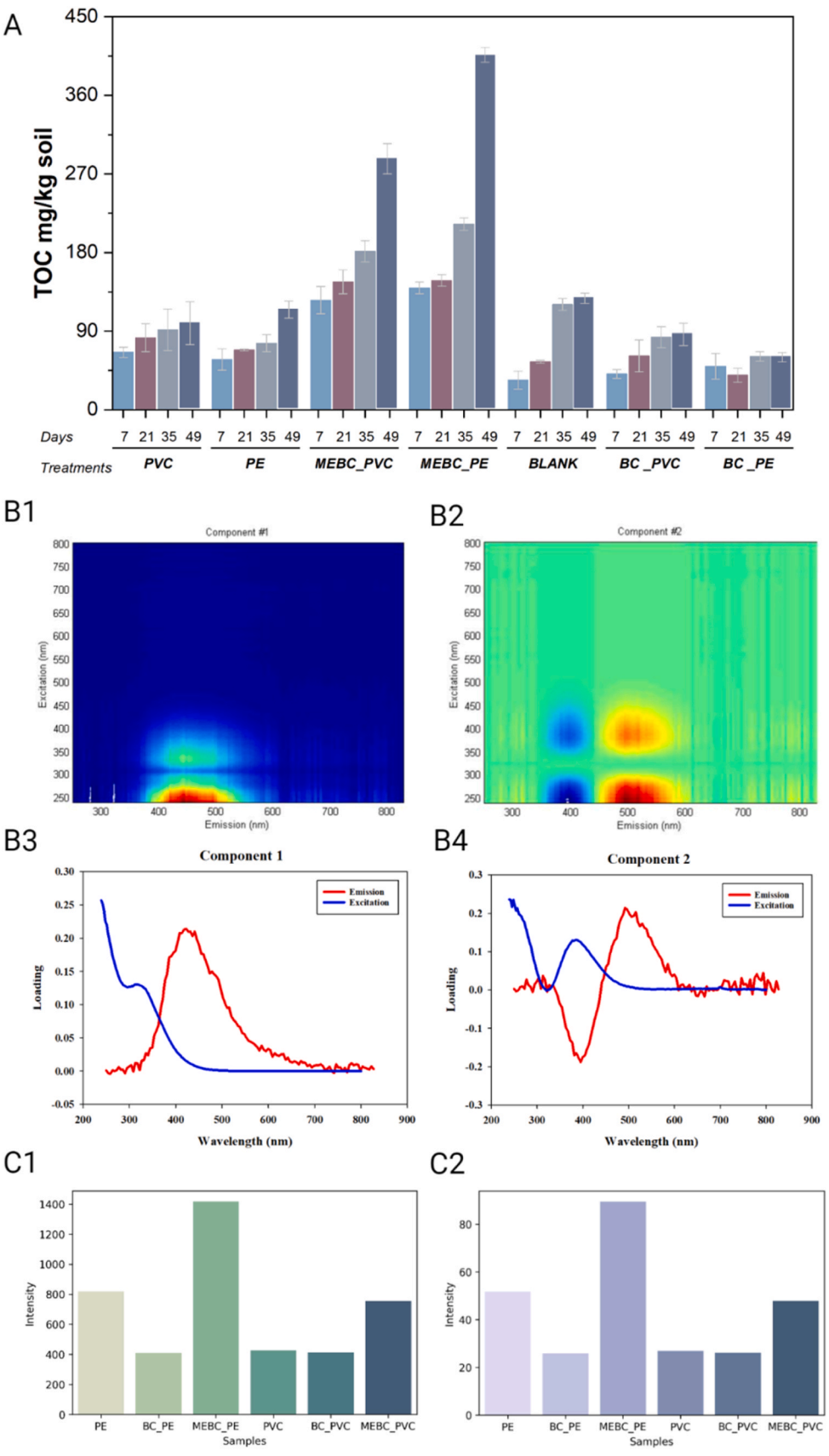

Fig. 1. Shifts in soil DOC. Total organic carbon levels of soil DOC measured for the different treatments. (B1–4) Soil DOM components on the 49th day identified by EEM spectroscopy. B1 refers to UVA humic acids, B2 to protein/phenol-like substances, B3 reports the wavelength of Ex/Em spectra for B1, and B4 reports the wavelength of Ex/Em spectra for B2. (C1–2) Fluorescence intensities of the two components among different treatments. C1 represents UVA humic acids, C2 represents protein/phenol-like substances.

Table 2
Excitation and emission maxima of the fluorescent components of the DOM samples.

Components	Ex/Em (nm)	Description
C1	250,325/425	Humic acid-like
C2	275/340	Protein/Phenol-like

substrates coming from MPs. The MPs' degradation can be divided into two parts. In the first one, an upstream pathway leads to the depolymerization of macromolecular polymers into smaller oligomers, which are further reduced into monomers by specific enzymes. In the second part, downstream pathways contribute to the mineralization of the monomers released in the first step [54]. According to this process, the increased abundance of genes involved in the metabolic processes of the intermediate compounds, and the related transporters are indicative of an increased MPs degradation. Under PE and PVC MPs treatment, some genes encoding oligosaccharides, lipids, and amino acids transporters changed in abundance (Log_2 FC exceeded $\pm$ 2). In addition, when MEBC remediation is carried out, the fraction of genes encoding transporters with a Log_2 FC > 2 was increased (Fig. 3A, Table S6). Based on the KEGG annotation results obtained from the genes predicted on the global assembly, the metabolic pathways including enzymes potentially associated with the MPs degradation potential were reconstructed. For the selected pathways the fraction of genes significantly increasing in relative abundance in each treatment was reported in Fig. 3B. Compared to PVC MPs, PE MPs showed stronger effects on some pathways. BC addition resulted in an increased abundance in the microbiome of genes involved in pyruvate metabolism, propanoate metabolism, chloroalkane-chloroalkene degradation, and fatty acid degradation (FAD) of PE. In contrast, it was found a decreased abundance of genes related to the degradation of aromatic compounds. MEBC addition resulted in an increased abundance of genes encoding ABC transporters and those involved in butyrate metabolism, suggesting a more efficient mineralization of the degradation products derived from PE MPs. Addition of MEBC on PVC MPs resulted in a more pervasive effect, and genes having an increased abundance were associated with pathways involved in the degradation of both aromatic compounds and fatty acids. Unexpectedly, there was no enrichment of genes involved in the chloroalkane-chloroalkene degradation pathway.

Some key enzymes involved in the degradation of the polymeric structures of MPs into monomers were selected and their relative abundance in the different samples was investigated. These enzymes include alkane monooxygenase, alkane dehalogenase, polyvinyl alcohol (PVA) dehydrogenase, and enzymes involved in the degradation of aromatic compounds, which play a crucial role in the degradation of MPs. The relative abundances of genes encoding these enzymes are shown in Fig. 3C. According to our reconstruction, alkane monooxygenases of the

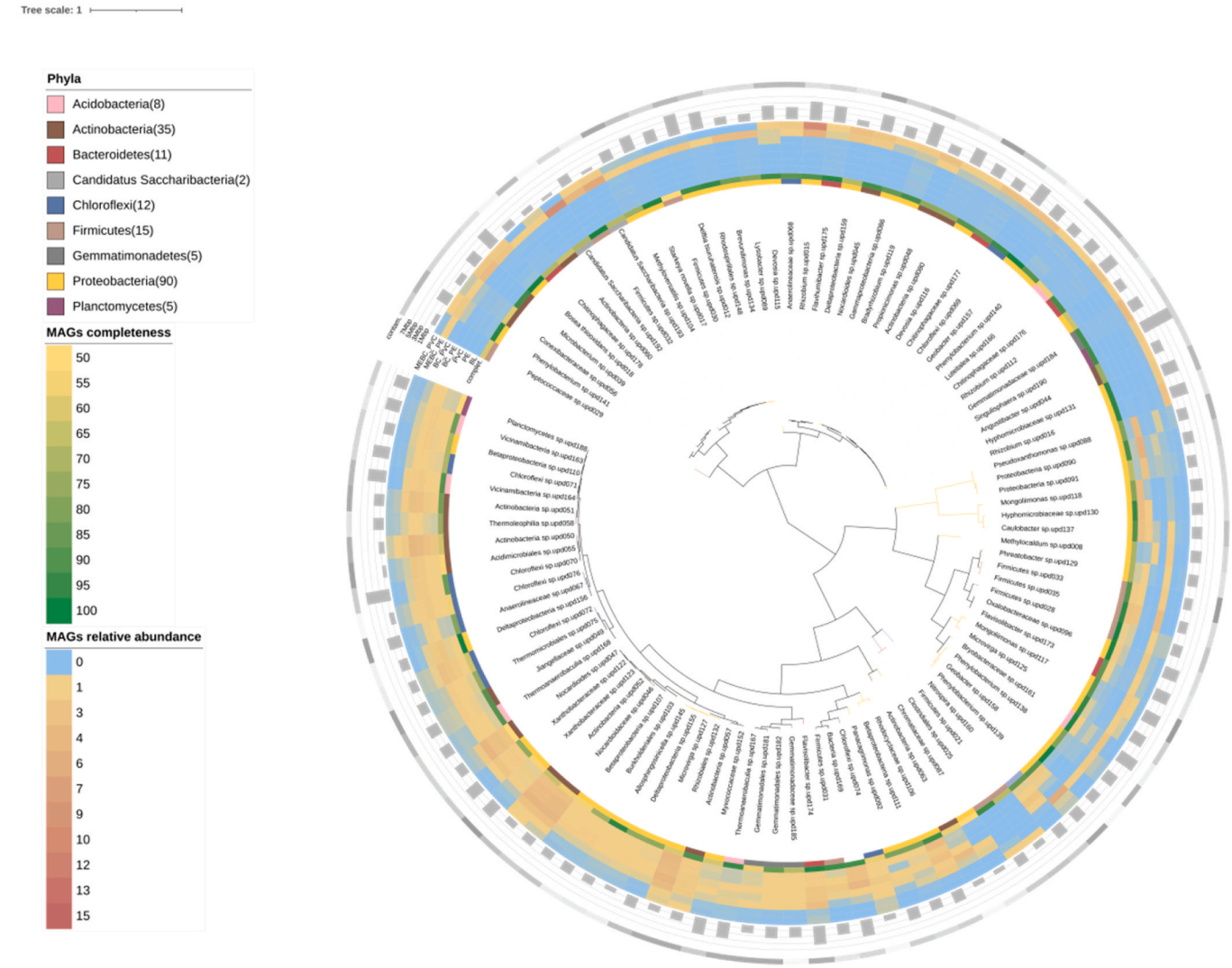

Fig. 2. Properties of 105 MAGs identified in the microbiomes: MAGs coverage, quality, and taxonomic assignment.

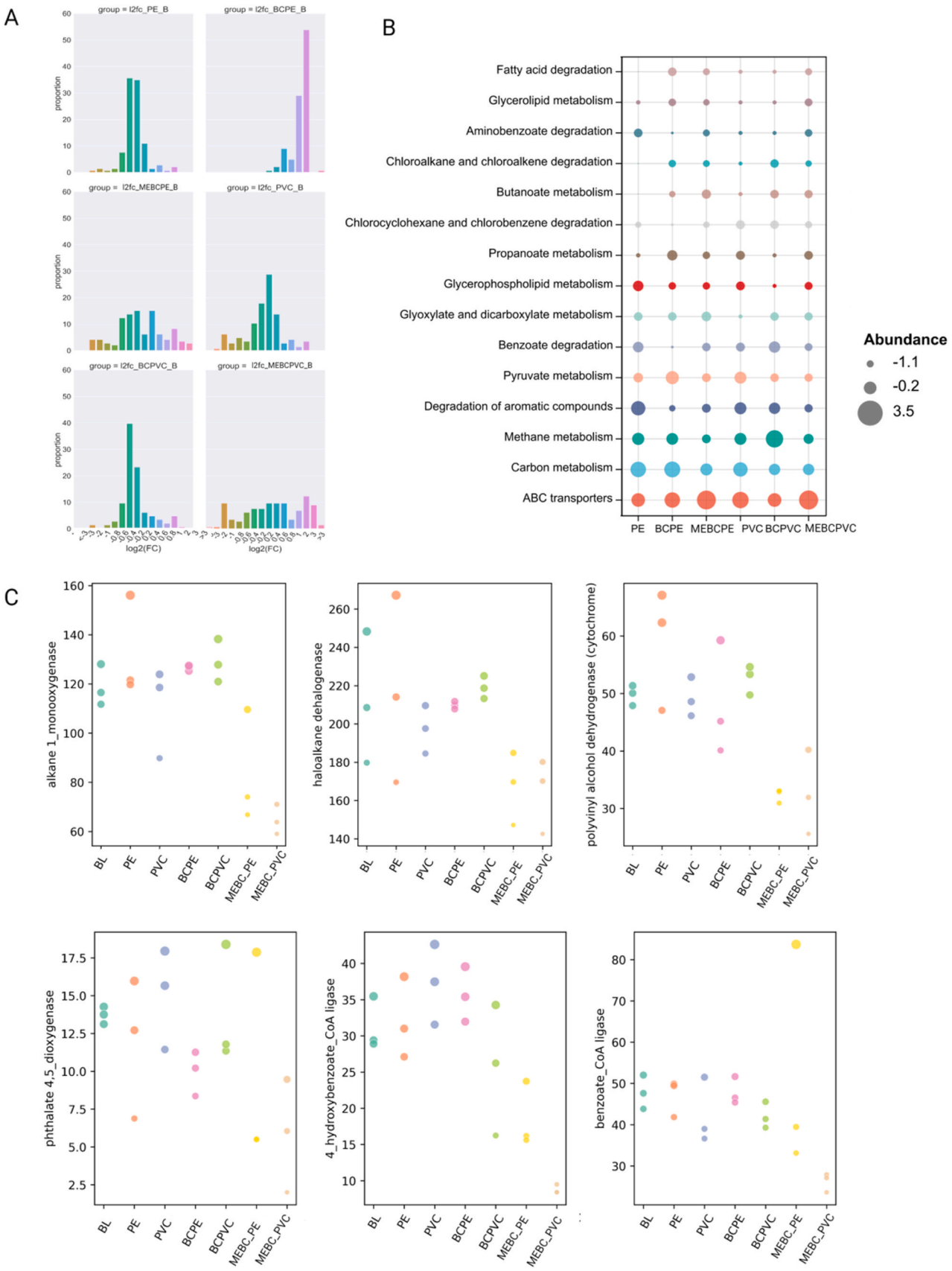

Fig. 3. Soil functional activities potentially associated with the MPs degradation. (A) Relative abundance determined for ABC transporters. (B) Fraction of genes with significantly increased relative abundance (compared to blank) in different treatments. (C) RPKM values of some selected key enzymes among different treatments.

AlkB family (EC 1.14.15.3) are important enzymes belonging to the long-chain alkane degradation pathway. The RPKM of the genes encoding enzymes EC 1.14.15.3 increased in the PE treatment in comparison to the control, but significantly decreased in the MEBC-PE and MEBC-PVC treatments. Haloalkane dehalogenases are hydrolases which break down halogenated aliphatic molecules to produce alcohols, halide ions, and protons as byproducts [55]. In this context, enzyme EC 3.8.1.5, which has alkane dehalogenation capability, is performing one of the crucial steps [56]. However, this gene revealed a decreased relative abundance only after exposure to MEBC-PE and MEBC-PVC. After the dehalogenation step, PVC can be converted to PVA [57,58]. For this reason, PVA dehydrogenase (PVADH) can be considered as a potential signature of the PVC degradation degree. Similar to alkane monooxygenase, the relative abundance of the PVADH gene was increased in the PE treatment, and significantly decreased in the MEBC-PE and MEBC-PVC treatments.

In the downstream degradation pathway, the aliphatic and aromatic compounds generated are further degraded and utilized. Given that aliphatic compounds are more easily degraded than aromatic compounds [59], the genes encoding the degradation of PAHs and benzoates enzymes were also investigated (Fig. 3C). According to the PAHs degradation pathway, the phthalates produced by the activity of 2-formylbenzoate dehydrogenase (EC 1.2.1.78) can be further degraded by enzymes of the phthalate 4,5-dioxygenase (EC 1.14.12.7), which acts on phthalates to generate protocatechuate degradation. In addition, the gene encoding 4-hydroxybenzoate-CoA ligase (EC 6.2.1.27) also had higher RPKM value in the PVC treatment compared to the blank, and its increased abundance predicted increased levels of anthranilate degradation.

3.4. MPs degradation process driven by key microbial species

3.4.1. Prediction of the peoxidized long-chain alkane utilization pathways by Nocardioides

Based on a genome-centric approach, 20% of the scaffold identified was assigned to the MAGs; the genome-centric approach allowed a more specific investigation of the functional role of some selected species. Nineteen MAGs harbor potential alkane C-C bond cleavage-related

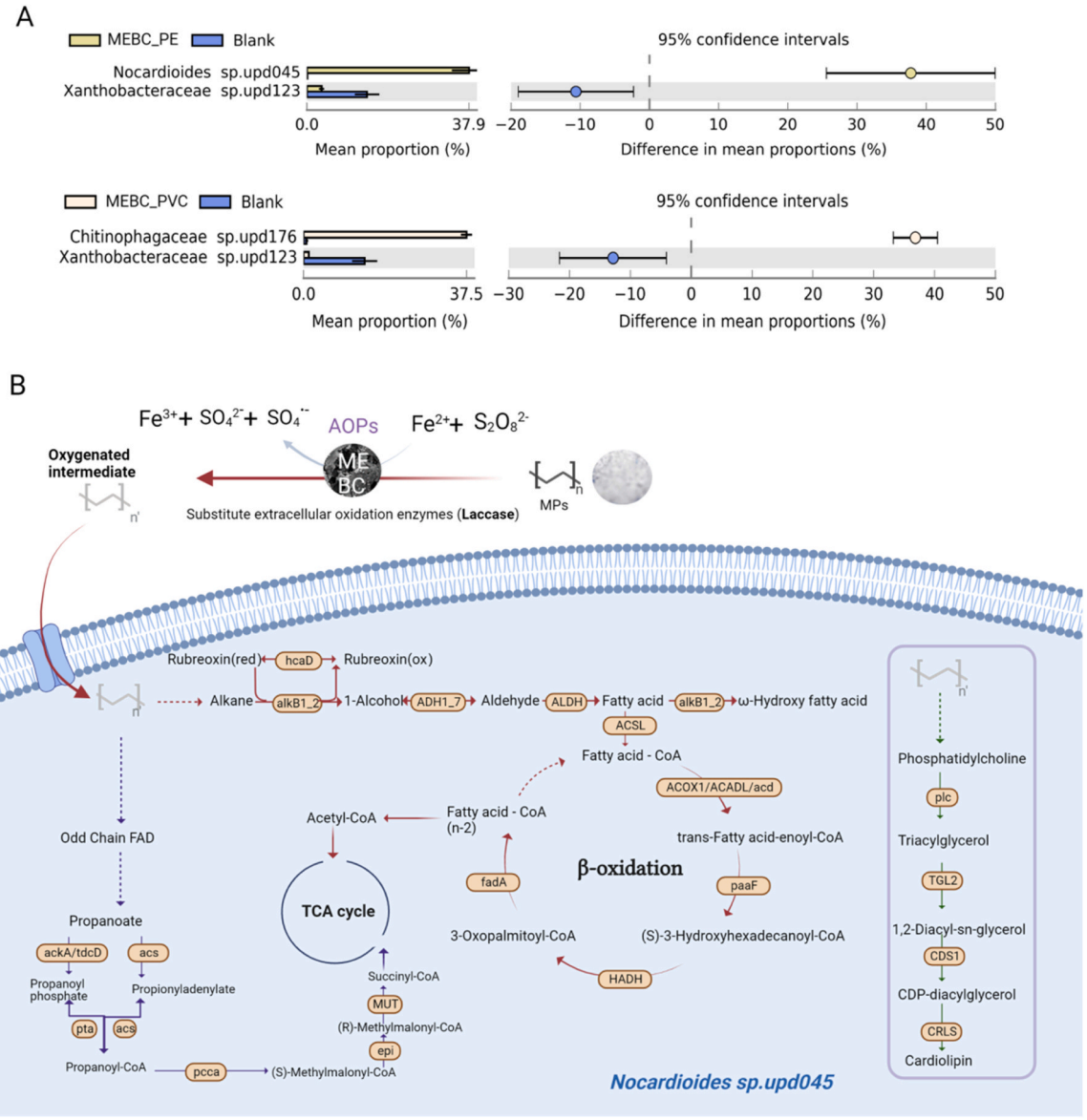

Fig. 4. (A) MAGs potentially involved in C-C bond cleavage have a highly different relative abundance in different treatments compared to the blank. (B) Graphical representation of the proposed n-alkane metabolic pathway in *Nocardioides* sp. upd045. All relevant genes used for metabolic reconstruction can be found in Table S10.

functions (alkane monooxygenase) (Fig. S8A). Among these MAGs, *Nocardioides* sp. upd045 was significantly enriched in the MEBC-treated treatment (Fig. 4A), showing that this microbial species may enhance the pro-oxidative function of magnetic biochar, resulting in accelerated MPs degradation. A specific functional investigation of this MAG performed according to KEGG annotation, revealed the presence of complete alkane cleavage and β-oxidation of FAD pathways (Fig. 4B). *Chitinophagaceae* sp. upd176 was significantly enriched only in the MEBC-PVC treatment. Despite this species missing acyl-CoA oxidase and does not have a complete β-oxidation pathway, it possesses glutaryl-CoA dehydrogenase. This enzyme can integrate the odd-chain fatty acid product Glutaryl-CoA into the last step of β-oxidation, thus generating acetyl-CoA, which can enter the TCA cycle. In addition to the degradation occurring through β-oxidation, some saturated fatty acids require additional degradation steps [60]. For example, FAD degradation produces succinic semialdehyde (a short chain of four carbon atoms) or propionate. They require further production of succinyl-CoA by succinate-semialdehyde dehydrogenase (EC 1.2.1.16; EC 1.2.1.79), and propionyl-CoA carboxylase. The complete propionate metabolic pathway was observed in *Nocardioides* sp. upd045 and *Chitinophagaceae* sp. upd176.

3.4.2. Species involved in alkane dehalogenation in the paddy soil microbiome

Given the high fraction of MAGs (46.7%) containing alkane dehalogenase (EC 3.8.1.5) (Fig. S8B), attention was focused on the 22 members significantly enriched ($p < 0.05$) in specific samples in comparison to the blank. Most of the species were increased in relative abundance in MEBC-PE and MEBC-PVC treatments, with *Rhizobium* sp. upd015 and *Microbacterium* sp. upd039 being the most significant (Fig. 5A). *Bryobacteraceae* sp. upd161 resulted in significantly increased abundance in BCPVC. Additionally, there were 15 MAGs with PVADH-related genes potentially involved in PVA degradation (Table S6). *Phenylobacterium* sp. upd141 was enriched in MEBC treatments, and it encodes enzymes acting both as dehalogenase and also PVADH. Among all the PVA potential degraders, *Proteobacteria* sp. upd090 was dominant (5.23%) in the PE treatment. While compared to PVC treatment, the relative abundances of *Phenylobacterium* sp. upd138 and *Bryobacteraceae* sp. upd161 in BCPVC treatment increased by 1.6% and 1.8%, respectively.

3.4.3. Species involved in downstream benzoate metabolism

In addition to long-chain alkanes, various additives can be potentially released from MPs, undergoing a further degradation process. Most of the additives belong to complex PAHs organic compounds, and their degradation byproducts are usually further funneled into the benzoate metabolic pathway. To gain more insights on this process, a dedicated analysis was performed on 27 MAGs encoding benzoate ligase (EC 6.2.1.25) (Fig. S8C). Among them, *Pseudacidovorax* sp. upd097, *Bradyrhizobium* sp. upd119 and *Blastocatellia* sp. upd162 showed a significant increase in samples treated with MEBC (Fig. 6A). According to the results of the KEGG reconstruction, these three MAGs have a complete pathway to degrade benzoate to 5-Carboxy-2-pentenoyl-CoA (Fig. 6B). It is worth noting that *Pseudacidovorax* sp. upd097 and *Bradyrhizobium* sp. upd119, which are significantly enriched in the MEBC-PVC treatment, also have a complete pathway for 4-Hydroxybenzoate degradation. This latter compound can be generated from benzoate through the action of benzoate 4-monooxygenase. The enrichment of the three MAGs mentioned above in the MEBC-PVC treatment could be related to phthalate plasticizers commonly used in PVC production [61]. We further discussed the species involved in the transformation of the critical intermediate catechol in the supplement note. Interestingly, *Rhizobium* sp. upd015 not only has genes that encode enzymes EC 6.2.1.25, Catechol 1,2-dioxygenase (EC 1.13.11.1), and catechol 2, 3-dioxygenase (EC 1.13.11.2) but also has the potential to perform alkane dehalogenation, providing a possible explanation for the versatility of this strain potentially involved in PVC MPs degradation.

4. Discussion

Generally, soil DOM can be considered a reliable indicator of changes in biochemical reactions. Currently, a combination of TOC analysis and EEM spectroscopy has been successfully used to investigate DOM properties in multiple environmental systems [62]. According to our findings, MEBC can considerably increase TOC, while MPs alone had an inhibiting effect on the accumulation of total dissolved organic matter in the soil. Moreover, MEBC addition led to the accumulation of a large amount of C1, consistently with the high TOC measured. There are

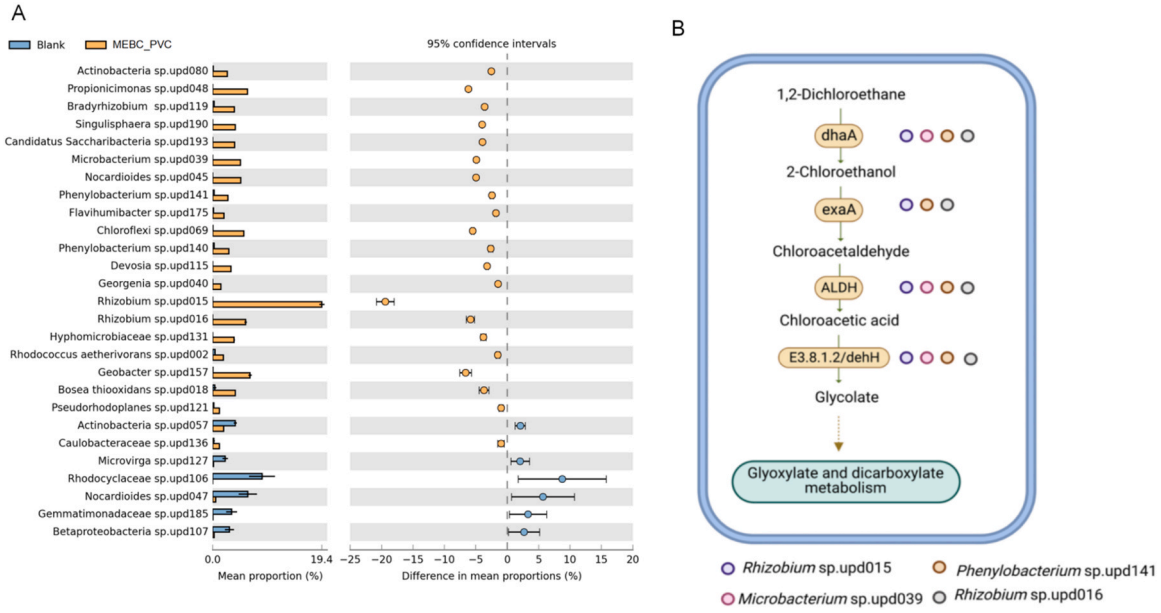

Fig. 5. (A) Relative abundance of dehalogenation-related MAGs in MEBC-PVC treatment compared to the control. Genome information of MAGs with dehalogenation potential is shown in Fig. S9. (B) Microbial species potentially involved in the downstream dehalogenation process. All relevant genes used for metabolic reconstruction can be found in Table S10.

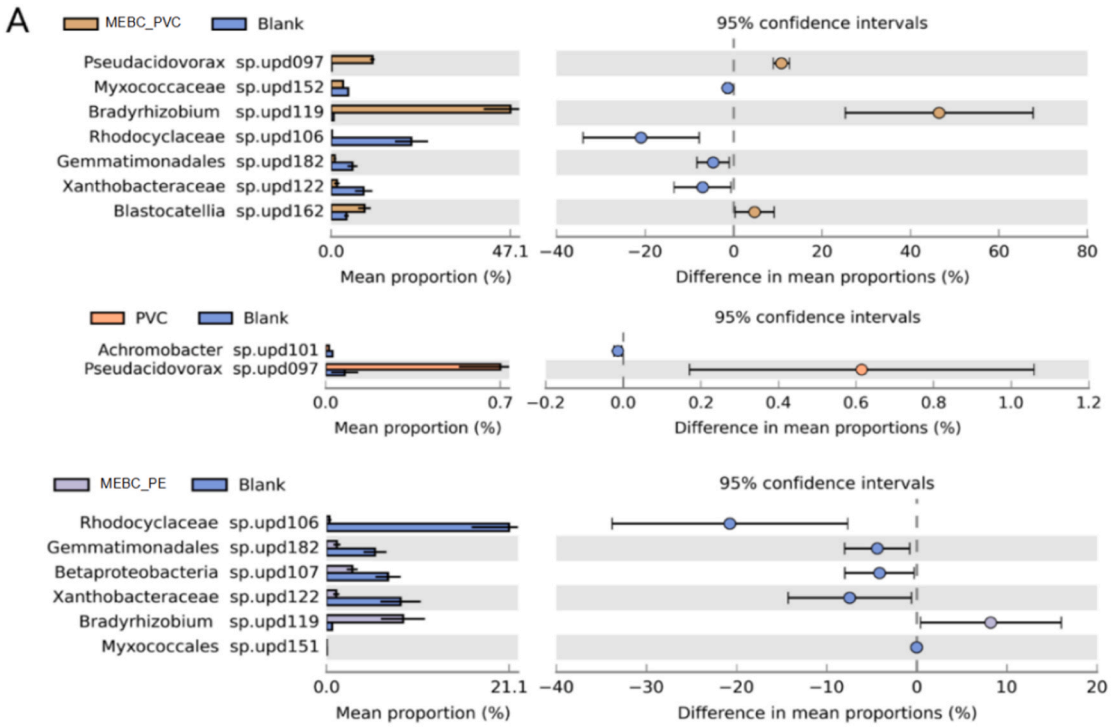

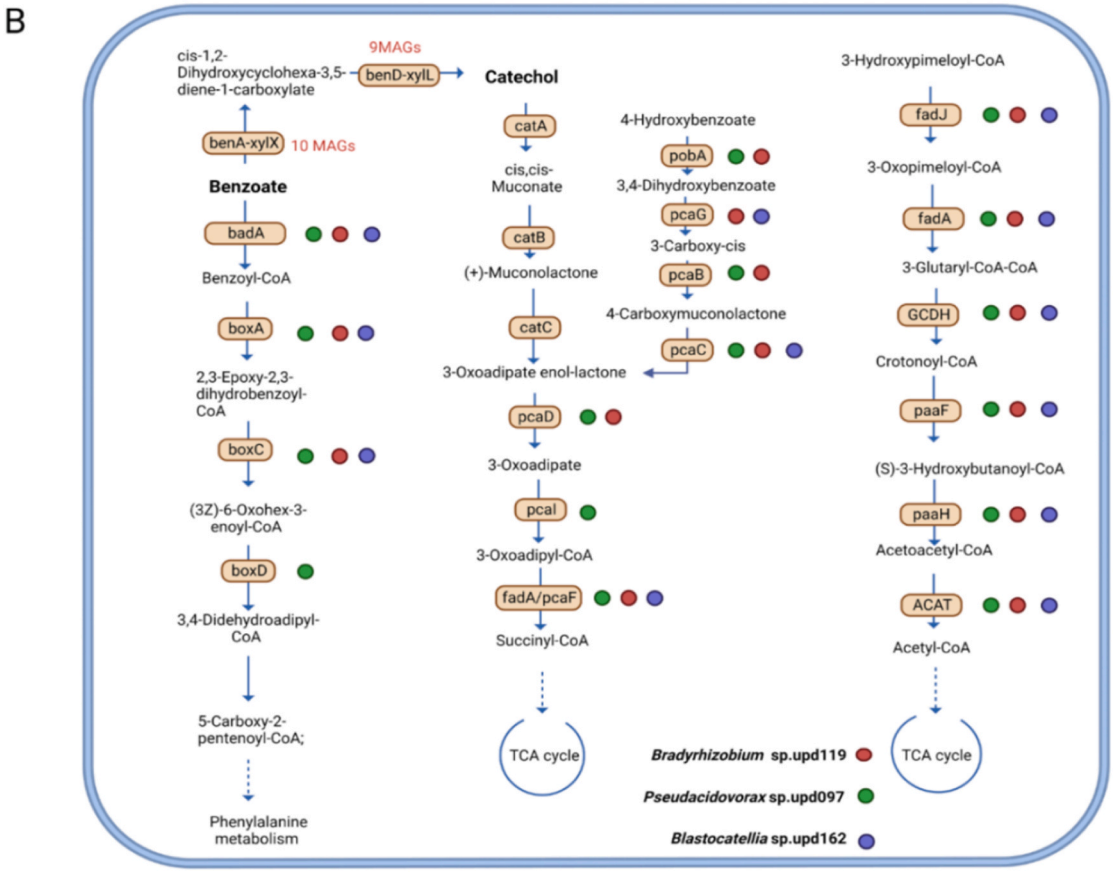

Fig. 6. (A) MAGs containing benzoate ligase revealed a significantly different abundance in the comparisons performed between blank and some other treatments such as MEBC-PVC, PVC and MEBC-PE. (B) Potential benzoate metabolic pathways identified in MAGs enriched in MEBC treatments. All relevant genes used for metabolic reconstruction can be found in Table S10.

various possible explanations for the change in the fluorescence intensity evidenced in DOM, including for example processes leading to its oxidation, concentration, electronic group change, etc. [63,64]. In this case it can be assumed that MEBC can promote the oxidation reaction, thereby increasing the fluorescence intensity of the aromatic compounds. It should be noted that the soil microbiome is complex, and many species possess specific degradative activities. These microorganisms may respond to plasticizer-like pollutants, utilizing them as a carbon source, resulting in a ripple effect on soil biochemical functions. For microplastics, even though the proportion of readily biodegradable fraction may be low, the dissolved substances can still affect the microbial community structure, particularly in PVC MPs with a high proportion of plasticizers [65]. While our study observed an increased content of total organic carbon and macromolecular organic matter in MEBC treatment, further evidence is required to directly identify the organic matter source. The complex composition of soil leachate poses challenges to the detection of high molecular weight compounds and the quantification of various organic compounds, as they exist in low concentrations. We concentrated the sample via evaporation to dryness and analyzed it using GC-MS to obtain a more detailed understanding of the liquid phase composition. However, even after concentrating the sample tenfold and dissolving it in toluene, no prominent peaks were detected. Further investigation of the product using high-resolution mass spectrometry is therefore warranted and could prove valuable in future studies.

Hybrid assembly and metagenomic binning are advanced techniques for studying microbial communities involved in microplastic degradation. The microbial communities in microvials of different treatments were analyzed in the current study to reveal the dynamic characteristics of microbial responses to MPs treatment in paddy soil systems. The analysis identified a highly complex metagenome consisting of 193 MAGs. Only 32 MAGs were present in the sample with relative abundance higher than 3% (Fig. S3). Both PE and PVC MPs increased the abundance of Actinomycetes. In addition, *Pseudoxanthomonas* sp. upd088 was also specifically enriched in the PE treatment; species belonging to this taxon were previously reported to have the ability to degrade a range polysaccharides like lignin and cellulose, but also polyester [66,67]. A significant increase in the abundance of *Phenylobacterium* sp. upd139 was also observed in the BCPVC treatment. Species of this taxon were frequently found in herbicide and crude oil-contaminated soils [68,69] and were associated to the metabolic processing of PAH) [70]. The dominant MAGs identified in the MEBC treatment group were markedly different in comparison to the other treatments (Fig. S3). *Rhizobium* sp. upd015 was dominant in both MEBC-PE and MEBC-PVC treatments. The *Rhizobium* genus has been reported as enriched in soils contaminated by MPs [71], and it has the potential to degrade polyesters to synthesize polyhydroxyalkanoates [72]. In summary, the enriched MAGs seem to be involved in the degradation of a variety of polyesters, lignin, and carbonaceous organics. An investigation of putative obligate and/or facultative syntrophic among 104 members of the paddy soil microbiome was conducted using co-occurrence analysis. The results of this analysis showed that multiple MAGs within the paddy soil community exhibited significant reciprocal co-occurrence (Fig. S4). An example of this is the MEBC-enriched *Rhizobium* sp. upd015, which was found to have a significant positive correlation with *Microbacterium* sp. upd039, *Clostridiales* sp. upd025, *Flavihumibacter* sp. upd175, and *Chitinophagaceae* sp. upd176, suggesting their potential to establish a facultative reciprocal relationship. Considering the diversity of organic sources in soil, analysis of species abundance cannot provide a detailed picture of the functional roles related to MPs degradation, which can be clarified by investigating the metabolic pathways. Therefore, genome-centric functional analysis is important to reveal changes in the degradation potential of MPs.

Through the investigation of the PRKM value of the enzyme at the overall level, it was found that MEBC treatment seems not to determine a significant increase in their relative abundance. One possible explanation is that the redox reactions induced by MEBC may reduce the dependence of the degradation process on enzymes on the global level. As evidenced by the distribution of the relative abundance of ABC transporter genes reported in Fig. 4B, some transporters were significantly promoted in MEBC treatments. Additionally, the genes encoding the acetyl-CoA transporter assigned to the last step of the fatty acid and benzoate metabolism did not reduce in abundance in MEBC treatments. According to this finding, the results obtained from the analysis of the global assembly cannot provide a detailed view of the process at the species level, so we further reconstructed the metabolic pathways of species containing key enzymes.

Both degradation and dehalogenation pathways involving PE and PVC MPs were investigated. Besides the common β-oxidation pathway, since it was reported in previous studies that polyethylene would affect the glycerolipid metabolism in microorganisms [73], the changes in glyceride and glyceophospholipid metabolism were examined in the "global assembly analysis (Fig. 3A). Some genes related to this pathway were significantly more abundant in PE, BCPE, MEBC-PE and MEBC-PVC treatments. The completeness of these pathways was checked in some selected MAGs. The results indicate that *Nocardioides* sp. upd045 specifically encodes diacylglycerol kinase, which can convert diacylglycerol to phosphatidic acid, and may ultimately generate cardiolipin (CL) which is relevant to determine the composition of the bacterial membrane structure (Fig. 5B) [74]. It is worth noting that CL is a lipid with unique properties that exist only in membranes that generate electrochemical potentials, it contains four acyl chains and tends to form non-lamellar structures, potentially acting as a proton sink [75]. Moreover, global-level analysis revealed a higher abundance of *btaA/btaB* genes involved in 1,2-Diacyl-sn-glycerol metabolism in the MEBC-PE samples. Regarding the MEBC-PVC samples, an increase was also observed in the RPKM value of the diacylglycerol kinase enzyme (EC 2.7.1.107), which plays an important role in the phosphatidylcholine (PC) biosynthesis pathway. These findings are consistent with previous studies reporting that some bacteria can efficiently integrate and modify n-alkanes into membrane fatty acids [76]. Additionally, the biodegradation of MPs, especially n-alkanes from the oxidized PVC MPs, was not limited to the metabolism of fatty acids but can also lead to synthesis of compounds that can be integrated in bacterial membranes. On the other hand, pre-oxidation processes can be enzymatically or chemically-mediated. For example, secreted laccase (EC 1.10.3.2) has been reported to play a key role in PE biodegradation by promoting pre-oxidation [71]. The enzyme EC 1.10.3.2 was found in 28 MAGs (Table S6). However, the cumulative abundance of these MAGs was not significantly higher in the MEBC-treated treatment, suggesting that the pre-oxidation of MPs in these samples was not strictly dependent on laccase activity but probably to other AOPs mediated by MEBC (Fig. 4B).

There are some unresolved aspects regarding the dehalogenation of MPs, especially PVC. For example, it is still undefined whether the dehalogenation process occurs mainly before or after the C–C backbone cleavage. In theory, if the extracellular long-chain vinyl chloride undergoes dechlorination first, it can be converted to polyvinyl alcohol or to partially depolymerized PVA. PVA can be imported into the periplasm, where it is oxidized by intracellular pyrroloquinoline quinone-dependent PVADH, which uses cytochrome c as an electron acceptor [77]. Finally, it can be hydrolyzed by the enzyme oxidized PVA hydrolase (OPH) or by β-diketone hydrolase [78]. Experimental results obtained in the present study do not support this hypothesis, because the RPKM of the gene encoding PVADH has low values in MEBC treatments, and MAGs containing PVADH did not increase in abundance in MEBC treatments. These findings are inconsistent with the enrichment of the final step dehalogenation MAGs evidenced in MEBC-PVC treatments. Therefore, we speculate that long vinyl chloride chains could first undergo C-C chain scission, which is followed by intracellular dehalogenation, rather than being firstly converted into PVA. By integrating

genomic information from MAGs containing alkane dehalogenase, the complete dehalogenation pathway of 1,2-dichloroethane belonging to short-chain alkanes was observed in *Rhizobium* sp. upd015, *Rhizobium* sp. upd016 and *Phenylobacterium* sp. upd141(Fig. 5B). Furthermore, alkene monooxygenase EC1.14.13.69 was predicted in *Geobacter* sp. upd157 and *Bryobacteraceae* sp. upd161, suggesting a putative tetrachloroethylene degradation activity in these MAGs. Although MEBC treatment did not increase the RPKM value of EC 3.8.1.5 at the global level, some MAGs with dehalogenation potential were significantly enriched in the MEBC-PVC treatment. However, the pathways from long-chain chlorinated alkanes to 1,2-dichloroethane is still not completely clarified, and more in-depth studies are needed in the future to investigate the precise enzymatic steps converting MPs to short-chain chlorinated alkanes.

5. Conclusion

This study shows that the cooperation of soil microbes and magnetic biochar significantly increased the dissolved organic matter level in microplastic-contaminated soil. Additionally, species belonging to *Nocardioides* and *Rhizobium* are able to perform a key step in long-chain alkane utilization and alkane dehalogenation, and they can work in cooperation with benzoate metabolizing species that were found significantly enriched in MEBC treatments. Overall, this work showed that a hybrid Illumina-Nanopore metagenomic approach can tackle the complexity of the soil microbiome and clarify its response to MPs degradation. The present study paves the way to clarify these processes and is crucial to delineate an in-situ remediation strategy of soil microplastic pollution.

Environmental implication

Microplastics (MPs) in soil ecosystems are challengingto remove and separate. The recycling of MPs through a combination of chemicaloxidation and biological conversion has advanced significantly, but it is stillunclear how microorganisms cooperate with external stimuli to influence thefate of MPs. In this study, we investigated the microbiome properties of paddysoil exposed to two different MPs and employed magnetic biochar (MEBC) to trigger the oxidation process. An intriguing Nocardioidesspecies showed multiple metabolic patterns for long-chain alkanes. Some specieswith dehalogenation potential enriched in MEBC treatment also suggest the possibility of chlorine removalusing in-situ remediation.

CRediT authorship contribution statement

Mengyuan Ji: Conceptualization, Methodology, Software, Formal analysis, Investigation, Visualization, Writing – original draft, editing. **Ginevra Giangeri, Fengbo Yu, Filippo Sessa:** Investigation. Writing – review & editing. **Chao Liu, Wenjing Sang, Fangbai Li, Paolo Canu:** Validation, Writing – review & editing. **Laura Treu:** Funding acquisition, Resources. **Stefano Campanaro:** Methodology, Data curation, Writing – review & editing, Supervision, Funding acquisition.

Declaration of Competing Interest

The authors declare that they have no known competing financial interests or personal relationships that could have appeared to influence the work reported in this paper.

Data availability

The data that has been used is confidential.

Acknowledgments

This work was supported by the grant “Sviluppo Catalisi dell’Innovazione nelle Biotecnologie” (MIUR ex D.M.738 dd 08/08/19) of the Consorzio Interuniversitario per le Biotecnologie (CIB) and by the China Scholarship Council (No. 202008310162).

Appendix A. Supporting information

Supplementary data associated with this article can be found in the online version at doi:10.1016/j.jhazmat.2023.131950.

References

[1] J.-J. Guo , X.-P., Huang , Y.-Z., Wang , L. Xiang , H. Li, Q.-Y. Cai et al. Migration and toxicology of microplastics in soil: A review, Environment international, (2019).
[2] Zhao, S., Zhang, Z., Chen, L., Cui, Q., Cui, Y., Song, D., et al., 2022. Review on migration, transformation and ecological impacts of microplastics in soil. Appl Soil Ecol 176, 104486.
[3] Xu, C., Zhang, B., Gu, C., Shen, C., Yin, S., Aamir, M., et al., 2020. Are we underestimating the sources of microplastic pollution in terrestrial environment. J Hazard Mater 400, 123228.
[4] Zhang, L., Xie, Y., Liu, J., Zhong, S., Qian, Y., Gao, P., 2020. An overlooked entry pathway of microplastics into agricultural soils from application of sludge-based fertilizers. Environ Sci Technol 54, 4248–4255.
[5] Rillig, M.C., Leifheit, E., Lehmann, J., 2021. Microplastic effects on carbon cycling processes in soils. PLoS Biol 19, e3001130.
[6] Zhang, S., Wang, J., Yan, P., Hao, X., Xu, B., Wang, W., et al., 2021. Non-biodegradable microplastics in soils: a brief review and challenge. J Hazard Mater 409, 124525.
[7] Hu, Y., He, X., Shali, Y., Luo, M., Zhang, Y., Zhang, S., 2020. Screening of polyethylene film-degrading bacteria from gut microbiota of Galleria mellonella and Tenebrio Molitor. Microbiol China 47, 4029–4041.
[8] Scott, G., Wiles, D.M., 2001. Programmed-life plastics from polyolefins: a new look at sustainability. Biomacromolecules 2, 615–622.
[9] Labuzek, S., Nowak, B., Pajak, J., 2004. The susceptibility of polyethylene modified with bionolle to biodegradation by filamentous fungi. Pol J Environ Stud 13.
[10] Kaeberlein, T., Lewis, K., Epstein, S.S., 2002. Isolating" uncultivable" microorganisms in pure culture in a simulated natural environment. Science 296, 1127–1129.
[11] Handelsman, J., 2004. Metagenomics: application of genomics to uncultured microorganisms. Microbiol Mol Biol Rev 68, 669–685.
[12] Prayogo, F.A., Budiharjo, A., Kusumaningrum, H.P., Wijanarka, W., Suprihadi, A., Nurhayati, N., 2020. Metagenomic applications in exploration and development of novel enzymes from nature: a review. J Genet Eng Biotechnol 18, 1–10.
[13] Tang, J., Zhu, W., Kookana, R., Katayama, A., 2013. Characteristics of biochar and its application in remediation of contaminated soil. J Biosci Bioeng 116, 653–659.
[14] Tong, M., He, L., Rong, H., Li, M., Kim, H., 2020. Transport behaviors of plastic particles in saturated quartz sand without and with biochar/Fe3O4-biochar amendment. Water Res 169, 115284.
[15] Kumar, M., Xiong, X., Sun, Y., Yu, I.K., Tsang, D.C., Hou, D., et al., 2020. Critical review on biochar-supported catalysts for pollutant degradation and sustainable biorefinery. Adv Sustain Syst 4, 1900149.
[16] Yi, Y., Huang, Z., Lu, B., Xian, J., Tsang, E.P., Cheng, W., et al., 2020. Magnetic biochar for environmental remediation: a review. Bioresour Technol 298, 122468.
[17] Zhao, Y., Yuan, X., Li, X., Jiang, L., Wang, H., 2021. Burgeoning prospects of biochar and its composite in persulfate-advanced oxidation process. J Hazard Mater 409, 124893.
[18] Wang, R.-Z., Huang, D.-L., Liu, Y.-G., Zhang, C., Lai, C., Wang, X., et al., 2019. Recent advances in biochar-based catalysts: properties, applications and mechanisms for pollution remediation. Chem Eng J 371, 380–403.
[19] Li, R., Wang, Z., Zhao, X., Li, X., Xie, X., 2018. Magnetic biochar-based manganese oxide composite for enhanced fluoroquinolone antibiotic removal from water. Environ Sci Pollut Res 25, 31136–31148.
[20] Luo, X., Shen, M., Liu, J., Ma, Y., Gong, B., Liu, H., et al., 2021. Resource utilization of piggery sludge to prepare recyclable magnetic biochar for highly efficient degradation of tetracycline through peroxymonosulfate activation. J Clean Prod 294, 126372.
[21] Kang, J., Zhou, L., Duan, X., Sun, H., Ao, Z., Wang, S., 2019. Degradation of cosmetic microplastics via functionalized carbon nanosprings. Matter 1, 745–758.
[22] Sullivan, K.P., Werner, A.Z., Ramirez, K.J., Ellis, L.D., Bussard, J.R., Black, B.A., et al., 2022. Mixed plastics waste valorization through tandem chemical oxidation and biological funneling. Science 378, 207–211.
[23] Li, X., Jia, Y., Zhou, M., Su, X., Sun, J., 2020. High-efficiency degradation of organic pollutants with Fe, N co-doped biochar catalysts via persulfate activation. J Hazard Mater 397, 122764.
[24] Li, X., Wang, C., Zhang, J., Liu, J., Liu, B., Chen, G., 2020. Preparation and application of magnetic biochar in water treatment: a critical review. Sci Total Environ 711, 134847.
[25] Yamashita, Y., Jaffé, R., Maie, N., Tanoue, E., 2008. Assessing the dynamics of dissolved organic matter (DOM) in coastal environments by excitation emission

matrix fluorescence and parallel factor analysis (EEM-PARAFAC). Limnol Oceanogr 53, 1900–1908.
[26] Ji, M., Sang, W., Tsang, D.C., Usman, M., Zhang, S., Luo, G., 2020. Molecular and microbial insights towards understanding the effects of hydrochar on methane emission from paddy soil. Sci Total Environ 714, 136769.
[27] Li, D., Luo, R., Liu, C.-M., Leung, C.-M., Ting, H.-F., Sadakane, K., et al., 2016. MEGAHIT v1. 0: a fast and scalable metagenome assembler driven by advanced methodologies and community practices. Methods 102, 3–11.
[28] Chen, Y., Nie, F., Xie, S.-Q., Zheng, Y.-F., Dai, Q., Bray, T., et al., 2021. Efficient assembly of nanopore reads via highly accurate and intact error correction. Nat Commun 12, 1–10.
[29] De Maio, N., Shaw, L.P., Hubbard, A., George, S., Sanderson, N.D., Swann, J., et al., 2019. Comparison of long-read sequencing technologies in the hybrid assembly of complex bacterial genomes. Microb Genom 5.
[30] F. Zhang, J. Zhang, Y. Yang, Y. Wu, A chromosome-level genome assembly for the beet armyworm (Spodoptera exigua) using PacBio and Hi-C sequencing, BioRxiv, (2020) 2019.2012. 2026.889121.
[31] Gurevich, A., Saveliev, V., Vyahhi, N., Tesler, G., 2013. QUAST: quality assessment tool for genome assemblies. Bioinformatics 29, 1072–1075.
[32] Alneberg, J., Bjarnason, B.S., de Bruijn, I., Schirmer, M., Quick, J., Ijaz, U.Z., et al., 2013. CONCOCT: clustering contigs on coverage and composition. arXiv Prepr arXiv 1312, 4038.
[33] Kang, D.D., Froula, J., Egan, R., Wang, Z., 2015. MetaBAT, an efficient tool for accurately reconstructing single genomes from complex microbial communities. PeerJ 3, e1165.
[34] Kang, D.D., Li, F., Kirton, E., Thomas, A., Egan, R., An, H., et al., 2019. MetaBAT 2: an adaptive binning algorithm for robust and efficient genome reconstruction from metagenome assemblies. PeerJ 7, e7359.
[35] Nissen, J.N., Johansen, J., Allesøe, R.L., Sønderby, C.K., Armenteros, J.J.A., Grønbech, C.H., et al., 2021. Improved metagenome binning and assembly using deep variational autoencoders. Nat Biotechnol 39, 555–560.
[36] Wu, Y.-W., Simmons, B.A., Singer, S.W., 2016. MaxBin 2.0: an automated binning algorithm to recover genomes from multiple metagenomic datasets. Bioinformatics 32, 605–607.
[37] Sieber, C.M., Probst, A.J., Sharrar, A., Thomas, B.C., Hess, M., Tringe, S.G., et al., 2018. Recovery of genomes from metagenomes via a dereplication, aggregation and scoring strategy. Nat Microbiol 3, 836–843.
[38] Parks, D.H., Imelfort, M., Skennerton, C.T., Hugenholtz, P., Tyson, G.W., 2015. CheckM: assessing the quality of microbial genomes recovered from isolates, single cells, and metagenomes. Genome Res 25, 1043–1055.
[39] Chaumeil, P.-A., Mussig, A.J., Hugenholtz, P., Parks, D.H., 2020. GTDB-Tk: a toolkit to classify genomes with the Genome Taxonomy. Database, Oxf Univ Press.
[40] Lagesen, K., Hallin, P., Rødland, E.A., Stærfeldt, H.-H., Rognes, T., Ussery, D.W., 2007. RNAmmer: consistent and rapid annotation of ribosomal RNA genes. Nucleic Acids Res 35, 3100–3108.
[41] Yilmaz, P., Parfrey, L.W., Yarza, P., Gerken, J., Pruesse, E., Quast, C., et al., 2014. The SILVA and "all-species living tree project (LTP)" taxonomic frameworks. Nucleic Acids Res 42, D643–D648.
[42] Hyatt, D., Chen, G.-L., LoCascio, P.F., Land, M.L., Larimer, F.W., Hauser, L.J., 2010. Prodigal: prokaryotic gene recognition and translation initiation site identification. BMC Bioinforma 11, 1–11.
[43] De Bernardini, N., Basile, A., Zampieri, G., Kovalovszki, A., De Diego Diaz, B., Offer, E., et al., 2022. Integrating metagenomic binning with flux balance analysis to unravel syntrophies in anaerobic CO_2 methanation. Microbiome 10, 1–18.
[44] Cantalapiedra, C.P., Hernández-Plaza, A., Letunic, I., Bork, P., Huerta-Cepas, J., 2021. eggNOG-mapper v2: functional annotation, orthology assignments, and domain prediction at the metagenomic scale. Mol Biol Evol 38, 5825–5829.
[45] Yu, H., Fan, P., Hou, J., Dang, Q., Cui, D., Xi, B., et al., 2020. Inhibitory effect of microplastics on soil extracellular enzymatic activities by changing soil properties and direct adsorption: an investigation at the aggregate-fraction level. Environ Pollut 267, 115544.
[46] Qin, X.-q, Yao, B., Jin, L., Zheng, X.-z, Ma, J., Benedetti, M.F., et al., 2020. Characterizing soil dissolved organic matter in typical soils from China using fluorescence EEM–PARAFAC and UV–visible absorption. Aquat Geochem 26, 71–88.
[47] Liu, H., Yang, X., Liang, C., Li, Y., Qiao, L., Ai, Z., et al., 2019. Interactive effects of microplastics and glyphosate on the dynamics of soil dissolved organic matter in a Chinese loess soil. Catena 182, 104177.
[48] Yamashita, Y., Tanoue, E., 2003. Chemical characterization of protein-like fluorophores in DOM in relation to aromatic amino acids. Mar Chem 82, 255–271.
[49] Kalam, S., Basu, A., Ahmad, I., Sayyed, R., El-Enshasy, H.A., Dailin, D.J., et al., 2020. Recent understanding of soil acidobacteria and their ecological significance: a critical review. Front Microbiol 11, 580024.
[50] Větrovský, T., Steffen, K.T., Baldrian, P., 2014. Potential of cometabolic transformation of polysaccharides and lignin in lignocellulose by soil Actinobacteria. PloS One 9, e89108.
[51] Starr, E.P., Shi, S., Blazewicz, S.J., Probst, A.J., Herman, D.J., Firestone, M.K., et al., 2018. Stable isotope informed genome-resolved metagenomics reveals that Saccharibacteria utilize microbially-processed plant-derived carbon. Microbiome 6, 1–12.
[52] Alteio, L., Schulz, F., Seshadri, R., Varghese, N., Rodriguez-Reillo, W., Ryan, E., et al., 2020. Complementary metagenomic approaches improve reconstruction of microbial diversity in a forest soil. Msystems 5 e00768-00719.
[53] Larsbrink, J., McKee, L.S., 2020. Bacteroidetes bacteria in the soil: glycan acquisition, enzyme secretion, and gliding motility. Adv Appl Microbiol 110, 63–98.
[54] Lin, Z., Jin, T., Zou, T., Xu, L., Xi, B., Xu, D., et al., 2022. Current progress on plastic/microplastic degradation: Fact influences and mechanism. Environ Pollut, 119159.
[55] Nagata, Y., Ohtsubo, Y., Tsuda, M., 2015. Properties and biotechnological applications of natural and engineered haloalkane dehalogenases. Appl Microbiol Biotechnol 99, 9865–9881.
[56] Mitter, E.K., Germida, J.J., de Freitas, J.R., 2021. Impact of diesel and biodiesel contamination on soil microbial community activity and structure. Sci Rep 11, 1–14.
[57] Al-Harahsheh, M., Al-Nu'airat, J., Al-Otoom, A., Al-jabali, H., Al-zoubi, M., 2019. Treatments of electric arc furnace dust and halogenated plastic wastes: a review. J Environ Chem Eng 7, 102856.
[58] H. Vanheule, INSIGHTS INTO BACTERIAL DEGRADATION OF THERMOPLASTIC POLYMERS AT MESOPHILIC CONDITIONS, in, Ghent University, 2020.
[59] Bouwer, E.J., Zehnder, A.J., 1993. Bioremediation of organic compounds-putting microbial metabolism to work. Trends Biotechnol 11, 360–367.
[60] Pfeuffer, M., Jaudszus, A., 2016. Pentadecanoic and heptadecanoic acids: multifaceted odd-chain fatty acids. Adv Nutr 7, 730–734.
[61] Krauskopf, L.G., 2003. How about alternatives to phthalate plasticizers. J Vinyl Addit Technol 9, 159–171.
[62] Han, H., Hwang, J., Kim, G., 2021. Characterizing the origins of dissolved organic carbon in coastal seawater using stable carbon isotope and light absorption characteristics. Biogeosciences 18, 1793–1801.
[63] Lu, Q., Yuan, Y., Tao, Y., Tang, J., 2015. Environmental pH and ionic strength influence the electron-transfer capacity of dissolved organic matter. J Soils Sediment 15, 2257–2264.
[64] Phong, D.D., Hur, J., 2015. Insight into photocatalytic degradation of dissolved organic matter in UVA/TiO2 systems revealed by fluorescence EEM-PARAFAC. Water Res 87, 119–126.
[65] Wiedner, K., Polifka, S., 2020. Effects of microplastic and microglass particles on soil microbial community structure in an arable soil (Chernozem). Soil 6, 315–324.
[66] Kumar, M., Revathi, K., Khanna, S., 2015. Biodegradation of cellulosic and lignocellulosic waste by Pseudoxanthomonas sp R-28. Carbohydr Polym 134, 761–766.
[67] Yue, W., Yin, C.-F., Sun, L., Zhang, J., Xu, Y., Zhou, N.-Y., 2021. Biodegradation of bisphenol-A polycarbonate plastic by Pseudoxanthomonas sp. strain NyZ600. J Hazard Mater 416, 125775.
[68] Lopez-Echartea, E., Strejcek, M., Mukherjee, S., Uhlik, O., Yrjälä, K., 2020. Bacterial succession in oil-contaminated soil under phytoremediation with poplars. Chemosphere 243, 125242.
[69] Yang, S., Wen, X., Zhao, L., Shi, Y., Jin, H., 2014. Crude oil treatment leads to shift of bacterial communities in soils from the deep active layer and upper permafrost along the China-Russia crude oil pipeline route. PloS One 9, e96552.
[70] Rodgers-Vieira, E.A., Zhang, Z., Adrion, A.C., Gold, A., Aitken, M.D., 2015. Identification of anthraquinone-degrading bacteria in soil contaminated with polycyclic aromatic hydrocarbons. Appl Environ Microbiol 81, 3775–3781.
[71] Zhang, N., Ding, M., Yuan, Y., 2022. Current advances in biodegradation of polyolefins. Microorganisms 10, 1537.
[72] Jendrossek, D., Handrick, R., 2002. Microbial degradation of polyhydroxyalkanoates. Annu Rev Microbiol 56, 403.
[73] Gravouil, K., Ferru-Clément, R., Colas, S., Helye, R., Kadri, L., Bourdeau, L., et al., 2017. Transcriptomics and lipidomics of the environmental strain Rhodococcus ruber point out consumption pathways and potential metabolic bottlenecks for polyethylene degradation. Environ Sci Technol 51, 5172–5181.
[74] Mileykovskaya, E., Dowhan, W., 2009. Cardiolipin membrane domains in prokaryotes and eukaryotes. Biochim Et Biophys Acta (BBA)-Biomembr 1788, 2084–2091.
[75] Unsay, J.D., Cosentino, K., Subburaj, Y., García-Sáez, A.J., 2013. Cardiolipin effects on membrane structure and dynamics. Langmuir 29, 15878–15887.
[76] Naether, D.J., Slawtschew, S., Stasik, S., Engel, M., Olzog, M., Wick, L.Y., et al., 2013. Adaptation of the hydrocarbonoclastic bacterium Alcanivorax borkumensis SK2 to alkanes and toxic organic compounds: a physiological and transcriptomic approach. Appl Environ Microbiol 79, 4282–4293.
[77] Wei, Y., Fu, J., Wu, J., Jia, X., Zhou, Y., Li, C., et al., 2018. Bioinformatics analysis and characterization of highly efficient polyvinyl alcohol (PVA)-degrading enzymes from the novel PVA degrader Stenotrophomonas rhizophila QL-P4. Appl Environ Microbiol 84 e01898-01817.
[78] Amann, M., Minge, O., 2011. Biodegradability of Poly (vinyl acetate) and related polymers. Synth Biodegrad Polym 137–172.

Chapter III

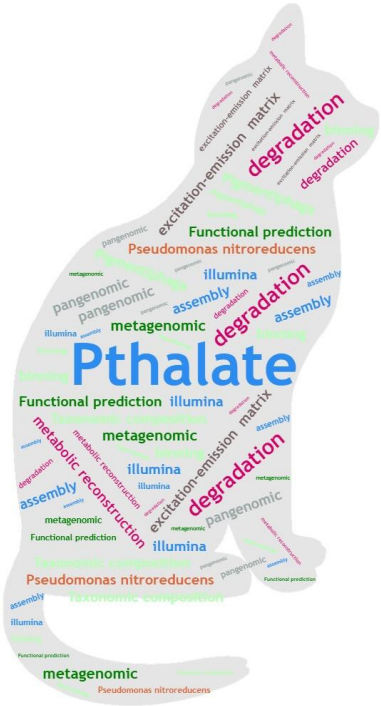

An integrated Metagenomic-Pangenomic strategy revealed native microbes and magnetic biochar cooperation in plasticizer degradation

Mengyuan Ji [a] , Ginevra Giangeri [a] , Muhammad Usman [b] , Chao Liu [c] , Matteo Bosaro [d] , Filippo Sessa [e] , Paolo Canu [e] , Laura Treu [a] , Stefano Campanaro [a,*]
Chemical Engineering Journal, Volume 468, 15 July 2023, 143589
https://doi.org/10.1016/j.cej.2023.143589

[a] Department of Biology, University of Padova, Via U. Bassi 58/b, 35121 Padova, Italy
[b] Department of Civil and Environmental Engineering, University of Alberta, Edmonton, AB T6G 2W2, Canada
[c] Guangdong Key Laboratory of Integrated Agro-Environmental Pollution Control and Management, Institute of Eco-environmental and Soil Sciences, Guangdong Academy of Sciences, Guangzhou 510650, China
[d] Italiana Biotecnologie, Via Vigazzolo 112, 36054 Montebello Vicentino, Italy
[e] Department of Industrial Engineering, University of Padova, Via Marzolo 9, 35131 Padova, Italy

*Corresponding author

Chemical Engineering Journal 468 (2023) 143589

Contents lists available at ScienceDirect

Chemical Engineering Journal

journal homepage: www.elsevier.com/locate/cej

An integrated Metagenomic-Pangenomic strategy revealed native microbes and magnetic biochar cooperation in plasticizer degradation

Mengyuan Ji [a], Ginevra Giangeri [a], Muhammad Usman [b], Chao Liu [c], Matteo Bosaro [d], Filippo Sessa [e], Paolo Canu [e], Laura Treu [a], Stefano Campanaro [a,*]

[a] Department of Biology, University of Padova, Via U. Bassi 58/b, 35121 Padova, Italy
[b] Department of Civil and Environmental Engineering, University of Alberta, Edmonton, AB T6G 2W2, Canada
[c] Guangdong Key Laboratory of Integrated Agro-Environmental Pollution Control and Management, Institute of Eco-environmental and Soil Sciences, Guangdong Academy of Sciences, Guangzhou 510650, China
[d] Italiana Biotecnologie, Via Vigazzolo 112, 36054 Montebello Vicentino, Italy
[e] Department of Industrial Engineering, University of Padova, Via Marzolo 9, 35131 Padova, Italy

ARTICLE INFO

Keywords:
Plasticizers
Magnetic biochar
Degradation
Metagenome
Pangenome

ABSTRACT

There has been growing concern over the release of plasticizers from plastic products, and the high levels of plasticizers in the environment have led to a threat to ecological security. Although some plasticizers may naturally degrade, their slow removal and prolonged life cycle remain challenges. To address this, this study explored a unique hybrid strategy using native field microorganisms and magnetic biochar (MBC) to support the upstream degradation of plasticizers. Diethyl phthalate (DP) was used as the test subject. The study found that MBC treatment led to high level of total organic carbon (TOC) and various organic products, demonstrating the degradation of DP. Analysis of the hybrid metagenomic model showed that several species of *Pseudomonas* can degrade downstream phenylmethanal and *Pseudomonas nitroreducens* has the ability to cooperate well with MBC due to its iron receptor and transporter. Additionally, a *Pigmentiphaga* species was found to have the ability to fully mineralize DP. Analysis of the *Pigmentiphaga* pangenome revealed that genes related to DP biodegradation were shared by members of this genus. Although some members of *Pseudomonas* is known to be pathogenic, the species identified in the study may not be harmful as they lack virulence factors. The study provides evidence regarding the cooperation between native biodegraders and MBC in mineralizing plasticizers, offering a new solution for removing phthalate plasticizers from soil and surface water.

1. Introduction

Phthalates (PAEs) are commonly utilized as plasticizers within the plastic industry to enhance the flexibility, transparency, durability, and lifespan of plastics [1]. However, these phthalate-based plasticizers have a tendency to leach into the environment rather than forming a covalent bond with the resin [2]. Due to their extensive use, plasticizer contaminants have been identified in various environments such as surface waters, sediments, agricultural fields, and soils located near industrial sites [3]. Hence, the development of a sustainable and efficient method to remove these pollutants is imperative as PAEs have a limited biodegradation rate [4].

The behavior of plasticizer pollutants is controlled by complex dynamic physical, chemical, and biological processes, including adsorption/desorption [5], leaching [6,7], chemical/biological degradation [8,9], plants uptake [10], and runoff [11]. However, these traditional methods are not without risks and limitations. Potential concerns include ineffectiveness for certain pollutants, recontamination, mobilization, generation of harmful byproducts, and persistence in the environment [12,13]. In contrast, microbial degradation provides a sustainable and eco-friendly approach to soil remediation that effectively treats a broad range of pollutants without generating harmful

Abbreviations: MBC, Magnetic biochar; DP, Diethyl phthalate; TOC, Total organic carbon; PA, Phenylmethanal; PAEs, Phthalates; EEM, Excitation-emission matrix; GC–MS, Gas chromatography-mass; BC, Biochar; SP, Sodium persulfate; AOPs, Advanced oxidation process; DOM, Dissolved organic matter; PARAFAC, Parallel Factor; EI, Electron impact; MAGs, Metagenome assembled genomes; RPKM, Reads per kilobase million; ARGs, Antibiotic resistance genes; Ex, Excitation; Em, Emission; envMAGs, MAGs obtained from environmental.

* Corresponding author.
E-mail address: stefano.campanaro@unipd.it (S. Campanaro).

https://doi.org/10.1016/j.cej.2023.143589
Received 21 March 2023; Received in revised form 13 May 2023; Accepted 15 May 2023
Available online 18 May 2023

byproducts or emissions [14]. However, the potential for release and degradation as well as microbial responses to PAEs in farmland-water systems are not well understood, yet. Although various studies have focused on the potential of natural microorganisms to digest PAEs [15,16], the microbial degradation of PAEs in environments often takes a long time and requires specific conditions favoring microbial growth and acclimatization [17]. For instance, a 35 days-long experiment revealed that native soil microorganisms alone were unable to reduce dioctyl phthalate concentrations by more than 20% [18]. Another investigation revealed that di-n-octyl phthalate degraded slowly even when bioaugmentation was made using adaptive activated sludge [19]. However, a recent investigation found that a combination of oxidation processes and stressors significantly accelerated the biodegradation of bis(2-ethylhexyl) phthalate decreasing the degradation time to just 24 days [20]. This highlights the crucial role of external stimulation in enhancing the degradation of plasticizer pollutants known as PAEs. The distinct nature of paddy soil, characterized by frequent flooding, creates favorable conditions for various chemical reactions, making it important to conduct further research on the degradation potential of PAEs in this type of farmland-water system. A more detailed investigation of this environment will provide relevant information that will help in mitigating the negative impacts of these pollutants.

Biochar (BC)-based multifunctional materials have gained widespread recognition for their environmental friendliness, efficiency, and ability to remediate contaminated soils [21,22]. One particular type of biochar-based material, Magnetic Biochar (MBC), is formed through the pyrolysis activation or chemical co-precipitation of transition metals such as Fe, Co, and Ni with the biochar substrate [23]. These transition metals on MBC can help activate free radicals in the environment, such as sulfate radicals, to selectively degrade recalcitrant pollutants like PAEs [20]. BC has the ability to indirectly stimulate microorganisms by providing a favorable habitat within its porous structure, and its nutrient absorption capacity can continuously support microbial growth [24], thereby enabling certain microorganisms to synergistically remove pollutants with BC. Despite the potential benefits of MBC in degrading PAEs, there has been limited research on the degradation potential obtained through the interaction between MBC and native microbes in response to external stimulation. While some studies have focused on changes in soil microbial communities in the presence of PAEs, few have investigated the functional responses of specific microbial species. As a result, it remains unclear which microorganisms are responsible for PAE degradation in farmland-water systems and how MBC-microbe interactions play a role in the degradation of PAEs. Further investigation is needed to fully understand these interactions and the potential of biochar-based materials in remediation efforts.

The current study aims to investigate the collaborative degradation of plasticizers in flooded soil using MBC and naturally occurring field microorganisms. Diethyl phthalate (DP) was selected as the model PAEs for this investigation since it is one of the most widely utilized PAEs in comparison to other plasticizer types and has been found in numerous contaminated fields [25]. A multidisciplinary approach was employed to characterize the metabolic processes involved in DP degradation. This approach involved identifying the organic levels and components present in contaminated soil leachate and DP released in the aqueous environment. Total organic carbon (TOC) analyzer, excitation-emission matrix (EEM) fluorescence spectroscopy, and gas chromatography-mass (GC–MS) spectrometry were combined to analyze the samples. In addition, high-precision Illumina short-reads and large-span nanopore long-reads were used together to obtain detailed information on the microbial communities present in the complex farmland soil–water system. Putative MBC cooperating species and microbes with the ability to autonomously degrade DP were obtained, and their potential pathways for metabolizing DP were investigated. Pangenomic evidence suggests that related members of the *Pigmentiphaga* genus share the ability to degrade DP, and we further investigated these species for their potential antibiotic resistance and pathogenicity in the environment.

2. Materials and methods

2.1. Preparation of biochar and chemicals

The preparation of biochar and magnetic biochar was conducted using rice straw as the raw material. Rice straw was subjected to drying, crushing, and sieving with a 60-mesh sieve prior to use. A portion of the treated rice straw was then mixed with urea, ascorbic acid, and $FeSO_4{\cdot}7H_2O$, placed in an autoclave, sealed, and subjected to a heating process at 160 °C for 10 h. After the mixed material was taken out and dried for 24 h, it was subjected to pyrolysis in a tube furnace at the temperature of 700 °C under N_2 gas for 2 h. The solid material obtained after pyrolysis was then taken out. The solid material that has undergone mixed liquid pretreatment was named MBC, and the material obtained by pyrolysis of the original rice straw was named BC. Fig. S1 presents the surface structure and elemental composition of the magnetic biochar. The diethyl phthalate (C_6H_4-1,2-$(CO_2C_2H_5)_2$, ≥99%), Sodium persulfate (SP, $Na_2S_2O_8$, ≥ 99.5%), urea (NH_2CONH_2, 99%), and ascorbic acid used in the experiment were purchased from Sigma-Aldrich.

2.2. Release experiment in water

To explore the potential and characteristics of DP dissolution in water under different conditions, a release experiment was conducted. DP was dissolved in ultra-high quality Milli-Q water by adding 0.45 mL DP to 80 mL of water in a 120 mL amber glass bottle, and the mixture was shaken at 150 rpm for 24 h to evaluate the release properties. A separate set of experiments was performed to assess the impact of MBC on the DP aqueous solution. In these experiments, 0.5 g of MBC and 2.25 mmol of sodium persulfate (SP) were added to the DP aqueous solution. The contact time was maintained at 24 h, and dissolved organic matter samples were collected through a 0.45 μm membrane filter and stored at −20 °C for further analysis.

2.3. Microcosm incubations and sampling

Soil samples were collected from a depth of 2–20 cm in a paddy field located in Grumolo delle Abbadesse (VI, Italy) (45°30′36.8″N 11°39′29.3″E). The samples were dried, ground, and sieved through a 40-mesh sieve for later use. A microcosm incubation experiment was conducted with three replicates for each of the following treatments: Control, BC and DP, MBC and DP, and DP-contaminated treatment. The experimental setup involved filling 120 mL serum bottles with 50 g of soil and 80 mL of sterile ultrapure water. Then, 2.25 mmol DP were added to the microcosm to achieve of 1% (w/w) ratio of the dry weight of soil. The advanced oxidation process (AOPs) was then triggered by adding SP to the MBCDP treatment (SP were added according to the DP ratio of 1:1). The microcosms were incubated in the dark at 25 °C and wrapped in aluminum foil to prevent evaporation.

After the first week of incubation, the liquid phase was collected, and the collection was repeated every two weeks thereafter. The liquid phase was sampled with a 2 mL syringe, centrifuged at 4000 rpm (Eppendorf 5804R centrifuge) for 10 min, and the upper liquid layer was stored at −20 °C for the subsequent analysis of dissolved organic matter (DOM). After the long-term incubation, the mixture in the microcosm was subjected to high-speed centrifugation for 10 min at 4000 rpm (Eppendorf 5804R centrifuge). The obtained liquid samples were stored at −20 °C for later determination of organic matter.

2.4. Methodology for integrated liquid analysis

The TOC content of liquid samples was measured using high-temperature catalytic combustion to CO_2 on a TOC analyzer (TOC-L CPH, Shimadzu, Japan). The instrument was calibrated with potassium hydrogen phthalate. Prior to analysis, the liquid samples were filtered through 0.45 μm filters to remove any particulate matter.

The structural properties of the liquid samples were characterized using EEM fluorescence spectroscopy (Aqualog; Horiba-Jobin Yvon, USA). Using MATLAB Version 8.5.0197613 for Parallel Factor (PARAFAC) modeling as previously described [26].The instrument had an excitation range of 240 to 600 nm and an emission range of 280 to 550 nm. To correct for Rayleigh scattering, the raw EEM data was normalized. The fluorescence spectra of Milli-Q water was taken under the same conditions to control for the effects of Raman scattering.

Organic components of the liquid samples were analyzed using GC–MS (Clarus® 580, Clarus® SQ 8, USA). The instrument was operated in full scan mode (m/z 50–350), with electron impact (EI) mode at 70 eV and an ion source temperature of 220 °C. The temperature program for the GC oven started at 40 °C, held for 2 min, then ramped up to 280 °C at a rate of 10 °C/min and held for 9 min. Helium was used as the carrier gas. Chemical identification was based on comparison of the obtained mass spectra to the NIST mass spectral database [27]. Details regarding the samples preparation for GC–MS are available in the Supporting Information.

2.5. DNA extraction and sequencing

After long-term incubation, collect the homogenized soil mixture from each microcosm for microbialanalysis. DNA was extracted from the soil slurry using DNeasy PowerSoil® (QIAGEN GmbH, Hilden, Germany) with minor modifications according to the protocol of manufacturer. NanoDrop (ThermoFisher Scientific, Waltham, MA) and Qubit fluorometer (Life Technologies, Carlsbad, CA) were used to check the quantity and quality of extracted samples. Shotgun sequencing was performed using the Illumina NovaSeq platform at the Sequencing Facility of the DPartment of Biology, University of Padova. Total DNA from all samples was pooled and used to build a long-read library with the Rapid Barcoding kit (SQK-RBK004). A FLO-MIN106 R9 flow cell on a MinION device was then used to sequence the long-read library (Oxford Nanopore Technologies, Oxford, UK).

2.6. Hybrid assembly and genomic data analysis

Sequence data were deposited at the Sequence Read Archive (SRA, NCBI) under Bioproject PRJNA892267. The process of hybrid assembly, binning, functional annotation, and classification of metagenome assembled genomes (MAGs), as well as the calculation of reads per kilobase million (RPKM) per sample, are thoroughly described in the Supporting Information.

Additional genomes/MAGs associated with putative DP degraders were downloaded from the NCBI database and used for pangenome analysis. Genome was assessed for completeness and contamination using Checkm2 [28] and subsequently annotated individually for each metagenome following the above protocol. The maximum-likelihood trees were generated with fasttree2 [29] using the binary presence and absence of accessory genes, and were visualized in phandango [30]. Antibiotic resistance genes (ARGs) were annotated using the Comprehensive Antibiotic Research Database [31]. Predict the bacterial virulence of selected MAGs using the VFanalyzer [32].

2.7. Statistical

The two-sided Welch's t-test was used to determine the significance of differences in the number of genes associated to different functional categories in MAGs. Difference in the number of genes belonging to different categories were also estimated considering treatments and blank. Based on statistical results from the Fisher exact test, the "annotate" and "enrichment" functions of the EnrichM (v0.6.30) were used to identify enzymes enriched in MAGs associated to particular treatments (https://github.com/geronimp/enrichM).

3. Results and discussion

3.1. Liquid phase organic properties of different treatments

The effect of AOPs activated by MBC on DP in a water environment was evaluated through a release experiment. Figure S1 illustrates the successful loading of Fe and N onto the surface of the prepared MBC. Previous research has shown that Fe-N co-doped BC has the ability to activate PS through a series of free-radical and non-free-radical pathways, resulting in the production of highly oxidizing free radicals such as •OH, $\bullet SO_4^-$, and $^1O_2$ that are capable of attacking and breaking the chemical bonds of pollutants [33]. Fig. 1 shows the organic structure properties and composition of the DP and MBCDP treatments after 24 h of shaking release. The excitation and emission (Ex/Em) peak at 275/340 nm excited by DP is consistent with the position of tryptophan and protein-like substances, and the application of MBC significantly reduced the fluorescence intensity at this position. It has been reported in the literature [34] that the fluorescence intensity of furans and organic acids can be significantly lower compared to phenolic aromatic compounds. The use of MBC in this study resulted in a decrease in fluorescence intensity, which is believed to be caused by the formation of degradation products like acetic acid, besides, the presence of redox reactions may also lead to fluorescence quenching in DOM [35]. The GC–MS analysis showed clearly that the peak area of DP (16.32 min) after treatment with MBC was significantly reduced by 52% (Fig. 1b). The released products were identified as Phenylmethanal (PA) (7.34 min) and benzylic alcohol (8.56 min). The high peak value of PA revealed a successful attack on the single bonds "C-C" and "C-O", as well as the double bond "C = O" of DP.

Fig. 2 presents the organic properties of the soil leachate obtained from the long-term incubation experiment. The changes in the TOC of soil leachate among different treatments during the incubation period are depicted in Fig. 2a. Initially, no significant differences were observed among the DP, BCDP, and MBCDP treatments. However, a marked decrease in TOC was observed in the BCDP treatment after 21 days of incubation and it remained similar to the blank group in the later stages, while the TOC of the DP and MBCDP groups increased over time, reaching 4270 mg/kg soil and 3480 mg/kg soil respectively on the 49th day. The observation that the BCDP group showed low TOC values is consistent with previous reports of efficient DP adsorption by biochar soil composites [36,37]. The elevated TOC in the MBCDP treatment indicated that adsorption is no longer the dominant mechanism, and that the buildup of intermediate products could contribute to the increase in TOC content. It can be inferred that MBC, which has a similar porous structure to BC, is capable of adsorbing and aggregating organic pollutants. The aggregation of DP on the surface of MBC makes it more susceptible to attack by free radicals such as $\bullet SO_4^-$ generated by AOPs. Additionally, studies have shown that the oxygen-containing functional groups of MBC promote the generation of $\bullet SO_4^-$ in the Fe_3O_4/PS system [38], enhancing the attack efficiency on organic matter and leading to the accumulation of more intermediate products. This warrants further experimental validation in the future. The increase in TOC in soil solely contaminated with DP can be attributed to the high solubility of DP in water (1080 mg/L at 25 °C) [39], which resulted in its gradual integration into the soil leachate over time.

EEM equipped with PARAFAC identified four principal components with distinct Ex/Em (Fig. 2b, Table1). Component 1 (C1) evidenced two prominent EX/Em peaks at 250 nm and 425 nm, as well as at 325 nm and 425 nm. This spectral pattern aligns with the characteristics of substances similar to humic acids. Prior studies have established the widespread presence of C1 in rice soil [40]. Component 2 (C2) displayed a maximum EX/Em peak at 275 nm/340 nm and is related to substances similar to tryptophan and proteins [41]. Furthermore, its spectral position matches that of the excitation spectrum of DP solvent. Component 3 (C3) exhibited a peak position at 250 nm/500 nm, which is indicative of anthropogenic UVA humic or fulvic acid substances originating from

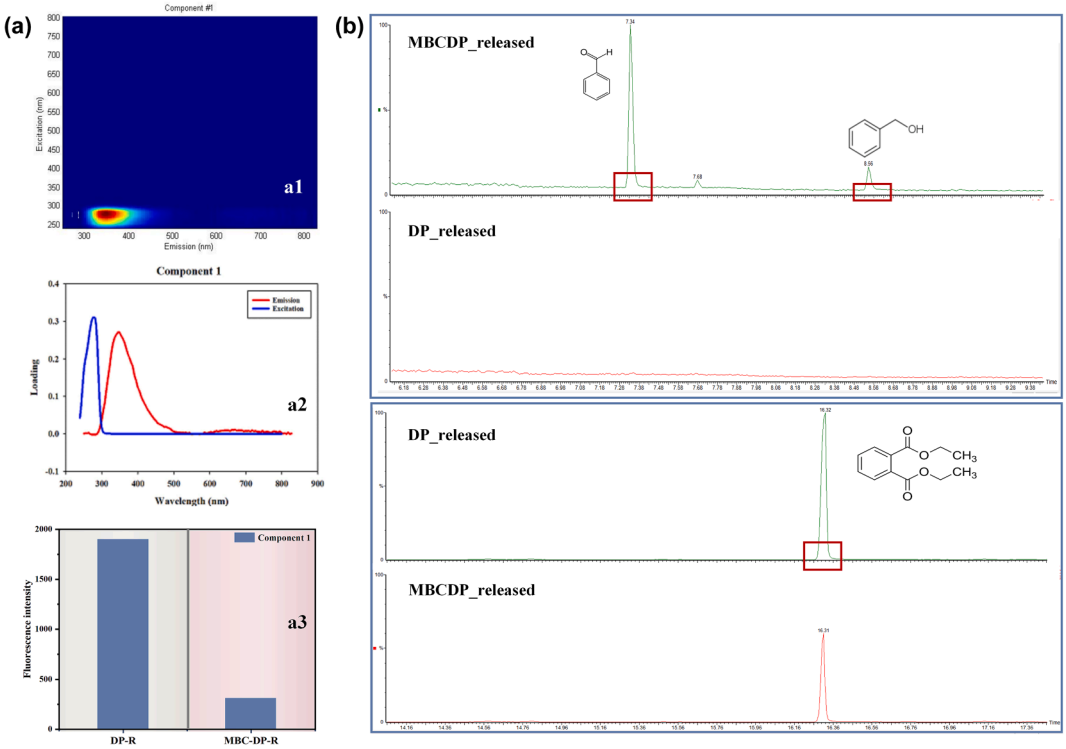

Fig. 1. The properties of organic matter obtained from the oscillatory release experiments of DP and MBCDP treatments. (a) Fluorescence properties of released substances identified by EEM spectroscopy. The fluorescence spectrum excited by DP in aqueous solution is referred to as a1, the corresponding excitation/emission wavelength is designated as a2, and the fluorescence intensity resulting from DP and MBCDP aqueous solution is represented by a3. (b) Organic compounds identified in DP and MBCDP aqueous solutions via GC–MS analysis.

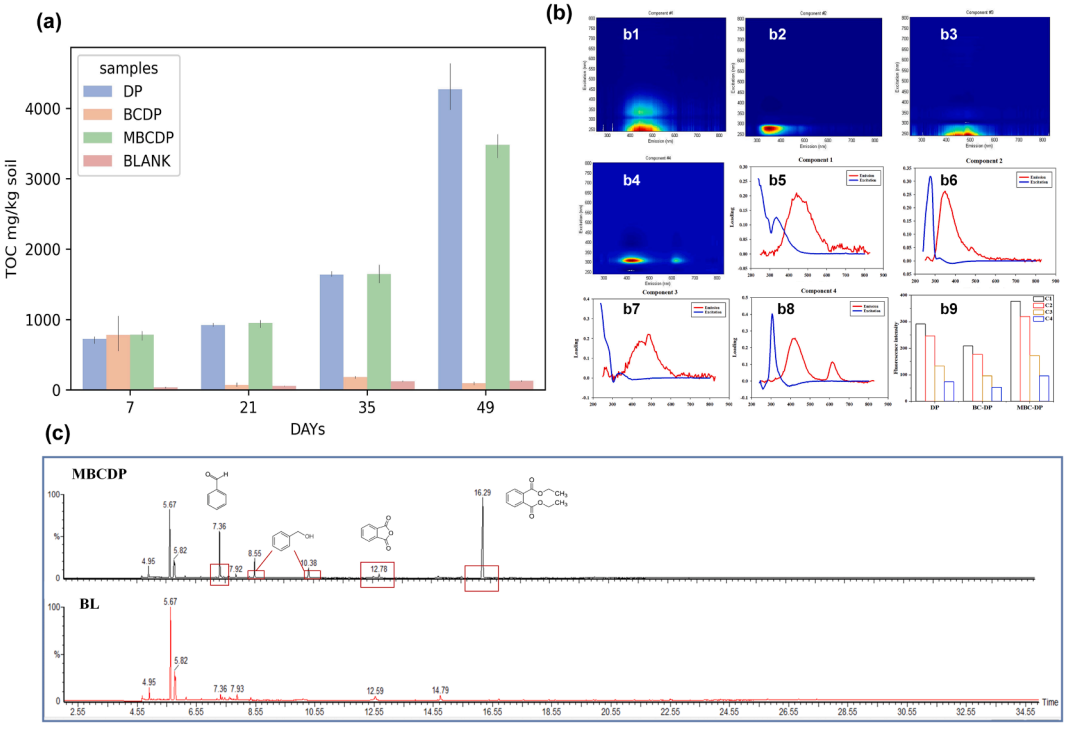

Fig. 2. Shifts in liquid phase. (a) Total organic carbon levels of soil solution from different treatments. (b) Structural features of liquid organic matter identified by EEM spectroscopy. The fluorescence spectrums excited by DOM in soil leachate are referred to as b1-4, the corresponding excitation and emission wavelengths are designated as b5-8, and the fluorescence intensity of the identified components among different treatments is denoted as b9. (c) Organic components in the liquid phase of MBCDP treatment identified by GC–MS spectroscopy.

Table 1
The fluorescent components of the DOM samples.

Components	Ex/Em(nm)	Description	Source
C1	250,325/425	Humic acid-like	Autochthonous
C2	275/340	tryptophan-like, protein-like	Autochthonous
C3	250/500	UVA humic-like	fulvic acid, terrestrial, autochthonous
C4	310/410,610	UVA marine humic-like	anthropogenic from wastewater and agriculture

terrestrial systems [42]. Component 4 (C4) displayed two emission peaks at (310, 410) nm and (310, 610) nm, which are attributed to UVA marine humic substances of anthropogenic origin from wastewater and agriculture [43]. This component was also in agreement with the fluorescence peak position of benzaldehyde, 4-hydroxy-3,5-dimethoxy, as reported in a previous study [34]. The distinct emission peak at 610 nm suggests the presence of higher molecular weight aromatic compounds [44]. These results showed that the fluorescence intensity of each component in the MBCDP treatment was significantly higher than that of the other two treatments. Although the TOC value of the DP treatment was higher than that of the MBCDP treatment, the fluorescence intensity of the fluorescent substances was lower in the DP treatment compared to the MBCDP treatment. The observed difference in soil organic matter may be attributed to a variety of factors, including redox reactions, condensation, concentration, and changes in ion exchange. For example, the polymerization and condensation of soil organic matter has been shown to lead to an increase in humic and fulvic acids [45]. Fenton oxidation has also been found to enhance the fluorescence intensity of aromatic functional groups in DOM by increasing the production of non-aromatic compounds and inorganic residues from proteins or humic substances [46]. Furthermore, the increase in C3 and C4 may be related to the accumulation of degradation products of DP in MBC treatment.

Soil leachate is known to have a complex composition that hinders the detection of high molecular weight compounds and limits the ability to directly quantify the products due to low concentrations of various organic compounds. To overcome these limitations, the samples were concentrated through evaporative drying and analyzed by GC–MS to provide qualitative evidence of liquid phase components (Fig. 2c). Despite the difficulties in detecting high-intensity peaks, the MBCDP treatment still produced distinct peaks for benzyl alcohol, phthalic anhydride, and diethyl phthalate. The larger peak area for PA at 7.36 min also indicated an increase in the content of benzaldehyde. In short, the presence of these components is in agreement with the results of the release experiment, providing direct evidence that the AOPs in the flooded soil environment were also successfully activated by elements of the MBC load, resulting in the attack of free radicals on DP and the accumulation of intermediate products such as PA.

3.2. Taxonomic composition of the microbiome in different treatments

Both a “global assembly analysis” and a “genome-centric metagenomic” approach were used to ascertain the role of the microbiome in various microcosm bottles. The former was based on gene finding and annotation on the entire assembly obtained from the combined assembly of Illumina and nanopore reads. The scaffolds underwent a binning process to identify the microbial genomes. This process allowed to recover 193 MAGs (completeness $\geq$ 50% and contamination $\leq$ 10%). 74 MAGs with a relative abundance greater than 1% were taxonomically assigned to 9 bacterial phyla, as depicted in Fig. 3. *Proteobacteria,* with 38 MAGs, dominated the microbial community and have been reported

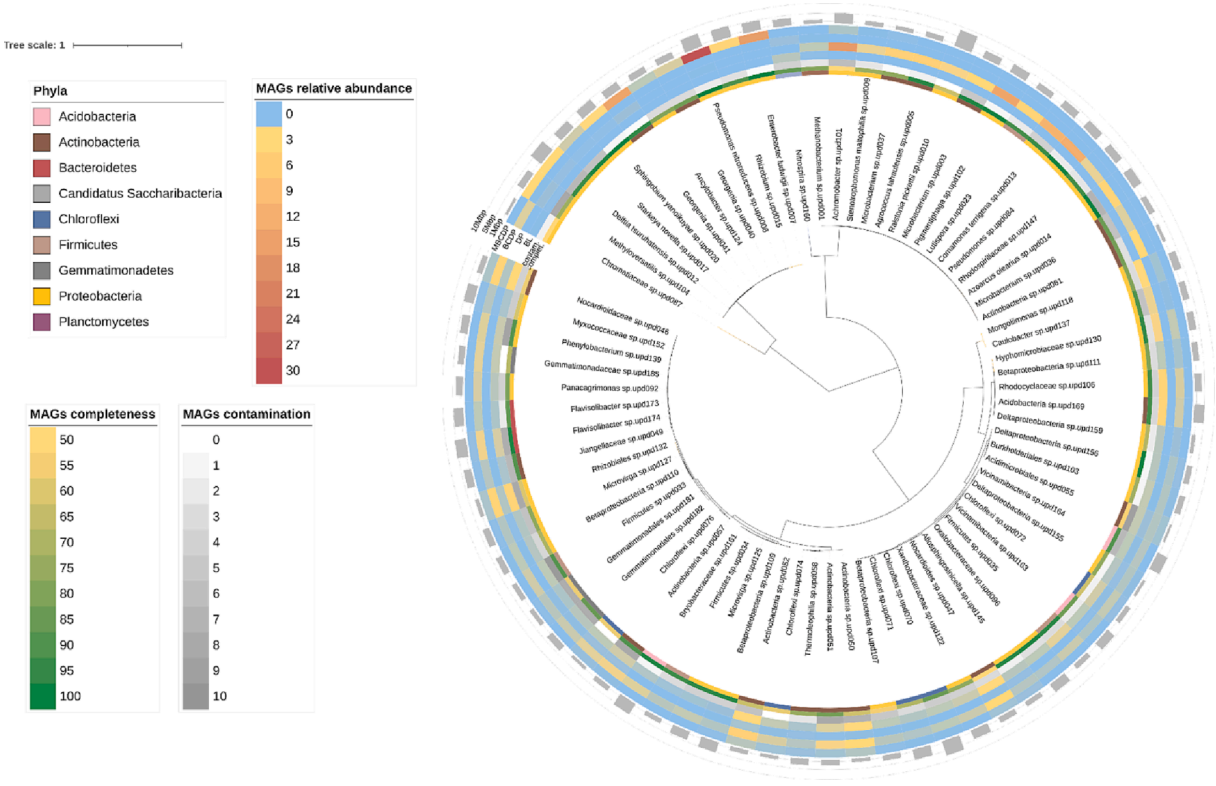

Fig. 3. Properties of 74 MAGs identified in the microbiome with relative abundance higher than 1%: MAG coverage, quality (completeness and contamination), and taxonomic assignment.

to play important roles in global nutrient cycling and carbohydrate metabolism [47]. The increased relative abundance of this phylum (37.5% in MBCDP and 32.2% in DP treatment compared to the blank) suggested an elevated level of carbohydrate metabolism in both treatments. *Firmicutes* (4 MAGs), previously reported to play key roles in lignocellulosic decomposition [48], showed a significant decrease in relative abundance in MBCDP treatment, suggesting that soil natural organic matter is not the main degradant of this group. Other phyla such as *Gemmatimonadetes* (3MAGs), *Chloroflexi* (5MAGs), *Bacteroidetes* (2MAGs), and *Acidobacteria* (3MAGs) were significantly reduced in both DP and MBCDP treatments, while the relative abundance of *Actinobacteria* (17 MAGs) remained unchanged among the various treatments. These phyla have diverse metabolic pathways which are relevant for important biogeochemical cycles, decomposition of biopolymers, and secretion of exopolysaccharides [49–51]. The addition of DP may have altered the organic substrate levels of the paddy soil, affecting the abundance of these phyla.

Some specific MAGs belonging to the aforementioned phyla showed significant enrichment in response to different conditions. For instance, *Pseudomonas nitroreducens* sp. upd006 was found to have a relative abundance of up to 37.6% in the MBCDP group. Previous studies have linked this species with the degradation of aromatic compounds, including simazine and nicosulfuron [52]. Additionally, some of the highly abundant MAGs in the MBCDP treatment, such as *Georgenia* sp. upd041, *Rhizobium* sp. upd015, and *Methyloversatilis* sp. upd104, have been reported to be associated with the degradation of phthalic acid esters by soil bacterial communities [53,54]. This enrichment further supports the changes in microbial community composition observed as a result of the degradation of DP. The treatment of DP contamination also resulted in the significant enrichment of *Achromobacter* sp. upd101, *Pigmentiphaga* sp. upd102, *Pseudomonas* sp. upd084, and *Comamonas terrigena* sp. upd013. These microorganisms have the potential of utilizing DP as a direct carbon source for their growth. Nevertheless, microbial composition analysis alone provides limited information, and the evidence presented in later sections, based on genome-centric functional analysis, provides a more comprehensive and convincing assessment.

The variation in microbial community composition among the different treatments was illustrated through principal component analysis (PCA) (Figure S4). As depicted, the microbial composition in the BCDP treatment was similar to the Blank group, while the DP and MBCDP treatments were noticeably distinct from the control. This is in line with the observed changes in species relative abundance. The potential obligate or facultative nutritional modes of the microbiome members across the different treatments were further explored through a co-occurrence analysis (Figure S5). Fig. S5(b) depicts the co-occurrence network of several highly abundant MAGs that exhibit significant correlation (r greater than 0.5) (considering only the top 50 abundant MAGs). Notably, a significant positive association (r greater than 0.5, $P < 0.05$) was observed between *Pseudomonas nitroreducens* sp. upd006 and several MAGs, including *Georgenia* sp. upd041, *Rhizobium* sp. upd015, *Delftia tsuruhatensis* sp. upd012, *Sphingobium yanoikuyae* sp. upd020, and *Enterobacter ludwigii* sp. upd007. It has been reported that under simulated shallow aquifer conditions, *Sphingobium yanoikuyae* can convert DP to phthalic acid through successive hydrolysis or demethylation pathways [55]. Additionally, *Georgia*, *Ancylobacter*, and *Rhizobium* have been widely recognized for their ability to degrade polycyclic aromatic and xenobiotic organic pollutants [56–58]. This further suggests the possibility of complementary functional roles among these MAGs in response to the MBCDP treatment.

3.3. Functional prediction at the global level

Examining enzyme abundance among treatments can provide a clear understanding of how microbial communities contribute to the degradation of contaminants. The degradation of DP can be divided into two processes: upstream degradation (DP demethylation to form phthalic acid) and downstream degradation (phthalic acid mineralization). In this study, the RPKM values of genes in all samples were calculated and used as a proxi to assess the impact of different treatments on the upstream and downstream degradation of DP.

Fig. 4a compares the changes in abundance levels (calculated as RPKM values) of enzymes involved in the biodegradation process among different treatments. It is evident that the DP treatment had significantly higher levels of genes encoding phthalate transporter (ophD), phthalate 4,5-*cis*-dihydrodiol dehydrogenase (EC 1.3.1.64), phthalate 4,5-dioxygenase (EC 1.14.12.7), and phthalate 4,5-dioxygenase reductase component (EC:1.18.1.-) compared to the other treatments (Fig. 4A). Studies have shown that dioxygenase of Gram-negative bacteria first catalyze the formation of *cis*-4,5-dihydro-4,5-dihydroxyphthalate, followed by oxidation to 4,5-dihydroxyphthalate through NAD-dependent dehydrogenase [59]. Meanwhile, Gram-positive bacteria first oxidize PAEs to 3,4-dihydro-3,4-dihydroxyphthalate, which is deelectronized and dehydrogenated to produce 3,4-dihydroxyphthalate, followed by dehydrodecarboxylation [60]. Therefore, it is evident that the biodegradation process, which was controlled by gram-negative bacteria, dominated the DP treatment. In contrast, the levels of genes involved in the upstream degradation of DP in the MBCDP treatment were not significantly different from the blank sample. This suggests that the high organic matter levels in the MBCDP group did not result from direct degradation of DP by microorganisms. Further analysis was conducted to investigate the changes in genes encoding downstream benzoate metabolism among the treatments. It was observed that the MBCDP treatment showed higher levels of the gene encoding benzoate 1,2-dioxygenase (EC 1.14.12.10) compared to the other treatments, suggesting that the MBCDP group utilized MBC to directly achieve the upstream degradation of DP and relied on soil microorganisms for the cooperative mineralization of downstream PA.

The phylogenetic origins of DP degradation genes were explored by taxonomic classification of phthalate 4,5-dioxygenase (EC 1.14.12.7) and phthalate 4,5-dioxygenase reductase component (EC 1.18.1.-) genes, which control the first step in phthalate degradation (Fig. 4b). A total of 41 MAGs were found to contain genes encoding the enzymes EC 1.14.12.7 and EC 1.18.1.-. Among them, several species including *Pseudomonas nitroreducens* upd006, *Pigmentiphaga* sp. upd102, *Pseudomonas* sp. upd084, *Azoarcus olearius* sp. upd014, and *Methyloversatilis* sp. upd104, exhibited high gene copy numbers of these two enzymes (Fig. 4B). The distribution of these MAGs among different treatments is further displayed in Figure S6. It is clear that *Pseudomonas nitroreducens* sp. upd006, *Pseudomonas* sp. upd084 and *Pigmentiphaga* sp. upd102 not only exhibited high gene copy numbers of critical enzymes, but also were significantly enriched in the DP treatment or MBCDP treatment. This further qualifies them as potential DP degraders or possibly as species cooperating in MBC degradation.

The discovery of *Pigmentiphaga* sp. upd102, a microaerophilic, aromatic compound-degrading bacterium found exclusively in the DP treatment, is of significance. Previous studies have shown that species belonging to the genus *Pigmentiphaga* are capable of metabolizing aromatic compounds [61,62], and in this study *Pigmentiphaga* sp. upd102 showed a direct degradation potential for DP, therefore, it could represent a new DP degrader existing in natural paddy soil. To provide more logical and convincing proof of how these several MAGs contribute to the degradation of DP in different treatments, we further reconstructed the metabolic pathways of these MAGs and carried out comparative gene analysis.

3.4. Putative degradation pathways identified from metabolic reconstruction

3.4.1. Pseudomonas nitroreducens sp. upd006 and Pseudomonas sp. upd084

In this study, the species *Pseudomonas nitroreducens* sp. upd006 and *Pseudomonas* sp. upd084 were identified as being enriched in the

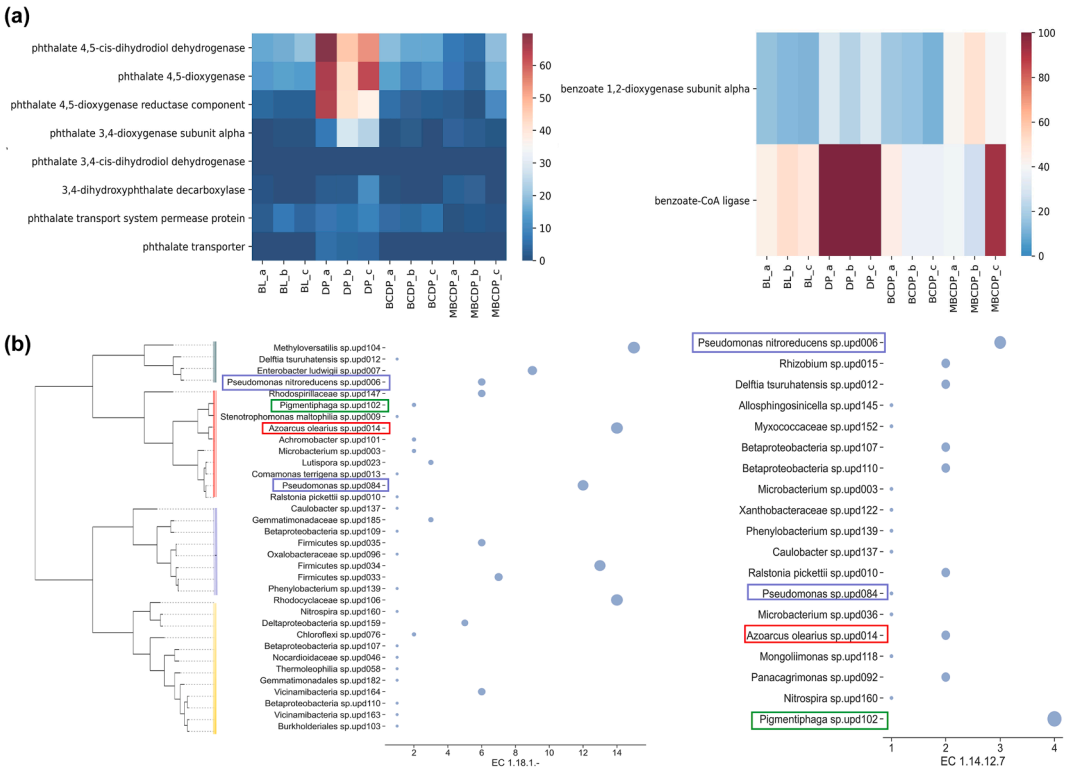

Fig. 4. Microbial functional activities potentially associated with DP degradation at the global level. (a) RPKM values of selected DP degrading enzymes among different treatments. RPKM values of all genes are reported in Table S2. (b) Gene copy numbers of phthalate 4,5-dioxygenase in MAGs.

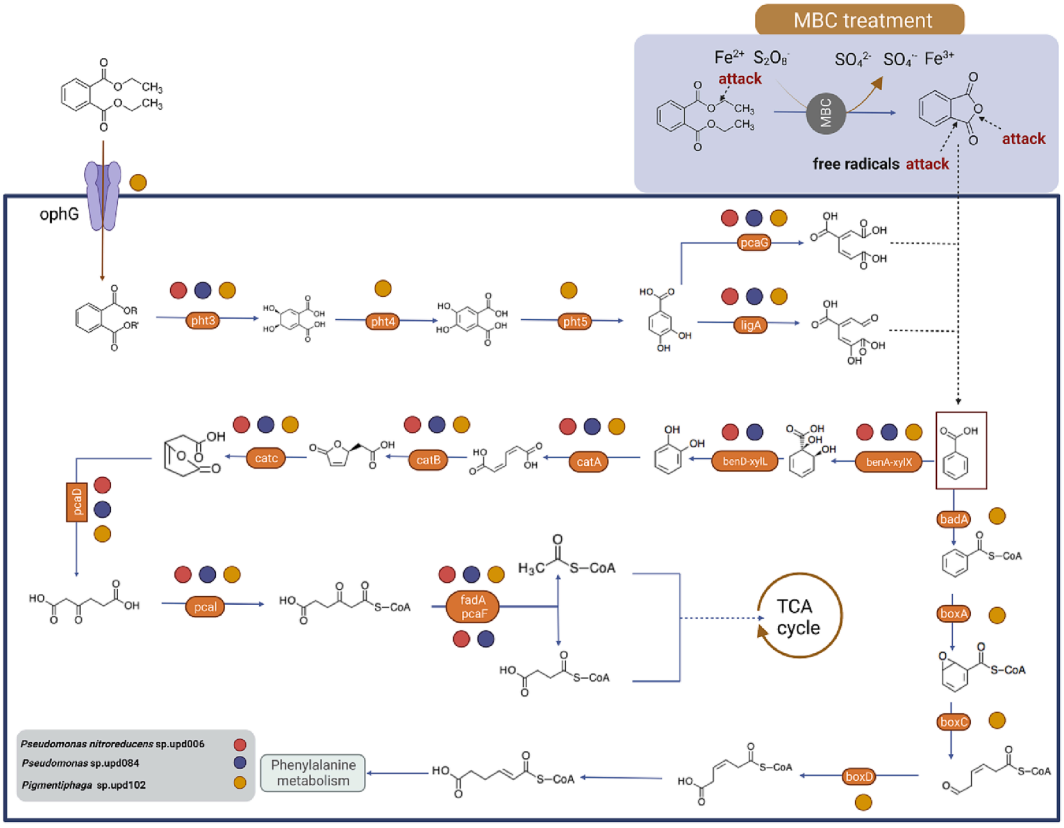

Fig. 5. Graphical representation of the proposed DP metabolic pathway based on three key species. The red, purple and yellow dots represent genes present in *Pseudomonas nitroreducens* sp. upd006, *Pseudomonas* sp. upd084, and *Pigmentiphaga* sp. upd102, respectively. All relevant genes considered for metabolic reconstruction can be found in Table S5. (For interpretation of the references to colour in this figure legend, the reader is referred to the web version of this article.)

MBCDP and DP groups, respectively. Previous research has indicated that members of the genus *Pseudomonas* have a role in the degradation of various phthalic lipids, such as dibutyl phthalate [63]. To gain further insight into the metabolic potential of these two MAGs, metabolic reconstructions were performed on their genomes, as depicted in Fig. 5. The red and purple dots indicate the annotated genes in *Pseudomonas nitroreducens* sp. upd006 and *Pseudomonas* sp. upd084, respectively. Our results indicated that although both *Pseudomonas nitroreducens* sp. upd006 and *Pseudomonas* sp. upd084 contain the gene encoding the phthalate 4,5-dioxygenase (pht3), they are lacking other essential genes in the upstream biodegradation pathway of DP and the transporter genes for PAEs (oph cluster). Despite the lack of these genes can be attributed to the incomplete genome reconstruction, this finding suggests that they cannot directly convert DP into PA. However, the downstream degradation pathway from PA is complete in both MAGs. PA was converted to catechol through the action of benzoate 1,2-dioxygenase and dihydroxycyclohexadiene carboxylate dehydrogenase, followed by a series of oxidases, isomerases, lipases, and transferases. This ultimately results in the production of Succinyl-CoA or Acetyl-CoA, which entered the tricarboxylic acid cycle.

The results obtained from the MBCDP treatment indicate a high prevalence of *Pseudomonas nitroreducens* sp. *upd006* in the samples. This suggests that this species is likely to be highly enriched with PA as a carbon source, particularly after intermediate PA is produced through oxidation. GC–MS analysis (Fig. 2C) supports the finding that firstly the C-O bond of DP is degraded to form phthalic anhydride, which was then further broken down to PA, and metabolized by *Pseudomonas nitroreducens* sp. upd006. The enrichment of *Pseudomonas* sp. *upd084* in the DP group appears to be linked to a mutualistic co-culture of microorganisms. As demonstrated in Figure S3, *Pseudomonas* sp. *upd084* exhibited a significant positive correlation with several MAGs that possess degradative potential. This suggests that the species may be able to metabolize intermediates produced by other species. In consideration of the functional similarity of *Pseudomonas nitroreducens* sp. upd006 and *Pseudomonas* sp. upd084 in the benzoate metabolism pathway, we conducted a comparative analysis of their gene content. The results of the comparison showed a high level of homology between the two MAGs (Figure S7).

The ability of *Pseudomonas* species to uptake and metabolize iron has been well documented [64]. In our study, both *Pseudomonas nitroreducens* sp. upd006 and *Pseudomonas* sp. upd084 possess complete polycyclic aromatic hydrocarbon degradation pathways. However, only *Pseudomonas nitroreducens* sp. upd006 was observed to be significantly enriched in the MBCDP group. This disparity between the two MAGs could be associated with the presence of ferrous iron (Fe(II)) and ferric iron (Fe(III)) in the reaction system activated by MBC. The Feo system is widely recognized as the primary ferrous (Fe(II)) transport system in prokaryotes [65]. FeoB, a large integral membrane protein, is believed to function as a ferrous permease, while FeoA can directly bind to FeoB. This FeoA-FeoB interaction is essential for the uptake of Fe(II) [66]. Our results, as anticipated, indicated the presence of genes encoding FeoA and FeoB in *Pseudomonas nitroreducens* sp. upd006 and their absence in *Pseudomonas* sp. upd084 (Table S3).

Furthermore, to postulate how the conversion process of Fe(II) to free ferric iron (Fe(III)) is working upon activation of the AOPs, we conducted an investigation into the related functional genes involved in Fe(III) recognition and transport in these two MAGs. The outer membrane TonB-dependent receptor and transporter FpvA and FptA, known for their high selectivity and affinity for Fe(III) [67], were only present in *Pseudomonas nitroreducens* sp. upd006 and absent in *Pseudomonas* sp. upd084. To assess the similarity of the Fe(II) and Fe(III) uptake and transport functions among members of the *Pseudomonas nitroreductase* species, a pangenome analysis was conducted (Table S4). The results showed that genes encoding ferrous (Fe(II)) transport were present in all of the analyzed MAGs/genomes, with the exception of one downloaded genome named *P. nitroreducens_contig1* having low completeness (87.57%), and the majority of them contained FpvA and FptA. These findings highlight the exceptional potential of *Pseudomonas nitroreducens* as a cooperative partner in MBC, with its ability to absorb both Fe(II) and Fe(III) generated during AOPs, while degrading upstream accumulated PA. In short, DP was initially attacked by free radicals activated by MBC in this soil–water environment, causing chemical bond cleavage as well as the release of iron elements. Co-occurring microorganisms such as *Sphingobium yanoikuyae* sp. upd020 and *Rhizobium* sp. upd015 may help mineralize DP and other intermediate products, leading to a significant accumulation of PA, which serves as a substrate for *Pseudomonas nitroreducens* sp. upd006. Furthermore, Fe(II) and Fe(III) in the process were absorbed by *Pseudomonas nitroreducens* sp. upd006, achieving harmless recycle of resources while mineralizing DP. This MBC-functional microbial combined system thus holds great promise for future biotechnological applications.

3.4.2. *Pigmentiphaga sp. upd102*

The yellow dots in Fig. 5 depict the genes annotated in *Pigmentiphaga* sp. upd102, whose whole-genome information is presented in Figure S8. Our analysis revealed the presence of a complete DP metabolic pathway in this MAG. The transport of PAEs into the bacterial cell is a critical metabolic step, which is facilitated by either the ABC transporter-type PAE transport system or, alternatively, by the permease-type PAE transporter [68]. In *Pigmentiphaga* sp. upd102, the phthalate transport protein (ophG) mediates the entry of DP into the cell, which is then converted into protocatechuate via the pht gene cluster. Finally, the protocatechuate undergoes degradation through protocatechuate dioxygenase to enter the benzoate degradation process. Compared to *Pseudomonas nitroreducens* sp. upd006 and *Pseudomonas* sp. upd084, *Pigmentiphaga* sp. upd102 exhibits a novel PA degradation pathway, converting PA to Benzoyl-CoA through benzoate-CoA ligase, ultimately generating 2,3-Didehydroadipyl-CoA which can enter the phenylalanine metabolism. The complete metabolic pathway of 2,3-Didehydroadipyl-CoA in *Pigmentiphaga* sp. upd102 is presented in the reconstructed phenylalanine metabolism map shown in Figure S9.

The degradation of DP by the genus *Pigmentiphaga* has not been previously reported. In order to determine the presence of DP degradation capability within the genus, a pangenome investigation was conducted utilizing information from *Pigmentiphaga*-related genomes/MAGs obtained from environmental (envMAGs) samples in the NCBI database (Table S6). The completeness of these envMAGs and *Pigmentiphaga* sp. upd102 varied between 73% and 100%, and the degree of contamination varied between 0% and 4.5%. In contrast, *Pigmentiphaga* sp. upd102 had low sequence homology to other *Pigmentiphaga* genomes/MAGs retrieved in the NCBI database. We further retrieved the annotations of the core gene clusters involved in phthalate metabolism in the *Pigmentiphaga* genomes (Fig. 6B). The gene *pht5* encoding 4,5-dihydroxyphthalate decarboxylase and terephthalate 1,2-dioxygenase oxygenase component (*tphA3*) were detected in all envMAGs and *Pigmentiphaga* sp. upd102. The complete pathway for converting phthalate to protocatechuate, as encoded by genes pht3-5, was observed in all MAGs except Pigmentiphaga sp. landfill_2 (73% completeness). Additionally, multiple envMAGs have genes (*ophG*, *ophH*) encoding PAE transporters, which may facilitate directly incorporating DP into the cell cytoplasm. Therefore, our putative DP mineralization pathway may be a ubiquitous capability in *Pigmentiphaga* based on evidence provided by the MAGs/genomes belonging to this genus.

3.5. *Antibiotic resistance and virulence factor of putative DP-degrading species*

The widespread presence of microplastics has raised concerns about the dissemination of antibiotic resistance genes (ARGs) [69] and pathogenic organisms [70]. The impact of chemical additives in plastics on the proliferation of ARGs and virulence factors is currently unclear. Hence, it is important to examine whether microbes performing DP

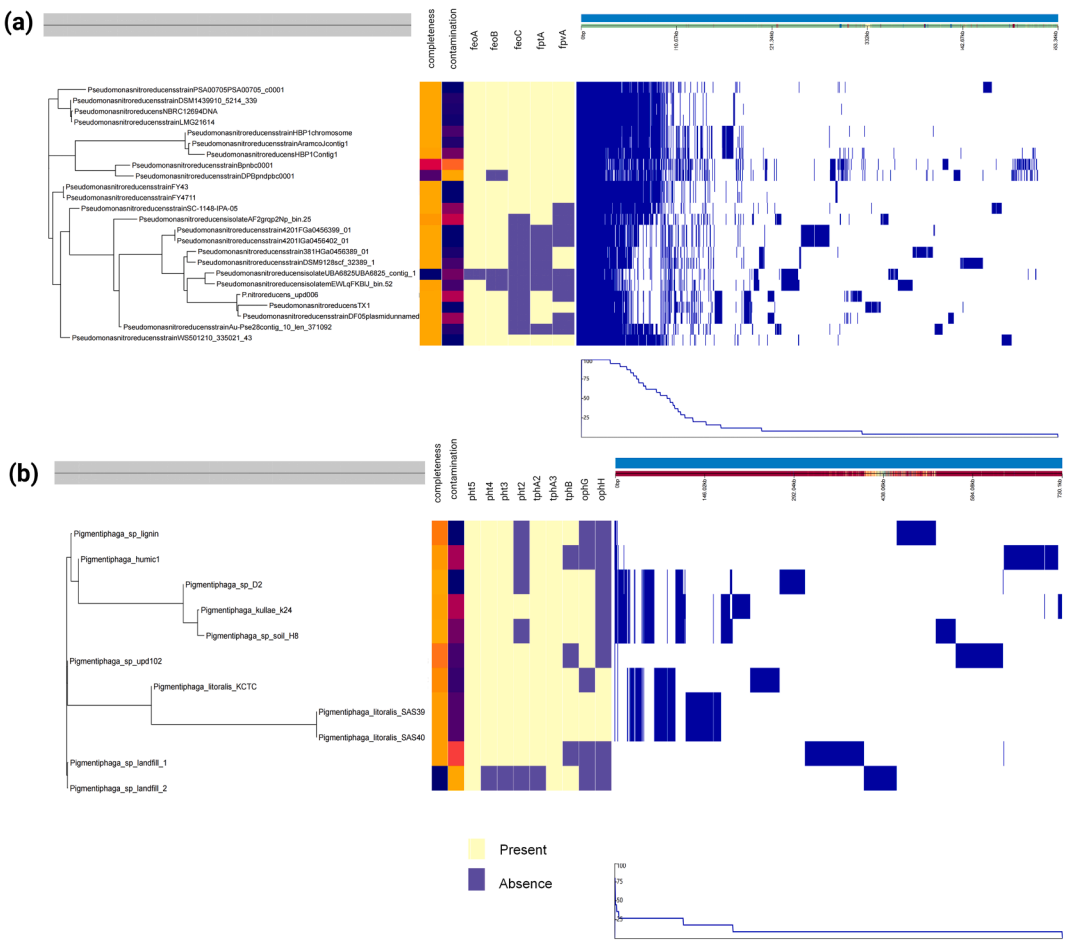

Fig. 6. Pangenome analysis of (a) *Pseudomonas nitroreducens* sp. upd006 and (b) *Pigmentiphaga* sp. upd102. All MAGs/genomes were retrieved from the NCBI database. The maximum-likelihood tree is generated using the binary presence and absence of accessory genes.

degradation contain ARGs and virulence factors, as this could impact their applicability in biodegradation of plasticizers.

All these three MAGs derived from the Pseudomonadota phylum contain ARGs that are linked to the resistance to specific types of drugs (Table S7). The most frequently occurring ARGs found in *Pigmentiphaga* sp. upd102 were those related to fluoroquinolone and tetracycline resistance. Similarly, both the two MAGs from the *Pseudomonas* genus showed strict hits for resistance to fluoroquinolone and tetracycline, as well as aminocoumarins, diaminopyrimidines, and phenols. Additionally, *Pseudomonas* sp. upd084 showed high hits for genes associated with resistance to benzalkonium chloride antibiotics. A more diverse set of ARGs was found in *Pseudomonas nitroreducens* sp. upd006, including those related to macrolide monobactam, carbapenem, cephalosporin, penam, peptide, sulfonamide, glycylcycline, and acridine dye resistance. These findings align with previous studies [71,72] and suggest that these three MAGs has the potential of spreading antibiotic resistance in the environment.

The existence of bacterial virulence factors can hinder the applicability of bacteria for engineering/bioremediation purposes, as they enable pathogenic bacteria to replicate and disseminate within a host by circumventing host defenses [73]. Our analysis identified multiple virulence factor-associated genes in three MAGs (Table S8). These included genes involved in amino acid and purine metabolism, biofilm formation, efflux pumps, and antiphagocytosis. Furthermore, genes related to Type IV pili biosynthesis, a key component of primary epithelial cell adhesion [74], were present in *Pseudomonas nitroreducens* sp. upd006 and *Pseudomonas* sp. upd084. The presence of known harmful virulence gene clusters in *Pseudomonas*, such as exotoxin A and metallophores [75,76], were not identified in the selected MAGs. In particular, the gene related to phytotoxin phaseolotoxin (*cysC1*) was detected in *Pseudomonas nitroreducens* sp. upd006. Although several virulence factors were identified, many of them serve essential metabolic functions necessary for bacterial survival, thus, it is conceivable that the potential DP degraders proposed in this work won't be pathogenic, making them suitable for use in the remediation of plasticizers in paddy soils and field runoff. However, the possible negative impact of *Pseudomonas nitroreducens* sp. upd006 on some plants should be noted.

4. Conclusion

Human activities have resulted in the influx of plastic waste into agricultural fields, leading to the accumulation of plastic additives in these environments. While the traditional methods of microbial degradation can be sluggish, incorporating magnetic biochar to activate the peroxidation process offers a promising avenue for facilitating the in-situ degradation of plasticizers. Indeed, this study demonstrated that hybrid magnetic biochar and field microorganisms, such as *Pseudomonas nitroreducens* sp. *upd006* that can uptake Fe(II) and Fe(III), were capable of mineralizing DP plasticizer. Additionally, the species *Pigmentiphaga* sp. upd102 was observed to have the potential of completely metabolize plasticizers in contaminated soil. A pangenome analysis also suggested that plasticizer mineralization may be a common trait among members of the *Pigmentiphaga* genus. The absence of pathogenicity virulence factors in the proposed potentially degrading or MBC-cooperating species makes them a promising option for removing plasticizers from surface water and farmland soils. However, to ensure the safe and

effective application of MBC in environmental remediation, it is crucial to consider how to design MBC to control its own toxicity and the environmental risks associated with free radicals.

Declaration of Competing Interest

The authors declare that they have no known competing financial interests or personal relationships that could have appeared to influence the work reported in this paper.

Data availability

Sequence data were deposited at the Sequence Read Archive (SRA, NCBI) under Bioproject PRJNA892267

Acknowledgments

This work was supported by the grant “Sviluppo Catalisi dell’Innovazione nelle Biotecnologie” (MIUR ex D.M.738 dd 08/08/19) of the Consorzio Interuniversitario per le Biotecnologie (CIB) and by the China Scholarship Council (No. 202008310162).

Appendix A. Supplementary data

Supplementary data to this article can be found online at https://doi.org/10.1016/j.cej.2023.143589.

References

[1] C. Luís, M. Algarra, J.S. Câmara, R. Perestrelo, Comprehensive insight from phthalates occurrence: from health outcomes to emerging analytical approaches, Toxics 9 (2021) 157.
[2] Y. Ma, S. Liao, Q. Li, Q. Guan, P. Jia, Y. Zhou, Physical and chemical modifications of poly (vinyl chloride) materials to prevent plasticizer migration-Still on the run, React. Funct. Polym. 147 (2020), 104458.
[3] P. Chakraborty, N.W. Shappell, M. Mukhopadhyay, S. Onanong, K.R. Rex, D. Snow, Surveillance of plasticizers, bisphenol A, steroids and caffeine in surface water of river Ganga and Sundarban wetland along the Bay of Bengal: occurrence, sources, estrogenicity screening and ecotoxicological risk assessment, Water Res. 190 (2021), 116668.
[4] M. Zhou, J. Yang, Y. Li, A model for phthalic acid esters’ biodegradability and biotoxicity multi-effect pharmacophore and its application in molecular modification, J. Environ. Sci. Health A 56 (2021) 361–378.
[5] X. Zhang, L. He, A.K. Sarmah, K. Lin, Y. Liu, J. Li, H. Wang, Retention and release of diethyl phthalate in biochar-amended vegetable garden soils, J. Soil. Sediment. 14 (11) (2014) 1790–1799.
[6] R. Jamarani, H.C. Erythropel, J.A. Nicell, R.L. Leask, M. Marić, How green is your plasticizer? Polymers 10 (2018) 834.
[7] J. Kastner, D.G. Cooper, M. Marić, P. Dodd, V. Yargeau, Aqueous leaching of di-2-ethylhexyl phthalate and “green” plasticizers from poly vinyl chloride, Sci. Total Environ. 432 (2012) 357–364.
[8] C.M. Chan, R. Lyons, P.G. Dennis, P. Lant, S. Pratt, B. Laycock, Effect of toxic phthalate-based plasticizer on the biodegradability of polyhydroxyalkanoate, Environ. Sci. Tech. 56 (24) (2022) 17732–17742.
[9] L. Xu, W. Chu, L. Gan, Environmental application of graphene-based CoFe2O4 as an activator of peroxymonosulfate for the degradation of a plasticizer, Chem. Eng. J. 263 (2015) 435–443.
[10] A. Kumari, R. Kaur, Uptake of a plasticizer (di-n-butyl phthalate) impacts the biochemical and physiological responses of barley, PeerJ 10 (2022) e12859.
[11] J.A. Pedersen, M. Soliman, I.H.(. Suffet, Human pharmaceuticals, hormones, and personal care product ingredients in runoff from agricultural fields irrigated with treated wastewater, J. Agric. Food Chem. 53 (5) (2005) 1625–1632.
[12] R.T. Lumio, M.A. Tan, H.D. Magpantay, Biotechnology-based microbial degradation of plastic additives, 3, Biotech 11 (2021) 350.
[13] M.W. Lim, E.V. Lau, P.E. Poh, A comprehensive guide of remediation technologies for oil contaminated soil—present works and future directions, Mar. Pollut. Bull. 109 (1) (2016) 14–45.
[14] S. Bala, D. Garg, B.V. Thirumalesh, M. Sharma, K. Sridhar, B.S. Inbaraj, M. Tripathi, Recent strategies for bioremediation of emerging pollutants: a review for a green and sustainable environment, Toxics 10 (2022) 484.
[15] S. Shariati, A.A. Pourbabaee, H.A. Alikhani, Biodegradation of diethyl phthalate and phthalic acid by a new indigenous Pseudomonas putida, Folia Microbiol. (2023) 1–12.
[16] Z.-D. Wen, D.-W. Gao, W.-M. Wu, Biodegradation and kinetic analysis of phthalates by an Arthrobacter strain isolated from constructed wetland soil, Appl. Microbiol. Biotechnol. 98 (10) (2014) 4683–4690.
[17] M. Boll, R. Geiger, M. Junghare, B. Schink, Microbial degradation of phthalates: biochemistry and environmental implications, Environ. Microbiol. Rep. 12 (1) (2020) 3–15.
[18] Y. Wang, Q. Ren, W. Zhan, K. Zheng, Q.i. Liao, Z. Yang, Y. Wang, X. Ruan, Biodegradation of di-n-octyl phthalate by Gordonia sp Lff and its application in soil, Environmental Technology 43 (17) (2022) 2604–2611.
[19] W. Jianlong, Z. Xuan, W.u. Weizhong, Biodegradation of phthalic acid esters (PAEs) in soil bioaugmented with acclimated activated sludge, Process Biochem. 39 (12) (2004) 1837–1841.
[20] Y. Xie, H. Liu, H. Li, H. Tang, H. Peng, H. Xu, High-effectively degrade the di-(2-ethylhexyl) phthalate via biochemical system: Resistant bacterial flora and persulfate oxidation activated by BC@ Fe3O4, Environ. Pollut. 262 (2020), 114100.
[21] M. Ji, X. Wang, M. Usman, F. Liu, Y. Dan, L. Zhou, S. Campanaro, G. Luo, W. Sang, Effects of different feedstocks-based biochar on soil remediation: a review, Environ. Pollut. 294 (2022) 118655.
[22] C. Zhang, G. Zeng, D. Huang, C. Lai, M. Chen, M. Cheng, W. Tang, L. Tang, H. Dong, B. Huang, Biochar for environmental management: Mitigating greenhouse gas emissions, contaminant treatment, and potential negative impacts, Chem. Eng. J. 373 (2019) 902–922.
[23] Y. Yi, Z. Huang, B. Lu, J. Xian, E.P. Tsang, W. Cheng, J. Fang, Z. Fang, Magnetic biochar for environmental remediation: A review, Bioresour. Technol. 298 (2020) 122468.
[24] A.R. Zimmerman, B. Gao, M.-Y. Ahn, Positive and negative carbon mineralization priming effects among a variety of biochar-amended soils, Soil Biol. Biochem. 43 (6) (2011) 1169–1179.
[25] X. Zhang, A.K. Sarmah, N.S. Bolan, L. He, X. Lin, L. Che, C. Tang, H. Wang, Effect of aging process on adsorption of diethyl phthalate in soils amended with bamboo biochar, Chemosphere 142 (2016) 28–34.
[26] M. Ji, W. Sang, D.C. Tsang, M. Usman, S. Zhang, G. Luo, Molecular and microbial insights towards understanding the effects of hydrochar on methane emission from paddy soil, Sci. Total Environ. 714 (2020), 136769.
[27] I. Koo, X. Zhang, S. Kim, Wavelet-and Fourier-transform-based spectrum similarity approaches to compound identification in gas chromatography/mass spectrometry, Anal. Chem. 83 (14) (2011) 5631–5638.
[28] A. Chklovski, D.H. Parks, B.J. Woodcroft, G.W. Tyson, CheckM2: a rapid, scalable and accurate tool for assessing microbial genome quality using machine learning, bioRxiv (2022) 2022.2007. 2011.499243.
[29] C. Piñeiro, J.M. Abuín, J.C. Pichel, Very Fast Tree: speeding up the estimation of phylogenies for large alignments through parallelization and vectorization strategies, Bioinformatics 36 (2020) 4658–4659.
[30] J. Hadfield, N.J. Croucher, R.J. Goater, K. Abudahab, D.M. Aanensen, S.R. Harris, Phandango: an interactive viewer for bacterial population genomics, Bioinformatics 34 (2018) 292–293.
[31] B.P. Alcock, A.R. Raphenya, T.T.Y. Lau, K.K. Tsang, M. Bouchard, A. Edalatmand, W. Huynh, A.-L. Nguyen, A.A. Cheng, S. Liu, S.Y. Min, A. Miroshnichenko, H.-K. Tran, R.E. Werfalli, J.A. Nasir, M. Oloni, D.J. Speicher, A. Florescu, B. Singh, M. Faltyn, A. Hernandez-Koutoucheva, A.N. Sharma, E. Bordeleau, A. C. Pawlowski, H.L. Zubyk, D. Dooley, E. Griffiths, F. Maguire, G.L. Winsor, R. G. Beiko, F.S.L. Brinkman, W.W.L. Hsiao, G.V. Domselaar, A.G. McArthur, antibiotic resistome surveillance with the comprehensive antibiotic resistance database, Nucleic Acids Res. (2020).
[32] B. Liu, D. Zheng, Q. Jin, L. Chen, J. Yang, VFDB 2019: a comparative pathogenomic platform with an interactive web interface, Nucleic Acids Res. 47 (2019) (2019) D687–D692.
[33] M. Xi, K. Cui, M. Cui, Y. Ding, Z. Guo, Y. Chen, C. Li, X. Li, Enhanced norfloxacin degradation by iron and nitrogen co-doped biochar: revealing the radical and nonradical co-dominant mechanism of persulfate activation, Chem. Eng. J. 420 (2021), 129902.
[34] S. Hao, X. Zhu, Y. Liu, F. Qian, Z. Fang, Q. Shi, S. Zhang, J. Chen, Z.J. Ren, Production temperature effects on the structure of hydrochar-derived dissolved organic matter and associated toxicity, Environ. Sci. Tech. 52 (13) (2018) 7486–7495.
[35] J.A. Korak, E.C. Wert, F.L. Rosario-Ortiz, Evaluating fluorescence spectroscopy as a tool to characterize cyanobacteria intracellular organic matter upon simulated release and oxidation in natural water, Water Res. 68 (2015) 432–443.
[36] R. Guo, L. Yan, P. Rao, R. Wang, X. Guo, Nitrogen and sulfur co-doped biochar derived from peanut shell with enhanced adsorption capacity for diethyl phthalate, Environ. Pollut. 258 (2020), 113674.
[37] J. Yan, G. Quan, Sorption behavior of dimethyl phthalate in biochar-soil composites: implications for the transport of phthalate esters in long-term biochar amended soils, Ecotoxicol. Environ. Saf. 205 (2020), 111169.
[38] C.-D. Dong, C.-W. Chen, C.-M. Hung, Persulfate activation with rice husk-based magnetic biochar for degrading PAEs in marine sediments, Environ. Sci. Pollut. Res. 26 (33) (2019) 33781–33790.
[39] W.J. Adams, G.R. Biddinger, K.A. Robillard, J.W. Gorsuch, A summary of the acute toxicity of 14 phthalate esters to representative aquatic organisms, Environmental Toxicology and Chemistry: an Int. J. 14 (1995) 1569–1574.
[40] J. Gao, Z. Shi, H. Wu, J. Lv, Fluorescent characteristics of dissolved organic matter released from biochar and paddy soil incorporated with biochar, RSC Adv. 10 (10) (2020) 5785–5793.
[41] Y. Yamashita, E. Tanoue, Chemical characterization of protein-like fluorophores in DOM in relation to aromatic amino acids, Mar. Chem. 82 (3-4) (2003) 255–271.
[42] C.J. Williams, Y. Yamashita, H.F. Wilson, R. Jaffé, M.A. Xenopoulos, Unraveling the role of land use and microbial activity in shaping dissolved organic matter characteristics in stream ecosystems, Limnol. Oceanogr. 55 (3) (2010) 1159–1171.

[43] P.G. Coble, Marine optical biogeochemistry: the chemistry of ocean color, Chem. Rev. 107 (2007) 402–418.
[44] N. Ferretto, M. Tedetti, C. Guigue, S. Mounier, R. Redon, M. Goutx, Identification and quantification of known polycyclic aromatic hydrocarbons and pesticides in complex mixtures using fluorescence excitation–emission matrices and parallel factor analysis, Chemosphere 107 (2014) 344–353.
[45] J. Šerá, F. Huynh, F. Ly, Š. Vinter, M. Kadlečková, V. Krátká, D. Máčalová, M. Koutný, C. Wallis, Biodegradable polyesters and low molecular weight polyethylene in soil: interrelations of material properties, Soil Organic Matter Substances, and Microbial Community, International Journal of Molecular Sciences 23 (2022) 15976.
[46] B. Aftab, H.-S. Shin, J. Hur, Exploring the fate and oxidation behaviors of different organic constituents in landfill leachate upon Fenton oxidation processes using EEM-PARAFAC and 2D-COS-FTIR, J. Hazard. Mater. 354 (2018) 33–41.
[47] K. Li, W. Jia, L. Xu, M. Zhang, Y. Huang, The plastisphere of biodegradable and conventional microplastics from residues exhibit distinct microbial structure, network and function in plastic-mulching farmland, J. Hazard. Mater. 442 (2023), 130011.
[48] P.V. Gavande, A. Basak, S. Sen, K. Lepcha, N. Murmu, V. Rai, D. Mazumdar, S. P. Saha, V. Das, S. Ghosh, Functional characterization of thermotolerant microbial consortium for lignocellulolytic enzymes with central role of Firmicutes in rice straw depolymerization, Sci. Rep. 11 (2021) 1–13.
[49] M.N. Fawaz, Revealing the ecological role of Gemmatimonadetes through cultivation and molecular analysis of agricultural soils, (2013).
[50] P.H. Janssen, P.S. Yates, B.E. Grinton, P.M. Taylor, M. Sait, Improved culturability of soil bacteria and isolation in pure culture of novel members of the divisions Acidobacteria, Actinobacteria, Proteobacteria, and Verrucomicrobia, Appl. Environ. Microbiol. 68 (5) (2002) 2391–2396.
[51] N. Ren, Y. Wang, Y. Ye, Y. Zhao, Y. Huang, W. Fu, X. Chu, Effects of continuous nitrogen fertilizer application on the diversity and composition of rhizosphere soil bacteria, Front. Microbiol. 11 (2020) 1948.
[52] M. Hernández, P. Villalobos, V. Morgante, M. González, C. Reiff, E. Moore, M. Seeger, Isolation and characterization of a novel simazine-degrading bacterium from agricultural soil of central Chile, Pseudomonas sp. MHP41, FEMS microbiology letters 286 (2008) 184-190.
[53] M.A. Pereyra-Camacho, V.E. Balderas-Hernández, A. De Leon-Rodriguez, Biodegradation of diisononyl phthalate by a consortium of saline soil bacteria: optimisation and kinetic characterisation, Appl. Microbiol. Biotechnol. 105 (8) (2021) 3369–3380.
[54] S.-G. Woo, Y. Cui, M.-S. Kang, L. Jin, K.K. Kim, S.-T. Lee, M. Lee, J. Park, Georgenia daeguensis sp. nov., isolated from 4-chlorophenol enrichment culture, Int. J. Syst. Evol. Microbiol. 62 (2012) 1703–1709.
[55] Y. Wang, H. Liu, Y. Peng, L. Tong, L. Feng, K. Ma, New pathways for the biodegradation of diethyl phthalate by Sphingobium yanoikuyae SHJ, Process Biochem. 71 (2018) 152–158.
[56] X. Zhang, R. Li, J. Song, Y. Ren, X.i. Luo, Y.i. Li, X. Li, T. Li, X. Wang, Q. Zhou, Combined phyto-microbial-electrochemical system enhanced the removal of petroleum hydrocarbons from soil: a profundity remediation strategy, J. Hazard. Mater. 420 (2021) 126592.
[57] C. Dai, H. Wu, X. Wang, K. Zhao, Z. Lu, Network and meta-omics reveal the cooperation patterns and mechanisms in an efficient 1, 4-dioxane-degrading microbial consortium, Chemosphere 301 (2022), 134723.
[58] Y. Teng, X. Wang, L. Li, Z. Li, Y. Luo, Rhizobia and their bio-partners as novel drivers for functional remediation in contaminated soils, Front. Plant Sci. 6 (2015) 32.
[59] C. Pagnout, G. Frache, P. Poupin, B. Maunit, J.-F. Muller, J.-F. Férard, Isolation and characterization of a gene cluster involved in PAH degradation in Mycobacterium sp. strain SNP11: Expression in Mycobacterium smegmatis mc2155, Res. Microbiol. 158 (2007) 175–186.
[60] D.-W. Liang, T. Zhang, H.H. Fang, J. He, Phthalates biodegradation in the environment, Appl. Microbiol. Biotechnol. 80 (2008) 183–198.
[61] G. Wang, W. Yue, Y. Liu, F. Li, M. Xiong, H. Zhang, Biodegradation of the neonicotinoid insecticide Acetamiprid by bacterium Pigmentiphaga sp. strain AAP-1 isolated from soil, Bioresour. Technol. 138 (2013) 359–368.
[62] H. Yang, X. Wang, J. Zheng, G. Wang, Q. Hong, S. Li, R. Li, J. Jiang, Biodegradation of acetamiprid by Pigmentiphaga sp. D-2 and the degradation pathway, International Biodeterioration & Biodegradation 85 (2013) 95-102.
[63] H. Yu, L. Wang, Y. Lin, W. Liu, D. Tuyiringire, Y. Jiao, L. Zhang, Q. Meng, Y. Zhang, Complete metabolic study by dibutyl phthalate degrading Pseudomonas sp. DNB-S1, Ecotoxicol. Environ. Saf. 194 (2020), 110378.
[64] P. Cornelis, Iron uptake and metabolism in pseudomonads, Appl. Microbiol. Biotechnol. 86 (6) (2010) 1637–1645.
[65] C. Gómez-Garzón, J.E. Barrick, S.M. Payne, E.G. Ruby, Disentangling the evolutionary history of Feo, the major ferrous iron transport system in bacteria, MBio 13 (1) (2022).
[66] H. Kim, H. Lee, D. Shin, The FeoA protein is necessary for the FeoB transporter to import ferrous iron, Biochem. Biophys. Res. Commun. 423 (4) (2012) 733–738.
[67] F. Hoegy, H. Celia, G.L. Mislin, M. Vincent, J. Gallay, I.J. Schalk, Binding of iron-free siderophore, a common feature of siderophore outer membrane transporters of Escherichia coli and Pseudomonas aeruginosa, J. Biol. Chem. 280 (21) (2005) 20222–20230.
[68] R. Hu, H. Zhao, X. Xu, Z. Wang, K. Yu, L. Shu, Q. Yan, B. Wu, C. Mo, Z. He, Bacteria-driven phthalic acid ester biodegradation: Current status and emerging opportunities, Environ. Int. 154 (2021), 106560.
[69] L. Niu, W. Liu, A. Juhasz, J. Chen, L. Ma, Emerging contaminants antibiotic resistance genes and microplastics in the environment: Introduction to 21 review articles published in CREST during 2018–2022, Crit. Rev. Environ. Sci. Technol. 52 (2022) 4135–4146.
[70] D. Zhu, J. Ma, G. Li, M.C. Rillig, Y.-G. Zhu, Soil plastispheres as hotspots of antibiotic resistance genes and potential pathogens, ISME J. 16 (2) (2022) 521–532.
[71] M. Hernandez, S. Roy, C.W. Keevil, M.G. Dumont, Identification of diverse antibiotic resistant bacteria in agricultural soil with H218O stable isotope probing and metagenomics, bioRxiv (2023) 2023.2001. 2024.525391.
[72] H. Liao, H. Li, C.-S. Duan, X.-Y. Zhou, X.-L. An, Y.-G. Zhu, J.-Q. Su, Metagenomic and viromic analysis reveal the anthropogenic impacts on the plasmid and phage borne transferable resistome in soil, Environ. Int. 170 (2022), 107595.
[73] A.S. Cross, What is a virulence factor? Crit. Care 12 (2008) 1–2.
[74] L.L. Burrows, Pseudomonas aeruginosa twitching motility: type IV pili in action, Annu. Rev. Microbiol. 66 (1) (2012) 493–520.
[75] G. Ghssein, Z. Ezzeddine, A review of Pseudomonas aeruginosa metallophores: Pyoverdine, pyochelin and pseudopaline, Biology 11 (2022) 1711.
[76] M. Michalska, P. Wolf, Pseudomonas Exotoxin A: optimized by evolution for effective killing, Front. Microbiol. 6 (2015) 963.

Chapter IV

Different microplastics in anaerobic paddy soils: Altering methane emissions by influencing organic matter composition and microbial metabolic pathways

Mengyuan Ji [a,b] , Lurui Xiao [a] , Muhammad Usman [d] , Chao Liu [e] , Wenjing Sang [a,*] , Laura Treu [b] , Stefano Campanaro [b] , Gang Luo [c] , Yalei Zhang [f]
Chemical Engineering Journal, Volume 469, 1 August 2023, 144003
https://doi.org/10.1016/j.cej.2023.144003

[a] Textile Pollution Controlling Engineering Center of Ministry of Environmental Protection, College of Environmental Science and Engineering, Donghua University, Shanghai 201620, China
[b] Department of Biology, University of Padua, 35131 Padova, Italy
[c] Shanghai Key Laboratory of Atmospheric Particle Pollution and Prevention (LAP3), Department of Environmental Science and Engineering, Fudan University, Shanghai 200433, China
[d] Department of Civil and Environmental Engineering, University of Alberta, Edmonton, AB T6G 2W2, Canada
[e] Key Laboratory for Water Quality and Conservation of the Pearl River Delta, Ministry of Education, Guangzhou University, Guangzhou 510006, China f College of Environmental Science and Engineering, Tongji University, Shanghai 200092, China
*Corresponding author

Chemical Engineering Journal 469 (2023) 144003

Contents lists available at ScienceDirect

Chemical Engineering Journal

journal homepage: www.elsevier.com/locate/cej

Different microplastics in anaerobic paddy soils: Altering methane emissions by influencing organic matter composition and microbial metabolic pathways

Mengyuan Ji [a,b], Lurui Xiao [a], Muhammad Usman [d], Chao Liu [e], Wenjing Sang [a,*], Laura Treu [b], Stefano Campanaro [b], Gang Luo [c], Yalei Zhang [f]

[a] Textile Pollution Controlling Engineering Center of Ministry of Environmental Protection, College of Environmental Science and Engineering, Donghua University, Shanghai 201620, China
[b] Department of Biology, University of Padua, 35131 Padova, Italy
[c] Shanghai Key Laboratory of Atmospheric Particle Pollution and Prevention (LAP3), Department of Environmental Science and Engineering, Fudan University, Shanghai 200433, China
[d] Department of Civil and Environmental Engineering, University of Alberta, Edmonton, AB T6G 2W2, Canada
[e] Key Laboratory for Water Quality and Conservation of the Pearl River Delta, Ministry of Education, Guangzhou University, Guangzhou 510006, China
[f] College of Environmental Science and Engineering, Tongji University, Shanghai 200092, China

ARTICLE INFO

Keywords:
Microplastics
Paddy soil
Methane emission
Anaerobic metabolic

ABSTRACT

Microplastics are widespread in farmland and threaten soil ecology. However, how different microplastics affect methane emission in paddy soil are still unclear. To address this knowledge gap, three typical microplastics, polyethylene, polypropylene, and polyvinyl chloride were added to paddy soil with different doses (0.01%, 0.1%, and 1%), and a 50-day incubation experiment was conducted. Compared with polyethylene and polypropylene microplastics, 1% of polyvinyl chloride microplastic resulted in the highest increase in methane production. According to the integrated liquid phase analysis, all three microplastics contributed to the accumulation of humus in the soil solution. Differential microbial taxa analysis indicated that some denitrifying bacteria such as *Gemmatimonadetes* and *Omnitrophicaeota* were significantly enriched in 1% polyethylene and polypropylene microplastics groups on day 30, and *Rice Cluster I* methanogens archaea were enriched specially in the 1% polyvinyl chloride microplastic group. The predicted soil metabolic functions suggested that polyethylene and polyvinyl chloride microplastics enhanced oxidative phosphorylation and amino acid reduction pathways. Macromolecular humus induced by microplastics may play a critical role in the dynamic equilibrium of anaerobic systems in paddy soils. These findings highlighted the threat of microplastics in agricultural fields greenhouse gas emissions. The identified quinone reductive metabolic pathways may provide potential strategies to reduce methane emissions.

1. Introduction

Microplastics (MPs) are tiny particles (<5 mm) that form as a result of physicochemical and biological processes acting on plastic waste [1]. Due to their high durability, slow degradation rates, and potential toxicity to ecosystems [2,3], they have emerged as a significant environmental pollutant, generating increasing concern. It has been reported that MPs are widespread in terrestrial ecosystems and pose a threat to

Abbreviations: MPs, Microplastics; GHG, Greenhouse gases; PE, Polyethylene; PP, Polypropylene; PVC, Polyvinyl chloride; DOC, Dissolved organic carbon; EEM, Excitation emission matrix; TCD, Thermal conductivity detector; TOC, Total organic carbon; Ex, Excitation; Em, Emission; OTUs, Operational taxonomic units; PCoA, Principal coordinate analysis; PERMANOVA, Permutation multivariate analysis of variance; LDA, Linear discriminant analysis; LEfSe, Linear discriminant analysis coupled with effect size; KO, KEGG ortholog; C1, Component 1; C2, Component 2; C3, Component 3; C4, Component 4; C5, Component 5; C6, Component 6; C7, Component 7; C8, Component 8; SSA, Specific surface area; TEAs, Terminal electron acceptors; PAHs, Polycyclic aromatic hydrocarbons.

* Corresponding author.
E-mail addresses: mengyuan.ji@studenti.unipd.it (M. Ji), musman4@ualberta.ca (M. Usman), chao3299@gmail.com (C. Liu), wjsang@dhu.edu.cn (W. Sang), laura.treu@unipd.it (L. Treu), stefano.campanaro@unipd.it (S. Campanaro), gangl@fudan.edu.cn (G. Luo), zhangyalei@tongji.edu.cn (Y. Zhang).

https://doi.org/10.1016/j.cej.2023.144003
Received 9 January 2023; Received in revised form 20 May 2023; Accepted 6 June 2023
Available online 7 June 2023

the balance of these systems [4]. While there has been extensive research on the issues surrounding MPs in aquatic environments [5], comparatively limited attention has been given to the study of MPs in soil environments. This disparity can be attributed primarily to the challenges associated with detecting and isolating MPs within soil aggregates [6]. Nevertheless, it is imperative to investigate the impact of MPs on terrestrial biogeochemical processes, given the documented effects of MPs on soil microbiology, faunal populations, and carbon cycling [7,8].

Agricultural activities, particularly the application of mulch film, are identified as the main source of MPs pollution in soil [9]. The unique flooded conditions of paddy soil provide anaerobic habitats for soil microorganisms, making it susceptible to changes in greenhouse gases (GHG) emissions due to external factors. Although thermoplastic MPs such as polyethylene (PE) are not directly utilized by soil microorganisms, they can indirectly affect soil GHG emission by increasing soil microporosity and aeration [10]. For example, a previous study demonstrated that the introduction of PE MPs into anaerobic soils with high nitrogen content increased the abundance of the denitrification functional gene (nirS), resulting in a rise in GHG emissions [11]. Additionally, a recent study found that PE MPs can inhibit methane emissions from paddy fields by reducing the abundance of the methane production gene mcrA in acidic soil or increasing the abundance of the methane oxidation gene pmoA in alkaline soil [12]. Han and colleagues observed a substantial increase in the mcrA values in paddy fields when PE MPs were applied in conjunction with hydrochar [13]. Despite recent studies investigating the impact of MPs on GHG emission-related functional genes in paddy soil, conclusive results are limited due to the restricted range of tested MPs. Furthermore, the mechanisms underlying the observed gene changes remain unclear. Besides specific functional genes, the impact of MPs on soil microbial communities and carbon cycling remains unclear. Growth of some gram-negative bacteria such as *Ktedonobacteriales* and *Oligoflexales* was found to be enhanced by PE and PVC MPs in agriculture soil, while the growth of gram-positive bacteria was suppressed by the presence of these MPs [14,15]. A study conducted by Wu et al. demonstrated that the impact of low-density PE MPs on microbial communities varied depending on the applied dose (0.2%, 1%, and 2% w/w) [16]. It was also reported that PE MPs at a concentration of 1% can enhance the mineralization of soil organic carbon by promoting the efficient utilization of low molecular weight organic substances by microorganisms such as *Syntrophomonadaceae*, *Anaerobacteriu*, *Papillibacter*, and *Mobilitalea* [17]. However, previous findings have been inconclusive, necessitating further research into the effects of various microplastic types on soil biogeochemical processes, particularly in paddy soils, where their potential impact on global warming can be significant.

PE, polypropylene (PP), and polyvinyl chloride (PVC) are commonly used in the production of mulch worldwide [18]. PE is distinguished by its inherent lightweight nature, exceptional flexibility, and notable resistance to chemical degradation. Conversely, PP manifests heightened strength, increased rigidity, and superior thermal stability [19]. In contrast, PVC showcases moderate mechanical strength along with commendable resistance to chemical agents, often encompassing additives to confer additional flexibility or desired characteristics [20]. These plastics have been shown to alter the content and structure of soil organic carbon, leading to changes in microbial composition and metabolism [21,22]. The introduction of plastic pollution into soil environments can result in the subsequent release of micro- and nanoscale particles. Emerging evidence suggests that micro- and nanoscale particles can exert both direct and indirect influences on soil microorganisms and enzymatic processes [23]. For instance, the application of high doses of multi-walled carbon nanotubes has been shown to significantly diminish microbial activity and biomass in soil [24]. Adverse effects on soil enzymatic activity have been observed in the presence of nanosilver [25], while a pronounced decline in microbial biomass has been detected in soils amended with nanoscale titanium dioxide [26]. various nano-composite fertilizers have been widely applied in agricultural practices [27,28], influencing soil organic fertility [29] and microbial communities. For instance, the type of carbon nanotubes has been reported as a major factor distinguishing bacterial communities after exposure in previous studies, and single-walled carbon nanotubes were found to exert a stronger influence on soil bacterial community composition (β diversity) compared to multi-walled carbon nanotubes [30]. Furthermore, renewable materials such as biomass and coke have also been found to have varying effects on greenhouse gas emissions [31–33], including NOx and CO_2. These discrepancies may arise from various factors, including the toxicological variances among micro- and nanoscale particles, exposure doses and durations, and soil physicochemical properties [34]. Considering the differences in physicochemical properties between plastics and these well-studied nanomaterials, the previous findings cannot be directly extrapolated to MPs. While the occurrence of MP particles at the micrometer scale in terrestrial ecosystems is increasingly being recognized, limited information is available regarding their impacts on soil biogeochemical processes. The dearth of comprehensive and well-defined experimental investigations conducted under comparable conditions hinders a comprehensive understanding of the effects of MPs on environmental microbiology.

Table 1
Physicochemical properties of soil.

Sample	pH	TOC (g/kg soil)	C content (wt%)	H content (wt%)	N content (wt%)	Available phosphorus (mg/kg soil)
Soil	7.6	17.8	3.29%	0.94%	0.26%	7.86

The primary objective of this study is to systematically examine the comparative effects of PP, PE, and PVC plastics, administered at varying doses on the micrometer scale, on the biogeochemical processes in paddy soil. Furthermore, employing advanced bioinformatics methodologies, this investigation endeavors to elucidate the potential mechanistic underpinnings behind the observed disparities in methane emission levels, offering novel insights at a comprehensive metabolic pathway level. A 50-day incubation experiment was conducted to investigate the effects of these three typical types of MPs on methane emission at three doses (0.01%, 0.1%, and 1% w/w). Shifts in soil dissolved organic carbon (DOC) was characterized using total organic carbon (TOC) analyzer and excitation emission matrix (EEM) spectra. High-throughput sequencing combined with bioinformatics analysis was used to examine the abundance of functional genes related to quinone reduction and anaerobic respiration, which may suppress methane emissions. Thus, an in-depth understanding of the mechanism of MPs affecting methane emissions from farmland can be obtained, laying the foundation for the development of future emission reduction technologies.

2. Materials and methods

2.1. Soil and MPs preparation

Soil samples was collected from the surface (2–20 cm depth) of paddy rice field which was located in Songjiang District, Shanghai, China. After air-drying and mixing, the soil samples were sieved with a 2 mm sieve. The basic physicochemical properties of soil are shown in Table 1.The plastics (PP, PE and PVC) used in this study were purchased from Huixing Environmental Protective Material Co., Ltd. (Guangdong, China). Before using, the plastics were processed through a crusher to reduce their size and then sieved to less than 5 mm to obtain MPs.

2.2. Incubation experiment

To simulate the flooding conditions of paddy fields, an anaerobic soil

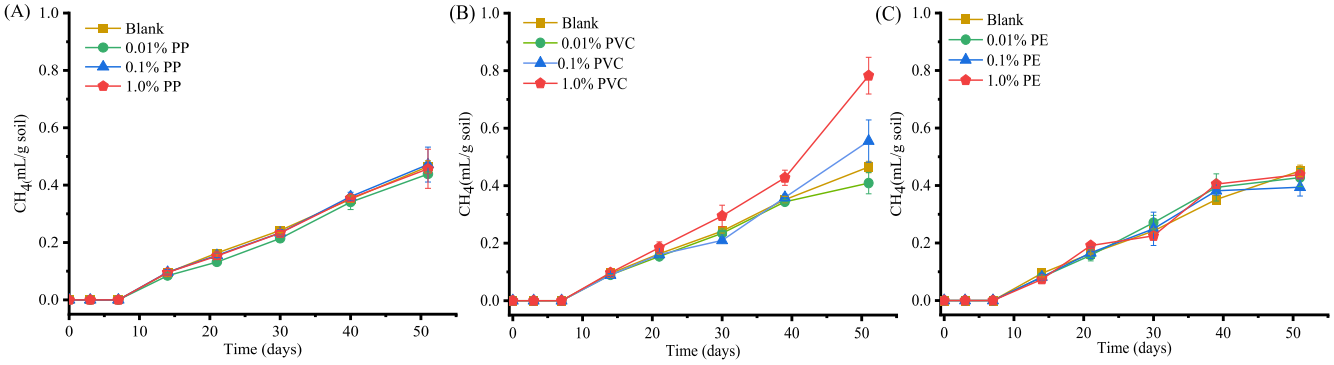

Fig. 1. Effects of typical MPs with different mass ratios on soil methane emissions from paddy soil.(A) Polypropylene(PP); (B) Polyvinyl chloride(PVC); (C) Polyethylene(PE).

slurry incubation experiment was conducted. The incubation setup was based on previous anaerobic incubation experiments [35,36]. Each 120 mL serum bottle was filled with 50 g of dry paddy soil, and low, medium, and high dosages of different MPs were added (0.01%, 0.1%, and 1% w/w (MPs/dry soil)), which were selected based on their sensitivity to changes in functional gene abundance related to the soil carbon cycle [11,37]. The soil was then mixed with 60 mL of ultrapure water and sealed with butyl rubber septa and crimped with aluminum caps. The vials were shaken up and down and the headspace was flushed with nitrogen. A blank group was also included in which no MPs were added. All groups were tested in triplicates and then incubated in the dark at 28 °C. During the incubation period, gas samples from the top of the bottles were periodically collected using a syringe and analyzed for methane concentration using a gas chromatograph (Haixin, GC-960, China) combined with a thermal conductivity detector (TCD). After 30 days and 50 days of incubation, destructive soil sampling was performed. The obtained mixtures were centrifuged at 6000 rpm for 15 min to separate the solid and liquid phases and stored at −20 °C. The liquid and solid samples were then used for analysis of dissolved organics and DNA extraction, respectively.

2.3. Characterization of soil dissolved organic matter

The DOC content of liquid samples was analyzed using a TOC analyzer (TOC-L CPH, Shimadzu, Japan). The instrument was calibrated using potassium hydrogen phthalate. Liquid samples were filtered through 0.22 μm filters to eliminate any particulate matter before analysis.

The fluorescence spectrophotometer (Aqualog; Horiba-Jobin Yvon, USA) was used to conduct EEM Spectra measurement on the liquid phase. The excitation (Ex) range was from 240 to 600 nm and the emission (Em) range was from 280 to 550 nm to identify the components of the liquid phase. The spectra were recorded using excitation and emission slit widths of 3 nm. The initial data was zeroed to eliminate the effect of Rayleigh scattering and a Milli-Q water sample was run to remove the impact of Raman scattering. Parallel factor analysis was applied to determine the fluorescence properties of the DOC components [38].

2.4. High-throughput sequencing and bioinformatics analysis

Soil samples were collected at 30 and 50 days for microbial analysis, and DNA was extracted from 0.5 g of soil using the QIAamp DNA Isolation Kit (QIAGEN, 51504). The extracted DNA was quantified and checked for purity using a Nanodrop (2000). The archaeal and bacterial 16S rRNA genes were amplified using the 515F (GTGCCAGCMGCCGCGGTAA) and 806R (GGACTACHVGGGTWTCTAAT) primers [39]. The PCR reaction was carried out with the following conditions: preheating at 95 °C for 3 min, 40 cycles of denaturation at 98 °C for 30 s, annealing at 58 °C for 15 s, and elongation at 75 °C for 15 s, followed by a final step at 72 °C for 1 min. The PCR products were sequenced on the Illumina MiSeq platform according to standard protocols, and the resulting sequences were clustered into operational taxonomic units (OTUs) with a cutoff value of 0.03. Taxonomic classification of the sequences was performed using the RDP classifier with a confidence threshold of 80% [40]. The 16S rRNA sequences have been deposited in the NCBI Sequence Read Archive database with accession number PRJNA821636.

To assess the differences in microbial composition among the groups, the Shannon index and Bray-Cutris distance were calculated using the "Vegan" package in R (version 4.0.5). Principal coordinate analysis (PCoA) based on weighted UniFrac distances was employed to show community differences among groups, and the significance of these differences was confirmed through a permutation multivariate analysis of variance (PERMANOVA). Linear discriminant analysis (LDA) coupled with effect size (LEfSe) was used to determine species with significant differences in abundance among different groups [41]. The functions of different groups were predicted using PICRUSt2 software [42], which was installed as a QIIME2 plugin. The metabolic pathways were reconstructed using the KEGG ortholog (KO) group ids. To provide a more quantitative description, the following formula was used to calculate the change of the main phyla in each group relative to the blank:

$$R_p=(R_i-R_0)/R_0 \times 100\% \quad (1)$$

Where R_i is the relative abundance of a certain phylum exposed, and i represent different exposures, including the type, dose, and exposure time of MPs. R_0 is the relative abundance of this certain phylum in the blank group.

Linear regression [43] and random forest [44] models were utilized to predict the impact of dosage of MPs, major fluorescent products, and phyla responses on methane production. The statsmodels [45] and sklearn [46] packages of the Python software were employed for these analyses.

2.5. Statistical

The impact of MPs on the microbial community was evaluated using Kruskal-Wallis analysis for the Shannon Index, Bray-Curtis, unique OTUs, and main phyla. The statistical significance was considered as significant when the P-value was less than 0.05.

LEfSe analysis was conducted to identify key members with significant differences in abundance among the groups. The Kruskal-Wallis test was first applied to detect significant differences and the Wilcoxon signed-rank test was used to validate the sub-members of differential members. Finally, LDA was utilized to reduce the data dimensionality and assess the results. Members with the LDA score ≥ 2.0 were

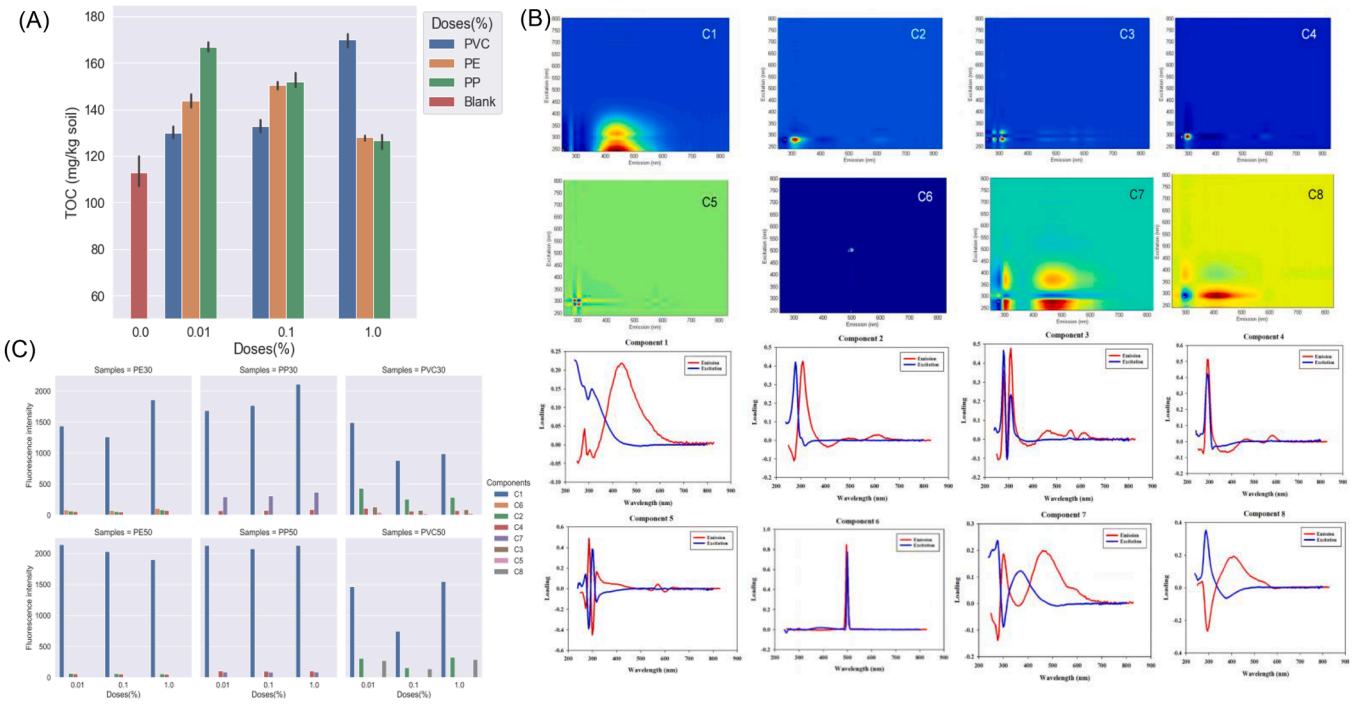

Fig. 2. Shifts in soil DOC. (A) Total organic carbon levels of soil DOC under different treatments. (B) Fluorescent components were identified from soil DOC. (C) Differences in fluorescence intensity induced by different MPs. The suffixes "30" and "50" denote day 30 and day 50 sampling, respectively.

considered as important biomarkers for each group.

A two-sided Welch's T-test was employed to evaluate the differences in functional genes between the treated and control samples. The significance level was determined as P-value less than 0.05. Additionally, Pearson correlation analysis was conducted to investigate the correlation between the dose and exposure time of MPs and microbial abundance. The statistical analysis was performed using SPSS 23.0.

3. Results and discussion

3.1. Effect of different MPs on soil methane emissions

The effect of different doses of PP, PVC, and PE MPs (0.01%, 0.1%, and 1%) on cumulative methane emissions from soil are shown in Fig. 1. The presence of PP and PE MPs did not significantly affect methane emissions compared to the blank group. However, methane emissions increased by 19.4% with 0.1% PVC MPs and by 68.32% with 1% PVC MPs. Linear regression analysis (Fig. S1A) further verified the promotion effect of PVC dosage on methane emissions (with a sensitivity = 0.10).

The effects of MPs on methane emissions have been attributed to variations in the response of methanogenic and methanotrophic bacteria, influenced by soil and MP characteristics. PET MPs have been reported to reduce methane emissions by increasing pmoA gene abundance, while PAN MPs showed negligible impact on mcrA and pmoA gene quantities [47]. In this study, only higher doses of PVC promoted methane production, while other MPs had minimal influence, possibly due to differences in their inherent properties. For example, PVC typically contains more plasticizer additives compared to PE and PP [48], which can be released into the soil and serve as a carbon source for microorganisms, potentially increasing the abundance of methanogenic bacteria. Additionally, the physicochemical properties of the soil are easily disturbed by external stimuli [49,50], MPs can disrupt soil aggregate protection and enhance phenol oxidase activity [51,52], leading to shifts in the ratio of methanogenic to methanotrophic bacteria ratio and increased DOC levels. Therefore, subsequent sections focus on investigating the response of soil organic matter and microbial composition to the different treatments.

3.2. Effect of MPs type and dosage on DOC content

The impact of various types and doses of MPs on the TOC levels of soil leachate after 50 days is shown in Fig. 2A. In comparison to the blank, all three types of MPs resulted in a significant increase in TOC levels. At low doses (0.01% and 0.1%), the increase in TOC caused by PP and PE was greater than that caused by PVC. However, at the high dose (1%), the increase in TOC caused by PVC was higher than that caused by PP and PE. As the dose of PVC increased from 0.01% to 1%, the TOC level increased from 129.42 mg/kg to 170.47 mg/kg. Conversely, as the dose of PP increased from 0.01% to 1%, the TOC level decreased from 170.46 mg/kg to 123.02 mg/kg. The 0.1% dose of PE (150.76 mg/kg) resulted in a larger increase in TOC compared to the 0.01% (144.19 mg/kg) and 1% (128.54 mg/kg) doses.

The study found a positive correlation between the dosage of PVC and TOC levels ($R = 1.000$, $P = 0.004$), which is in line with previous research showing that the leaching of DOC from PVC increases with the amount of PVC [53]. Additionally, the results showed that lower doses of PP and PE MPs had a greater effect on increasing TOC than the higher dose. In soils, conventional MPs such as PP and PE can potentially integrate into soil aggregates, competing with microorganisms for ecological niches and influencing the release of soil organic matter [10,54]. Moreover, higher doses of PP and PE MPs increase the total adsorption sites in the environment, potentially enhancing their adsorption capacity for various soil constituents, including cellulose, hemicellulose, lignin, proteins, lipids, monosaccharides, and carbohydrates [55,56]. Consequently, the elevated doses of PP and PE MPs are associated with a decrease in TOC levels. In contrast, As the dosage of PVC MPs increased, the release rate of the plasticizer of PVC may have outweighed the absorption rate, resulting in a significant increase in TOC. These plasticizers may serve as unstable carbon fractions that are accessible to microorganisms, as certain materials with coating additives have the potential to release vinyl alcohol into the environment [57]. It is worth noting that Li et al. also reported a more pronounced promotion of TOC by PP compared to PVC (In the dose range of 0.3% to 1.0%, w/w), attributing it to the differences in carbon content between PP (85.7%) and PVC (38.4%) [58]. Another possible factor is that MPs,

Table 2
Excitation and emission maxima of the fluorescent components of the DOC samples.

Components	Ex/Em (nm)	Description	References
C1	310/425	Humic acid-like	(Murphy et al., 2006; Qin et al., 2020)
C2	270/310	Protein/Phenol-like	(Yamashita and Tanoue, 2003)
C3	275, 310/ 275,310	Protein/Phenol-like	(Yamashita and Tanoue, 2003)
C4	290/290	Protein/Phenol-like	(Uchimiya et al., 2015; Al Riza et al., 2019)
C5	275,300/ 290,310	Protein/Phenol-like	(Yamashita and Tanoue, 2003)
C6	500/500	More complex molecular structures	(Hu et al., 2021)
C7	270/300,450	Aromatic, aliphatic, and humic-like	(Yu et al., 2020)
C8	270/410	Aromatic, aliphatic, and fulvic-like	(Yu et al., 2020)

considered contributors to TOC under current detection methods [59], are typically more resistant in PVC compared to PP and PE under the same detection conditions, resulting in significantly higher TOC levels in this study for PE and PP MPs at low doses compared to PVC MPs. However, it is important to note that the organic carbon contributed by MPs may differ in structure and functionality from natural soil organic matter [60]. While TOC values increased, this additional fraction cannot be considered genuine soil nutrients directly, to explore the variations in DOC structure caused by different MPs, further characterization of the DOC was conducted using EEM spectroscopy.

3.3. Effect of MPs type and dosage on DOC structure

The fluorescence spectra of the soil leachate are displayed in Fig. S2. Parallel factor analysis revealed the presence of eight components of soil dissolved organic matter, shown in Fig. 2B. The peak positions and descriptions of these components are listed in Table 2. Component 1 (C1) showed a peak at Ex/Em = 310/425 nm, which was identified as a UVA humic substance [61]. Components 2, 3 and 5 (C2, C3, and C5) showed peak positions in the range of Ex = 270–310 nm, Em = 275–310 nm and were similar to Protein/Phenol-like substances [62]. Component 4 (C4) was distinguished by its peak at Ex/Em = 290/290 nm with a lower emission wavelength compared to C3 and C5, potentially indicating a higher degree of aromaticity or molecular weight [63]. Component 6 (C6) exhibited a peak at Ex/Em = 500/500 nm, indicating the presence of complex macromolecules in the sample [64]. Furthermore, both component 7 (C7) and component 8 (C8) were identified as fulvic-like substances, with C7 exhibiting two excitation peaks at Ex 270 and 380 nm and two emission peaks at 320 and 450 nm, and C8 showing peaks at Ex/Em = 270/410 nm [65]. Fig. 2C further provides a comparison of the fluorescent components of the PE, PP, and PVC groups on the 30th and 50th days. The C6 was found in the PE MPs group on day 30, with a fluorescence position similar to that of rhodamine B [64]. This material was probably a symmetrical chain scission product of PE MPs, which biodegraded and disappeared by the end of the incubation period. C1 is a common soil humus-excited fluorescent component [66], and its intensity increased with time in multiple groups, especially the low-dose PE and PP groups. The fluorescence intensity of unique C7 in the PP group decreased over time, indicating that it may be a PP-derived intermediate. The PVC group had a higher intensity of easily biodegradable Protein/Phenol-like substances (C2, C3, C4, and C5) compared to the PE and PP groups, which was consistent with the increased methane emissions. On the 50th day, the intensity of aromatic humus (C8)

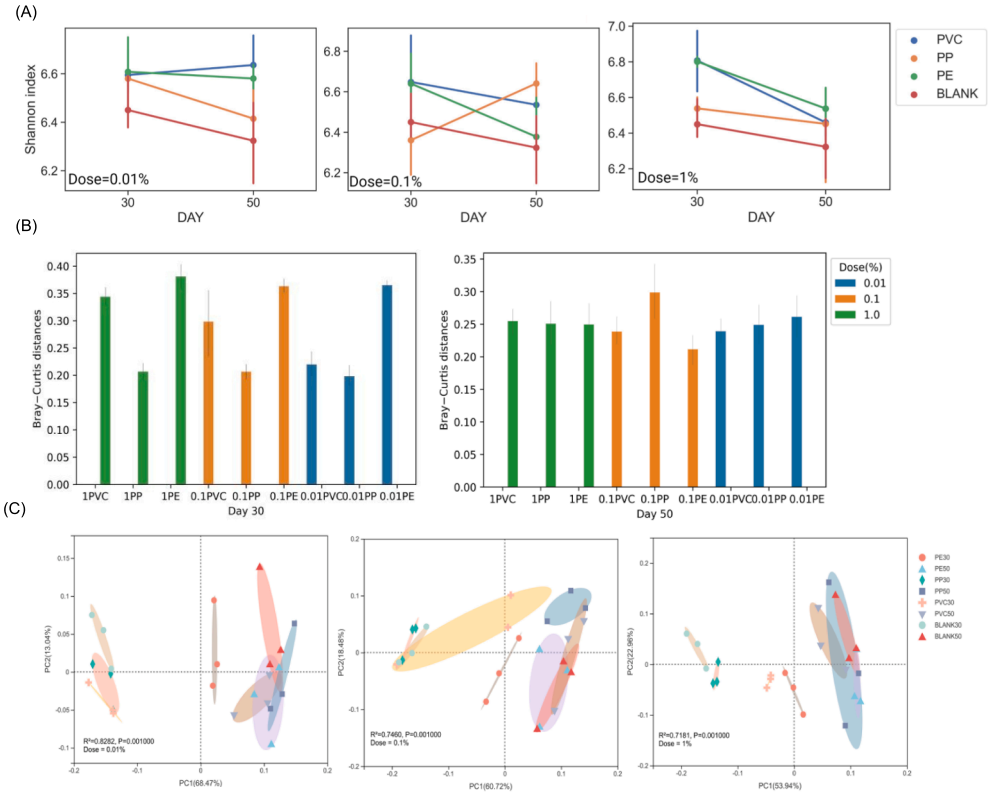

Fig. 3. (A) Alpha diversity variation trend of paddy soil communities with various typical MPs treatments under different mass ratios, indexed by Shannon index. (B) Beta diversity of bacterial communities in paddy soils treated with different MPs. (C) Bray-Curtis distance for each treatment relative to blank at the mid and late-term. PCoA analysis based on weighted UniFrac distances for different MPs treatments (p = 0.001 in adonis test for all three mass ratios).

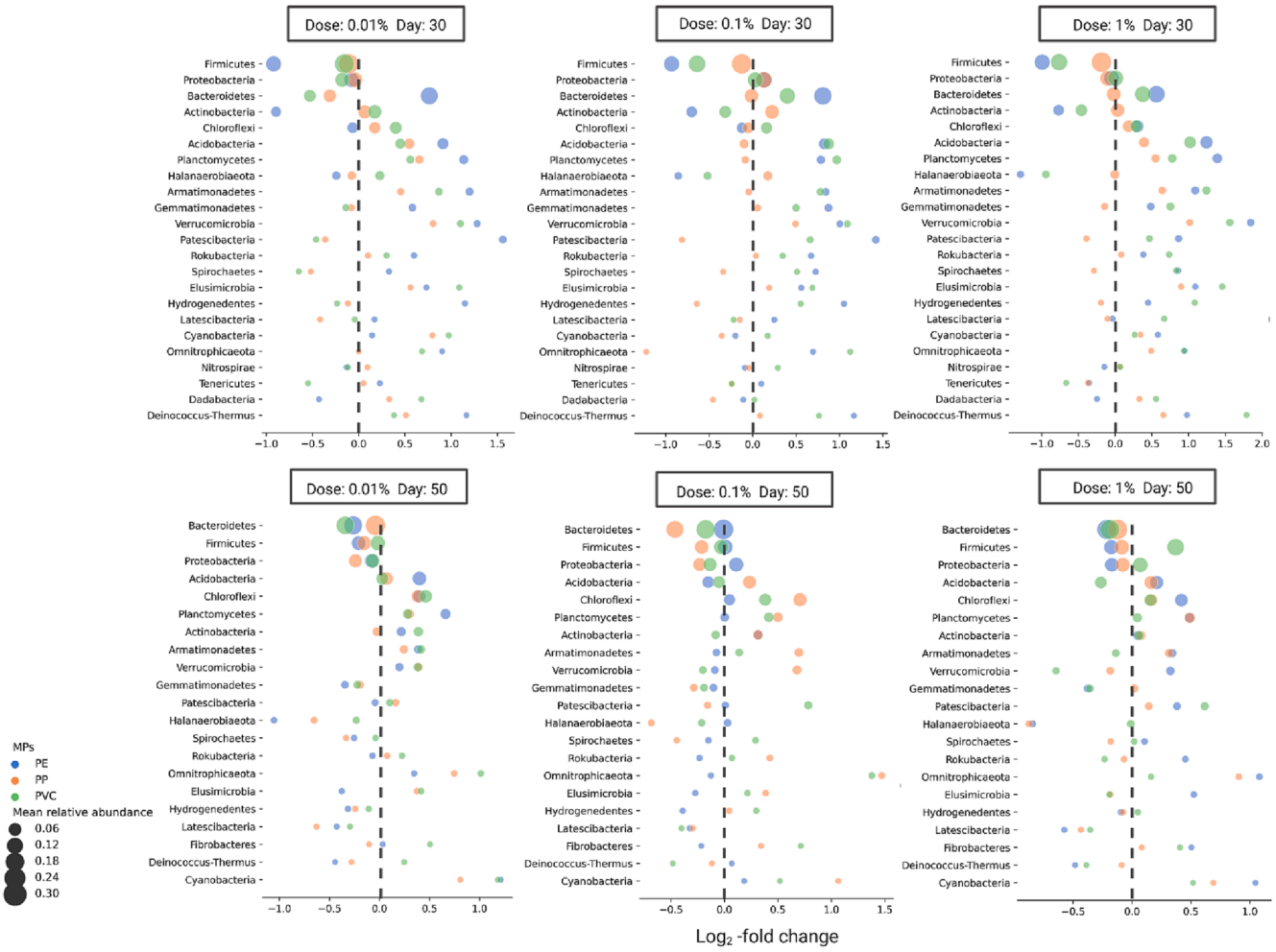

Fig. 4. The relative abundance changes of the main phyla in each treatment relative to the blank control under different mass ratios on day 30 and day50.

increased while the Protein/Phenol-like substances decreased, further supporting the biodegradability of these compounds. RF analysis (Fig. S1B) also verified that C4, C8, C1, and C2 were the main fluorescent organic indicators affecting methane emissions.

The DOC fluorescence intensity of the PP groups on the 30th day of exposure was significantly positively correlated with the dosage (P less than 0.01), while the fluorescence intensity of these group on the 50th day tended to be similar. Meantime, C1 accumulation was observed at 1% and 0.01% doses. For PVC MPs, the 0.01% dose resulted in the highest intensity at day 30, but the 1% dose exerted the highest intensity at day 50, and the intensity of C8 increased significantly. For PE MPs groups, the 1% dose resulted in the highest fluorescence intensity on day 30, and low doses (0.01% and 0.1%) of PE significantly promoted the accumulation of C1 after 50 days of incubation. It can be observed that lower doses of PP and PE resulted in significant accumulation of humic acids like, while all PVC treatments led to the accumulation of fulvic acids like. Both types of DOC typically exhibit high-molecular-weight complex structures and are difficult to degrade [67]. Generally, in the process of organic matter degradation, unstable components of DOC, such as carbohydrates, undergo degradation at an earlier stage, while refractory DOC components, such as high-molecular-weight tannins, accumulated. Over time, these refractory components transform into soil humus [52], contributing to the buildup of stable organic matter in the soil. This may partially explain the observed accumulation of C1 and C8 in this study.

It is worth noting that the inhibitory effect of humic substances on anaerobic wetland methanogenesis has been extensively documented [68,69]. Quinone groups in humic substances can act as terminal electron acceptors (TEAs), shifting the metabolic pathways of some methanogenic archaea towards the reduction of organic substrates, rather than methanogenesis. Gibbs free energy calculations (Table S1) also suggestted that the reduction of quinones coupled with organic compounds was more feasible than the methanogenesis process [70,71]. It can be seen that although all of the MPs released intermediates, the accumulation of humic substances likely resulted in a shift away from methanogenesis as the dominant metabolic pathway. In short, the alterations in stable and labile carbon substrates may play a pivotal role in shaping microbial community dynamics and functions, subsequently influencing the microplastic-mediated organic carbon cycling processes in paddy soil. Therefore, conducting a microbial analysis to investigate community composition and metabolic function is essential.

3.4. *Effect of MPs on soil microbial community diversity*

Fig. 3A illustrates the microbial diversity under different treatments. The alpha diversity of the PE and PVC groups was significantly higher than that of the Blank group and decreased over time at 0.1% and 1% doses. At the 0.01% dose, the alpha diversity in the PVC group increased over time, while the change in the PE group was not significant. Pearson correlation analysis revealed a significant negative correlation between the Shannon index and incubation duration for PVC and PE at the 1% dose ($r = -0.844$, $p = 0.035$; $r = -0.878$, $p = 0.021$). For PP MPs, the 0.1% dose induced significantly higher alpha diversity at day 50 than at day 30, while at the other two doses, the Shannon index decreased over time

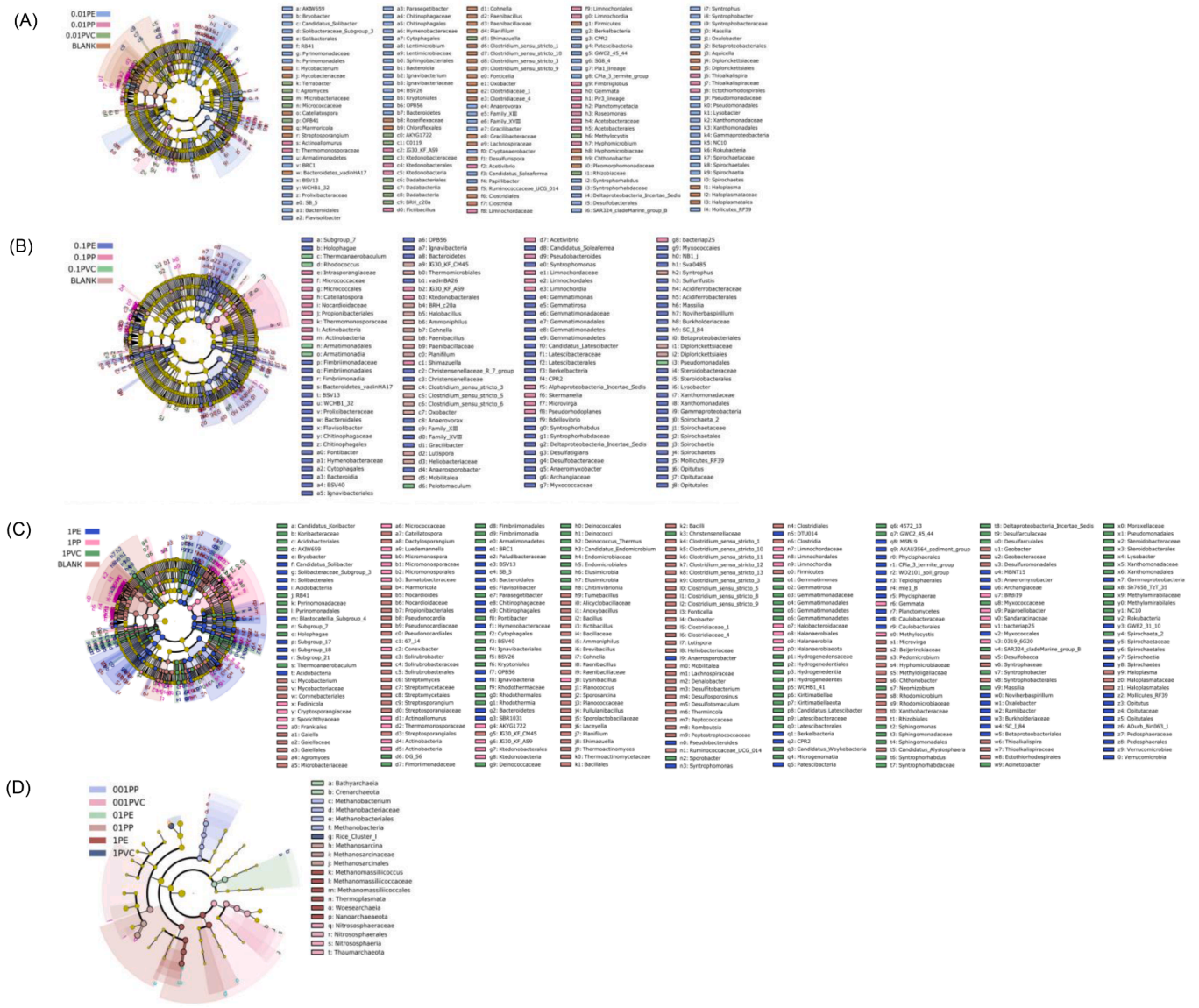

Fig. 5. Microbial members with significant relative abundance differences under (A) 0.01%, (B) 0.1% and (C) 1% MPs treatment after 30 days of incubation. (D) Archaeal members with significant relative abundance differences under various treatments incubated for 30 days. All labeled taxa are listed on the right of the figures. All marker members identified by LDA can be found in Table S3.

and was generally lower than that of PVC and PE. Furthermore, Pearson correlation analysis showed that the soil microbial diversity of these three types of MPs did not depend on the dosage ($p = 0.644$). The Bray – Curtis distance of each group relative to the Blank were calculated to compare the similarity of soil bacterial community composition between different groups (Fig. 3B). On day 30, the impact of PE on soil bacterial communities was the most significant, while the effect of PP was the weakest, regardless of the dose. On day 50, the impact of the three types of MPs on soil bacterial communities became more similar, except for PP, which had the strongest effect on soil bacterial communities at the 0.1% dose, consistent with its highest alpha diversity on day 50 (Fig. 3A). PCoA analysis for communities under each condition for mid-term and late-term is shown in Fig. 3C. The samples of the 30th and 50th days were significantly separated at different doses, and more overlaps have been observed between groups at day 50. PERMANOVA examination was consistent with the PCoA, indicating that different types of MPs led to significant differences in community diversity among groups ($p = 0.001$ for all doses). Additionally, the analysis showed that for these three types of MPs, dosage was not the main factor driving changes in the community diversity (PVC: $P = 0.402$, PP: $P = 0.95$, PE: $P = 0.167$).

Previous studies have reported significant differences in the overall bacterial community diversity of sediment in response to different MPs treatments [72]. These differences have been attributed to variations in soil characteristics (such as soil organic carbon content, texture, pH, and bacterial community composition) and microplastic properties (degradability, concentration, and morphology) [73]. In this study, the PE MPs consistently displayed the greatest separation on the PCoA plot at Day 30, regardless of the dosage. Zhao and colleagues also reported that PE MPs can enhance soil microaggregates and significantly reduce soil bulk density and stability of soil water aggregates, thereby influencing soil community structure [74]. Conversely, despite the three thermoplastic MPs used in the experiment sharing C-C backbones, PP possesses a methyl side chain that confers increased resistance to aerobic biodegradation. The presence of tertiary carbon in PP reduces its susceptibility to microbial degradation [75]. PVC exhibits notable resistance to biodegradation, primarily due to halogens, particularly chlorine, which enhance its resistance to aerobic biodegradation [76]. Furthermore, soil organic carbon is also influenced by microplastics,

thereby impacting community structure. For instance, PVC is typically supplemented with phthalates [77], which easily leach from the polymer structure and lead to the enrichment of certain functional communities. In this study, PVC MP treatments exhibited more diverse DOC structures compared to other MPs at Day 30, as evidenced by EEM analysis. Among them, C2, C3, C4, and C5 represent protein-like structures with degradable properties. The presence of C6 exclusively in PE may contribute to its greatest separation at Day 30. On the other hand, it is noteworthy that the different MPs had varying effects on the accumulation of humus, and the rate of humus decomposition played a crucial role in soil nutrient cycling [52]. Therefore, we extracted the typical humus component, C1, from the fluorescence results and performed correlation analysis with the Shannon Index and Bray-Curtis distance. It was found that the C1 content was negatively correlated with soil alpha diversity on the 30th day ($R = -0.783$, $P = 0.013$), which indicated that the increased humus component probably inhibited the growth of some microorganisms. Although community diversity appeared time-dependent (with most of the variations recovered on long-term scales), MPs would cause interspecific competition in specific communities in the soil, with further top-down effects on nutrient cycling [78]. Therefore, we focused on some notably affected taxa from the phylum to the genus level caused by various MPs in the following.

3.5. Effect of MPs on microbial community compositions at the phylum level

The changes of phyla relative abundance were calculated for every group relative to the blank control to better present the effects of different MPs on community composition (Fig. 4). After 50 days of incubation, all the three MPs determined an increase in the relative abundance of *Chloroflexi*, *Planctomycetes*, and *Patescibacteria* regardless of the dose levels. Comparing the abundance of the phyla on day 30 and day 50. Pearson correlation analysis showed that, after 50 days, the dose of PVC MPs was positively correlated with the abundance of *Proteobacteria*, *Firmicutes* ($r = 0.420$, $p = 0.029$; $r = 0.571$, $p = 0.002$). Meanwhile, an increase in the dose of PP MPs positively correlated with the relative abundance of *Gemmatimonadetes* ($r = 0.416$, $p = 0.031$). A higher dose of PE also demonstrated a growth-enhancing effect on *Omnitrophicaeota* and *Elusimicrobia* ($r = 0.695$, $p = 0.001$; $r = 0.657$, $p = 0.000$). RF analysis was used to identify the main genetic indicators of microbial response to the methane emission (Fig. S1C). Of all the phyla evaluated, *Halanaerobiaeota* was found to have the strongest effect on methane emission, followed by *Spirochaetes*, *Omnitrophicaeota*, *Elusimicrobia*, and *Proteobacteria*. This *Halanaerobiaeota* phylum has been previously identified as a type of anaerobic fermentative bacteria [79], The growth of *Halanaerobiaeota* is known to be strongly influenced by salt content, and its abundance changes are closely tied to nitrogen and ammonium metabolism in the system [80]. Therefore, the decreased relative abundance of *Halanaerobiaeota* in the PE and PP MPs groups may be attributed to the enhanced anammox reaction.

Omnitrophicaeota is known to thrive in anoxic environments and compete with methanogens for substrates such as formate or H_2 [81]. The observed negative correlation between *Omnitrophicaeota* and PVC dosage, as well as the positive correlation between *Omnitrophicaeota* and PE dosage, suggests that as PVC dosage increases. Methanogens have a competitive advantage in methane production. Conversely, with increasing PE dosage, *Omnitrophicaeota* may have a competitive advantage. These differences in microbial competition may contribute to the observed differences in methane emissions between the PVC and PE MPs groups. In anaerobic soil systems, there was not only methanogenesis but also denitrification and anammox processes. This study found that PE or PP enriched *Elusimicrobia*, *Gemmatimonadetes*, and *Planctomycetes*, which are involved in the nitrogen cycle process [82,83]. The nitrous oxide reductase gene (nosZ) associated with *Gemmatimonadetes*, for instance, is thought to be able to decrease N_2O in anaerobic environments [84], whereas anammox *Planctomycetes* play a significant part in the global nitrogen cycle by releasing fixed nitrogen back to the atmosphere as N_2 [85]. As a result of the enrichment of these heterotrophic denitrifying bacteria and anammox bacteria, the organic pollutants of the system would be consumed [86]; these bacteria then compete with methanogens for substrates, reducing methane emissions. Therefore, the difference in methane emissions between PVC and PP, and PE MPs cannot be solely attributed to the amount of carbon substrates released, but also to the differential growth of competing bacteria.

3.6. Effect of MPs at low taxonomic levels

The results of the LEfSe analysis are depicted in Fig. 5, highlighting the impact of different MPs on microbial community composition from phylum to genus. At the 0.01% dose (Fig. 5A), the classes *Bacteroidia*, *Spirochaetia*, *Berkelbacteria*, and *Gammaproteobacteria* were significantly enriched in the PE MPs groups, while the classes *Ktedonbaceria*, *Planctomycetacia*, and *Limnochordia* showed a noticeable enrichment in the PP MPs groups. Furthermore, the genera *Terrabacter*, *Agromyces*, *Shimazuella*, *Methylocystis*, and *Rhizobiaceae* were significantly enriched in the PVC MPs groups. Furthermore, at this dose, the PE MPs exhibited the highest number of significantly enriched taxa compared to the other two MPs. As the dose increased, most of the taxa that were enriched at lower doses continued to be specifically enriched by PP and PE MPs (as shown in Fig. 5B and 5C). Unlike the PE and PP MPs, there was a lower degree of overlap in the taxa that were enriched by different doses of PVC MPs. As compared to the 0.01% and 0.1% doses, the 1% PVC dose led to a significantly greater enrichment of taxa, such as the *Elusimicrobia* and *Holophagae* classes, *Acidobacteriales* order, and *Pedosphaeraceae*, *Christensenellaceae*, *Koribacteraceae* families, as well as the *Gemmatimonas* genus. Notably, *Spirochaetia*, significantly enriched in the PE group, has been reported to be positively correlated with the degradation of polycyclic aromatic hydrocarbons (PAHs) and phthalates [87]. *Terrabacter* and *Agromyces*, enriched by PVC MPs, have been reported to be closely associated with phthalate degradation [88,89]. The enrichment of *Methylocystis*, which fixes formaldehyde to cellular carbon via the serine pathway [90], is unexpected and suggests the possibility of anaerobic methane oxidation in our reactors. Given that PVC has a more complex haloalkane structure and different chemical additives than PE and PP [91], it is reasonable that PVC MPs have significantly different enriched taxa.

Rice Cluster I is a unique type of methanogen that has been reported to possess enzymatic capabilities for carbohydrate metabolism and assimilatory sulfate reduction, as well as an aerotolerant, H_2/CO_2-dependent lifestyle. This unique set of traits gives *Rice Cluster I* a selective advantage over other methanogens in its habitat, which may explain its prevalence in the rice rhizosphere [92]. The substantial enrichment of *Rice Cluster I* in the PVC groups (Fig. 5D) suggests that its presence is closely related to the observed increase in methane production in that group, while the corresponding PE and PP groups did not show such enrichment. Although the PP and PE MPs did not have a significant impact on cumulative methane production, they also lead to the enrichment of some other specific methanogenic archaeal during the incubation period. For instance, on day 30, Class *Methanomassiliicoccus* was significantly enriched by 1% PE, while *Methanobacterium* and *Methanosarcina* were enriched by 0.01% PP and 0.1% PP, respectively. Notably, these microorganisms have been shown to use redox organics as TEAs [71,93]. Given that these notable species suggest the possibility of altered anaerobic metabolic pathways, we focused on the enzymes and pathways associated with anaerobic respiration that may be affected by MPs in the next section.

Figure S3 illustrates the differential taxa of the communities after a 50-day exposure. Succession in soil community composition over time was observed, and on day 50, most of the enriched members recovered regardless of dose, but some unique species remained enriched. Specifically, at the 0.01% dose, *Halianglum* was enriched by PE,

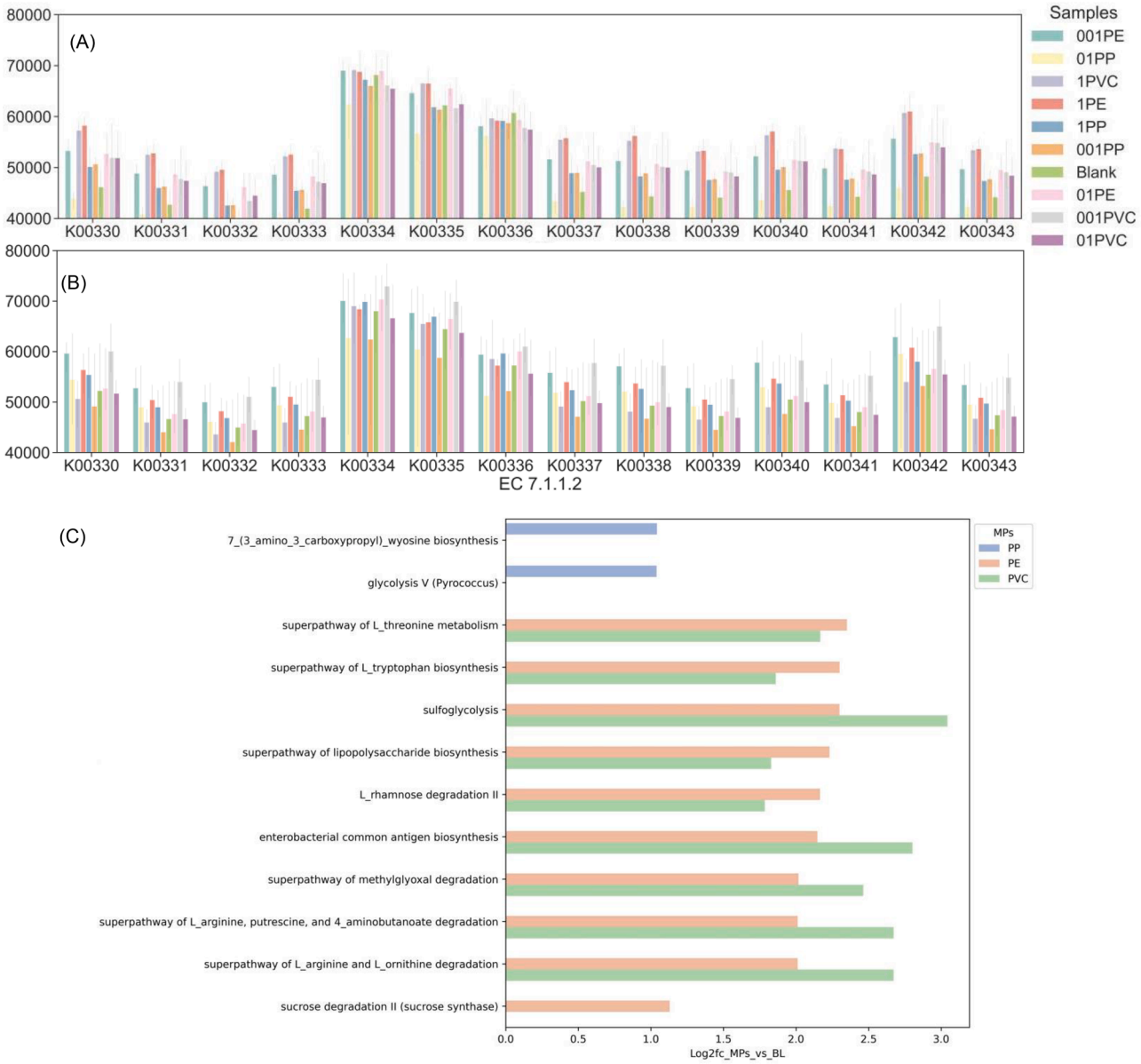

Fig. 6. Differences in gene copy numbers relating to quinone reductase (EC 7.1.1.2) among all groups. (A) Day 30 and.(B) Day 50. The Y-axis represents the normalized relative abundance of genes shown as 16S rRNA gene copy number. X-axis corresponds to KEGG homology IDs of genes encoding EC 7.1.1.2. (C) Identified and significantly enhanced pathways by different MPs (log2FC > 1, P less than 0.05).

Ruminococcaceae_UCG_010 was improved by PP, while *Mobilitalea*, *Thermincola*, and *Ruminococcaceae_UCG_014* were enriched by PVC. At a 0.1% dose, *Noviherbaspirillum* was enriched by PE, *Omnitrophaceae* by PP, while *Hydrogenedensaceae* and *Syntrophus* were enriched by PVC. As the dosage increased, it was observed that the presence of 1% of PVC led to a greater diversity of enriched taxa. Notably, this included the emergence of *Dehalogenimonas*, *Anoxybacillus*, *Ammoniphilus*, *Microvirga*, *Syntrophomonas*, and two species of *Clostridium*. At this point, *Methanomassiliicoccus* was the only methanogenic archaeon that was significantly enriched within the 0.01% PE MPs. *Dehalogenimonas* genus are known for their ability to couple growth with reductive dehalogenation of a variety of polychlorinated alkanes [94], and the enrichment of this genus in the PVC group after 50 days suggested the potential for dechlorination of PVC MPs. *Anoxybacillus*, *Microvirga* and *Ammoniphilus* use hydrolytic enzymes and metabolites to break down hydrocarbons, allowing them to grow on different plastic polymers and degrade high molecular weight compounds [95,96]. Moreover, *Syntrophomonas* can help oxidize benzene by releasing electrons to electron acceptors like *Desulfobulbaceae*, humic acids, and methanogens, and also promoted methane emissions by aiding in carbon dioxide reduction [97].

3.7. Effect of MPs on anaerobic metabolic pathways

The overall changes in soil functional profiles induced by different MPs were annotated to explore the impacts on anaerobic rice paddy soil metabolism. Fig. 6A and 6B show that the relative abundance of genes encoding ubiquinone reductase (EC 7.1.1.2) was elevated compared to the blank group, particularly in the 1% PE and 1% PVC groups, at day 30. Additionally, the relative abundance of genes encoding quinone oxidoreductase EC 7.1.1.2 was increased in the MP groups relative to the blank group, suggesting the presence of quinones as electron acceptors in the environment for the reduction of some universal substrates.

Considering that a total of 54 different samples were involved in this study, we selected the groups with the highest number of significant different taxa for metabolic pathway reconstruction (1% dose at 30 days). The MetaCyc database was used to examine the metabolic

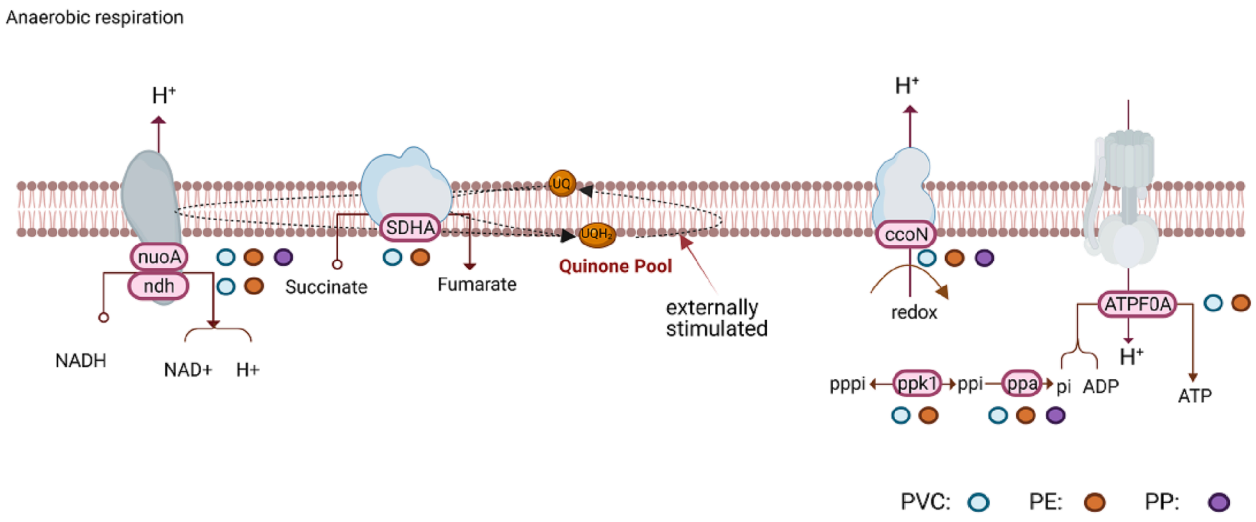

Fig. 7. Identified and upregulated genes involved in oxidative phosphorylation mapped over generic pathways induced by different MPs. The green, red and purple dots indicate PVC, PE, and PP treatments, respectively. All relevant genes used for metabolic reconstruction can be found in Table S4. (For interpretation of the references to colour in this figure legend, the reader is referred to the web version of this article.)

pathways that were significantly improved in the different groups [98] (Fig. 6C, Table S2). Notably, the groups treated with PE and PVC demonstrated significant enhancements in multiple pathways associated with amino acid metabolism, which exhibited a consistent correlation with the observed elevation in quinone reductase activity. The pathway belonging to the metabolism of glycine to pyruvate was significantly enhanced in the PE and PVC MPs groups (Fig. S4), and the enhancement of glycine dehydrogenase (EC:1.4.4.2) in this system also indicated that glycine may act as the terminal hydrogen receptor of anaerobic respiration. Furthermore, the carbon fixation pathway of pyruvate was also enhanced in PE and PVC MPs groups, which suggested the presence of CO_2 in our experimental system. In summary, a pathway derived from the reduction of glycine into pyruvate and further into carbon fixation was enhanced by PE and PVC MPs. The changes in oxidative phosphorylation (map00190) under anaerobic conditions were also examined in this study. As shown in Fig. 7, PE and PVC MPs enhanced the complete oxidative phosphorylation pathway, which is the last step energy-producing reaction of anaerobic respiration [99]. This upregulated oxidative phosphorylation further verified the existence of anaerobic respiration with inorganic or organic matter as terminal hydrogen acceptors in the MPs-contaminated paddy soil system.

In short, the anaerobic oxidation pathway, which involves amino acids as H + acceptors and quinone-like substances as electron acceptors, was enhanced by PVC and PE MPs. The balance between this quinone reduction pathway and the methane production activities ultimately determined the observed methane emissions. Considering the substantial increase in unstable organic carbon substrates and the significant enrichment of methanogens archaea of *Rice Cluster I* in the PVC groups, the methane production activity in these PVC groups surpassed quinone oxidation activity, leading to an overall promotion of methane emissions. In contrast, the PP and PE MPs groups exhibited a limited availability of utilizable carbon sources, and the carbon substrates of methane-producing archaea were depleted by various competing bacterial groups. Furthermore, it is noteworthy that the presence of abundant quinone-like humic substances in the MPs-contaminated soils has the potential to convert CH_4 into CO_2, thereby resulting in no overall increase in methane production levels in the PE and PP MPs group. However, the precise influence of humic acids on anaerobic pathways in soil remains inadequately elucidated and lacks consensus, warranting further experimental investigations to validate these findings.

4. Conclusion

The results of this study compared the effects of different types and doses of thermoplastic MPs on soil DOC, microbial community structure, and metabolic pathways. The type of MPs played a key role in shaping the response of soil bacterial communities to exposure, with PVC MPs being the most significant contributor to cumulative methane emissions. Additionally, humic substances were accumulated in all three MPs groups, and PVC MPs resulted in the most diverse DOC composition. On day 30, PE MPs had a stronger impact on paddy soil bacterial community composition than PVC and PP MPs, which is closely related to the chemical structure of the plastics themselves. Additionally, the type of MPs was more decisive than the dose of MPs. The respective enrichment of competing species and *Rice Cluster I* in the PE, PP, and PVC groups could partly explain the differences in methane emissions of these groups. More importantly, higher levels of quinone reductase in the PE and PVC groups enhanced the complete oxidative phosphorylation pathway, revealing the potential methane oxidation process with humic acid as an electron acceptor. Thus, this work has significant implications for future efforts to reduce the farmland additional methane emission brought by MPs.

Declaration of Competing Interest

The authors declare that they have no known competing financial interests or personal relationships that could have appeared to influence the work reported in this paper.

Data availability

The data that has been used is confidential.

Acknowledgments

This work was supported by the National Natural Science Foundation of China (No. 52270151), National Key Research and Development Program: Key Projects of International Scientific and Technological Innovation Cooperation Between Governments (2022YFE0120600), Natural Science Foundation of Shanghai (No. 22ZR1401700) and China Scholarship Council (No. 202008310162).

Appendix A. Supplementary data

Supplementary data to this article can be found online at https://doi.org/10.1016/j.cej.2023.144003.

References

[1] K.L. Law, R.C. Thompson, Microplastics in the seas, Science 345 (6193) (2014) 144–145.
[2] M. Padervand, E. Lichtfouse, D. Robert, C. Wang, Removal of microplastics from the environment. A review, Environ. Chem. Lett. 18 (3) (2020) 807–828.
[3] V.N. de Ruijter, P.E. Redondo-Hasselerharm, T. Gouin, A.A. Koelmans, Quality criteria for microplastic effect studies in the context of risk assessment: a critical review, Environ. Sci. Tech. 54 (19) (2020) 11692–11705.
[4] M.C. Rillig, R. Ingraffia, A.A. de Souza Machado, Microplastic incorporation into soil in agroecosystems, Frontiers, Plant Sci. 8 (2017) 1805.
[5] M. Kumar, X. Xiong, M. He, D.C. Tsang, J. Gupta, E. Khan, S. Harrad, D. Hou, Y. S. Ok, N.S. Bolan, Microplastics as pollutants in agricultural soils, Environ. Pollut. 265 (2020), 114980.
[6] J.P. da Costa, A. Paço, P.S. Santos, A.C. Duarte, T. Rocha-Santos, Microplastics in soils: assessment, analytics and risks, Environ. Chem. 16 (2018) 18–30.
[7] Q. Wang, X. Feng, Y. Liu, W. Cui, Y. Sun, S. Zhang, F. Wang, Effects of microplastics and carbon nanotubes on soil geochemical properties and bacterial communities, J. Hazard. Mater. 433 (2022), 128826.
[8] M.C. Rillig, E. Leifheit, J. Lehmann, Microplastic effects on carbon cycling processes in soils, PLoS Biol. 19 (3) (2021) e3001130.
[9] N. Khalid, M. Aqeel, A. Noman, Z. Fatima Rizvi, Impact of plastic mulching as a major source of microplastics in agroecosystems, J. Hazard. Mater. 445 (2023) 130455.
[10] F. Wang, Q. Wang, C.A. Adams, Y. Sun, S. Zhang, Effects of microplastics on soil properties: current knowledge and future perspectives, J. Hazard. Mater. 424 (2022), 127531.
[11] Y. Yu, X. Li, Z. Feng, M. Xiao, T. Ge, Y. Li, H. Yao, Polyethylene microplastics alter the microbial functional gene abundances and increase nitrous oxide emissions from paddy soils, J. Hazard. Mater. 432 (2022), 128721.
[12] Z. Zhang, Z. Yang, H. Yue, M. Xiao, T. Ge, Y. Li, Y. Yu, H. Yao, Discrepant impact of polyethylene microplastics on methane emissions from different paddy soils, Appl. Soil Ecol. 181 (2023), 104650.
[13] L. Han, B. Zhang, D. Li, L. Chen, Y. Feng, L. Xue, J. He, Y. Feng, Co-occurrence of microplastics and hydrochar stimulated the methane emission but suppressed nitrous oxide emission from a rice paddy soil, J. Clean. Prod. 337 (2022) 130504.
[14] J. Wang, M. Huang, Q. Wang, Y. Sun, Y. Zhao, Y. Huang, LDPE microplastics significantly alter the temporal turnover of soil microbial communities, Sci. Total Environ. 726 (2020), 138682.
[15] H. Zang, J. Zhou, M.R. Marshall, D.R. Chadwick, Y. Wen, D.L. Jones, Microplastics in the agroecosystem: are they an emerging threat to the plant-soil system? Soil Biol. Biochem. 148 (2020), 107926.
[16] C. Wu, Y. Ma, D. Wang, Y. Shan, X. Song, H. Hu, X. Ren, X. Ma, J. Cui, Y. Ma, Integrated microbiology and metabolomics analysis reveal plastic mulch film residue affects soil microorganisms and their metabolic functions, J. Hazard. Mater. 423 (2022), 127258.
[17] M. Xiao, Y. Luo, H. Zhang, Y. Yu, H. Yao, Z. Zhu, D.R. Chadwick, D. Jones, J. Chen, T. Ge, Microplastics shape microbial communities affecting soil organic matter decomposition in paddy soil, J. Hazard. Mater. 431 (2022), 128589.
[18] S.-K. Kim, J.-S. Kim, H. Lee, H.-J. Lee, Abundance and characteristics of microplastics in soils with different agricultural practices: Importance of sources with internal origin and environmental fate, J. Hazard. Mater. 403 (2021), 123997.
[19] H.A. Maddah, Polypropylene as a promising plastic: A review, Am. J. Polym. Sci 6 (2016) 1–11.
[20] P. Visakh, R.N. Darie-Nita, Polyvinylchloride (PVC)-Based Blends: State of Art, New Challenges and Opportunities, Polyvinylchloride-based Blends: Preparation, Characteriz. Appl. (2022) 1–17.
[21] J. Hou, X. Xu, H. Yu, B. Xi, W. Tan, Comparing the long-term responses of soil microbial structures and diversities to polyethylene microplastics in different aggregate fractions, Environ. Int. 149 (2021), 106398.
[22] J. Zhou, H. Gui, C.C. Banfield, Y. Wen, H. Zang, M.A. Dippold, A. Charlton, D. L. Jones, The microplastisphere: Biodegradable microplastics addition alters soil microbial community structure and function, Soil Biol. Biochem. 156 (2021), 108211.
[23] A.D. Servin, J.C. White, Nanotechnology in agriculture: next steps for understanding engineered nanoparticle exposure and risk, NanoImpact 1 (2016) 9–12.
[24] M. Chen, S. Zhou, Y. Zhu, Y. Sun, G. Zeng, C. Yang, P. Xu, M. Yan, Z. Liu, W. Zhang, Toxicity of carbon nanomaterials to plants, animals and microbes: Recent progress from 2015-present, Chemosphere 206 (2018) 255–264.
[25] S. Rahmatpour, M. Shirvani, M.R. Mosaddeghi, F. Nourbakhsh, M. Bazarganipour, Dose–response effects of silver nanoparticles and silver nitrate on microbial and enzyme activities in calcareous soils, Geoderma 285 (2017) 313–322.
[26] C. Xu, C. Peng, L. Sun, S. Zhang, H. Huang, Y. Chen, J. Shi, Distinctive effects of TiO2 and CuO nanoparticles on soil microbes and their community structures in flooded paddy soil, Soil Biol. Biochem. 86 (2015) 24–33.
[27] O. Khan, M.B.K. Niazi, G.A. Shah, A. Hazafa, Z. Jahan, M. Sadiq, F. Sher, Green synthesis and evaluation of calcium-based nanocomposites fertilizers: A way forward to sustainable agricultural, Journal of the Saudi Society of, Agric. Sci. 20 (2021) 519–529.
[28] U. Khalid, F. Sher, S. Noreen, E.C. Lima, T. Rasheed, S. Sehar, R. Amami, Comparative effects of conventional and nano-enabled fertilizers on morphological and physiological attributes of Caesalpinia bonducella plants, Journal of the Saudi Society of, Agric. Sci. 21 (2022) 61–72.
[29] B. Beig, M.B.K. Niazi, F. Sher, Z. Jahan, U.S. Malik, M.D. Khan, J.H.P. Américo-Pinheiro, D.-V. Vo, Nanotechnology-based controlled release of sustainable fertilizers, A review, Environmental Chemistry Letters 20 (4) (2022) 2709–2726.
[30] F. Wu, Y. You, X. Zhang, H. Zhang, W. Chen, Y.u. Yang, D. Werner, S. Tao, X. Wang, Effects of various carbon nanotubes on soil bacterial community composition and structure, Environ. Sci. Tech. 53 (10) (2019) 5707–5716.
[31] T. Rashid, S.A.A. Taqvi, F. Sher, S. Rubab, M. Thanabalan, M. Bilal, B. ul Islam, Enhanced lignin extraction and optimisation from oil palm biomass using neural network modelling, Fuel 293 (2021), 120485.
[32] C. Yin, S. Qiu, S. Zhang, F. Sher, H. Zhang, J. Xu, L. Wen, Strength degradation mechanism of iron coke prepared by mixed coal and Fe2O3, J. Anal. Appl. Pyrol. 150 (2020), 104897.
[33] S. Cai, S. Zhang, Y. Wei, F. Sher, L. Wen, J. Xu, J. Dang, L. Hu, A novel method for removing organic sulfur from high-sulfur coal: Migration of organic sulfur during microwave treatment with NaOH-H2O2, Fuel 289 (2021), 119800.
[34] H.J. Johnston, G.R. Hutchison, F.M. Christensen, S. Peters, S. Hankin, K. Aschberger, V. Stone, A critical review of the biological mechanisms underlying the in vivo and in vitro toxicity of carbon nanotubes: The contribution of physico-chemical characteristics, Nanotoxicology 4 (2010) 207–246.
[35] Y. Zhang, W. Hou, M. Chi, Y. Sun, J. An, N. Yu, H. Zou, Simulating the effects of soil temperature and soil moisture on CO2 and CH4 emissions in rice straw-enriched paddy soil, Catena 194 (2020), 104677.
[36] M. Usman, Z. Shi, M. Ji, S. Ren, G. Luo, S. Zhang, Microbial insights towards understanding the role of hydrochar in alleviating ammonia inhibition during anaerobic digestion, Chem. Eng. J. 419 (2021), 129541.
[37] Y. Zhang, X. Li, M. Xiao, Z. Feng, Y. Yu, H. Yao, Effects of microplastics on soil carbon dioxide emissions and the microbial functional genes involved in organic carbon decomposition in agricultural soil, Sci. Total Environ. 806 (2022), 150714.
[38] C. Stedmon, R. Bro, Characterizing Dissolved Organic Matter Fluorescence with Parallel Factor Analysis: A Tutorial, Limnol. Oceanogr. 6 (2008) 572–579.
[39] J.A. Peiffer, A. Spor, O. Koren, Z. Jin, S.G. Tringe, J.L. Dangl, E.S. Buckler, R.E. Ley, Diversity and heritability of the maize rhizosphere microbiome under field conditions, Proceedings of the National Academy of Sciences 110 (2013) 6548.
[40] M. Ji, W. Sang, D.C. Tsang, M. Usman, S. Zhang, G. Luo, Molecular and microbial insights towards understanding the effects of hydrochar on methane emission from paddy soil, Sci. Total Environ. 714 (2020), 136769.
[41] N. Segata, J. Izard, L. Waldron, D. Gevers, L. Miropolsky, W.S. Garrett, C. Huttenhower, Metagenomic biomarker discovery and explanation, Genome Biol. 12 (6) (2011) R60.
[42] G.M. Douglas, V.J. Maffei, J.R. Zaneveld, S.N. Yurgel, J.R. Brown, C.M. Taylor, C. Huttenhower, M.G.I. Langille, PICRUSt2 for prediction of metagenome functions, Nat. Biotechnol. 38 (6) (2020) 685–688.
[43] B. Iooss, P. Lemaître, A review on global sensitivity analysis methods, Uncertainty management in simulation-optimization of complex systems: algorithms and applications (2015) 101-122.
[44] A. Antoniadis, S. Lambert-Lacroix, J.-M. Poggi, Random forests for global sensitivity analysis: A selective review, Reliab. Eng. Syst. Saf. 206 (2021), 107312.
[45] S. Seabold, J. Perktold, Statsmodels: Econometric and statistical modeling with python, Proceedings of the 9th Python in Science Conference, Austin, TX, 2010, pp. 10-25080.
[46] F. Pedregosa, G. Varoquaux, A. Gramfort, V. Michel, B. Thirion, O. Grisel, M. Blondel, P. Prettenhofer, R. Weiss, V. Dubourg, Scikit-learn: Machine learning in Python, the Journal of machine Learning research 12 (2011) 2825–2830.
[47] L. Han, L. Chen, D. Li, Y. Ji, Y. Feng, Y. Feng, Z. Yang, Influence of polyethylene terephthalate microplastic and biochar co-existence on paddy soil bacterial community structure and greenhouse gas emission, Environ. Pollut. 292 (2022), 118386.
[48] J. Ru, Y. Huo, Y. Yang, Microbial degradation and valorization of plastic wastes, Front. Microbiol. 11 (2020) 442.
[49] K. Ibrahimi, K.B. Attia, R. Amami, J.H.P. Américo-Pinheiro, F. Sher, Assessment of three decades treated wastewater impact on soil quality in semi-arid agroecosystem, Journal of the Saudi Society of, Agric. Sci. 21 (2022) 525–535.
[50] R. Amami, K. Ibrahimi, F. Sher, P.J. Milham, D. Khriji, H.A. Annabi, K. Abrougui, S. Chehaibi, R. Dalal, Effects of conservation and standard tillage on soil physico-chemical properties and overall quality in a semi-arid agrosystem, Soil Res. 60 (6) (2021) 485–496.
[51] H. Yu, P. Fan, J. Hou, Q. Dang, D. Cui, B. Xi, W. Tan, Inhibitory effect of microplastics on soil extracellular enzymatic activities by changing soil properties and direct adsorption: An investigation at the aggregate-fraction level, Environ. Pollut. 267 (2020), 115544.
[52] H. Liu, X. Yang, G. Liu, C. Liang, S. Xue, H. Chen, C.J. Ritsema, V. Geissen, Response of soil dissolved organic matter to microplastic addition in Chinese loess soil, Chemosphere 185 (2017) 907–917.
[53] Y.K. Lee, K.R. Murphy, J. Hur, Fluorescence Signatures of Dissolved Organic Matter Leached from Microplastics: Polymers and Additives, Environ. Sci. Tech. 54 (2020) 11905–11914.
[54] G. Zhang, F. Zhang, Variations in aggregate-associated organic carbon and polyester microfibers resulting from polyester microfibers addition in a clayey soil, Environ. Pollut. 258 (2020), 113716.

[55] P. Wu, Z. Cai, H. Jin, Y. Tang, Adsorption mechanisms of five bisphenol analogues on PVC microplastics, Sci. Total Environ. 650 (2019) 671–678.
[56] W. Horwath, Carbon cycling and formation of soil organic matter, Soil microbiology, ecology and biochemistry, Elsevier (2007) 303–339.
[57] N. Zafar, M.B.K. Niazi, F. Sher, U. Khalid, Z. Jahan, G.A. Shah, M. Zia, Starch and polyvinyl alcohol encapsulated biodegradable nanocomposites for environment friendly slow release of urea fertilizer, Chemical Engineering Journal Advances 7 (2021), 100123.
[58] J. Li, Y. Yu, Z. Zhang, M. Cui, The positive effects of polypropylene and polyvinyl chloride microplastics on agricultural soil quality, J. Soil. Sediment. 23 (3) (2023) 1304–1314.
[59] S.W. Kim, S.-W. Jeong, Y.-J. An, Microplastics disrupt accurate soil organic carbon measurement based on chemical oxidation method, Chemosphere 276 (2021), 130178.
[60] M.C. Rillig, Microplastic disguising as soil carbon storage, Environ. Sci. Technol. 52 (11) (2018) 6079–6080.
[61] H. Chen, K. Lei, X. Wang, Terrestrial humic substances in Daliao River and its estuary: optical signatures and photoreactivity to UVA light, Environ. Sci. Pollut. Res. 23 (7) (2016) 6459–6471.
[62] Y. Yamashita, E. Tanoue, Chemical characterization of protein-like fluorophores in DOM in relation to aromatic amino acids, Mar. Chem. 82 (3-4) (2003) 255–271.
[63] M. Uchimiya, S. Hiradate, M.J. Antal, Influence of carbonization methods on the aromaticity of pyrogenic dissolved organic carbon, Energy Fuel 29 (4) (2015) 2503–2513.
[64] Y. Hu, H. Zhang, D. Zhao, Transform method in three-dimensional fluorescence spectra for direct reflection of internal molecular properties in rapid water contaminant analysis, Spectrochim. Acta A Mol. Biomol. Spectrosc. 250 (2021), 119376.
[65] D. Yu, J. Cui, X. Li, H. Zhang, Y. Pei, Electrochemical treatment of organic pollutants in landfill leachate using a three-dimensional electrode system, Chemosphere 243 (2020), 125438.
[66] X.-Q. Qin, B.o. Yao, L. Jin, X.-Z. Zheng, J. Ma, M.F. Benedetti, Y. Li, Z.-L. Ren, Characterizing soil dissolved organic matter in typical soils from China using fluorescence EEM–PARAFAC and UV–visible absorption, Aquat. Geochem. 26 (1) (2020) 71–88.
[67] N. Vikram, A. Sagar, C. Gangwar, R. Husain, R.N. Kewat, Properties of humic acid substances and their effect in soil quality and plant health, Humus and Humic Substances-Recent Advances, IntechOpen2022.
[68] F.J. Cervantes, C.H. Gutiérrez, K.Y. López, M.I. Estrada-Alvarado, E.R. Meza-Escalante, A.-C. Texier, F. Cuervo, J. Gómez, Contribution of quinone-reducing microorganisms to the anaerobic biodegradation of organic compounds under different redox conditions, Biodegradation 19 (2) (2008) 235–246.
[69] E.I. Valenzuela, C. Padilla-Loma, N. Gómez-Hernández, N.E. López-Lozano, S. Casas-Flores, F.J. Cervantes, Humic substances mediate anaerobic methane oxidation linked to nitrous oxide reduction in wetland sediments, Front. Microbiol. 11 (2020) 587.
[70] D.R. Bond, D.R. Lovley, Electricity production by Geobacter sulfurreducens attached to electrodes, Appl. Environ. Microbiol. 69 (3) (2003) 1548–1555.
[71] D.E. Holmes, T. Ueki, H.-Y. Tang, J. Zhou, J.A. Smith, G. Chaput, D.R. Lovley, N. Dubilier, A membrane-bound cytochrome enables Methanosarcina acetivorans to conserve energy from extracellular electron transfer, MBio 10 (4) (2019).
[72] M.E. Seeley, B. Song, R. Passie, R.C. Hale, Microplastics affect sedimentary microbial communities and nitrogen cycling, Nat. Commun. 11 (2020) 2372.
[73] J. Shi, J. Wang, J. Lv, Z. Wang, Y. Peng, J. Shang, X. Wang, Microplastic additions alter soil organic matter stability and bacterial community under varying temperature in two contrasting soils, Sci. Total Environ. 838 (2022), 156471.
[74] Z.-Y. Zhao, P.-Y. Wang, Y.-B. Wang, R. Zhou, K. Koskei, A.N. Munyasya, S.-T. Liu, W. Wang, Y.-Z. Su, Y.-C. Xiong, Fate of plastic film residues in agro-ecosystem and its effects on aggregate-associated soil carbon and nitrogen stocks, J. Hazard. Mater. 416 (2021), 125954.
[75] B. Gewert, M.M. Plassmann, M. MacLeod, Pathways for degradation of plastic polymers floating in the marine environment, Environ. Sci. Processes Impacts 17 (9) (2015) 1513–1521.
[76] G.S. Sayler, J. Sanseverino, K.L. Davis, Biotechnology in the sustainable environment, Springer Science & Business Media, 2012.
[77] L. Hermabessiere, A. Dehaut, I. Paul-Pont, C. Lacroix, R. Jezequel, P. Soudant, G. Duflos, Occurrence and effects of plastic additives on marine environments and organisms: a review, Chemosphere 182 (2017) 781–793.
[78] M.C. Rillig, A.A. de Souza Machado, A. Lehmann, U. Klümper, Evolutionary implications of microplastics for soil biota, Environ. Chem. 16 (2018) 3–7.
[79] S. Ma, J. Xiong, X. Wu, H. Liu, L. Han, G. Huang, Effects of the functional membrane covering on the gas emissions and bacterial community during aerobic composting, Bioresour. Technol. 340 (2021), 125660.
[80] M. Menéndez-Serra, X. Triadó-Margarit, E.O. Casamayor, Ecological and metabolic thresholds in the bacterial, protist, and fungal microbiome of ephemeral saline lakes, Microb Ecol 82 (4) (2021) 885–896.
[81] A. Baricz, C.M. Chiriac, A.Ş. Andrei, P.A. Bulzu, E.A. Levei, O. Cadar, K.P. Battes, M. Cîmpean, M. Şenilă, A. Cristea, Spatio-temporal insights into microbiology of the freshwater-to-hypersaline, oxic-hypoxic-euxinic waters of Ursu Lake, Environ. Microbiol. 23 (2021) 3523–3540.
[82] R. Méheust, C.J. Castelle, P.B. Matheus Carnevali, I.F. Farag, C. He, L.-X. Chen, Y. Amano, L.A. Hug, J.F. Banfield, Groundwater Elusimicrobia are metabolically diverse compared to gut microbiome Elusimicrobia and some have a novel nitrogenase paralog, ISME J. 14 (12) (2020) 2907–2922.
[83] X. Guo, S. Du, H. Guo, W. Min, Long-term saline water drip irrigation alters soil physicochemical properties, bacterial community structure, and nitrogen transformations in cotton, Appl. Soil Ecol. 182 (2023), 104719.
[84] J. Chee-Sanford, D. Tian, R. Sanford, Consumption of N2O and other N-cycle intermediates by Gemmatimonas aurantiaca strain T-27, Microbiology 165 (2019) 1345–1354.
[85] M.C. Van Teeseling, R.J. Mesman, E. Kuru, A. Espaillat, F. Cava, Y.V. Brun, M. S. VanNieuwenhze, B. Kartal, L. Van Niftrik, Anammox Planctomycetes have a peptidoglycan cell wall, Nat. Commun. 6 (2015) 6878.
[86] A. Sepehri, M.-H. Sarrafzadeh, Effect of nitrifiers community on fouling mitigation and nitrification efficiency in a membrane bioreactor, Chemical Engineering and Processing-Process Intensification 128 (2018) 10–18.
[87] Y. Liu, Y.-H. Huang, H. Lü, H. Li, Y.-W. Li, C.-H. Mo, Q.-Y. Cai, Persistent contamination of polycyclic aromatic hydrocarbons (PAHs) and phthalates linked to the shift of microbial function in urban river sediments, J. Hazard. Mater. 414 (2021), 125416.
[88] H.-M. Zhao, H. Du, J. Lin, X.-B. Chen, Y.-W. Li, H. Li, Q.-Y. Cai, C.-H. Mo, H.-M. Qin, M.-H. Wong, Complete degradation of the endocrine disruptor di-(2-ethylhexyl) phthalate by a novel Agromyces sp. MT-O strain and its application to bioremediation of contaminated soil, Sci. Total Environ. 562 (2016) 170–178.
[89] H. Habe, M. Miyakoshi, J. Chung, K. Kasuga, T. Yoshida, H. Nojiri, T. Omori, Phthalate catabolic gene cluster is linked to the angular dioxygenase gene in Terrabacter sp. strain DBF63, Appl. Microbiol. Biotechnol. 61 (1) (2003) 44–54.
[90] J.P. Bowman, Methylocystis, Bergey's Manual of Systematics of Archaea and Bacteria (2015) 1-7.
[91] G. Akovali, Plastic materials: chlorinated polyethylene (CPE), chlorinated polyvinylchloride (CPVC), chlorosulfonated polyethylene (CSPE) and polychloroprene rubber (CR), in: Toxicity of building materials, Elsevier, 2012, pp. 54–75.
[92] C. Erkel, M. Kube, R. Reinhardt, W. Liesack, Genome of rice cluster I archaea the key methane producers in the rice rhizosphere, Science 313 (5785) (2006) 370–372.
[93] D.R. Bond, D.R. Lovley, Reduction of Fe (III) oxide by methanogens in the presence and absence of extracellular quinones, Environ. Microbiol. 4 (2) (2002) 115–124.
[94] W.M. Moe, F.A. Rainey, J. Yan, The genus Dehalogenimonas, in: L. Adrian, F. E. Löffler (Eds.), Organohalide-Respiring Bacteria, Springer Berlin Heidelberg, Berlin, Heidelberg, 2016, pp. 137–151.
[95] Y.-X. Zhao, L. Guo, L. Wang, N.-D. Jiang, K.-X. Chen, Y.-J. Dai, Biodegradation of the pyridinecarboxamide insecticide flonicamid by Microvirga flocculans and characterization of two novel amidases involved, Ecotoxicol. Environ. Saf. 220 (2021), 112384.
[96] J. Singh, Y.K. Nandabalan, Prospecting Ammoniphilus sp. JF isolated from agricultural fields for butachlor degradation, 3 Biotech 8 (2018) 1–7.
[97] B.M. Van der Zaan, F.T. Saia, A.J. Stams, C.M. Plugge, W.M. de Vos, H. Smidt, A. A. Langenhoff, J. Gerritse, Anaerobic benzene degradation under denitrifying conditions: Peptococcaceae as dominant benzene degraders and evidence for a syntrophic process, Environ. Microbiol. 14 (2012) 1171–1181.
[98] R. Caspi, T. Altman, R. Billington, K. Dreher, H. Foerster, C.A. Fulcher, T. A. Holland, I.M. Keseler, A. Kothari, A. Kubo, M. Krummenacker, M. Latendresse, L. A. Mueller, Q. Ong, S. Paley, P. Subhraveti, D.S. Weaver, D. Weerasinghe, P. Zhang, P.D. Karp, The MetaCyc database of metabolic pathways and enzymes and the BioCyc collection of Pathway/Genome Databases, Nucleic Acids Res. 42 (D1) (2014) D459–D471.
[99] A.D. Moodie, W.J. Ingledew, Microbial anaerobic respiration, Adv. Microb. Physiol. 31 (1990) 225–269.

Chapter V

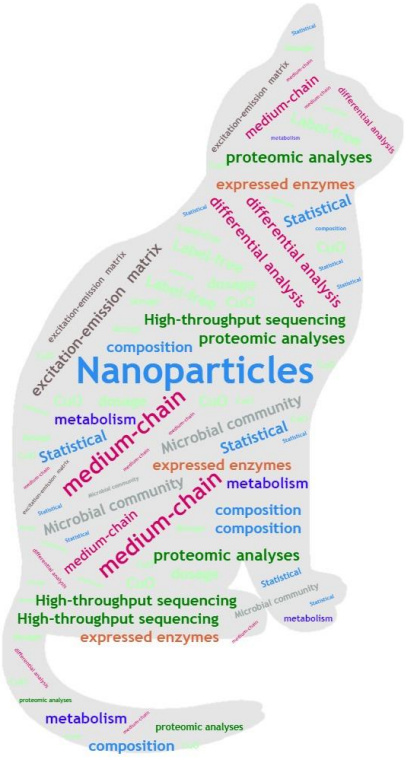

Nonmonotonic effect of CuO nanoparticles on medium-chain carboxylates production from waste activated sludge

Chao Liu [a] , Haiqing Wang [b] , Muhammad Usman [c] , Mengyuan Ji [d] , Jun Sha [a] , Zhenda Liang [a] , Lishan Zhu [a] , Li Zhou [a,*] , Bing Yan [a,*]
Water Research, Volume 230, 15 February 2023, 119545
https://doi.org/10.1016/j.watres.2022.119545

[a] Institute of Environmental Research at Greater Bay Area, Key Laboratory for Water Quality and Conservation of the Pearl River Delta, Ministry of Education, Guangzhou University, Guangzhou 510006, P R China
[b] School of Environmental Science and Engineering, Shandong University, Jinan 250100, PR China
[c] Bioproducts Science & Engineering Laboratory (BSEL), Department of Biological Systems Engineering, Washington State University (WSU), Richland, WA, USA
[d] Department of Biology, University of Padua, Via U. Bassi 58/b, 35121 Padova, Italy

*Corresponding author

Water Research 230 (2023) 119545

Contents lists available at ScienceDirect

Water Research

journal homepage: www.elsevier.com/locate/watres

Nonmonotonic effect of CuO nanoparticles on medium-chain carboxylates production from waste activated sludge

Chao Liu [a], Haiqing Wang [b], Muhammad Usman [c], Mengyuan Ji [d], Jun Sha [a], Zhenda Liang [a], Lishan Zhu [a], Li Zhou [a,*], Bing Yan [a,*]

[a] Institute of Environmental Research at Greater Bay Area, Key Laboratory for Water Quality and Conservation of the Pearl River Delta, Ministry of Education, Guangzhou University, Guangzhou 510006, P R China
[b] School of Environmental Science and Engineering, Shandong University, Jinan 250100, PR China
[c] Bioproducts Science & Engineering Laboratory (BSEL), Department of Biological Systems Engineering, Washington State University (WSU), Richland, WA, USA
[d] Department of Biology, University of Padua, Via U. Bassi 58/b, 35121 Padova, Italy

ARTICLE INFO

Keywords:
Waste activated sludge
Anaerobic fermentation
CuO nanoparticles
Medium chain carboxylate
Metaproteomic analysis

ABSTRACT

The growing applications of CuO nanoparticles (NPs) in industrial and agriculture has increased their concentrations in wastewater and subsequently accumulated in waste activated sludge (WAS), raising concerns about their impact on reutilization of WAS, especially on the medium-chain carboxylates (MCCs) production from anaerobic fermentation of WAS. Here we showed that CuO NPs at 10–50 mg/g-TS can significantly inhibit MCCs production, and reactive oxygen species generation was revealed to be the key factor linked to the phenomena. At lower CuO NPs concentrations (0.5–2.5 mg/g-TS), however, MCCs production was enhanced, with a maximum level of 37% compared to the control. The combination of molecular approaches and metaproteomic analysis revealed that although low dosage CuO NPs (2.5 mg/g-TS) weakly inhibited chain elongation process, they displayed contributive characteristics both in WAS solubilization and transport/metabolism of carbohydrate. These results demonstrated that the complex microbial processes for MCCs production in the anaerobic fermentation of WAS can be affected by CuO NPs in a dosage-dependent manner via regulating microbial protein expression level. Our findings can provide new insights into the influence of CuO NPs on anaerobic fermentation process and shed light on the treatment option for the resource utilization of CuO NPs polluted WAS.

1. Introduction

With the rapid innovation and commercialization of nanotechnology, large amounts of nanoparticles (NPs) have been incorporated into consumer and industrial products. Particularly, as a p-type semiconductor, CuO NPs were produced world-widely at a dosage of 570 t in 2014 and would be 1600 t by the year 2025 (Hou et al., 2017). Due to the unique physicochemical properties, CuO NPs have been widely used in various fields, such as industrial catalysis and sustainable agriculture (Otero-González et al., 2014; Ingle, 2021). The large production and widespread utilization of CuO NPs can lead to their environmental release and accumulation. In fact, CuO NP are commonly found in different environmental media and matrices (e.g., polluted sludge and water,). Particularly, waste activated sludge (WAS) is considered as a reservoir for CuO NPs accumulation, since many of NPs ultimately enter the wastewater treatment plants (WWTP) and concentrated in WAS (Kiser et al., 2010; Limbach et al., 2008). For instance, the content of CuO NPs in sludge is estimated to be approximately 2–5 mg/g of total solids (TS) according to the sample collected worldwide (Abdulsada et al., 2021; Mu et al., 2011). And the value can be higher in China as the concentration of Cu in 193 sludge samples was detected to be about 908.4 mg•kg^{-1} (Tou et al., 2017). Furthermore, a much greater level of CuO NPs may be measured in the near future considering their increasing production and use. CuO NPs have been reported to exhibit diverse adverse effects on individual organisms by causing oxidative stress, cell membrane disruption, and inactivation of key enzymes (Gonzalez-Estrella et al., 2013; Tian et al., 2017). Therefore, treatment and resource utilization of the large amount of WAS also faces risk posed by CuO NPs.

Anaerobic conversion, occurred in a syntrophic microbial community, has been strategically used as a cost-effective method to achieve simultaneously WAS reduction and valuable end-products production.

* Corresponding authors.
E-mail addresses: zhoul@gzhu.edu.cn (L. Zhou), drbingyan@yahoo.com (B. Yan).

https://doi.org/10.1016/j.watres.2022.119545
Received 7 June 2022; Received in revised form 18 December 2022; Accepted 27 December 2022
Available online 29 December 2022

Methane (CH_4), hydrogen (H_2), short-chain carboxylates (SCCs, mainly C2-C5 carboxylic acids) are the common products of anaerobic WAS fermentation, whereas medium-chain carboxylates (MCCs) is emerged recently as a class of novel product with a higher utilization value as it carries more energy and has better separability. As a type of fatty acid that contain 6 to 12 carbon atoms, MCCs can be produced through SCCs upgrading accompanying with electron donors (e.g., ethanol) by carboxylate platform in anaerobic reactor. The pivotal biochemical reactions for these bioproducts generation in anaerobic reactor involve solubilization, hydrolysis, acidification and chain elongation/methanogenesis (Wu et al., 2020b). The solubilization step has been considered the bottleneck of WAS anaerobic conversion as most organic content, such as carbohydrates and proteins, is enclosed inside the microbial cell membranes (Zheng et al., 2014). This soluble organic matter should be released and accessed by hydrolytic bacteria to produce polymers and monomers (Yang et al., 2020). Subsequently, acidogenic bacteria metabolize the polymer and monomers to yield SCCs (especially acetate) for further MCCs or CH_4 synthesis conducted by chain elongation microbe or methanogens, respectively (Angenent et al., 2016). In this regard, the variation of operated conditions can induce the dissimilarities in any aforementioned reactions (Liu and Ghosh, 1997; Zheng et al., 2014).

Although experimental setups could influence MCCs production from WAS, the characteristic of WAS such as its composition, is regarded as the foundational and key factor influencing the fermentation performance (Liu et al., 2012; Wang et al., 2020a). CuO NPs, as an accumulated material in WAS, can potentially affect functional microbial groups and catalytic reaction activity for WAS anaerobic conversion. Therefore, it is worth investigating the effect of CuO NP on MCCs generation and then providing information for further study to improve MCCs production and shorten fermentation duration, in case of some particle occurrence in the experimental sludge. Like most other syntrophic communities, it should be emphasized that the anaerobic conversion could not only be influenced by the activity of individual microorganisms, but also the syntrophic community. It has been reported that the negative effect of CuO NPs on CH_4 production was mainly attributed to their inhibition on methanogenesis (Ajay et al., 2020; Chen et al., 2020). However, a recent report by Wei et al. (2021) suggested that CuO at 5 mg/g-TS significantly promoted H_2 production due to the enhanced WAS solubilization. These studies revealed that the effect of CuO NPs on the anaerobic fermentation are greatly influenced by the unique biological process required for the production of each product. However, a comprehensive understanding of MCCs production in WAS anaerobic fermentation influenced by CuO NPs is lacking, such as how does CuO NP dosage in WAS impact its anaerobic fermentation? What is the mechanism of the effect of CuO NPs on various processes involved in MCC generation? Besides, only microbial community composition was used to explore the mechanisms behind the effect of CuO NPs on anaerobic conversion process, which was still not convincible (Huang et al., 2019; Luna-delRisco et al., 2011; Wang et al., 2017).

In this study, we explored the potential effects of CuO NPs on MCCs production from WAS anaerobic fermentation and the underlying mechanisms based on molecular approaches and label-free quantitative proteomic analysis. As a quantitative metaproteomic technology, label-free quantitative proteomic analysis could provides direct proof on the expressed genes and quantify the key proteins from multiple differential samples associated with various operations (Abram et al., 2011; Lü et al., 2014). The current study will focus on (1) systematically exploring the dosage-response relationship between CuO NPs and MCCs production, and the involved each step; (2) identification the contribution of generated intracellular reactive oxygen species (ROS), released ions as well as disturbed electron transfer activity to the change of MCCs yield; and (3) revealing the possible mechanism for the production of MCCs in the presence of CuO NPs from protein and genes aspects. This study is expected to contribute to the comprehensive understanding of the impact of CuO NPs on WAS anaerobic fermentation through complex microbial process, and provide important clues for resource utilization of CuO NPs-containing sludge.

2. Materials and methods

2.1. Inoculum, WAS and CuO NPs

The inoculum used in this study was derived from a well-characterized reactor with an operating period of more than one year, fed with WAS and ethanol to produce MCCs. The characteristics of the inoculum were as follows: total solid (TS) 21.3 ± 0.7 g/L, volatile solid (VS) 16.9 ± 1.1 g/L, total chemical oxygen demand (TCOD) 23.5 ± 0.9 g/L, soluble chemical oxygen demand (SCOD) 0.3 ± 0.1 g/L and pH 7.2 ± 0.5.

The WAS in present study was collected from the secondary settler of a WWTP (Shenzhen, China). The main characteristics of the WAS were as follows: TS 21.0 ± 0.3 g/L, VS 15.6 ± 0.3 g/L, TCOD 22.9 ± 0.5 g/L, SCOD 0.9 ± 0.1 g/L, total CuO NPs 0.05 ± 0.01 mg/g-TS and pH 6.9 ± 0.5. The CuO NPs (purity >99%) used in present study was purchased from Sigma-Aldrich (Shanghai, China). The transmission electron microscopy (TEM) image of CuO NPs was obtained using a FEI Talos F200s (Hillsboro, OR, USA)) using a voltage of 200 kV to visualize their shape and particle size (~40 nm) (Fig. S1, SI).

2.2. Effects of CuO NPs on the MCCs production from WAS

The experiments were conducted in 150 mL serum bottles with working volume of 70 mL (20 mL of inoculum and 50 mL of WAS together with 300 mM C ethanol), for MCCs potential tests. And the concentration of ethanol as electron donor was determined according to previous studies (Wang et al., 2020b; Wu et al., 2018). One reactor was labeled as the control without CuO NPs addition, while the other four reactors were dosage with CuO NPs (0.464, 2.464, 9.964 and 49.964 mg/g-TS) to the final concentrations of 0.5, 2.5, 10 and 50 mg/g-TS based on the initial CuO NPs in WAS. In addition, the reactors with only inoculum and basic anaerobic medium (BA medium) were used as negative controls. The detailed composition of BA medium was described in our previous study (Yang et al., 2019). All reactors were performed in triplicates and lasted for ~34 days. The pH was adjusted to 7 in all the reactors by adding 4 M NaOH and 4 M HCl. 2-Bromoethanesulfonate (BES; 100 mM) was added initially to inhibit methanogens. The above reactors were flushed with N_2 for 5 min to create an anaerobic environment, sealed with butyl rubber stoppers, and then placed in a 35 °C incubator with a shaking speed of 150 rpm. The electron transport system (ETS) activity analysis and ROS production were also evaluated according to the reference (Limbach et al., 2007; Tian et al., 2017). In order to explore the influencing mechanism of CuO NPs, their impacts on four processes (solubilization, hydrolysis, acidogenesis, and chain elongation) involved in MCCs production were assessed with model substrates (Supporting Information). The significance of results was evaluated using the analysis of variance (ANOVA), and $P < 0.05$ was considered to be statistically significant.

2.3. Effect of Cu^{2+} on the MCCs production

The effect of Cu^{2+} on the MCCs production were tested. $CuCl_2$ instead of CuO NPs was injected into the reactors according to the Cu^{2+} concentrations determined at the end of CuO NPs experiment in Section 2.2. The other operation conditions were similar to the CuO NPs experiment. The MCCs concentration were determined after 34 days. All the tests were performed in triplicates.

2.4. Microbial community compositions analyses

To characterize time-dependent microbial composition changes

among inoculum group, control group and 2.5 mg/g-TS CuO NPs group, the microbial communities in the three groups were analyzed at different operational times. Samples Control-7, Control-15 Control-30 and Control-34 were obtained from reactor C on days 7, 15, 30 and 34, respectively. Samples CuO-7, CuO-15 CuO-30 and CuO-34 were obtained from reactor 2.5 mg/g-TS CuO NPs on days 7, 15, 30 and 34, respectively. Then the microbial community composition between the control and the 2.5 mg/g-TS CuO NPs exposed fermenter on day 34 (at stable state) were compared detailedly to gain more insight into how low dosage of CuO NPs influenced MCCs production. Detailed information was described in SI.

2.5. Label-free quantitative proteomic analyses

Samples from control group (0 mg CuO/g-TS) and the experimental group (2.5 mg CuO/g-TS) were also collected at the end of the experiment for label-free quantitative proteomic analysis. The total protein in the samples was extracted and separated by polyacrylamide gel electrophoresis (PAGE), and the total protein concentration was determined through the Bradford method (Sengupta et al., 2011). 0.5 μg/μL of the peptide was taken out of each sample for protein identification by liquid chromatograph-mass spectrometer/mass spectrometer analysis. The raw data were processed using PEAKSStudio version 8.5 against the NCBI database. Detailed information can be found in the SI.

3. Results and discussion

3.1. Dosage-dependent promotion and suppression of MCC production by CuO NPs

With ethanol as electron donor, the production of carboxylates (SCCs and MCCs) from WAS at different dosages of CuO NPs were investigated and shown in Fig. 1 and Fig. S2. After operation for 34 days, the concentration of carboxylates and microbial community composition in all reactors reached a stationary level (Fig. S3). As the concentrations of n-heptanoate and n-caprylate were almost negligible (< 8 mg COD/L), n-caproate was thus considered as the sole MCC product in this study. As shown in Fig. 1, it was clear that CuO NPs affect the production of carboxylates and the consumption of ethanol in a dosage-dependent manner. The production of carboxylates increased significantly with the dosage of CuO NPs in the range of 0–2.5 mg/g-TS, and achieved the highest at 2.5 mg/g-TS CuO NPs. The generation of MCCs and consumption of ethanol displayed similar trend. And the maximum MCCs concentration achieved 6600 mg COD/L at 2.5 mg/g-TS CuO NPs, which was 37% higher than that of the untreated control (4800 mg COD/L, $P < 0.05$). Nevertheless, the yield of SCCs (valerate, butyrate, propionate, acetate) increased up to a maximum of only 5.7% when CuO NPs content was 2.5 mg/g-TS. These results suggested that low CuO NPs dosage ($\leq$ 2.5 mg/g-TS) could mainly stimulate MCCs production from SCCs and ethanol (Angenent et al., 2016). With further increase of the CuO NPs dosages to 50 mg/g-TS, however, the total yield of carboxylates decreased to 45.6%, SCCs to 52.9%, and MCCs to 28% of that observed in the control ($P < 0.05$), respectively. Meanwhile, the consumption of ethanol decreased to 4600 mg COD/L, which only correspond to 56.1% of that in the control group. Overall, these results suggested that low CuO NPs dosage ($\leq$ 2.5 mg/g-TS) addition could lead to significantly enhanced production of MCCs from WAS, but extended exposure to CuO NPs would cause severe toxicity and inhibition effect.

To date, most previous studies reported the inhibitory effects of CuO NPs even at low dosage on the anaerobic microorganisms (Chen et al., 2014b; Otero-González et al., 2014; Wang et al., 2017). Different with previous reports, our results showed that CuO NPs (0–50 mg/g-TS) displayed enhancement-to-inhibition effect on WAS anaerobic fermentation for MCCs production. Based on these distinct phenomena, it is of great and enlightening significance to explore the mechanisms on anaerobic conversion of WAS for MCCs production under different CuO NP stresses, which were carried out in the following section.

3.2. CuO NPs affected each stage of WAS anaerobic fermentation

To better understand the role of CuO NPs, the effects of CuO NPs on key processes (i.e., solubilization, hydrolysis, acidogenesis, and chain elongation) were further conducted. As the bottleneck steps of WAS anaerobic fermentation, solubilization is a non-bioprocess with the release of soluble substances as the organic matters mainly existed in the solid phase of WAS (Liu and Fang, 2002). Therefore, the extent of WAS solubilization could be expressed by the variations of soluble organic matters. As shown in Fig. S4A, all dosages of CuO NPs addition promoted the release of organic matters, with the amount of polysaccharide, protein, and SCOD in the bioreactor increased with the increasing CuO NPs dosage after initial 2 d fermentation. Three-dimensional excitation–emission matrix (EEM) fluorescence spectroscopy was also used to

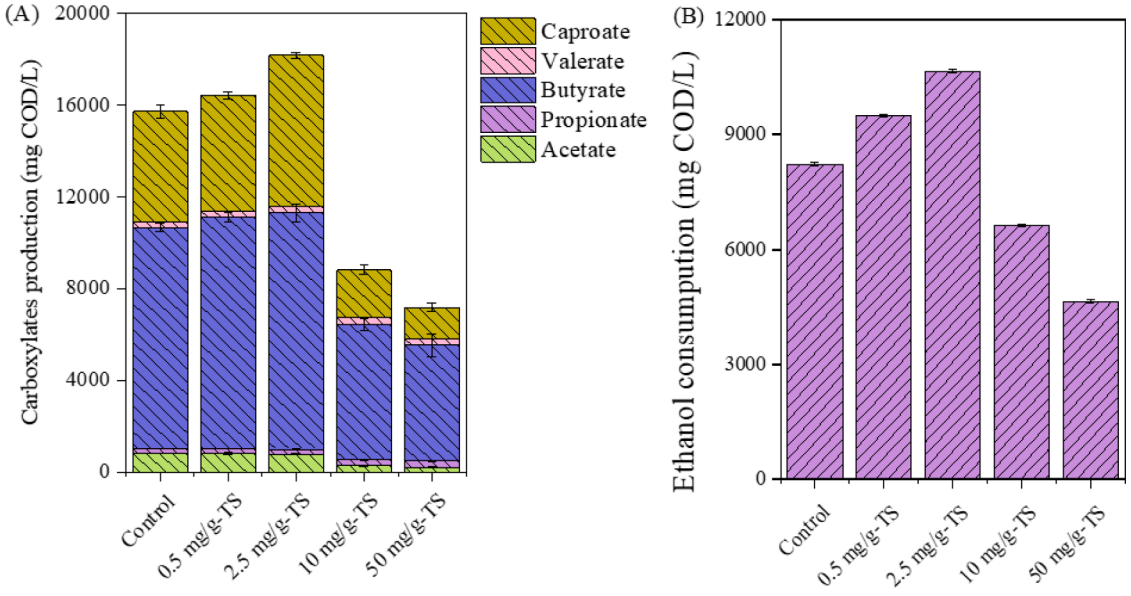

Fig. 1. (A) The production of carboxylates from WAS anaerobic fermentation and (B) consumption of ethanol with different concentrations of CuO NPs. Error bars represent standard deviations of triplicate tests.

characterize the soluble organic matters in fermentation liquor at different dosage of CuO NPs. As shown in Fig. S4(B)-(F), the Ex/Em peaks at 250–280/200–380 nm, which represented the areas related to the biodegradable soluble substances (Chen et al., 2003), was positively correlated with the dosage of CuO NPs. Similarly, the free lactate dehydrogenase (LDH) and DNA associated with the cell membrane integrity also increased (Fig. S4G), and was 74.5% and 76.1% higher than that of the control when the CuO NPs dosage was up to 50 mg/g-TS. All these results indicated that addition of CuO NPs improved solubilization of WAS, and the trend were positively related to CuO NPs dosage. Based on the characteristics of CuO NPs, three possibilities are proposed to explain the improved WAS solubilization. First, as a catalyst, CuO NP destroys the structure of WAS to make it easy to mix with water. Chen et al. (2014a) also demonstrated that CuNPs could ruin the layout of sludge and reduce its particle size by environmental scanning electron microscopy analysis. Second, CuO NPs improve the interaction between hydrophobic insoluble organic matters (mainly protein-like substances) in WAS and aqueous solution by its surface reactive property. In future research, determining the solubility and structure of protein-like substances in an abiotic environment and their interactions with CuO NPs may verify the hypothesis. Third, partially broken cells in WAS by CuO NPs may cause the release of internal macromolecular organics into the fermentation reactor. This has been shown by the SEM images and higher released LDH/free DNA (Fig. S5 and Fig. S4G).

The soluble organic matters released from WAS solubilization would be further biodegraded by the hydrolysis and acidification process, and further converted to MCCs through chain elongation step. The effect of CuO NPs on the hydrolysis step was examined using model proteins (bovine serum albumin, BSA) and model polysaccharide (dextran). Fig. S6(A) showed the degradation efficiency of BSA and dextran at different concentration of CuO NPs. At dosages of 0.5 and 2.5 mg/g-TS, the influences of CuO NPs on degradations of BSA and dextran were both insignificant compared to untreated control. However, the degradations rate of BSA and dextran at 10 mg/g-TS of CuO NPs were lower than that in the control (9.2% and 39% versus 24.5% and 81.1%, respectively), and the lowest degradations rate of both molecules was obtained at 50 mg/g-TS of CuO NPs (took only 17.9% and 24.8% of the control, respectively). Fig. S6(A) illustrated similar result for the acidogenesis of L-glutamate as model amino acid and glucose as model monosaccharide. The degradation rate of L-glutamate and glucose at dosages of 0.5 and 2.5 mg/g-TS CuO NPs were almost the same with that of control, whereas it started to decrease when CuO NPs concentration was above 10 mg/g-TS. The inhibition effect observed in the degradation assays suggested that high dosage of CuO NPs ($\geq$ 10 mg/g-TS) can disturb the hydrolysis and acidogenesis process. In the chain elongation step, with ethanol as electron donors, SCCs produced in fermentation are further converted to MCCs. By using acetate as model SCCs, it can be seen in Fig. S6B that the production of MCCs and consumption of ethanol at low concentration of CuO NPs (2.5 mg/g-TS) was slightly lower than that of the control group. However, the MCCs production further decreased to 57.3% and 26.1% of the control at 10 and 50 mg/g-TS of CuO NPs, respectively. These indicated that the CuO NPs pose negative effect on the chain elongation process, and the extent was highly concentration-dependent.

Taken together, all above results revealed that although chain elongation was weakly inhibited with CuO NPs at 2.5 mg/g-TS, WAS solubilization was enhanced, finally leading to the improved MCCs production during WAS fermentation. In contrast, high dosages of CuO NPs highly enhanced WAS solubilization, but hydrolysis, acidogenesis and chain elongation were all significantly inhibited; thus, the improvement were not enough to offset inhibition, resulting negative impact on overall MCCs production. As hydrolysis, acidification, and chain elongation are key bioprocess in anaerobic WAS fermentation, these findings suggested that the activity of related reactions and microorganisms has been significantly influenced by CuO NPs.

3.3. ROS generated in the bioreactor inhibited electron transport activity

All respiring microorganisms possess an active ETS which is an indicator of the biological activity of activated sludge (Blenkinsopp and Lock, 1990; Wang et al., 2013). Therefore, the ETS activity with CuO NPs was determined at the end of experiment (34^{th} day). The relative activities of ETS, which were dependent on CuO NP dosage, were illustrated in Fig. 2A. In the presence of 0.5 and 2.5 mg/g-TS of CuO NPs, the relative ETS activity was increased by 2% and 6% compared with that of the control, which was consistent with improved production of carboxylates shown in Fig.1. However, the presence of 10 and 50 mg/g-TS of CuO NPs significantly inhibited the ETS activity. For instance, the ETS activity at 50 mg/g-TS CuO NPs addition was about 51.2% lower than that of the control. These results consisted well with the inhibition findings for MCCs production from WAS, indicating that the impact of CuO NPs on the electron transfer activity directly related with the palmy or decay in WAS/ethanol conversion and carboxylates production.

It has been demonstrated that the electron transfer efficiency in anaerobic fermentation is highly correlated with the viability of microorganisms. Currently, the soluble metal ions were considered as an important parameter concerning the NPs biotoxicity to microorganisms (Tang et al., 2016). Therefore, the concentrations of Cu ions in all the reactors containing 0.5 to 50 mg/g-TS CuO NPs were measured, and the results revealed that the dissolution of CuO NPs was only 0.5–1.5% (0.15–36 mg/L Cu^{2+} released) (Fig. 2B). Moreover, the effects of the Cu ions on the MCCs production from WAS were explored. The results showed that such low concentrations of Cu ions (0.15–36 mg/L) cause negligible changes in anaerobic fermentation metabolism and MCCs production from WAS (Fig. 2B), indicating the effect of released ions on the performance of the bioreactor can be excluded.

It is well-known that NPs can influence the metabolism activity and viability of microcosm through generation of ROS (Degli Esposti and McLennan, 1998; Tian et al., 2019). Usually, ROS including superoxide (O_2-), hydrogen peroxide (H_2O_2), and hydroxyl radical (OH), are produced under aerobic/anaerobic conditions and show an increasing trend with increased amount of NPs (Degli Esposti and McLennan, 1998; Mu and Chen, 2011). These ROS could be depleted through reactions with some cellular components (e.g., phospholipids and proteins), and thus microbes can maintain normal metabolic activities (Wang and Chen, 2016). However, an excessive oxidative stress can lead to the reduction of cell viability and even cell death once this antioxidant self-defense is breached (Jeong et al., 2016). In the present study, ROS produced in the fermentation assay with or without CuO NPs were detected. As shown in Fig. 2C, CuO NPs promoted ROS generation in a concentration-dependent manner. In comparison with the control, the amount of ROS in system amended with 0.5 and 2.5 mg/g-TS of CuO NPs was increased only by 1.1% and 3.5%, respectively. Combined with the electron transfer activity, intracellular ROS generation at this level should not have impact on the microbial metabolism and the carboxylates production. Nevertheless, in the presence of 10 and 50 mg/g-TS of CuO NPs, the amount of intracellular ROS generated in the anaerobic system was dramatically 25.9% and 47.9% higher than that of the control, respectively. Under such conditions, a negative correlation between the intracellular ROS level and the electron transfer activity was observed. The results suggested that the decrease in electron transfer activity and thus declined carboxylates production with the dosage of CuO NPs exceeded 10 mg/g-TS could be mainly attributed to the generation of excessive ROS. Meanwhile the underlying mechanism of electron transfer activity and carboxylates production facilitated by lower dosages of CuO NPs was unclear and need to be further investigated.

3.4. CuO NP-induced alterations in microbial community

To gain more insight into how low dosage of CuO NPs influenced

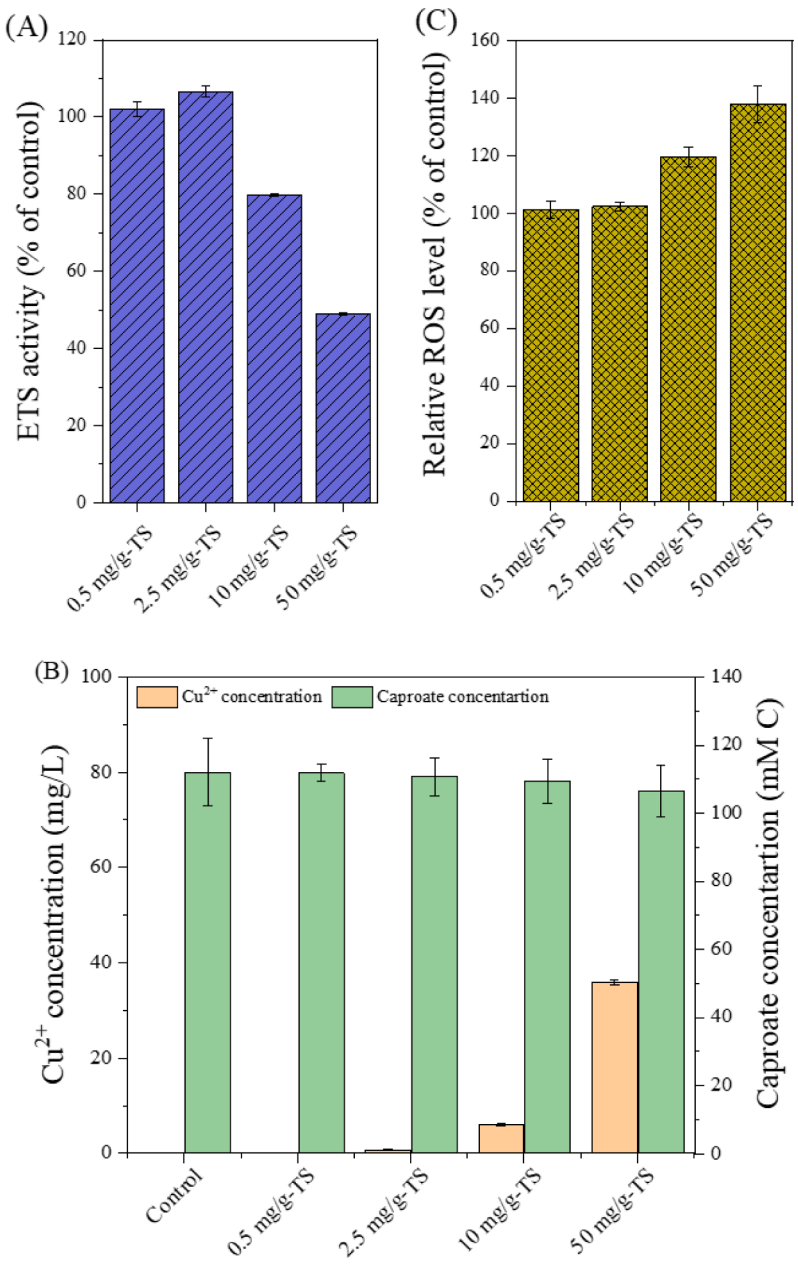

Fig. 2. Effects of CuO NPs at different concentrations on (A) the ETS activity, (B) the released Cu^{2+} concentration with their impacts on caproate production during WAS anaerobic fermentation, (C) the ROS level. Error bars represent standard deviations of triplicate tests.

MCCs production, the microbial community composition between the control and the 2.5 mg/g-TS CuO NPs exposed fermenter were compared using high-throughput sequencing of the 16S rRNA genes. The rarefaction curves (Fig. S7(A), SI) of the two samples gradually flattened, suggesting that the sequencing depth was enough to cover the whole diversity. The Shannon and Chao indices in 2.5 mg/g-TS CuO NPs group were 4.58 ± 0.03 and 1443 ± 11, respectively, which were a little lower to those in the control group (4.86 ± 0.07 and 1450 ±7). The results indicated that CuO NPs addition could decrease the microbial diversity, which was consistent with previous studies (Tang et al., 2016; Wei et al., 2021). Venn diagram based on 0.03 distance showed that the number of OTUs were 984 and 1176 in experimental and control groups, respectively, which further demonstrated that the microbial diversity was reduced with CuO NP addition (Fig. S7B). Fig. S8(A~B) showed the phylum and order levels distributions in control and experimental groups. The main phyla in both groups included *Synergistota, Proteobacteria, Actinobacteriota, Firmicutes, Bacteroidetes, Caldatribacteriota, Planctomycetota* and *Chloroflexi*, which totally accounted above 90% of the microbial population. More specially, *Actinobacteriota* and *Chloroflexi* were the dominate phyla in both two samples, and the dominance of two phyla was also found in other studies for the anaerobic fermentation of WAS (Wan et al., 2016; Wei et al., 2021). *Firmicutes* were also frequently found in the anaerobic digestion of WAS and chain elongation process (Angenent et al., 2016), and their abundance in experimental reactor was little lower than that obtained in the control (12.6% vs 13.9%), which indicated that the addition of 2.5 mg/g-TS CuO NPs might weakly inhibit the chain elongation process. In contrast, the abundances of *Caldatribacteriota* and *Synergistota* in the experimental group increased by 7.2 and 6.3 %, compared to those in the control group. The above phyla are closely related to the hydrolysis of organic matter (Hania et al., 2016). It was worth to note that a higher relative abundance of phylum *Planctomycetota* (both obligate and facultative aerobic chemoheterotrophs) was observed in the experimental group, which was probably related to the generation of ROS induced by

addition of CuO NPs (Glöckner et al., 2003). Therefore, the results revealed that the CuO NP addition could alter the overall taxonomic structure of bacterial communities in anaerobic fermentation of WAS. Fig. 3 showed the genus level identification of the sequences, and CuO NPs increased the relative abundances of functional microorganisms related to hydrolysis and acidogenesis. For example, the relative abundance of *Georgenia* sp., capable of performing hydrolysis, in the CuO NP was 15.8%, which showed an increase of 4.2% compared to the control group (Li et al., 2007). Moreover, the *Candidatus_Caldatribacterium sp.* is considered to participate in hydrolysis and acidogenesis (Vickers, 2017), and CuO NPs addition increased its abundances. *Clostridium sp.* Was reported to be responsible for chain elongation (Angenent et al., 2016), and its abundances in the CuO NP reactor was also little lower than that in the control group. Hence, CuO NP of 2.5 mg/g-TS could affect the microbial diversity, and thus promote both the hydrolysis and acidogenesis steps, while weakly inhibit chain elongation process.

3.5. CuO NP-induced changes in proteomic profiles related to carboxylates production

To deeply disclose the mechanism for the promotion of MCCs in the presence of 2.5 mg/g-TS CuO NPs, the identified and differentially expressed proteins based on label-free quantitative proteomic were analysed. Samples were obtained from control reactor and 2.5 mg/g-TS reactor at the end of the batch experiment and total 1785 proteins were identified from the samples. 483 of the 1785 proteins were identified as differentially expressed proteins, therein 294 proteins were up-regulated and 189 proteins were down-regulated. The changes of metabolic pathways induced by 2.5 mg/g-TS CuO NPs were further analyzed by KEGG database. Table S1 listed the significant enriched pathways ($P < 0.05$), and differentially expressed proteins were found to be enriched in Glycolysis/Gluconeogenesis (24.7%), Pyruvate metabolism (12.1%), Carbon fixation pathways in prokaryotes (5.4%), ABC transporters (9.5%) and Butanoate metabolism (13.5%). The above results can be attributed to that CuO NPs induced the changes of protein expression levels involved in various pathways for the conversion of WAS to MCCs. Therefore, the identified proteins were manually inspected and key enzymes were selected for analyzing the main metabolic reactions involved in the conversion of WAS and MCCs production, i.e., polysaccharide hydrolysis, proteolysis, central carbon metabolism and chain elongation pathway (Fig. 4 and 5, Table S2-S6).

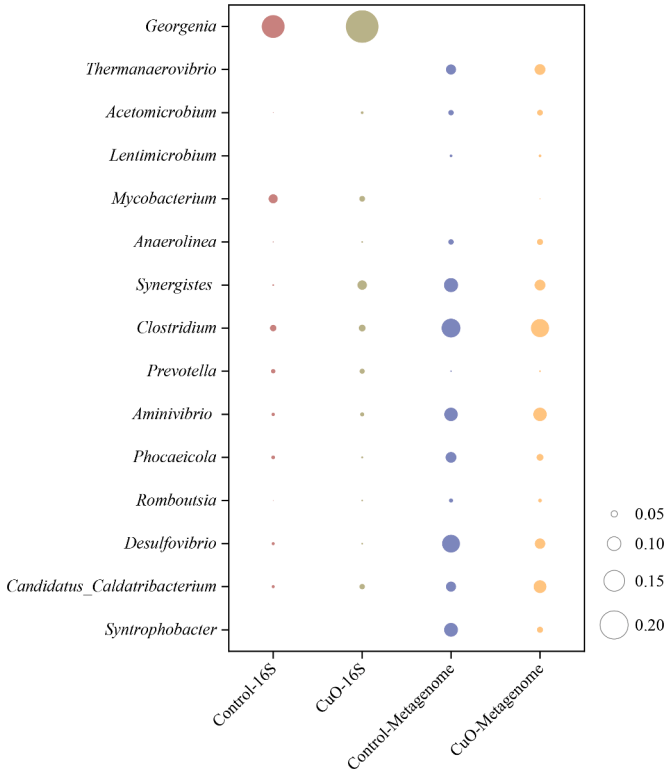

Fig. 3. Relative abundances of the dominant taxa in the 16S rRNA genes and metaproteomics at genus level in the control group (0 mg/g-TS CuO NPs) and the experimental group (2.5 mg/g-TS CuO NPs).

3.5.1. Hydrolysis-related expressional trait

Consistent with WAS being the main substrate for the incubations, proteins potentially involved in polysaccharide hydrolysis and proteolysis were identified (Table S2). According to the annotation to the CAZy database, 11 enzymes assigned to the Glycoside Hydrolases (GHs) and Carbohydrate-Binding Modules (CBMs) families were detected. It was obvious the differently expressed proteins, relating with the key hydrolysis enzymes (e.g., 4-α-glucanotransferase and β-1,4-glucan) were up-regulated. The result was inconsistent with the dextran degradation rate as shown in Fig. S5, which might be due to the diversity of polysaccharide and more abundant substrate regarding to the improved WAS solubilization. The enriched genus *Candidatus Caldatribacterium* and species *Acetomicrobium mobile* with the addition of CuO NPs, appeared as key actors for polysaccharide hydrolysis, which also had been studied as polysaccharide hydrolysis species (Fig.3) (Vickers, 2017). Meanwhile, the differently expressed proteins relating with the flagella and pilin monomer assigned to genus *Ca. Caldatribacterium* were up-regulated. Genus *Ca. Caldatribacterium* was motile through on flagella (Lin et al., 2014), and the higher expressed level of pilin monomer could help the microorganisms to move forward to nutrients, thereby promoting synthesis and metabolism of genus *Ca. Caldatribacterium*. Overall, the 2.5 mg/g-TS CuO NPs induced the up-regulated expression level of key enzymes involved in polysaccharide hydrolysis, which could be one reason for the promotion of MCCs production.

The extracellular protease activity was first supported by the identification of a putative extracellular protease, which could break proteins bonds to form peptides (Rawlings et al., 2014) (Table S3). Additionally, a membrane bound serine protease and carboxypeptidase protein, which could induce the fragmentation of proteins/polypeptide and formation of amino acids, were also detected. However, there were no significant regulation of these mentioned proteins involved in proteolysis, demonstrating that the addition of CuO NPs did not affect the proteolysis. The different expression level of proteins for polysaccharide hydrolysis and proteolysis might be due to the interaction between the functional microbial species and CuO NPs and thereby indirectly affect the proteins expression levels.

3.5.2. Metabolism of monosaccharides-related expressional trait

After polysaccharide hydrolysis and proteolysis, monosaccharides and amino acids were channeled to the central catabolic pathways to generate pyruvate. It is known that the transmembrane transport and intracellular metabolism are the indispensable steps for the utilization of monosaccharides and amino acids. The analysis of proteomic data revealed that the identified proteins related to monosaccharides (e.g., glucose and pentose) transporters was significantly up-regulated. In contrast, there were no significant changes of protein expression levels related to amino acids transporters. This was consistent with the results of hydrolysis, indicating that the exposure to low dosages of CuO NPs could promoted the monosaccharides transmembrane transport process, while shows no impact on the transport process of amino acids.

Regarding the intracellular metabolism of monosaccharides for pyruvate synthesis, only one enzyme assigned to the Enter-Doudoroff pathway for the production of glyceraldehyde 3-phosphate was detected (Fig. 4). In contrast, proteins from the complete Embden–Meyerhof pathway (glycolysis) were identified, along with the oxidative branch of the pentose phosphate pathway. Almost all identified proteins involved in glycolysis pathway were up-regulated, except the enzymes

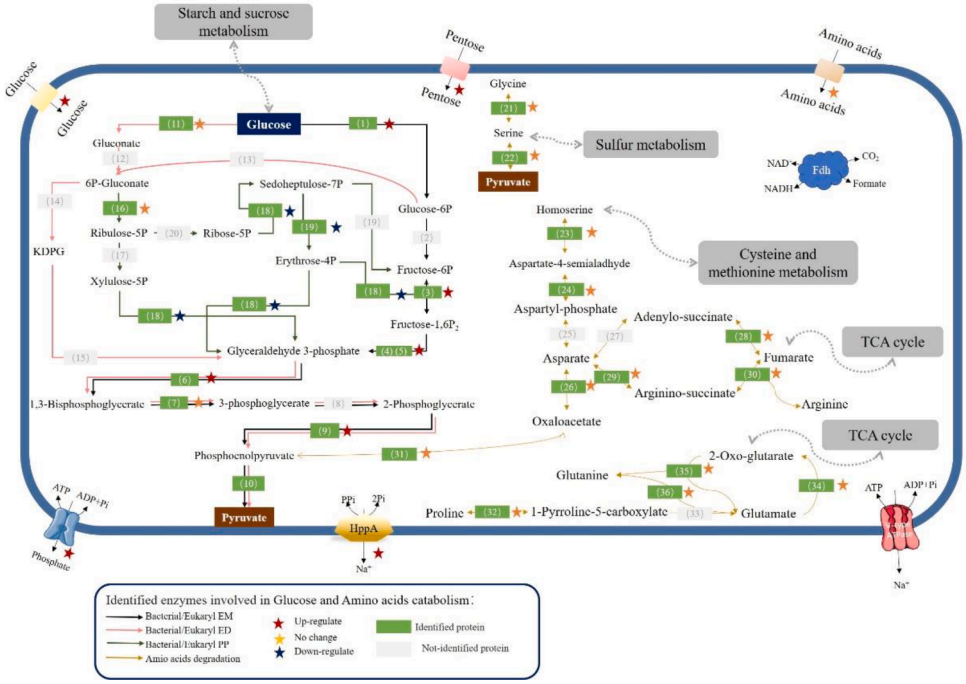

Fig. 4. Identified and differently expressed enzymes involved in the transmembrane hydrolysis products transport and intracellular metabolism mapped over generic pathways. Abbreviations: ATP, adenosine triphosphate; NAD(P)H, nicotinamide adenine dinucleotide (phosphate) hydrogen; Pi, phosphate; PPi, pyrophosphate; KDPG, 2-keto-3-deoxy-6-phosphogluconate. The detail description of these identified and differently expressed enzymes was provided in Supplementary Table S4.

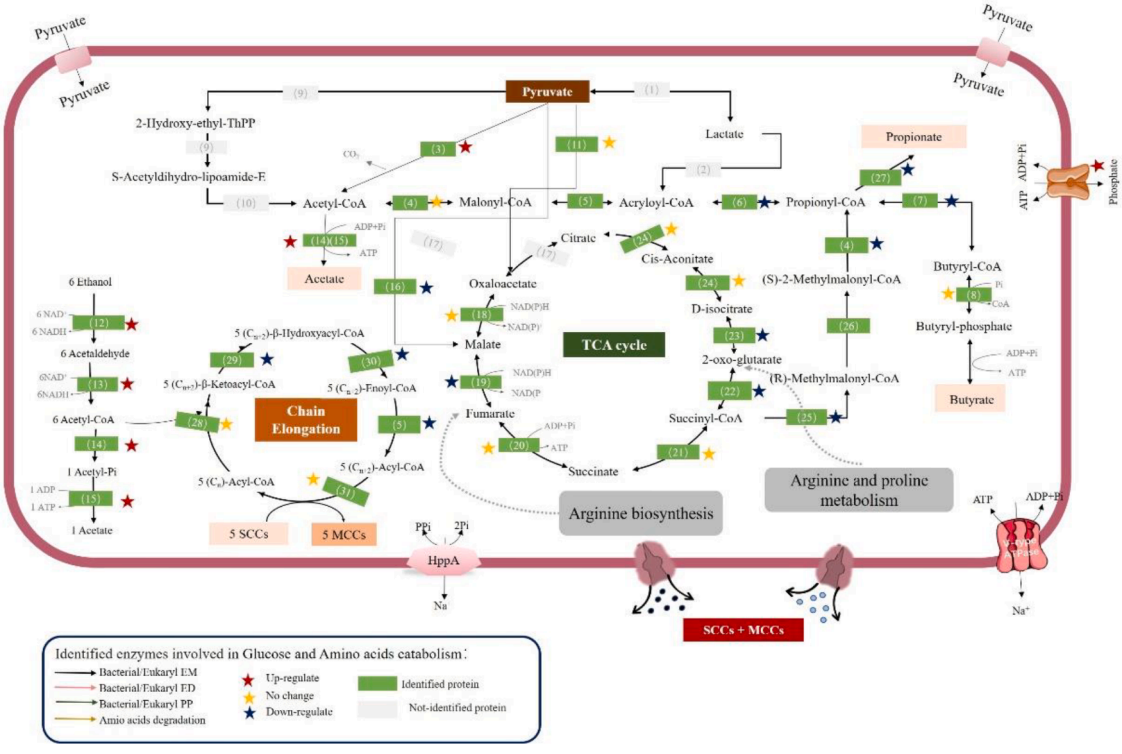

Fig. 5. Identified and differently expressed enzymes involved in the pyruvate metabolism and chain elongation process mapped over generic pathways. CoA, co-enzyme A. The detail description of these identified and differently expressed enzymes was provided in Supplementary Table S5.

phosphoglucose isomerase, while the identified proteins in pentose phosphate pathway were adverse (Fig. 4 and Table S4). These observations indicated that CuO NPs addition could change the metabolism pathway of monosaccharides. In addition, pyruvate synthase is a key enzyme involved in the glucose metabolism (Leiyu et al., 2009), which assigned 7 differentially expressed proteins as shown in Table. S4 (5 up-regulated and 2 down-regulated). According to the sourced microorganisms of each differentially expressed protein via proteomic, the up-regulated differentially expressed proteins involved in pyruvate synthase were originated from the species *Anaerolinea thermophila*, while

the down-regulated proteins could be assigned to genus *Acetomicrobium*. The results indicated that CuO NPs selectively induced the expression of proteins involved in pyruvate synthase from some bacteria in the mixed culture. Interestingly, several identified proteins assigned to superoxide dismutase from *A. thermophila* were highly expressed with 2.5 mg/g-TS CuO NPs (Table S6). As demonstrated by previous studies, superoxide dismutase is capable of scavenging ROS (Hu and Tirelli, 2012; Nantapong et al., 2019). The high expression level of superoxide dismutase could avoid the negative impact of intracellular ROS on the microbial metabolism with low dosage of CuO NPs. This phenomenon was in accordance with the result of electron transfer activity. In addition, the up-regulation of V/F-type reversible ATPases subunit (atpA and atpB) were also observed in CuO NP group (Table S6), which can transport protons or sodium cations across the membrane (Junge and Nelson, 2005). The up-regulated ATPases (two ~ three-fold higher than the control) was originated from the species *A. thermophila*, which further indicated that *A. thermophila* was the functional microorganism for the metabolism of monosaccharides. Taken together, the addition of low CuO NPs displayed contributive characteristics in transport and metabolism of monosaccharides.

Among the identified proteins involved in amino acid metabolism, 26 could be assigned to proline metabolism, 16 to arginine biosynthesis and 3 to serine metabolism. The proteins for glutamate, serine and arginine biosynthesis were all identified, except arginine-succinate synthase. Arginine, serine, and asparate could be converted into pyruvate and acetyl-CoA after oxidative decarboxylation for carboxylates biosynthesis. The proteins involved in glutamate, serine, and asparate metabolism into TCA cycle intermediates and pyruvate were also identified. However, there were no significant up-regulation or down-regulation of these identified proteins. Almost all the identified proteins related to amino acids degradation, except arginine, mainly attributed to strains from the *Aminivibrio pyruvatiphilus*. The relative abundances of this genus were similar in two samples both in 16S rRNA high-throughput sequencing and proteomic analysis (Fig. 3). Therefore, there was strong evidence that CuO NPs addition has negligible effect on amino acids consumption.

3.5.3. Carboxylates production-related expressional trait

There were 9 enzymes identified in the pyruvate metabolism (Fig. 5 and Table S5). The pathway module, involved in pyruvate converted to acetyl-CoA, was complete, and the pyruvate synthase subunit (porABCD) was observed in high expression level (1.5–3 fold higher than the control). The highly expressed pyruvate synthase could be a key reason for the promotion of SCCs production. Acetyl-CoA and other intermediates involved in tricarboxylic acid cycle would be further catalyzed into different products. According to the identified proteins, a variety of fermentation products, including acetate, propionate, butyrate could be generated. It is known that acetate is usually the end fermentation product, thus the activities of key acetate-forming enzymes (phosphotransacetylase, and acetate kinase) were determined. As shown in Fig. 5, the expression of phosphotransacetylase and acetate kinase in the experimental sample were up-regulated, relatively to the control, indicating that the acetogenesis could be stimulated in experimental group. Our previous study demonstrated that higher concentration of SCCs could accelerate the production of MCCs (Liu et al., 2020), thus the promotion of acetogenesis and acetate generation should be the main reason for the enhanced MCC (n-caproate) production.

In addition, alcohol dehydrogenase (responsible for acetyl-CoA formation from ethanol in chain elongation process) related proteins originated from *Clostridium sp.,* which known as chain elongation bacteria, was also up-regulated. This phenomenon was consistent with a higher ethanol consumption rate observed in experimental sample. Acetyl-CoA acyltransferase, acetoacetyl-CoA reductase, 3-Hydroxyacyl-CoA dehydrogenase, enoyl-CoA hydratase and acyl-CoA thioesterase involved in cycle pathway were also essential for MCCs production from acyl-CoA (Han et al., 2018; Wu et al., 2020a). In total, 17 proteins relating to above 5 essential enzymes were identified, and they were weakly down-regulated (took 0.7–0.8 of the control) except acetyl-CoA acyltransferase and acyl-CoA thioesterase (Results were shown in Table S5). Overall, although CuO NPs at 2.5 mg/g weakly inhibited chain elongation process, they induced high expression level of key enzymes involved in pyruvate metabolism and acetogenesis, ultimately leading to the enhanced MCCs production.

3.6. Current understandings of dosage-dependent effects of CuO NPs on MCCs production

Based on the above observations and discussions, the mechanism for the effect of CuO NPs on MCCs production from WAS during anaerobic fermentation was concluded. It has become a consensus that CuO NPs could cause inhibition on the anaerobic production of CH_4 from WAS, and the present study also found that the MCCs production was inhibited by CuO NPs exceeded 10 mg/g-TS. The ROS produced in anaerobic conversion system was inferred to be the primary cause of the phenomena. In contrast to the inhibition effect, the present study demonstrated that at CuO NPs lower than 2.5 mg/g-TS, MCCs production could be efficiently promoted. Combining metaproteomic analyses, chemical and molecular approaches, a model for the studied ecosystem is proposed (Fig. 6). Its main features with low dosage of CuO NPs exposure are as follows: (1) significant enhancement of WAS solubilization; (2) increased abundance of key microorganisms and enzymes associated with polysaccharide hydrolysis; (3) improved transport/metabolism of monosaccharides and acetogenesis; (4) higher expression level of superoxide dismutase despite the generation of ROS in WAS anaerobic fermentation; and finally, (5) only a weak inhibition of chain elongation. The information gained on the studied ecosystem highlights the possibility of regulation of functional microbial groups and catalytic reaction activity with CuO NPs, for MCCs production and complements the results gained from previous 16S rRNA genes or metagenomic studies (Huang et al., 2019; Luna-delRisco et al., 2011; Wei et al., 2021). While the current finding highlights the differential response and mechanism involved in the exposure of CuO NPs to MCC production fermentation system, future work is needed to determine the expression level of proteins for carbohydrate degradation and proteolysis, and understand how to steer the community further towards MCCs to increase the efficiency and selectivity of these systems and reduce the adverse effect of CuO NPs. Currently, several companies are paying attention to MCCs production from organic wastes. For example, a spin-off company named ChainCraft has made a great effort to establish setup and design for mass production of MCCs from WAS (www.chaincraft.nl). Thus, MCCs production from organic wastes is deemed as a promising and economic biotechnology and the increase obtained in present study could be quite helpful for recovery (extraction) in the further processing. As a proof-of concept study, here the highest selectivity of MCCs (36%) obtained at 2.5 mg/g-TS CuO NPs was relatively low. Some strategies, such as continuous product extraction and improving the ratio of ethanol to WAS, can also be adopted in future to improve the selectivity and production of MCCs from CuO NP-containing sludge. And last but certainly not least, repeated batch test or long-term continuous flow experiment should be conducted in the future study to explore more precise microbial mechanism and evaluate the long-term stability of MCC production process promoted by 2.5 mg/g-TS CuO to shed light for safer management and better practical utilization of CuO NPs polluted sludge.

4. Conclusion

This study comprehensively revealed that CuO NPs displayed dosage-dependent enhancement-to-inhibition effect on WAS anaerobic fermentation for MCCs production. It was found that the MCCs generation was inhibited by CuO NPs exceeded 10 mg/g-TS, and ROS produced in anaerobic conversion system was inferred to be the primary

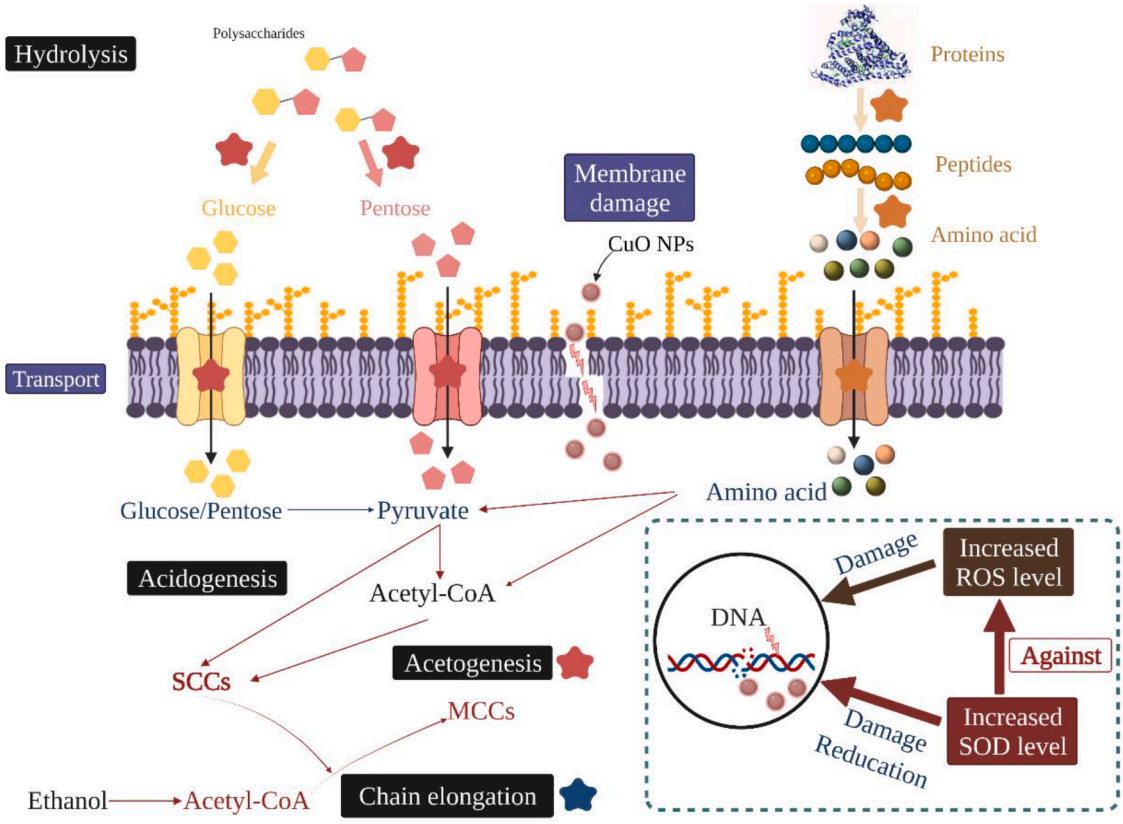

Fig. 6. Schematic diagram of 2.5 mg/g-TS CuO NPs-induced influences on anaerobic fermentation of WAS and intracellular metabolism for effective MCCs production. SOD: Superoxide dismutase.

cause of the phenomena. However, the present study demonstrated that at CuO NPs lower than 2.5 mg/g-TS (environmentally relevant concentrations), the SCCs and MCCs production could be efficiently promoted. Combining metaproteomic analyses, chemical and molecular approaches, the underlying mechanism may involve the enhanced WAS solubilization, increased electron transfer activities, increased abundances of key microorganisms and expression level of key enzymes associated with hydrolysis and acetogenesis process. Overall, this study provides important clues for resource utilization of CuO NP-containing sludge.

Declaration of Competing Interest

The authors declare no competing interest.

Data availability

Data will be made available on request.

Acknowledgment

This research was financially supported by the National Natural Science Foundation of China (21906033 and 22036002), Chinese Postdoctoral Science Foundation (2021M700922), the introduced innovative R&D team project under the “The Pearl River Talent Recruitment Program” of Guangdong Province (2019ZT08L387), and Funding by Science and Technology Projects in Guangzhou (202102020570).

Supplementary materials

Supplementary material associated with this article can be found, in the online version, at doi:10.1016/j.watres.2022.119545.

References

Abdulsada, Z., Kibbee, R., Örmeci, B., DeRosa, M., Princz, J., 2021. Impact of anaerobically digested silver and copper oxide nanoparticles in biosolids on soil characteristics and bacterial community. Chemosphere 263, 128173.
Abram, F., Enright, A.M., O'reilly, J., Botting, C., Collins, G., O'flaherty, V., 2011. A metaproteomic approach gives functional insights into anaerobic digestion. J. Appl. Microbiol. 110 (6), 1550–1560.
Ajay, C., Mohan, S., Dinesha, P., Rosen, M.A., 2020. Review of impact of nanoparticle additives on anaerobic digestion and methane generation. Fuel 277, 118234.
Angenent, L.T., Richter, H., Buckel, W., Spirito, C.M., Steinbusch, K.J., Plugge, C.M., Strik, D.P., Grootscholten, T.I., Buisman, C.J., Hamelers, H.V., 2016. Chain elongation with reactor microbiomes: open-culture biotechnology to produce biochemicals. Environ. Sci. Technol. 50 (6), 2796–2810.
Blenkinsopp, S., Lock, M., 1990. The measurement of electron transport system activity in river biofilms. Water Res. 24 (4), 441–445.
Chen, H., Chen, Y., Zheng, X., Li, X., Luo, J., 2014a. How does the entering of copper nanoparticles into biological wastewater treatment system affect sludge treatment for VFA production. Water Res. 63, 125–134.
Chen, J.L., Ortiz, R., Steele, T.W., Stuckey, D.C., 2014b. Toxicants inhibiting anaerobic digestion: a review. Biotechnol. Adv. 32 (8), 1523–1534.
Chen, W., Westerhoff, P., Leenheer, J.A., Booksh, K., 2003. Fluorescence excitation-emission matrix regional integration to quantify spectra for dissolved organic matter. Environ. Sci. Technol. 37 (24), 5701–5710.
Chen, Y., Yang, Z., Zhang, Y., Xiang, Y., Xu, R., Jia, M., Cao, J., Xiong, W., 2020. Effects of different conductive nanomaterials on anaerobic digestion process and microbial community of sludge. Bioresour. Technol. 304, 123016.
Degli Esposti, M., McLennan, H., 1998. Mitochondria and cells produce reactive oxygen species in virtual anaerobiosis: relevance to ceramide-induced apoptosis. FEBS Lett. 430 (3), 338–342.
Glöckner, F.O., Kube, M., Bauer, M., Teeling, H., Lombardot, T., Ludwig, W., Gade, D., Beck, A., Borzym, K., Heitmann, K., 2003. Complete genome sequence of the marine planctomycete Pirellula sp. strain 1. Proc. Natl. Acad. Sci. 100 (14), 8298–8303.

Gonzalez-Estrella, J., Sierra-Alvarez, R., Field, J.A., 2013. Toxicity assessment of inorganic nanoparticles to acetoclastic and hydrogenotrophic methanogenic activity in anaerobic granular sludge. J. Hazard. Mater. 260, 278–285.
Han, W., He, P., Shao, L., Lü, F., 2018. Metabolic interactions of a chain elongation microbiome. Appl. Environ. Microb. 84 (22), e01614–e01618.
Hania, W.B., Bouanane-Darenfed, A., Cayol, J.-L., Ollivier, B., Fardeau, M.-L., 2016. Reclassification of Anaerobaculum mobile, Anaerobaculum thermoterrenum, Anaerobaculum hydrogeniformans as Acetomicrobium mobile comb. nov., Acetomicrobium thermoterrenum comb. nov. and Acetomicrobium hydrogeniformans comb. nov., respectively, and emendation of the genus Acetomicrobium. Int. J. Syst. Evol. Micr. 66 (3), 1506–1509.
Hou, J., Wang, X., Hayat, T., Wang, X., 2017. Ecotoxicological effects and mechanism of CuO nanoparticles to individual organisms. Environ. Pollut. 221, 209–217.
Hu, P., Tirelli, N., 2012. Scavenging ROS: superoxide dismutase/catalase mimetics by the use of an oxidation-sensitive nanocarrier/enzyme conjugate. Bioconjugate Chem. 23 (3), 438–449.
Huang, H., Chen, Y., Yang, S., Zheng, X., 2019. CuO and ZnO nanoparticles drive the propagation of antibiotic resistance genes during sludge anaerobic digestion: possible role of stimulated signal transduction. Environ. Sci.: Nano 6 (2), 528–539.
Ingle, AP. (ED.), 2021. Nanotechnology in Plant Growth Promotion and Protection: Recent Advances and Impacts. In: John Wiley & Sons, Ltd., UK, pp. 79–92.
Jeong, C.-B., Won, E.-J., Kang, H.-M., Lee, M.-C., Hwang, D.-S., Hwang, U.-K., Zhou, B., Souissi, S., Lee, S.-J., Lee, J.-S., 2016. Microplastic size-dependent toxicity, oxidative stress induction, and p-JNK and p-p38 activation in the monogonont rotifer (Brachionus koreanus). Environ. Sci. Technol. 50 (16), 8849–8857.
Junge, W., Nelson, N., 2005. Nature's rotary electromotors. Science 308 (5722), 642–644.
Kiser, M.A., Ryu, H., Jang, H., Hristovski, K., Westerhoff, P., 2010. Biosorption of nanoparticles to heterotrophic wastewater biomass. Water Res. 44 (14), 4105–4114.
Leiyu, F., Yinguang, C., Xiong, Z., 2009. Enhancement of waste activated sludge protein conversion and volatile fatty acids accumulation during waste activated sludge anaerobic fermentation by carbohydrate substrate addition: the effect of pH. Environ. Sci. Technol. 43 (12), 4373–4380.
Li, W.-J., Xu, P., Schumann, P., Zhang, Y.-Q., Pukall, R., Xu, L.-H., Stackebrandt, E., Jiang, C.-L., 2007. Georgenia ruanii sp. nov., a novel actinobacterium isolated from forest soil in Yunnan (China), and emended description of the genus Georgenia. Int. J. Syst. Evolut. Microbiol. 57 (7), 1424–1428.
Limbach, L.K., Bereiter, R., Müller, E., Krebs, R., Gälli, R., Stark, W.J., 2008. Removal of oxide nanoparticles in a model wastewater treatment plant: influence of agglomeration and surfactants on clearing efficiency. Environ. Sci. Technol. 42 (15), 5828–5833.
Limbach, L.K., Wick, P., Manser, P., Grass, R.N., Bruinink, A., Stark, W.J., 2007. Exposure of engineered nanoparticles to human lung epithelial cells: influence of chemical composition and catalytic activity on oxidative stress. Environ. Sci. Technol. 41 (11), 4158–4163.
Lin, W., Bazylinski, D.A., Xiao, T., Wu, L.F., Pan, Y., 2014. Life with compass: diversity and biogeography of magnetotactic bacteria. Environ. Microbiol. 16 (9), 2646–2658.
Liu, C., Luo, G., Liu, H., Yang, Z., Angelidaki, I., Sompong, O., Liu, G., Zhang, S., Wang, W., 2020. CO as electron donor for efficient medium chain carboxylate production by chain elongation: microbial and thermodynamic insights. Chem. Eng. J. 390, 124577.
Liu, H., Fang, H.H., 2002. Extraction of extracellular polymeric substances (EPS) of sludges. J. Biotechnol. 95 (3), 249–256.
Liu, S., Zhu, N., Ning, P., Li, L.Y., Gong, X., 2012. The one-stage autothermal thermophilic aerobic digestion for sewage sludge treatment: effects of temperature on stabilization process and sludge properties. Chem. Eng. J. 197, 223–230.
Liu, T., Ghosh, S., 1997. Phase separation during anaerobic fermentation of solid substrates in an innovative plug-flow reactor. Water Sci. Technol. 36 (6-7), 303.
Lü, F., Bize, A., Guillot, A., Monnet, V., Madigou, C., Chapleur, O., Mazéas, L., He, P., Bouchez, T., 2014. Metaproteomics of cellulose methanisation under thermophilic conditions reveals a surprisingly high proteolytic activity. ISME J. 8 (1), 88–102.
Luna-delRisco, M., Orupõld, K., Dubourguier, H.-C., 2011. Particle-size effect of CuO and ZnO on biogas and methane production during anaerobic digestion. J. Hazard. Mater. 189 (1-2), 603–608.
Mu, H., Chen, Y., 2011. Long-term effect of ZnO nanoparticles on waste activated sludge anaerobic digestion. Water Res. 45 (17), 5612–5620.
Mu, H., Chen, Y., Xiao, N., 2011. Effects of metal oxide nanoparticles (TiO2, Al2O3, SiO2 and ZnO) on waste activated sludge anaerobic digestion. Bioresour. Technol. 102 (22), 10305–10311.
Nantapong, N., Murata, R., Trakulnaleamsai, S., Kataoka, N., Yakushi, T., Matsushita, K., 2019. The effect of reactive oxygen species (ROS) and ROS-scavenging enzymes, superoxide dismutase and catalase, on the thermotolerant ability of Corynebacterium glutamicum. Appl. Microbiol. Biotechnol. 103 (13), 5355–5366.
Otero-González, L., Field, J.A., Sierra-Alvarez, R., 2014. Inhibition of anaerobic wastewater treatment after long-term exposure to low levels of CuO nanoparticles. Water Res. 58, 160–168.
Rawlings, N.D., Waller, M., Barrett, A.J., Bateman, A., 2014. MEROPS: the database of proteolytic enzymes, their substrates and inhibitors. Nucleic Acids Res. 42 (D1), D503–D509.
Sengupta, D., Kannan, M., Reddy, A.R., 2011. A root proteomics-based insight reveals dynamic regulation of root proteins under progressive drought stress and recovery in Vigna radiata (L.) Wilczek. Planta 233 (6), 1111–1127.
Tang, Y., He, R., Zhao, J., Nie, G., Xu, L., Xing, B., 2016. Oxidative stress-induced toxicity of CuO nanoparticles and related toxicogenomic responses in Arabidopsis thaliana. Environ. Pollut. 212, 605–614.
Tian, T., Qiao, S., Yu, C., Tian, Y., Yang, Y., Zhou, J., 2017. Distinct and diverse anaerobic respiration of methanogenic community in response to MnO2 nanoparticles in anaerobic digester sludge. Water Res. 123, 206–215.
Tian, T., Qiao, S., Yu, C., Zhou, J., 2019. Effects of nano-sized MnO2 on methanogenic propionate and butyrate degradation in anaerobic digestion. J. Hazard. Mater. 364, 11–18.
Tou, F., Yang, Y., Feng, J., Niu, Z., Pan, H., Qin, Y., Guo, X., Meng, X., Liu, M., Hochella, M.F., 2017. Environmental risk implications of metals in sludges from waste water treatment plants: the discovery of vast stores of metal-containing nanoparticles. Environ. Sci. Technol. 51 (9), 4831–4840.
Vickers, N.J., 2017. Animal communication: when i'm calling you, will you answer too? Curr. Biol. 27 (14), R713–R715.
Wan, J., Jing, Y., Zhang, S., Angelidaki, I., Luo, G., 2016. Mesophilic and thermophilic alkaline fermentation of waste activated sludge for hydrogen production: focusing on homoacetogenesis. Water Res. 102, 524–532.
Wang, D., Chen, Y., 2016. Critical review of the influences of nanoparticles on biological wastewater treatment and sludge digestion. Crit. Rev. Biotechnol. 36 (5), 816–828.
Wang, W., Li, X., Wang, P., Song, X., Jiang, D., Wang, K., 2013. Long-term effects of Ni (II) on the performance and activity of activated sludge processes. Ecotoxicol. Environ. Saf. 92, 144–149.
Wang, X., Li, J., Liu, R., Hai, R., Zou, D., Zhu, X., Luo, N., 2017. Responses of bacterial communities to CuO nanoparticles in activated sludge system. Environ. Sci. Technol. 51 (10), 5368–5376.
Wang, Y., Wang, D., Yi, N., Li, Y., Ni, B.-J., Wang, Q., Wang, H., Li, X., 2020a. Insights into the toxicity of troclocarban to anaerobic digestion: sludge characteristics and methane production. J. Hazard. Mater. 385, 121615.
Wang, Y., Wei, W., Wu, S.-L., Ni, B.-J., 2020b. Zerovalent iron effectively enhances medium-chain fatty acids production from waste activated sludge through improving sludge biodegradability and electron transfer efficiency. Environ. Sci. Technol. 54 (17), 10904–10915.
Wei, W., Wu, L., Shi, X., Ni, B.-J., 2021. Mechanisms of CuO nanoparticles at an environmentally relevant level enhancing production of hydrogen from anaerobic fermentation of waste-activated sludge. ACS ES&T Water 1 (6), 1495–1502.
Wu, Q., Guo, W., Bao, X., Meng, X., Yin, R., Du, J., Zheng, H., Feng, X., Luo, H., Ren, N., 2018. Upgrading liquor-making wastewater into medium chain fatty acid: Insights into co-electron donors, key microflora, and energy harvest. Water Res. 145, 650–659.
Wu, S.-L., Sun, J., Chen, X., Wei, W., Song, L., Dai, X., Ni, B.-J., 2020a. Unveiling the mechanisms of medium-chain fatty acid production from waste activated sludge alkaline fermentation liquor through physiological, thermodynamic and metagenomic investigations. Water Res. 169, 115218.
Wu, S.-L., Wei, W., Sun, J., Xu, Q., Dai, X., Ni, B.-J., 2020b. Medium-Chain fatty acids and long-chain alcohols production from waste activated sludge via two-stage anaerobic fermentation. Water Res. 186, 116381.
Yang, Z., Ren, N.-q., Ho, S.-H., 2020. Optimizing the production of short and medium chain fatty acids (SCFAs and MCFAs) from waste activated sludge using different alkyl polyglucose surfactants, through bacterial metabolic analysis. J. Hazard. Mater. 384, 121384.
Yang, Z., Wang, W., Liu, C., Zhang, R., Liu, G., 2019. Mitigation of ammonia inhibition through bioaugmentation with different microorganisms during anaerobic digestion: selection of strains and reactor performance evaluation. Water Res. 155, 214–224.
Zheng, H.-S., Guo, W.-Q., Yang, S.-S., Feng, X.-C., Du, J.-S., Zhou, X.-J., Chang, J.-S., Ren, N.-Q., 2014. Thermophilic hydrogen production from sludge pretreated by thermophilic bacteria: analysis of the advantages of microbial community and metabolism. Bioresour. Technol. 172, 433–437.